PREPARATION OF ANTI-ADHESIVE AND ANTIBACTERIAL SURFACES
USING POLYMERS

A THESIS SUBMITTED TO
THE GRADUATE SCHOOL OF NATURAL AND APPLIED SCIENCES
OF
MIDDLE EAST TECHNICAL UNIVERSITY

BY

BORA ONAT

IN PARTIAL FULFILMENT OF THE REQUIREMENTS
FOR
THE DEGREE OF DOCTOR OF PHILOSOPHY
IN
BIOTECHNOLOGY

OCTOBER 2017

Approval of the thesis:

PREPARATION OF ANTI-ADHESIVE AND ANTIBACTERIAL SURFACES USING POLYMERS

submitted by **BORA ONAT** in partial fulfillment of the requirements for the degree of **Doctor of Philosophy in Department of Biotechnology, Middle East Technical University** by,

Prof. Dr. Gülbin Dural Ünver
Dean, Graduate School of **Natural and Applied Sciences**   _____

Assoc. Prof. Dr. Çağdaş Devrim Son
Head of Department, **Biotechnology**   _____

Assoc. Prof. Dr. İrem Erel Göktepe
Supervisor, **Chemistry Dept., METU**   _____

Assoc. Prof. Dr. Sreeparna Banerjee
Co-supervisor**, Dept. of Biological Sciences, METU**   _____

Examining Committee Members:

Prof. Dr. Ali Çırpan
Chemistry Dept., METU   _____

Assoc. Prof. Dr. İrem Erel Göktepe
Chemistry Dept., METU   _____

Assoc. Prof. Dr. Pınar Yılgör Huri
Dept. Of Biomedical Engineering, Ankara University   _____

Assoc. Prof. Dr. Fevzi Çakmak Cebeci
Faculty of Engineering and Natural Sciences,
 Sabancı University   _____

Assist. Prof. Dr. Özgül Persil Çetinkol
Chemistry Dept., METU   _____

Date:

I hereby declare that all information in this document has been obtained and presented in accordance with academic rules and ethical conduct. I also declare that, as required by these rules and conduct, I have fully cited and referenced all material and results that are not original to this work.

Name, Last name: Bora ONAT

Signature:

ABSTRACT

PREPARATION OF ANTI-ADHESIVE AND ANTIBACTERIAL SURFACES USING POLYMERS

Onat, Bora

Ph.D., Department of Biotechnology

Supervisor: Assoc. Prof. İrem Erel Göktepe

Co-supervisor: Assoc. Prof. Sreeparna Banerjee

October 2017, 218 pages

Layer-by-layer self-assembly of polymers is a versatile technique which can impart new functions to the surfaces of biomedical instruments and biomaterials. Materials which are coated by this technique can exhibit response towards environmental stimuli, such that the controlled release of drugs and similar biologically functional molecules under different stimuli can be observed.

In the span of this thesis study, ultra-thin polymer films were prepared through the layer-by-layer self-assembly technique, the physicochemical properties of the films were assessed and their potential functions in biomedical studies which cover coating surfaces to impart anti-adhesive and antibacterial properties were discovered. As described in the first chapter of the thesis, multilayer films of zwitterionic block copolymer micelles has shown bacterial anti-adhesive and pH-responsive antibacterial agent releasing properties. The antibacterial agent was released from the pH-

responsive cores of the block copolymer micelles. In the second chapter of the thesis, for the purpose of supporting the bone regeneration and reducing the time of acceptance of the implants in the body, multilayer films of antibacterial Tannic Acid (TA) and biodegradable poly(4-hydroxy-L-proline ester) (PHPE) was studied. It was determined that, these films are osteoconductive and support the regeneration of the bone. In the third chapter of the thesis, multilayer films of TA and thermoresponsive poly(N-vinyl caprolactam) (PVCL) was deposited on hydrogels composed of chitosan and polyethylene glycol (PEG). It was shown that, at physiological temperature, antibiotic release from the hydrogel membranes was enhanced. It was also determined that, hydrogels with TA and PVCL multilayer-film surface modifications enhance the viability of fibroblasts in the skin. This type of hydrogels hold promise in use as antibacterial wound dressings.

Layer-by-layer self-assembly technique is a facile and versatile method of preparing biologically functional surfaces. The films which are prepared in the extent of this thesis are not only promising for bacterial anti-adhesive and antibacterial applications, but also for bone regeneration and wound healing.

Keywords: Layer-by-layer films, Stimuli-response, Antibacterial, Anti-adhesive, Tissue regeneration

ÖZ

POLİMERLERİN KULLANIMI İLE ANTİBAKTERİYEL VE YAPIŞMA ÖNLEYİCİ YÜZEYLERİN HAZIRLANMASI

Onat, Bora

Doktora, Biyoteknoloji Bölümü

Tez Yöneticisi: Doç. Dr. İrem Erel Göktepe

Yardımcı Tez Yöneticisi: Doç. Dr. Sreeparna Banerjee

Ekim 2017, 218 sayfa

Polimerlerin katman-katman kendiliğinden yapılanma tekniği biyomedikal cihazların veya biyomalzemelerin yüzeylerine yeni fonksiyonlar katmakta kullanılan uygulaması basit bir yöntemdir. Bu yöntem ile kaplanan malzemeler çevresel etmenlere duyarlılık kazanabilmekte, ilaç vb. biyolojik moleküllerin kontrollü salımını gerçekleştirebilmektedir.

Bu tez çalışmasında, katman-katman kendiliğinden yapılanma yöntemi kullanılarak ultra-ince polimer filmler hazırlanmış, fizikokimyasal özellikleri incelenmiş ve yapışma önleyici ve antibakteriyel polimer yüzeylerin hazırlanmasını da kapsayan biyomedikal uygulamalar için potansiyelleri ortaya çıkarılmıştır. Tezin ilk bölümünde, zwitteriyonik blok kopolimer miseller içeren çok-katmanlı filmlerin bakteri yapışma önleyici özellikler gösterdiği, aynı zamanda pH'a duyarlı misel çekirdekleri sayesinde yüzeyden antibakteriyel ajan salımı gerçekleştirebildikleri gösterilmiştir. Tezin ikinci

bölümünde, kemik oluşumunu desteklemek ve implantların vücuda uyum sağlama sürecini kısaltmak amacıyla antibakteriyel Tannik Asit'in (TA) ve biyobozunur bir polimer olan poli(4-hidroksi-L-prolin ester)'in (PHPE) kullanarak çok-katmanlı filmler hazırlanmış ve bu filmlerin kemik rejenerasyonunu desteklediği ve osteokondüktif özellik gösterdiği ortaya çıkarılmıştır. Tezin üçüncü bölümünde, kitozan ve polietilen glikol'den oluşan hidrojellerin üzerinde TA ve sıcaklığa duyarlı poli(N-vinil kaprolaktam) (PVCL) çok-katmanlı filmleri biriktirilmiş, hidrojellerin yüzeyinden vücut sıcaklığında antibiyotik (Siprofloksasin) salımı gerçekleştiği gösterilmiştir. Yüzeyleri TA ve PVCL çok-katmanlı filmleri ile modifiye edilen hidrojellerin deri içerisinde bulunan fibroblastların viabilitesini artırdığı bulunmuştur. Bu tip hidrojellerin yara sargısı olarak kullanılabilme potansiyeli vardır.

Katman-katman kendiliğinden yapılanma yöntemi, biyolojik olarak işlevsel filmlerin hazırlanması için kolay uygulanabilir ve çok yönlü bir yöntemdir. Bu tez çalışması kapsamında hazırlanan filmler, yapışma önleyici ve antibakteriyel olmaları yanında kemik dokusu rejenerasyonu ve yara iyileştirme uygulamaları için de ümit verici niteliktedir.

Anahtar Kelimeler: Katman-katman filmler, Uyarıcıya duyarlı filmler, Antibakteriyel, Yapışma önleyici, Doku yenilenmesi

To My Dearest Ezgi
and to
My Family…

ACKNOWLEDGMENTS

TABLE OF CONTENTS

LIST OF TABLES

TABLES

LIST OF FIGURES

LIST OF SCHEMES

SCHEME

LIST OF ABBREVIATIONS

ANOVA	Analysis of variance
ATCC	American type culture collection
BCA	Bicinchoninic acid
BCM	Block copolymer micelle
βPDMA-*b*-PDPA	Betainized poly[3-dimethyl (methacryloyloxyethyl) ammonium propane sulfonate-b-2-(diisopropylamino)ethyl methacrylate]
bp	Base pair
bPEI	Branched poly(ethylene imine)
BSA	Bovine Serum Albumin
CCD	Charge-coupled device
cDNA	Complementary DNA
CFU	Colony forming unit
CHO	Chinese Hamster Ovary
DI	Deionized
DMEM	Dulbecco's modified Eagle's medium
DMF	Dimethylformamide
DNA	Deoxyribonucleic acid
DOX	Doxorubicin
D-PBS	Dulbecco's Phosphate Buffered Saline
ECM	Extracellular matrix
EDTA	Ethylenediaminetetraacetic acid
FBS	Fetal bovine serum
FGF	Fibroblast Growth Factor
FITC	Fluorescein isothiocyanate

FTIR	Fourier Transform Infrared Spectroscopy
GPC	Gel permeation chromatography
HA	Hyaluronic acid
HAIs	Hospital acquired infections
HEMAPTMC	h-Hydroxyethyl methacrylate-poly(trimethylene carbonate)
hrBMP-2	Human recombinant bone morphogenetic protein-2
HUVEC	Human umbilical vein endothelial cells
Hyp	*trans*-4-hydroxy-L-proline
I-CAM	Inter-cellular adhesion molecule
L	Liter
LCST	Lower critical solution temperature
LB	Langmuir-Blodgett, Luria Bertani
LbL	Layer-by-layer
M	Molarity
MDR	Multiple drug resistant
MIC	Minimum inhibitory concentration
mL	Milliliter
MAC	Mineralization activation cocktail
MEM	Minimal essential medium
M_N	Molecular weight by number average
MRSA	Methicillin-resistant *S. aureus*
MTT	3-(4,5-dimethylthiazolyl-2)-2,5-diphenyltetrazolium bromide
M_W	Molecular weight by weight average
MW	Molecular weight
NIPAAm	N-isopropylacrylamide
NIR	Near-infrared light
NMR	Nuclear magnetic resonance
ns	Not significant
OD	Optical density

OQAS	[3-(trimethoxysilyl)propyl]octadecyl-dimethylammonium chloride
PAA	Poly(acrylic acid)
PAA-BOH	Poly(acrylic acid)-phenyl boronic acid
PAAm	Poly(acrylamide)
PAH	Poly(allylamine hydrochloride)
PAMA	Poly(alkyl methacrylate)
PAMAM	Poly(amidoamine)
PAzoMA	Poly(6-[4-(4- methoxyphenylazo) phenoxy] hexyl methacrylate
PBA	Poly(butyl acrylate)
PBS	Phosphate buffered saline
PCL	Poly(caprolactam)
PDAC	Poly(diallyldimethyl ammonium chloride)
Pd/C	Palladium on Carbon
PDDA	Poly(diallyldimethyl ammonium chloride)
PDEAEMA	Poly(2-(diethylamino)ethyl methacrylate)
PDI	Poly dispersity index
PDMA-*b*-PDEA	Poly[2-(dimethylamino)ethyl methacrylate-*block*-poly(2-(diethylamino)ethyl methacrylate)]
PDMS	Poly(dimethylsiloxane)
pDNA	Plasmid DNA
PDPA	Poly(diisopropylamino)ethyl methacrylate
PEG	Poly(ethylene glycol)
PEI	Poly(ethylene imine)
PEO	Poly(ethylene oxide)
PHCP	Poly(4-hydroxy-*N*-cbz-L-proline ester)
PHPE	Poly(4-hydroxy-L-proline ester)
PIPOX	Poly(2-isopropyl-2-oxazoline)
pK_a	Acid dissociation constant
PGA	Poly(glycolic acid)
PLGA	Poly(lactide-*co*-glycolic acid)

PLL	Poly(L-lysine)
PLLA	Poly(lactic acid)
PMA	Poly(methyl acrylate)
PMEMA-*b*-PDPA	Poly[2-(N-morpholino)ethyl methacrylate-*block*-2-(diisopropylamino)ethyl methacrylate]
PNIPAAm	Poly(N-isopropylacrylamide)
pNPP	*para*-Nitophenylphosphate
PNVC-*co*-PAAEM-*co*-PVIm	Poly(vinylcaprolactam-*co*-acetoacetoxyethyl methacrylate-*co*-vinylimidazole)
POEGMA–PDPA	Poly(oligo(ethylene glycol) methacrylate)-*block*-poly(2-diisopropyl aminoethyl methacrylate)
pPBMA	Poly(phosphobetaine methacrylate)
PPG	Poly(propylene glycol)
PSS	Poly(styrene sulfonate)
PTFE	Poly(tetrafluoro ethylene)
PVA	Poly(vinyl alcohol)
PVCL	Poly(N-vinyl caprolactam=
PVME	Poly(vinyl methyl ether)
PVP	Poly(N-vinylpyrrolidone)
PVPON	Poly(N-vinylpyrrolidone)
rhBMP-2	Recombinant human bone morphogenetic protein-2
RNA	Ribonucleic acid
RPM	Revolutions per minute
RT-qPCR	Reverse transcriptase quantitative polymerase chain reaction
SAM	Self-assembled monolayer
SD	Standard deviation
SE	Standard error
siRNA	Small Interfering RNA
SP-DiOC$_{18}$(3)	3,3′-dioctadecyl-5,5′-di(4-sulfophenyl) oxacarbocyanine sodium salt

SPR	Surface plasmon resonance
TA	Tannic acid
U	Unit
UCST	Upper critical solution temperature
UV	Ultra violet
UV-Vis	Ultra violet - visible
VEGF	Vascular endothelial growth factor

xxx

CHAPTER 1

INTRODUCTION

1.1. Layer-by-Layer Self-Assembly Technique

Various strategies of building ultra-thin films have been applied in coating surfaces and the most prominent ones are the Langmuir-Blodgett (LB) technique [1] and the self-assembled monolayer (SAM) method [2]. Even though LB and SAM techniques have been widely used in the literature, the LB technique is mostly only applicable to the assembly of amphiphilic molecules onto surfaces and the SAM technique is limited to a single layer and do not allow the assembly of multiple layers on surfaces. Layer-by-layer (LbL) self-assembly technique is a cheap and versatile technique allowing the build-up of polymer multilayers as ultra-thin films, and is highly tunable due to the range of materials that can be incorporated in film structures [3,4].

LbL self-assembly technique was first introduced by Iler in 1966. Alumina and silica colloidal particles were deposited on substrates to form LbL structures. By Decher et al. in the 90s, LbL technique was adopted to polyelectrolytes, which resulted in the formation of ultrathin multilayers [5–7]. These alternating multilayer structures developed by Decher, Hong, and Schmitt, were composed of polyanions and polycations and were the frontiers of the LbL self-assembled polymer thin films. The basic procedure in the LbL self-assembly of molecules is the alternating deposition of two polyelectrolytes with opposite charges to a substrate. Basically, negatively charged substrate is immersed into a polycation solution for a determined period, and then rinsed. Then, the polycation-coated substrate is immersed into the polyanion solution for a determined period of time and rinsed again. The procedure is repeated until the desired thickness or layer number is achieved [8] (Scheme 1. 1.).

1
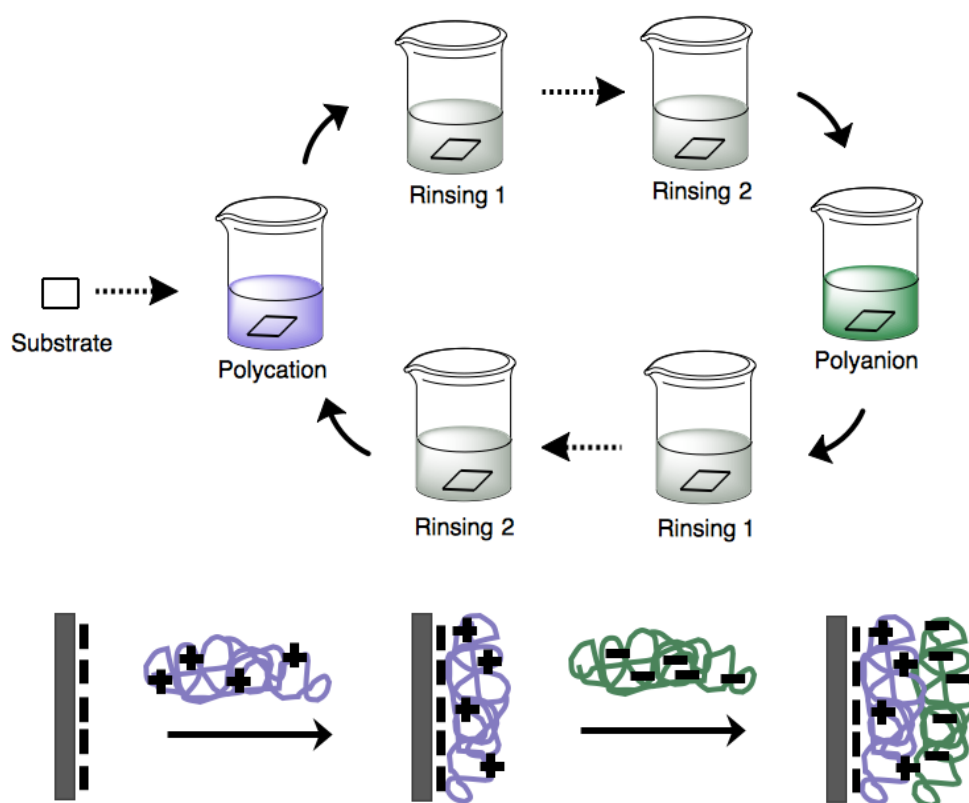
Scheme 1. 1. The schematic representation of LbL deposition of polyelectrolytes via dip-coating.

Although electrostatic interactions are the main driving force for LbL self-assembly of polymers at the surface, hydrogen-bonding interactions have also been investigated to construct LbL films (Scheme 1. 2.). In 1994, Rubner and colleagues introduced the use of hydrogen-bonding interactions between polymers to form LbL films of poly(vinyl pyrrolidone) (PVP), poly(vinyl alcohol) (PVA), poly(acrylamide) (PAAm), or poly(ethylene oxide) (PEO) with polyaniline [9]. Further studies showed that water-soluble non-ionic polymers with hydrogen-accepting functional groups could also be LbL constructed at the surface using hydrogen-donating polyacids [10,11].

Hydrogen-bonding interactions   Electrostatic interactions
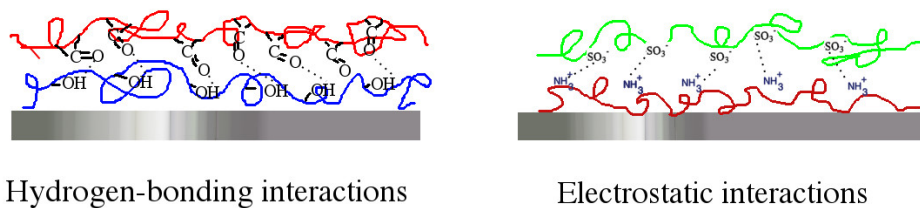
Scheme 1. 2. The schematic representation of LbL films via hydrogen-bonding interactions or electrostatic interactions as the driving force.

One significantly important advantage of LbL films is that they are composed of water-soluble molecules and polymers, thus LbL films can be prepared in aqueous environment in the absence of toxic organic solvents. Although majority of LbL films are prepared in aqueous solutions, there are studies where different solvents were used to deposit water insoluble polymers at surfaces. For example, alternating deposition of a dimethylformamide (DMF)-soluble azo-containing polymer as the anionic counterpart and poly(diallyldimethyl ammonium chloride) (PDAC) as the cationic counterpart was reported to form polyelectrolyte LbL films of varying thicknesses with linear growth patterns [12]. As also reported, "reverse-phase LbL deposition" is a potential approach in the self-assembly of anionic or cationic polymers in their non-ionized forms. As reported by Beyer et al., suspensions of poly(diallyldimethyl ammonium) (PDADMA) and poly(methyl acrylate) (PMA) in ethanol render them non-ionized, though diffusion forces them to self-assemble on surfaces in a non-similar fashion to the aqueous LbL technique where the primary driving force for polymers to self-assemble on surfaces is the Coulomb interactions [13].

The growth pattern of LbL films is basically divided into two: linear growth and exponential growth [14]. In linear growth, the thickness increase by one bilayer is constant, thus the growth is considered to be linear. In exponential growth, the overall thickness of the film increases exponentially as the layer number increases. Specifically, there are two hypotheses on the occurrence of the exponential growth of

LbL films. In the first hypothesis, thickness increases by increasing number of layers, because the molecules used in the LbL deposition form complexes throughout the self-assembly process. After each layer deposition, some part of the film dissociates into the solution, forms complexes with the molecules that are present in the solution and these complexes self-assemble again at the surface [15]. In the second hypothesis, the substrate with few deposited layers is immersed inside a solution of a particular polyelectrolyte. That polyelectrolyte, other than getting deposited as the topmost layer, can cross the energy barrier provided by the film and diffuses inside the film. These polyelectrolytes do not always interact with the oppositely charged polyelectrolytes inside the film, thus some of them diffuse back into the rinsing solution. However, still some remain within the multilayers making complexes inside the film [16]. This case fits suitably for poly(glycolic acid) (PGA)/ poly(L-lysine) (PLL) films [14], however note that, as reported by Ruths et al. [17], interfacial roughness of the films can be the mechanism behind the exponential growth of polyelectrolyte films [such as poly(styrene sulfonate)(PSS)/poly(allyamine hydrochloride (PAH) films]. Multilayer films of PLL and alginate [18] and PLL and hyaluronan [19,20] were the first reports of LbL films where researchers detected an exponential growth pattern on surfaces. The first five layers generally tend to be omitted in considering the type of the growth pattern, due to the substrate effect. Substrate-polymer interactions can reduce the extent of polymer-polymer interactions in the first layers. The substrate acts like a mechanical support for the LbL build-up of polymers, but this does not always mean that a successful LbL deposition can be achieved as further layers.

When it comes to the methods scientists use in obtaining LbL films, dip-coating is the prominent method used, but is not always the most advantageous one. In dip-coating applications, once a substrate is immersed inside the solution that contains a polymer, the polymer adsorbs onto the surface in a two-step fashion. At the fast initial step, the polymer chains interact with the surface through some of the functional groups. At the slow second step, polymer chains relax on the surface to pack densely and reorganize the thin film [21,22]. Spin-coating and spray-coating methods also found large place in the literature. The spin-coating method introduced shorter deposition times and smoother surfaces of multilayer structures compared to the films prepared by the same

molecules by dip-coating method [23]. Fabrication of LbL films via spray-coating method was first described by Schlenoff group in 2000, as an alternative to dip-coating method [24]. By spray-coating, the deposition of polymer layers on substrates was found to be achieved in much shorter times, compared to the time in dip-coating process. The surface properties and thickness values achieved via spray-coating are generally considered to be similar to that obtained via dip-coating process. So the advantage is solely the time spent on the process.

1.2. Factors Affecting the Properties of LbL Films

1.2.1. The Composition of the LbL Film

Use of polymers in LbL film applications hold great promise due to the broad range of functionalities and properties possessed by the polymers. The presence of functional groups in every repeating unit of polymers and their high molecular weight make them suitable counterparts in LbL applications. Polyelectrolytes are either anionic or cationic depending on the charge of the functional group in the repeating unit. Alternatively, polymers can also make hydrogen-bonding interactions between each other through the hydrogen accepting/donating functional groups. The functional groups on the polymers are highly critical on the behavior of polymers in solution, thus the LbL film properties, so the primary factor that affects the film deposition is the type of the polycation or the polyanion [25]. Functional groups induce conformational changes in polymers, affect how they interact with themselves, other polymers or molecules, or the solvent molecules.

1.2.2. pH

pH controls the charge density on weak polyelectrolytes, thus the conformation of the polymers. Most of the preliminary work on the LbL self-assembly of weak polyelectrolytes were performed under conditions in which polyelectrolytes are in their most highly charged form [26,27]. Some initial studies of poly(acrylic acid) (PAA)/poly(allylamine hydrochloride) (PAH) films of Rubner and coworkers have

5

focused on the complex behaviors of these weak polyacid/weak polybase pairs that occur over a wide range of pH values [28–30]. For example, film depositions carried out under highly acidic conditions (pH 2.5) ended up with thinner films compared to the deposition under mildly acidic conditions (pH 4.5) of the same polymer pairs [28]. Charge density on weak polyelectrolytes can be controlled by pH and allows facile control over the thickness of each self-assembled polymer layer [29,31].

1.2.3. Ionic Strength

The role of salts and free polyions in the polyelectrolyte solutions is another factor influencing the deposition mechanism of polymers on surfaces. For example, poly(alkyl methacrylate) (PAMA) and PAA multilayer structures, at pH 6.8 showed a linear growth pattern under 1 mM $NaNO_3$ concentration in the solution of deposition, but the film did not grow steadily under 5 mM $NaNO_3$ concentration, due to the screening effect of the free ions in solution between charged polymers [32]. As reported by Hammond and coworkers, the ionic strength dramatically affects the behaviour of polyion depositions. In the LbL deposition of PSS and poly(diallyldimethyl ammonium chloride) (PDAC), addition of low concentrations of salts (NaCl) changed the conformation of polymers from rods to barrels, resulting in thicker films. On the other hand, very high salt concentrations caused electrostatic screening and reduced polyion depositions [33].

1.2.4. Temperature

On the other hand, temperature is another stimuli that controls the conformation of polymers [34]. As described by Lvov and coworkers, the deposition temperature of PDAC and PSS films controls the thickness of the film. Alternating deposition of PDAC/PSS and PDAC/silica layers showed that when the deposition temperature was 60°C, the film thickness was higher compared to the thickness obtained at room temperature. The thickness was observed to be even higher at 90°C [35]. In another study, Tan et al. reported on the temperature-sensitive film deposition of PDAC/PSS films. As the temperature increased to 70°C, both PDAC and PSS self-assembled to

6

make thicker films, compared to the films assembled at room temperature [36]. Even though the mechanism behind the effect of temperature on polymer self-assembly is currently not clear, this group hypothesized that the mechanism behind this phenomenon would be the increased conformational mobility of the polymer chains at higher temperature, which give them the freedom to interact with the polyions present in solutions. Not only the deposition behavior of synthetic polymers is temperature-dependent, but also natural polymers can behave similarly in terms of temperature-sensitive deposition. Chitosan/alginate hydrogels form thicker multilayer films with higher drug encapsulation and release once they are deposited at higher temperatures than the room temperature, most probably because of the conformational changes in chitosan and alginate at high temperatures [37].

1.3. Stimuli-Responsive Polymer LbL Films

1.3.1 LbL Films Responsive to pH and Ionic Strength

Electrostatic and hydrogen-bonded LbL films are responsive to pH and ionic strength as the interaction between two polymers could be reduced via change in pH or ionic strength of the solution. pH and ionic response of polymer films stand out more when the polymers are weak polyelectrolytes, such as PAA and PAH [28]. For example, carboxylic acid groups of PAA deprotonates at pH values above its pK_a of 4.25 [38] (Figure 1.1.) Such polyelectrolytes shift charges easily around their pK_a values, leading to higher or lower electrostatic interactions with other charged molecules and polyelectrolytes [39]. This is an important property in LbL applications, because reduced interactions between polyelectrolytes would easily lead to the dissociation of the films. Similarly, polyelectrolyte interactions in LbL films decrease once ion concentration in their solution increases, due to the screening of charges on functional groups via circulating ions.
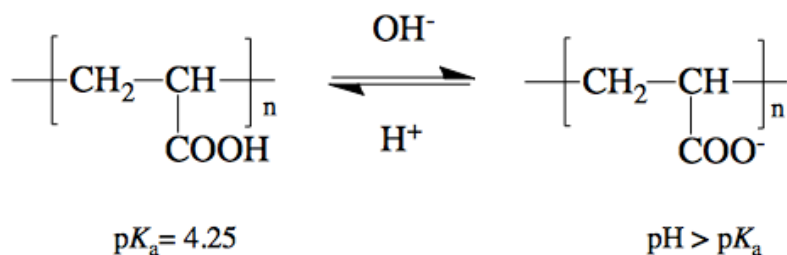
Fig. 1. 1. Chemical structure of the unimer of poly(acrylic acid) (PAA) with at the point where pH meets the pK_a value and when pH is higher than the pK_a value (Image modified from Chan et al., 2013 [40].

In pH-responsive LbL films, the primary mechanism that drives film compositional change is the protonation or deprotonation of specific chemical groups on polymers. Protonation or deprotonation weakens the interactions between polyions, and changes the conformation of the polyelectrolytes. For example, highly charged forms of PAA and PAH tend to form rod-like conformations, but as the interactions weaken under mildly acidic conditions, polymers form barrels and swell [41]. The secondary mechanism is related with the pK_a values of weak polyacids and polybases, but results in the dissociation of the LbL film. As the interaction between polyelectrolytes is weakened and the polymer-water interactions become dominant compared to polymer-polymer interactions, the LbL film dissociates. Both mechanisms drive the release of encapsulated molecules in LbL films [42]. pH-responsive LbL films have been thoroughly studied in the literature, and the most significant property of these films is the release of encapsulated agents (loaded cargo) from the thin film via pH-trigger [43]. Similarly, hollow capsules of LbL films can show reversible porosity under pH shifts, which is of important use in pH-responsive delivery of loaded cargo from capsules [44]. pH-dependent permeability of cargo molecules in LbL films is an important property for the encapsulation and release of agents in films. A schematic representation of the mechanisms of the release of cargo molecules from LbL hollow capsules is represented in Scheme 1. 3. For example, dextran and albumin can penetrate inside LbL films of PSS and PAH at neutral and acidic pH, but not at basic pH [45,46]. This makes the film load and release its cargo at acidic or neutral pH range. Oppositely, the cargo can be prone to release from LbL films at basic pH only. As

8

reported by Akashi and coworkers, Allura Red, a negatively-charged dye was released slowly at neutral and acidic pH, but much faster at basic pH from PVA/PAA LbL films [47]. This was reported to be due to the enhanced electrostatic repulsion between Allura Red and PAA at basic pH, due to the deprotonation of the carboxylic acid group.
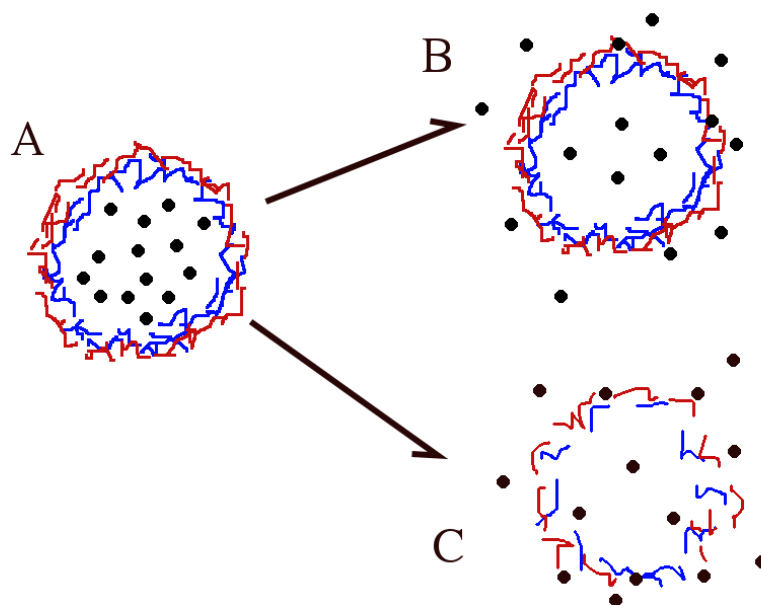
Scheme 1. 3. Schematic representation of LbL hollow capsules with loaded cargo molecules (A), release of cargo molecules from the hallow capsule upon changing stimuli through diffusion or conformational changes in the polymer chains (B), and through the dissociation of the LbL film (C).

The use of poly(carboxybetaine)s, due to their zwitterionic nature, have shown great promise in forming pH-responsive LbL films. In a report by the Sukhishvili group, (poly(4-vinylpyridiniopentanecarboxylate) (PCB5), was able to interact electrostatically with quatermized poly(4-vinyl pyridine) (P4VP) derivative, and poly(methylacrylic acid) (PMAA) or PSS to form hybrid films. P4VP/PCB5/PMAA hybrid films were able to dissociate at pH < 4 due to the deionization of the carboxylic acid groups of PCB5 and P4VP/PCB5/PSS hybrid films were able to dissociate pH > 7 due to the ionization of carboxylic acid groups, making it highly tunable [48]. Although LbL films can be designed to dissociate or get into conformational changes at different pH, not all of them are suitable for the release of active agents for biomedical applications. Especially the pH range from 5.5 to 7.5, which is commonly

observed inside living cells or in the extracellular area of cells have been of significant focus in designing LbL films or capsules with pH-responsive bahavior. Hammond and coworkers have reported on several LbL films with biodegradable and pH-responsive properties, where physiological pH induced faster degradation of the film components due to the nucleophilicity of amine, which induce the degradation at higher pH [49,50]. To functionalize LbL films with pH-responsive drug release (such as antibiotics or growth factors), block copolymer micelles with pH-responsive polybasic cores have been of great use, due to their ease of demicellization under mildly acidic conditions [51].

pH-responsive LbL films that were deposited by the hydrogen-bonding driving force between tannic acid (TA) and thermoresponsive polymers were reported before. Kharlampieva et al. reported that microcapsules of LbL films of poly(N-vinylpyrrolidone) (PVPON) and tannic acid (TA) could be successfully deposited on SiO$_2$ microparticles and the film permeability increased under mildly acidic conditions, in contrast to TA/PAH multilayers which possessed higher permeability at neutral or basic pH. This was attributed to a conformational change in the LbL film of TA/PVPON where TA was ionized at higher pH [52]. Similarly, TA/PVPON films can be deposited on living cells, however these films reduced cell viability, so needs more insight in terms of biomedical applications [53].

One natural carrier of biological compounds is a pathogen that causes epidemic diseases on a broad range of species. Such non-organismal pathogens are called viruses. They carry their load in biocompatible capsids which carry antigens that can form lock-and-key structures and allow them through cellular membranes by intracytosis. Viruses are great natural examples of DNA and RNA vehicles which trick prokaryotic and eukaryotic cells to internalize them as biocompatible agents. As Kataoka et al. mentioned in a review article 15 years ago, polymer micelles can be designed to mimic viruses and lipoproteins, especially in terms of structure, size and methods to penetrate in tissues [54]. One type of copolymers that can form micelles are block copolymer micelles (BCMs). BCMs are nanometer-scale micellar aggregates of varying sizes with blocks of two different solubility properties. In case of a two-

block copolymer micelle, one block forms the outer shell (coronae) of the structure due to its higher solubility in the solvent of the polymer solution, compared to the solubility of the other block. The inner (core) region of the structure forms an insoluble aggregate in the center of the structure, as it is not either soluble in the solvent or its solubility is low [55]. As polar or charged groups would form the coronae in a water-soluble micellar system, the opposite is also possible for non-polar groups in non-polar solvents.

Research on controlled release of compounds by BCMs were pioneered by Kataoka and coworkers [54,56]. Rather than drugs, model hydrophobic compounds (e.g. pyrene) were preferred as the cargo of BCMs in these initial reports. This was due to the easy detection of these compounds using fluorescence spectroscopy and UV-Vis spectroscopy techniques. One facile method of releasing the cargo out of the BCM is to adjust the pH of the polymer solution only. As the core of the micelle is hydrophobic in a specific pH range and hydrophilic out of this range, hydrophobic compounds such as pyrene can be easily encapsulated in the core of these micelles and released once the core becomes hydrophilic. For example, Zhang and coworkers were the first to report on thin films of block copolymer micelles. They reported on the LbL films of micelles of poly(styrene-*b*-acrylic acid) and poly(diallyl dimethylammonium chloride) (PDAC) where the hydrophobic dye pyrene was encapsulated in the polystyrene micellar cores of poly(styrene-*b*-acrylic acid) copolymer micelles and pyrene was released from the surface by increasing the concentration of NaCl in the solution. In their report, the release of functional molecules from LbL films where the agent was released at higher amounts by increasing NaCl concentration in solution was reasoned to be due to the loosening of the micelle core and shrinkage of the coronae due to the screening effect of Na^+ and Cl^- ions [57].

Drug-loaded BCM containing LbL films are highly useful in constructing surfaces of biological value. Such studies have been extensively carried out by Hammond and co-workers. First reports on the drug release from micelle-incorporated nano-films for extended periods of time (more than couple of days) were reported by this group of researchers [58,59]. In one study, multilayers of PAA and PEO-*b*-PCL micelles with

poly(ethylene oxide) (PEO)-corona were deposited at mildly acidic conditions when carboxylic acid groups of PAA were protonated and disintegrated when these groups were deprotonated at physiological pH. After the disintegration of the micelles from the films, drug release from micelle cores was observed due to the diffusion of the drug [58]. Another report by this group focused on using block copolymer micelles in LbL films for the release of triclosan, a bactericidal agent. Here, authors claimed that the high encapsulation efficiency of triclosan by the block copolymer micelles with poly(propylene glycol) (PPG)-core and poly(amidoamine) (PAMAM)- coronae was due to the dendritic architecture of the coronae part of the micelle [60], which showed that the architecture of the BCM coronae can influence the amount of cargo loaded.

Drug-conjugated BCMs has found use in LbL films. First of all, conjugating drug molecules to micelle forming BCMs for cancer therapy was first introduced by Kataoka and coworkers [61–63]. Hammond and coworkers pioneered the studies on pH-responsive release of doxorubicin from LbL films that incorporated drug-conjugated BCMs. In this study, they conjugated doxorubicin to the PHEMA-cores of poly(ethylene oxide)-*block*-poly(2-hydroxylethyl methacrylate) (PEO-*b*-PHEMA) micelles via carbamate linkage which could be cleaved under acidic conditions leading to release of doxorubicin from the micellar cores as well as from the surface [64].

Although many thin films with micelles released drugs because the core-forming block of the block copolymer micelle was stimuli-responsive, Kim and coworkers came up with the idea of micelle-releasing thin films. The poly(2-ethyl-2-oxazoline) block of the BCM effectively made hydrogen-bonding with PAMAM dendrimers with peripheral carboxyl groups under mildly acidic conditions, micelles released from films at pH ≥ 5.6 due to ionization of the carboxylic acid groups. The hydrophobic agent in the core of the micelle was released sequentially with the micelles out of the thin film [65].

Addison, Biggs, Armes, York and coworkers carried out significant amount of research on the deposition of block copolymer micelles with core blocks that are pH-responsive and shell blocks with tunable charge. They showed that micellization pH

12

could be altered by varying the chain length of the core block. This group of researchers synthesized BCMs with cationic [66], anionic [67] and zwitterionic corona [68] that greatly increased the range of potential applications of pH-responsive micelles. Some of these reports were specifically focusing on BCMs immobilized on core templates such as silica [66], polystyrene latex [69] and calcium carbonate [68]. One important publication by this group reported that LbL deposition of BCMs on substrates can hinder the effect of critical micelle concentration, but on the other hand, once micelles dissociate below the pH of micellization, they do not desorb out of the film. For example, poly[2-(dimethylamino)ethyl methacrylate-*block*-poly(2-(diethylamino)ethyl methacrylate)] (PDMA-*b*-PDEA) copolymers were able to form micellar structures at pH 7 - 8. They figured out that, once these micelles were immobilized on substrates, some of the micelles that dissociated under mildly acidic conditions regained their micellar structure on substrates when the pH of the solution was raised above pH 8 [68]. These researchers has worked extensively on coating microparticles with layers of BCMs and to achieve hollow microparticles. The major problem with preparation of hollow microcapsules was described by Addison et al. BCM dissociation and drug release could not be prevented during the removal of the sacrificial core template once silica templates were used for LbL assembly [66]. This problem was solved only when calcium carbonate templates were used. Templates could be removed by a treatment with dilute EDTA. This removal did not affect the micelle structure physically or cause any loss of the cargo drug, resolving the concerns on encapsulated cargo loss from BCMs coated on microparticles [68]. Hong et al. achieved similar hollow particles after removing polystyrene templates, though these capsules were only stable when specific M_W ratio of the core-forming and coronae-forming blocks was chosen. This study showed that electrostatic attractions between the coronae of loaded micelles immobilized on polystyrene templates could be stable after removal from the template and additional cross-linking were not necessary [70].

Hammond and coworkers were the first to report on the hydrogen-bonded BCM multilayers of poly(ethylene oxide)-block-poly(e-caprolactone) (PEO-b-PCL) micelles and polyacrylic acid (PAA) showing the diffusion of an antibacterial agent from the micelle cores [58]. A study by Erel et al. showed that, the hydrogen-bonded

LbL films of block copolymer micelles of poly[2-(N-morpholino)ethyl methacrylate-*block*-2-(diisopropylamino) ethyl methacrylate] (PMEMA-*b*-PDPA) could be successfully deposited at neutral pH and the film dissociation was triggered at either mildly acidic or mildly basic pH. Release from the micellar cores as well as from the surface at acidic conditions was due to dissolution of the micellar cores. However, at basic pH, PMEMA-*b*-PDPA micelles were released from the surface due to ionization of the polyacid component of the film and loss of hydrogen bonding interactions among the layers [71].

1.3.2. Polymer LbL Films Responsive to Biological Stimuli

As described previously, screening or the elimination of the charges on functional groups, or any elimination of the interactions between polymers in LbL films would lead to their dissociation in their aqueous environment. Competitive binding is one of the methods to eliminate the interactions between polymers, and is observed when externally provided molecules make interactions between particular functional groups, thus screen the interactions between polymers that make up the LbL film. Incorporation of moieties that trigger conformational changes in polymers under the influence of biomolecules is the first mechanism of LbL films that are responsive to biological stimuli. Living cells commonly release enzymes in their extracellular matrix (ECM) to design the ECM they live, migrate, and proliferate in. They sometimes release factors as signaling molecules that target integrins in other cells. A great number of studies described the use of natural polymers in LbL films. For example, the presence of natural polysaccharides (such as chitosan, hyaluronic acid, chondroitin sulfate) or protein fibrils, such as collagen type I can be used to build LbL films that are biodegradable, thus sensitive to biological activity [72–74].

In 2008, Levy et al. reported on carbohydrate-sensitive LbL microcapsules composed of PAA and a phenylboronic acid moiety (PAA-BOH). Mannan and PAA-BOH multilayer films were successfully deposited on surfaces in solutions at basic pH (9-11). These films, due to the selective interaction between phenylboronic acid and fructose, mannose, glucose, and galactose, were prone to lose their structure and

dissociate inside polysaccharide-containing solutions. One drawback of these multilayer films was that, they were dissociating at neutral pH and physiological conditions [75], so were not suitable for biomedical applications. To provide carbohydrate-sensitive responses to LbL films at physiological conditions, several groups have tried variety of modifications of LbL films possessing phenylboronic acid moieties. Zhang and coworkers reported on poly(butyl acrylate) (PBA)-PAAm and PVA films which were unable to dissociate at physiolocial pH, unless 5-30 mM glucose was present in the buffer [76]. More rapid film dissolution was observed when PAMAM dendrimers were modified by phenylboronic acid and self-assembled on substrates together with PVA [77].

Polysaccharides are significant examples of biological molecules which can stimulate the dissociation of LbL films. Note that, in biological media which carry all necessary nutrients (e.g. vitamins, metals, and ions) LbL films are prone to degradation or drug release due to the constant non-covalent interactions between these molecules and the polymers that compose LbL films. Most growth media of cell lines for *in vitro* cultures, or the human blood or the body fluid carry sugars and other nutrients which possess variety of functional groups. These functional groups would induce biological molecule aggregation and diffusion in surfaces, while facilitating the interchange of polymers with molecules.

Proteases, nucleases, and enzymes which degrade polysaccharides have been commonly studied in the literature as agents which facilitate the degradation of LbL films. Sukhorukov and coworkers have published several significant articles related with this phenomenon [78,79]. A notable article described the release of DNA from protease-responsive LbL polymer capsules [79]. Such capsules could be successful delivery agents of anti-cancer drugs to tumor sites, where tumor-specific enzymes are released. Recently, Sun et al. described the formation of a hollow LbL capsule made out of synthetic polymers PSS and PAH as multilayers and biological heparin/chitosan layers on top of them. These LbL capsules were prone to degradation by heparinase enzyme and had high loading capacity due to their large size [80].

Enzymes have significant roles as constituents of LbL films. For example, organophosphorus hydrolase is an enzyme produced by organisms for the hydrolyzation of organophosphorus compounds, which are known to have neurotoxic property [81]. Adsorption of organophosphorus hydrolase in chitosan/poly(thiophene-3-acetic acid) was carried out to form organophosphate-sensitive LbL film sensors. These films were called "sensors", because the interaction between organophosphorus hydrolase and poly(thiophene-3-acetic acid) was reduced due to the conformational changes occurred following the enzyme-substrate binding. The reduction in film thickness due to enzyme-substrate complex formation showed the presence of higher enzymatic activity, thus higher concentration of substrate molecules [82].

Another advantage of LbL deposition of polyelectrolytes comes in the development of biosensors and biochips. Micelles of diblock copolymers can induce a homogenous coverage of the template and high number of enzyme molecules can be immobilized on such surfaces. In terms of enzyme immobilization on surfaces, BCMs were found to improve the surface adsorption of enzymes, thus elevating the amount of enzymes, such as tyrosinase and choline oxidase immobilized on surfaces [83]. Qu et al. reported on the modification of a BCM with hemin to impart peroxidase-like activity to it. This modification was a significant example of a nanometer-scale biosensor, without the need of another polymer counterpart for surface immobilization [84].

Streptavidin and biotin are two molecules commonly used in biological experiments, such as chromatography, due to their high affinity towards each other [85]. Inoue et al. reported on the LbL films of streptavidin and 2-iminobiotin-labeled poly(ethylene imine) (PEI). Due to the strong affinity between biotin and avidin, the presence of biotin or analogues triggered a strong interaction between these molecules and the avidin in the film, resulting in the film dissociation [86]. As reported in a review by Takahashi et al., concanavalin A is a lectin-type protein with very high affinity towards variety of sugars. The LbL films that incorporate concanavalin A, due to strong interactions with macromolecules that contain sugars or polysaccharides, were triggered to dissociate easily under the presence of variety of sugars and polysaccharides, such as starch and hyaluronic acid [87].

16

Recently, Sukhishvili and coworkers reported on the bacteria-triggered release of antibacterial agents from surfaces. LbL films of Tannic Acid (TA) and an antibiotic (Gentamicin, Tobramicin, or Polymyxin B) was deposited on surfaces. Due to the protonation of the hydroxyl groups of TA at mildly acidic pH, the dissociation of the LbL film, and thus the antibiotics was triggered once the pH was lower than the physiological pH [88]. As bacteria release acidic side-products due to a variety of biological reactions, the antibiotic release was observed only in the vicinity where bacteria adhered [89].

1.3.3. Temperature-Responsive LbL Films

Temperature-responsive LbL films can be classified into two groups:

1) Films incorporating polymers with upper critical solution temperature (UCST) behavior

2) Films incorporating polymers with lower critical solution temperature (LCST) behavior

The LCST and UCST behavior can be imparted to LbL films through the incorporation of thermoresponsive polymers into the films. Poly(N-isopropylacrylamide) (PNIPAAm) has been the most commonly studied polymer, due to its LCST-based behavior close to normal body temperature. PNIPAAm displays lower critical solution temperature (LCST) at 32°C. Above its LCST, conformational transition from extended to globular coil is observed resulting in loss of hydrogen-bonding interactions among PNIPAAm and water molecules, followed by phase separation of the polymer from its aqueous solution (Scheme 1. 4.) [34]. In case of LCST multilayers, film collapsing could be observed at physiological conditions. Steitz et al. was the first to use PNIPAAm in LbL self-assembly [90] Glinel et al. coated polystyrene latex or melamine formaldehyde nanoparticles using PSS-PNIPAAm and PDEAEMA-PNIPAAm copolymers in a LbL fashion [91]. In this system electrostatic interaction was the primary force that drived the capsule formation and the variation

of temperature was thought to induce the variations in morphology and permeability of capsules due to LCST-type phase behaviour of PNIPAAm.
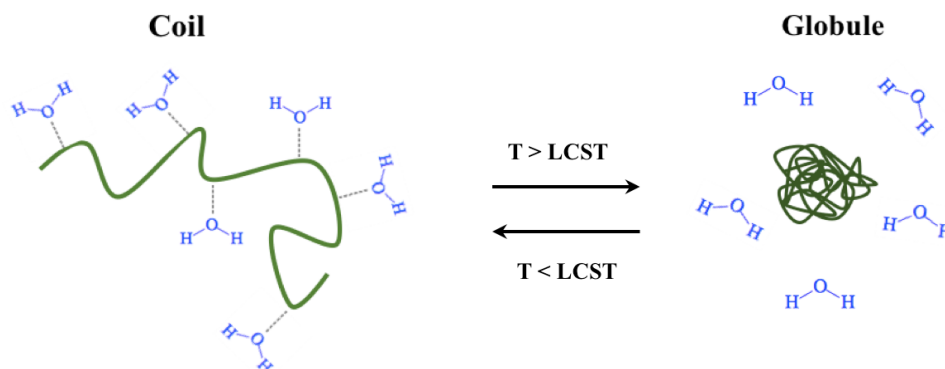
Scheme 1. 4. Schematic representation of the coil to globule transition of a polymer which possesses LCST-type phase behavior (Image modified from Phillips et al., 2015) [92].

Similar to PNIPAAm, poly(2-alkyl-2-oxazoline)s with short alkyl chain on the pendant groups are also water-soluble and express temperature responsive behaviors [93,94]. Poly(2-alkyl-2-oxazoline)s, can also be called as pseudo-peptides as they are structural similarity to polypeptides [95]. In addition, similar to poly(ethylene glycol) (PEG), poly(2-alkyl-2-oxazoline)s possess water-binding properties and can be used to functionalize surfaces to make them anti-adhesive [96]. Very recently, our group has reported on the pH and temperature-induced release of doxorubicin (DOX) from poly(2-isopropyl-2-oxazoline) (PIPOX) and Tannic Acid based LbL films. This study showed that, LbL films of PIPOX/TA, once at physiological temperatures could release higher amount of DOX, compared to the amount at room temperature. This was reported to be due to LCST behavior of PIPOX and increased kinetic energy of DOX molecules and PIPOX at higher temperatures [97].

LbL thin films of thermoresponsive polymers were also studied by Quinn and Caruso. Multilayer thin films of PAA and PNIPAAm were successfully fabricated and the temperature of fabrication showed effect on the film growth. The thickness of the film

was reported to be higher as solution temperatures were increased from 10°C to 21°C and to 30°C, most probably due to conformational changes in polymers and reduction in the water solubility of PNIPAAm. Similarly dye release kinetics were effected by temperature. At higher temperatures, encapsulated dye (Rhodamine B) in films was released from the films in a shorter time compared to the situation at room temperature due to the phase transition of PNIPAAm [98]. A significant amount of work on microcapsules of LbL films consisting of thermoresponsive polymers, e.g. PVPON, poly(N-vinylcaprolactam) (PVCL), and poly(N-isopropylacrylamide) (PNIPAAm) and tannic acid (TA) was carried out by Tsukruk and coworkers [52,53] and Sukhishvili and coworkers [99]. The main driving force for the assembly of these films was the hydrogen-bonding between TA and the thermoresponsive polymers. Temperature-responsive permeability of PMAA/PVME and PMAA/PVCL multilayers was reported by Kharlampieva et al. in 2005. According to this study, the reason behind enhanced permeability of LbL films at temperatures close to or above the LCST was the appearance of voids in the films due to temperature-induced conformational changes in the polymer chains. This was reported to be the reason for the permeability of dyes at higher rates under temperature above LCST of polymers [100].

LbL films was also shown to exhibit thermal transitions at higher degrees, even though specific thermoresponsive polymers with LCST or UCST behavior were not incorporated in films. Lutkenhaus and coworkers reported that two strong polyelectrolytes, PDAC and PSS can exhibit thermal transition at 49-56°C to a glassy state. At lower degrees, the glassy state can transit to a rubbery state, releasing loaded compounds (cargo) out from layers [101,102].

Studies on temperature-responsive hydrogels have been published for decades, but coating surfaces with temperature-responsive polymers is relatively new. Since early 90's, building hydrogels with temperature-response relied primarily on the use of poly(N-isopropylacrylamide) (PNIPAAm) or its copolymers [103]. PNIPAAm displays lower critical solution temperature (LCST) at 32°C, thus a transition of solubility in aqueous media at lower temperatures to insolubility and phase separation

at higher temperatures than this degree [34]. Due to its LCST behavior, crosslinked PNIPAAm hydrogels swell at low temperatures but can collapse suddenly once placed under temperatures above 32°C, such as the normal body temperature [103]. This makes the hydrogel release the bound water, thus the drugs within it, once the hydrogel is placed inside the body. Similarly, BCMs with thermoresponsive groups have been designed for drug encapsulation and release [104,105], primarily composed of PNIPAAm copolymers, but exceptions exist [106,107].

The first LbL self-assembled polyelectrolyte microgel thin film with temperature response was established by Serpe et al. in 2003. This report demonstrated the deposition of the microparticles of poly(*N*-isopropylacrylamide-*co*-acrylic acid) with poly(allylamine hydrochloride) (PAH) polymer counterpart at room temperature on surfaces [108]. Hydrogels do not possess some of the physical properties that could be essential in biomaterial science, such as toughness or rigidity. Therefore, surface modification of bulk materials with microgels of thermoresponsive polymers established the temperature-responsive release of drugs from materials without conceding the properties of the bulk material.

1.3.4. Light-Responsive (Photosensitive) LbL Films

Light responsiveness (photoresponsiveness) of multilayer thin films can be achieved through several pathways:
- encapsulated metal nanoparticles in multilayer films
- encapsulated metal oxide nanoparticles in multilayer films
- multilayer films with azobenzene-containing surfactants

Responsive behavior of metal nanoparticle to the visible light makes them highly advantageous in terms of biological applications [109]. After optical irradiation, metal nanoparticles (e.g. gold nanoparticles) due to Surface Plasmon Resonance (SPR) undergo lattice rearrangement and heating, which is the driving force for drug release or reduced interaction with surrounding polymers. Metal nanoparticles also emit fluorescence under light, which could be useful in detection in diagnostic applications

20

[110]. When it comes to medical therapy, light can be a very advantageous stimulus once nano- and micro-particles reach a target destination. Light-responsive microcapsules have been thoroughly studied in biomedical sciences. Palankar et al. developed polymeric microcapsules that were deposited on gold nanoparticles for the delivery of peptides onto Chinese hamster ovary (CHO) cells and used the thermoresponsive property of gold nanoparticles during the development of hollow capsules [111]. In 2007, Bedard et al. designed microshells that can shrink under UV light, due to the presence of azo-groups in one of the polymers that are present in the capsule. In 30 min., 27% surface area loss was achieved in the capsules, causing extensive shrinkage and release of the cargo [112]. Azo-groups undergo conformational changes when triggered with light, and can release heat. In this study, heated capsules did not undergo shrinkage, which could mean that the mechanism was only dependent on the conformational changes upon excitation with light.

The light-responsiveness of LbL films can also be activated through the presence of inorganic nanoparticles (e.g. CdS) [113] and molecules which undergo transition under several wavelengths of the light. As reported by Zhu and McShane, novel photosensitive diazo resins can be incorporated into LbL films to impart light-responsiveness to them [114]. The interaction between diazo resins and PSS is weak once the LbL is assembled, but then as the UV-light is applied on the system, inducing covalent-bond formation between diazo resin and PSS. Covalent bonds induce compact film formation thus, small molecules such as glucose oxidase and peroxidase can be released. Dissociation of dye aggregates from LbL films is another mechanism for the light-responsiveness of films As described by Tao and Möhvald, LbL films built up by alternating deposition of PSS/PAH and PDDA/azo dye can become permeable to polysaccharides under visible light. Near-infrared light (NIR) has shown great promise in biomedical sciences due to the weak absorption of the light by tissues. As described by Caruso and coworkers, LbL films of PSS and PAH were successfully deposited on gold nanoparticles. FITC-dextran was loaded in the films of the capsules under mildly acidic conditions, due to the permeation of the film under these conditions. As gold can absorb light energy and release heat, the driving mechanism in LbL film dissociation would be the conformation change in the polymers upon the

heat formation in the nanoparticle with NIR pulses, or the complete dissociation of the film due to extreme temperatures occurring on the gold nanoparticle [115]. Due to the formation of azo dye aggregates inside the films, visible light triggered the dissolution of these dye molecules, allowing dextran to penetrate inside films [116].

1.3.4.1. Light-Responsive BCMs

LbL films can incorporate BCMs with variety of response to environmental stimuli. One another stimuli is light. A block copolymer is regarded as light-responsive when it contains a light-responsive group at the side chain, the main chain, or at the block junction [117]. Light can induce the drug release from block copolymer micelle cores reversibly or irreversibly [118].

Trans-cis photoisomerization of nitrogen double bonds is the primary force driving the shifts in the polarity of photocrosslinkable groups. For example, azobenzene groups that are present in the core-forming group of a BCM, once activated by UV light, conversion to the *cis* form is observed, which is more polar compared to the molecule's *trans* form. This shift increases the hydrophilicity of the core-forming block of the BCM, thus causing the stimulus for the release of encapsulated hydrophobic compounds. This property of azobenzene was studied by Wang et al. in BCMs [119]. Basically, azobenzene-poly(methacrylate) (PAzoMA)-*b*-PAA BCMs with the core-forming azobenzene polymethacrylate block was able to go into demicellization under UV light, but micellization was reversed once the block copolymer was treated with visible light.

1.3.5. Magnetic Field-Responsive LbL Films

Magnetic field trigger is either dependent on the heat emission of superparamagnetic compounds that are in contact with polymers [120], or on the oscillatory motion of the particles under an applied frequency [121]. The temperature response of the multilayer films is achieved primarily due to heat emitted by metal nanoparticles which then induces conformational changes in the temperature-responsive polymer. For example,

one significant study by Katagiri et al. described that melaimine formaldehyde particles can be LbL coated by PSS and PAH. Magnetite (Fe_3O_4) was immobilized on these nanoparticles and the nanoparticle cores were removed. The irradiation of hollow capsules triggered a temperature increase and release of loaded cargo inside the capsule [122].

Other than the magnetothermal response, Lvov and coworkers described that ferromagnetic gold-coated cobalt nanoparticles, when coated with PSS and PAH LbL shells can build nanoparticles with magnetic field-responsive cargo release. The reason behind the cargo release under magnetic field was due to the ferromagnetic property of the nanoparticle core. Gold-coated cobalt nanoparticles, when under magnetic field, oscillate and twist, thus agitate the surrounding thin film and cause it to change conformationally. This conformational change was thought to be the driving force behind the cargo release from nanoparticles [123]. The mechanisms of the release of cargo molecules from LbL film coated magnetic nanoparticles can be seen in Scheme 1. 5.
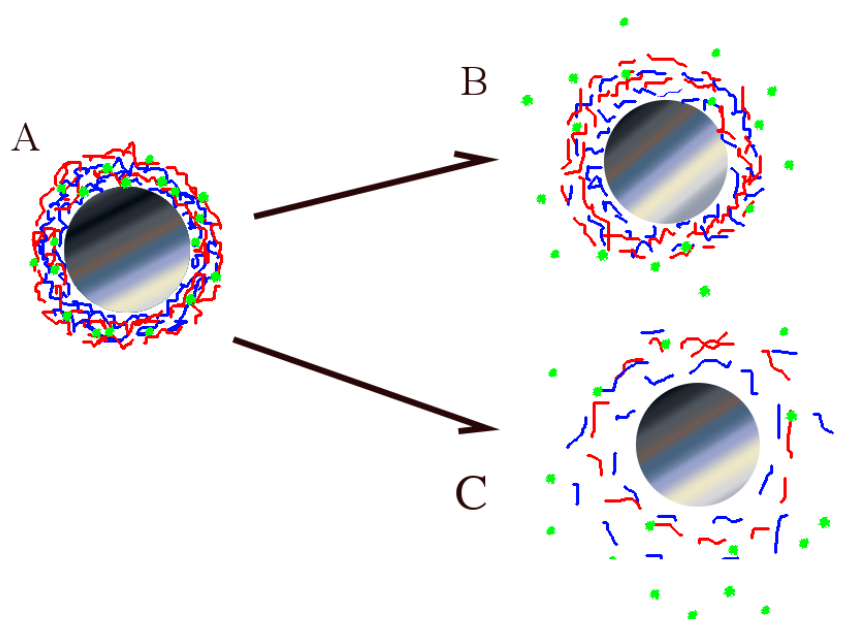
Scheme 1. 5. Schematic representation of a nanoparticle with magnetic-field responsive metallic core and LbL film deposited onto it (A). The applied magnetic

field can conformationally change the polymers in the LbL film, triggering the release of drugs (B), or trigger the dissocation of the LbL film, thus the drugs.

1.4. Biomedical Applications of LbL Films

Therapeutic nanomaterials created a broader perspective on how we deal with medical problems. The last two decades, researchers came up with brand new ideas of medical diagnostics and therapy by using nanomaterials that can target specific tissues. Although BCMs can be designed to target specific antigens, carry varying charges or be responsive to variable environmental stimuli, they are prone to dissociation once the micelle concentration goes below to the critical value upon dilution when injected in the body. Another disadvantage of BCMs is that they interact with other molecules around the target tissue or the blood stream. Such interaction of BCMs with surrounding molecules could mask them and hinder their property to target tissues or have controlled release. It could even affect their characteristic structure.

LbL deposition of micelles as ultrathin films brought the possibility of preventing micelle dissociation in the blood stream [66]. This has made micelles possible to circulate in bloodstream for extended periods of time without losing any of their loaded agent. Some biomaterials are designed to carry drugs in the human body for treatment purposes and LbL films have advantages on carrying genetic materials (such as DNA and siRNA) and circulating them in the blood stream for prolonged durations and target them to the desired cells. In this respect, BCM-containing LbL capsules have been of interest in recent years. One significant report showed that, block copolymer micelles could be deposited onto silica nanoparticles for the prevention of the BCM against environmental factors, or for triggering the targeting of the nanoparticle to specific locations in the human body, such as the tumor area [124]. This report showed that pH-responsive poly(oligo(ethylene glycol) methacrylate)-*block*-poly(2-diisopropyl aminoethyl methacrylate) (POEGMA–PDPA) micelles could be loaded with plasmid DNA. Just below the pK_a value of PDPA, the block is positively-charged, thus can undergo electrostatic interaction with DNA. The outermost shell of the micelle-deposited silica core particle was composed of tannic acid/poly(N-vinyl

pyrrolidone)/tannic acid (TA/PVPON/TA) LbL film respectively. The middle layer between the core nanoparticles and the LbL film was the micelles. Micelles could release plasmid DNA (pDNA) at pH 5, which corresponds to the pH of endosomes in cancer cells. Such polymersomes could additionally carry two different anti-cancer agents which target two different pathways, for the purpose of dual-drug delivery directed to the tumor area.

1.4.1. Anti-Adhesive and Antibacterial LbL Films

Superhydrophobic or superhydrophilic surfaces repel charged molecules that can potentially interact with the surface. On a hydrophobic surface, there is only an indefinite interaction with aqueous-based molecules with the surface. On the other hand, on hydrophilic surfaces, strong interaction with the water molecules in an aqueous system is observed. In biological studies, anti-adhesiveness is desired to overcome the adherence of organisms on the surface of a material building a tough structure, so called "biofouling". Anti-biofouling films are generally made out of superhydrophobic surfaces, which can repel the water and any microorganism in the water, or superhydrophilic surfaces, so that the surface can bind so much water that microorganisms do not even find the chance to adhere to.

The biofouling of microorganisms is observed primarily as a form of biofilm. Biofilms are primarily composed of polysaccharides that are secreted by the bacteria, providing a safe and strong extracellular environment for them to live and proliferate in. The most important property that a polysaccharide biofilm provides to bacteria is improved resistance to antibiotics. Even though bacteria are not resistant to a particular antibiotic, biofilms could provide the barrier in which antibiotics cannot penetrate inside, thus they are unable to kill the bacteria [125]. If a surface is antibacterial or anti-adhesive against bacteria, biofilm formation is eliminated or postponed. A combination with the surface anti-adhesiveness and antibiotic release from the surface or from outside the surface could eliminate the biofilm formation. This could reduce the number of hospitalized people around the world due to bacterial infections.

Grafts or sutures are commonly used biomaterials which provide support to tissues in the body during their regeneration or completely take on the function of a tissue, but they are always prone to bacterial accumulation. Anti-adhesiveness could prevent and postpone the biofilm formation on such biomaterials, spreading the area use of biomaterials by patients and increasing the number of cases of biomaterial production for clinical studies [126]. More information on bacterial anti-adhesive LbL films can be found in the first section of this thesis.

Antibacterial LbL films can be designed in two methods:
1) Loading antibiotics or antibacterial agents inside films
2) Using synthetic or natural polymers with contact killing properties

As previously mentioned in this section, LbL films can either release cargo through diffusion, or through response to environmental stimuli. Once antibiotics or antibacterial agents are loaded in LbL films, they can be released by diffusion, or by a variety of stimuli that triggers the antibiotic release only, or the dissociation of the whole film. As reported by Hammond and coworkers, sequential release of an antibiotic (Gentamicin) and a growth factor (recombinant human bone morphogenetic protein-2) (rhBMP-2) was possible through the hydrolytic degradation of the polymers in the LbL film. Poly(β-amino esters) were incorporated in these LbL films to render them hydrolytically degradable. The rate of release of the agents was tuned through incorporating bilayers of chitosan and laponite in the LbL film, through an addition of an interrupting film between the layers that contain rhBMP-2 and Gentamicin, and a covering film that is the outermost layer [127].

Bacteria can be killed through contact with natural or synthetic polymers, due to the presence of specific functional groups in these polymers. Fu et al. reported on antibacterial LbL films of heparin and chitosan, which were biocompatible and biodegradable. The protonated amino groups of chitosan, when in contact with the negatively-charged bacterial cell wall, conformationally affects the bacterial cell wall, causing it to leak. Similarly, chitosan-bearing LbL films possess contact killing against bacteria [128,129]. Synthetic polymers on surfaces of LbL films also possess contact

26

killing properties. As reported by Rubner and coworkers, [3-(trimethoxysilyl)propyl]octadecyl-dimethylammonium chloride (OQAS), which bears a quaternary ammonium salt structural unit coupled with a long hydrophobic alkyl chain (C_{18}), interacts with bacterial cell walls and trigger the cytoplasmic leak to kill them [129].

Another method to prevent biofouling on surfaces through LbL films is to coat surfaces with bio-inert or low-fouling polymers. PEG has been the keystone of low-fouling polymers as PEG creates a hydration layer which prevents adhesion [130]. Due to the same mechanism, polyzwitterions also found applications on surfaces to provide anti-adhesive films. One of us has reported on the monolayer of poly[3-dimethyl (methacryloyloxyethyl) ammonium propane sulfonate-*b*-2-(diisopropylamino)ethyl methacrylate] (βPDMA-*b*-PDPA) BCM as a potential anti-adhesive surface against bacteria [131].

LbL films can be designed to be dually-sensitive, such that they repel bacteria and kill them through the release of antibacterial agents. Electrostatic interactions between polymers of cationic and anionic functional groups drive the force in LbL buildup, but this interaction is not limited with the functional groups with one single charge. Recently, our group pioneered the research on incorporating BCMs with zwitterionic coronae-forming blocks in LbL films. Due to the pH-responsive PDPA core of βPDMA-*b*-PDPA, when the core is loaded with an antibacterial agent (triclosan), the agent could be released in mildly acidic media, due to the protonation of tertiary amine groups in the micelle core. This block copolymer micelle was also designed to be stable under physiological pH, making the micelle and the film suitable for biomedical applications [132]. Such drug loaded micelles release cargo in a shorter time around the tumor sites or the infection sites in the body, where products of anaerobic respiration could decrease the pH in the zone of 6 - 6.5.

1.4.2. Bioactive LbL Films

Bioactive thin films activate a biological response from particular cell lines or particular tissues of organisms. These responses could be the increase in metabolic activity, differentiation towards a lineage, proliferation of cells and thus the regeneration of tissue. It can also be any other upregulation or downregulation of genetic expression to suppress or induce a metabolic pathway, such as for the ones for the secretion of proteins and related globular structures from the cells.

As cells live and proliferate inside their extracellular matrix (ECM), they bind and interact with the ECM components, mainly through integrins and adhesins. This binding activates a cascade leading to several genetic regulations, and even differentiation of stem cells or progenitor cells to primary cells. When modifying surfaces, it is important to modify the surface such that the components of the surface are biological macromolecules such as collagen, fibrinogen, and hyaluronic acid [73,133,134] or synthesized polymers which mimic the ECM components [72].

Growth factors possess important functions in stem cell differentiation to primary cells and regeneration of tissues. Due to the presence of charged amino acids in these large proteins, they can interact with oppositely-charged polymers in thin films. They can also make polymer complexes and can be delivered into the body without further modifications. Also, they can be deposited on surfaces. Stimuli-responsive growth factors delivery under different stimuli is possible once growth factors are loaded inside LbL films. In 2005, Mao et al. reported on fibroblast growth factor (FGF)-heparin mixture/poly(ethylene imine) (PEI) multilayer films which induced collagen type I secretion and proliferation of fibroblasts seeded onto the coated surface [135]. Hammond and coworkers designed LbL films which elute growth factors through biodegradation of poly(βamino esters), followed by the disintegration of multilayers. Such growth factors released from the films of poly(β-amino esters) and chondroitin sulfate and induced bone tissue regeneration on bone defect sites [136,137]. These LbL films were also doped with hydroxyapatite to provide osteophilicity to the film, again to be used for bone tissue regeneration [134]. Recombinant human bone

morphogenetic protein-2 (rhBMP-2) induces osteogenic differentiation of mesenchymal stem cells and preposteoblasts into osteoblasts. They are secreted by osteoblasts to signal surrounding cells to differentiate. Picart and coworkers demonstrated rhBMP-2 release from LbL films composed of PLL and hyaluronic acid. In one of their study, C2C12 cells, which are myoblasts with ability to differentiate into an osteoblastic lineage, were observed to differentiate into osteoblasts by the release of rhBMP-2 from surfaces [72]. LbL thin films, in terms of growth factor release are suitable structures for the tenability of agent throughout the film, and also suitable structures for the control of the amount of the released agent.

1.5. Hydrogels for Biomedical Applications

Biodegradability is the ability of a biomedical device or a tissue scaffold or matrix to perform its intended functions successfully for a desired period through incorporation to the host local or systemic reactions in the body. Biocompatible scaffolds need to sustain cellular activity and optimize tissue regeneration [138]. Hydrogels for biomedical applications need to be biocompatible and this biocompatible property is Organisms on Earth are primarily composed of carbon-based molecules though they intake and retain very high amounts of water. Water is an inorganic molecule, thus not produced by the human body and should be replaced when lost. Water is the primary solvent in the human body, is the primary factor that stabilizes the osmotic pressure of cells, maintains the body temperature and brings excretions out [139]. As water is the most abundant inorganic molecule in the mammalian body, materials that intake and retain high amounts of water would be very suitable for biomedical applications. Hydrogels are networks of natural and synthetic polymers that absorb (at least) 10-20% or their weight as water. Examples are known to absorb water w/w in the level of thousands of times more than their original weight. High water content in hydrogels is the reason why hydrogels have been of great use in biomedical sciences since especially 70's [140,141].

Hydrogels are held together due to molecular entanglements or forces exerted between molecules, such as hydrogen-bonding, hydrophobic, and ionic forces [142,143].

Hydrogels are only permanent and stable when their polymers are covalently-crosslinked. This crosslinking can be achieved either by copolymerization with a crosslinker [144], or by the addition of water-soluble crosslinkers such as glutaraldehyde [145] and sodium periodate [146]. Cross-links among the polymer chains of hydrogels render them stable for long periods, making possible to be used for biomedical studies such as tissue engineering.

Hydrogels have found broad range of applications in biomedical sciences. This includes drug release and controlled drug release, scaffolds for tissue engineering, cell carriers, fillers, membranes, sheets, and wound dressings. An article published in 1980 showed that hydrogels had resolved one important issue related with immune rejection of pancreatic islet transplantation, which was the rejection of the implanted islet by the pancreas. PLL/sodium alginate hydrogels that were crosslinked with calcium chloride were able to encapsulate pancreatic islet cells, reducing the immune reaction after implantation, without any loss in insulin secretion by cells [147].

Collagen and shark cartilage were two of the first natural molecules that were used to design cell-carrying hydrogels as wound dressings [148]. Chitin and chitosan, cationic polysaccharides owing to their ability to induce skin regeneration, and prevent bacterial and fungal infections have been commonly used in hydrogels to prepare dressings to repair severe burns [149]. One ideal wound dressing should support the penetration of gases through the material, protect the covered tissue from microorganisms, physically support the tissue and provide the environment in which cells can regenerate and repair the defect [150]. Thus, chitosan, alginate and derivatives can be considered as ideal materials to prepare hydrogels as wound dressings.

Chemical nature of the hydrogel material is critical for drug release properties. Polyesters such as poly(glycolic acid) (PGA) and poly(lactide-*co*-glycolide) (PLGA) are biodegradable, thus degrade under the activity of enzymes in the body, or by hydrolysis and oxidation. This degradation induces the release of the drug molecules as bonds are broken from the polymers of the hydrogel and smaller molecules are set

free. As reported by Jeong et al., PEG-PLGA-PEG triblock copolymers form hydrogels at body temperature. This gelling at body temperature was reported to be due to micellar growth and intra- and inter-micelle phase mixing and packing. As the PLGA block is hydrolytically degradable, it enhanced the hydrogel to be biodegradable in body [151,152]. Similarly, oligo(poly(ethylene glycol) fumarate) hydrogels gellate at body temperature and are biodegradable. As reported by Mikos and coworkers, transforming growth factor-β1 (TGF-β) release was controlled with the polymer molecular weight and the degree of crosslinking [153].

One important field of application of hydrogels is tissue engineering and regenerative medicine. Biocompatible hydrogels, due to their physical similarities to extracellular matrices, and ability to deliver cargo such as growth factor, drugs, or cells are one of the materials that can be used in tissue engineering [154]. Hydrogels can be designed to possess pores that can perfectly accommodate cells once seeded. One disadvantage is that these pores are not connected through channels, which are essential for cells to communicate with each other. For example, collagen scaffolds with ceramic particles as porous scaffolds found place in the literature couple of times [155–157]. Hydrogels are suitable injectable materials for tissue regeneration, proved by a large number of studies. For example, hydroxyapatite-collagen with alginate which carried BMP-2 showed successful results as a bone filler. The material was able to get crosslinked by itself at the site of injection, at around 30 min [158]. Modification of PEG and PVA with the cell-adhesion peptides even enhanced the tissue engineering applications of hydrogels, making cells adhere into and interact with the hydrogel, such that they do with their extracellular matrix (ECM) [159,160]. Hydrogels are not only useful in bone tissue engineering, they can also be used as matrices for epithelial cell cyst formations once their surfaces is modified. Recently, Enemchukwu et al. described that epithelial cells form cysts in hydrogels possessing optimal range of elasticity, optimal amount of adhesive peptide density, and a threshold level of protease degradability like they do in their native ECM [161].

1.5.1. Stimuli Responsive Hydrogels

1.5.1.1. pH-Responsive Hydrogels

Stimuli responsive hydrogels release the loaded drug molecules by changing environmental stimuli, such as pH and temperature. For example, pH responsive hydrogels control drug release through a determined swelling and de-swelling mechanism induced by protonation/deprotonation of functional groups or higher or lower interaction with water molecules [162] (Scheme 1. 6.). Hydrogels of synthetic polymers, such as poly(acrylamide-*co*-maleic acid) [163] or synthetic-natural polymer hybrids [164], such as PEO-chitosan exhibit pH responsive behavior, due to the protonation or deprotonation of charged functional groups on polyions, which lead to higher swelling.
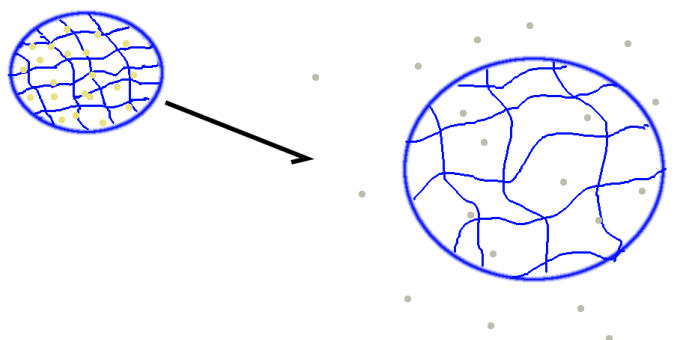
Scheme 1. 6. The swelling of the hydrogel induces the release of cargo molecules trapped inside the hydrogel.

1.5.1.2. Temperature-Responsive Hydrogels

Similarly, temperature responsive hydrogels are composed of temperature-responsive polymers. PNIPAAm [165] or its derivatives have been extensively investigated to prepare temperature-responsive hydrogels. Several studies recently have shown that solutions of polymers can gel at physiological temperatures. When such polymer

solutions are injected in defected tissues in the human body, they fill the defect, and then form the hydrogel by temperature-responsive gelation. Very recently, Payne et al. described that methycellulose/β-glycerophosphate hydrogels can form at 39°C, but with an addition of collagen, this degree can be decreased to 37°C, which is the body temperature [166]. Wagner and coworkers reported on biodegradable copolymer hydrogels with thermoresponsive property. These hydrogels which are made up of N-isopropylacrylamide (NIPAAm), acrylic acid, and hydroxyethyl methacrylate-poly(trimethylene carbonate) (HEMAPTMC) were able to form hydrogels at 37°C and degrade slowly inside the body in about 5 months. This was an attractive hydrogel designed specifically for the treatment of ischemic cardiomyopathy [167].

1.5.1.3. Light-Responsive Hydrogels

Light is another environmental stimulus which triggers hydrogels to conformationally change and swell. For example, hydrogels with triphenylmethane units (e.g. triphenylmethane leucocyanide) can swell in the presence of UV-light. The photodissociation of triphenylmethane to triphenylmethane cations and cyanide anions increases the ion concentration inside the hydrogel and the increased osmotic pressure causes more water molecules to penetrate into the gel and force it to swell [168]. Azobenzene molecules can be triggered to shift from *trans* isomer to cis isomer as UV light is applied. Presence of cyclodextrins that can associate with the trans isomer of azobenzene can form hydrogels. As the UV light is applied, the hydrogel dissociates to form a solution, due to reduction in cyclodextrin-azobenzene associations [169].

1.5.1.4. Magneto-Responsive Hydrogels

One another class of stimuli-responsive hydrogels is magneto-responsive hydrogels. For example Bhattacharya et al. reported on the microgels of poly(vinylcaprolactam-*co*-acetoacetoxyethyl methacrylate-*co*-vinylimidazole) (PNVC-*co*-PAAEM-*co*-PVIm) with BIS cross-linker. These polymers with thermosensitive PVCL units and pH-sensitive PVIm units exhibited pH and thermoresponsive behaviour. The most significant factor that modifies the phase transition temperature of the hydrogel is the weight fractions of PVIm

and PAAEM. At pH of 4 or lower, the PVIm was protonated, thus causing swelling and shifting the LCST higher. These protonated hydrogels were used as the templates of magnetic nanoparticles, which shifted the volume phase-transition temperature to higher values. These hybrid materials possess multiple response behaviour, to temperature, pH, and magnetic fields and they can be used in controlled and targeted drug release studies [170].

1.5.2. Surface Functionalization of Hydrogels

Even though hydrogels have a broad range of applications in biomedical sciences, primarily due to their water-binding abilities, the bulk biomaterial do not always possess all of the properties of a suitable biointerface. Cells that interact with the hydrogel would need to be able to adhere to the hydrogel and proliferate or differentiate on it. This interaction would be highly necessary for the regeneration of a defected tissue. As described in the previous section, adhesive proteins or growth factors can be loaded inside scaffolds to induce tissue regeneration, though a high amount of growth factor released from the scaffold could have off-target effects in organisms. Besides, they would be cost-effective. Modification of the hydrogel properties (e.g. by blending or crosslinking with other molecules) could reduce its properties, such as elasticity, or water-binding ability. The surface modification of a hydrogel would be sufficient to impart functions to the core hydrogel without physically modifying it.

Recently, Yesilyurt et al. reported on the coating of alginate hydrogel microspheres using zwitterionic phosphorylcholine polymers. This surface modification significantly reduced foreign body responses and fibrosis in the body [171]. Sanyasi et al. reported that the surface modification of tamarind kernel polysaccharide-based hydrogel using acrylic acid induces the osteogenic differentiation of mouse preosteoblasts [172]. In 2015, Grossutti et al. reported on modification of a hydrogel through coating. Coating the hydrogel surface with a hydrophobic phospholipid decreased the surface hydrophilicity and acted as a barrier, controlling the permeability of the bulk material [173].

1.5.2.1. Surface Functionalization of Hydrogels via the LbL Technique

Biomedical applications of LbL coated hydrogels have found significant place in the scientific literature (Scheme 1.7.). Sakaguchi et al. reported on the LbL deposition of dextran sulfate and chitosan on poly(vinyl alcohol) hydrogels [174]. This report was the first example of the LbL deposition of natural polymers on hydrogels. Grossin et al. further reported on a relatively opposite method where PLL/PGA and (PLL-hyaluronic acid)/PLL multilayers were deposited separately on a surface, and then the hydrogel that was loaded with fibroblasts were spray-deposited on them. This system was designed to investigate the biological activity of cells in hydrogels that were in direct contact with multilayers [175]. Mehrotra et al. developed LbL coated porous agarose hydrogels with alternating PAA/PEG and protein/PEG multilayers for time-controlled release of proteins [176]. In these LbL films, one of every two layers was PEG, and the remaining layers were PAA and the protein, respectively. Additional to these, Choi et al. reported on coating bPEI/TA and PDAC/lignin LbL films on collagen hydrogels to increase the strength and toughness of the hydrogel core and to prevent the burst release of an anti-cancer agent out of the hydrogel core [177].Very recently, Gentile et al. reported on deposition of PSS/PAH films doped with a specific peptide and transforming growth factor-β1 (TGF-β1) onto alginate microgels. These functionalized hydrogels were found to be ideal biomaterials to be used for chondrogenic tissue regeneration [178].

Bare hydrogel   LbL-coated hydrogel

Scheme 1. 7. Schematic representation of a bare hydrogel and LbL coated hydrogel.

1.6. Aim of the Thesis

The aim of this thesis study was to prepare functional LbL coatings which may find use in various biomedical applications, specifically in preparation of anti-adhesive and antibacterial surfaces; osteoconductive surfaces and wound dressings.

The work presented in Chapter 2 aimed preparation of dual functional LbL films which exhibit bacterial anti-adhesiveness and pH-responsive antibacterial agent delivery from surfaces to reduce hospital-acquired bacterial infections. In this context, bacterial anti-adhesiveness was aimed to be achieved by controlling the surface chemistry and pH-responsive release of an antibacterial agent was aimed to be achieved by using block copolymer micelles with pH-responsive polybasic cores as building blocks and cargo carrier in LbL assembly.

The work presented in Chapter 3 aimed preparation of LbL films which conducts bone tissue formation by SaOS-2 osteoblast-like cells. Conducting bone formation was aimed to achieve by constructing a LbL assembly based on a biodegradable polymer whose degradation products were expected to induce osteogenic differentiation. Our hypothesis was that poly(4-hydroxy-L-proline ester) (PHPE), which comprises trans-hydroxyproline resembles collagen, which is the dominant organic compound in the bone. In this context, osteogenic differentiation of osteoblast-like cells was aimed to be achieved through the induction of collagen synthesis by the cells, thorugh the treatment of the cells with PHPE.

The work presented in Chapter 3 aimed preparation of LbL modified chitosan/PEG membranes with enhanced antibacterial and cell adhesive properties for potential wound healing applications. Antibacterial activity was aimed to be enhanced by modifying the hydrogel surfaces using antibiotic incorporated temperature-responsive multilayer films via LbL technology. Cell adhesive property of the hydrogels was aimed to be enhanced by LbL coating the hydrogel surface to diminish the suppression of the proliferation of fibroblasts adherent on chitosan/PEG hydrogels.

1.7. References

[1]   J.A. Zasadzinski, R. Viswanathan, L. Madsen, J. Garnaes, D.K. Schwartz, Langmuir-Blodgett films, Science (80). 263 (1994) 1726. doi:10.1126/science.8134836.

[2]   D.S. Ginger, H. Zhang, C.A. Mirkin, The Evolution of Dip-Pen Nanolithography, Angew. Chemie - Int. Ed. 43 (2004) 30–45. doi:10.1002/anie.200300608.

[3]   W. Knoll, Self-assembled microstructures at interfaces, Curr. Opin. Colloid Interface Sci. 1 (1996) 137–143. doi:10.1016/S1359-0294(96)80054-9.

[4]   K. Ariga, J.P. Hill, Q. Ji, Layer-by-layer assembly as a versatile bottom-up nanofabrication technique for exploratory research and realistic application, Phys. Chem. Chem. Phys. 9 (2007) 2319. doi:10.1039/b700410a.

[5]   G. Decher, J.D. Hong, Buildup of ultrathin multilayer films by a self-assembly process, 1 consecutive adsorption of anionic and cationic bipolar amphiphiles on charged surfaces, Makromol. Chemie. Macromol. Symp. 46 (1991) 321–327. doi:10.1002/masy.19910460145.

[6]   G. Deeher, J.D. Hong, Buildup of ultrathin multiplayer films by a self-assembly process. II. Consecutive absorption of anionie and cationic bipolar amphiphiles and polyeleetrolytes on charged surfaces, Ber Bunsen-Ges Phys Chem. 95 (1991) 1430–1434. doi:10.1002/bbpc.19910951122.

[7]   G. Decher, J.D. Hong, J. Schmitt, Buildup of ultrathin multilayer films by a self-assembly process: III. Consecutively alternating adsorption of anionic and cationic polyelectrolytes on charged surfaces, Thin Solid Films. 210–211 (1992) 831–835. doi:10.1016/0040-6090(92)90417-A.

[8]   S. Schwarz, K.J. Eichhorn, E. Wischerhoff, A. Laschewsky, Polyelectrolyte adsorption onto planar surfaces: A study by streaming potential and ellipsometry measurements, in: Colloids Surfaces A Physicochem. Eng. Asp.,

(1999) 491–501. doi:10.1016/S0927-7757(99)00289-7.

[9]   W.B. Stockton, M.F. Rubner, Molecular Layer Processing of Polyaniline via the Use of Hydrogen Bonding Interactions, MRS Proc. 369 (1994) 587. doi:10.1557/PROC-369-587.

[10]   W.B. Stockton, M.F. Rubner, Molecular-Level Processing of Conjugated Polymers. 4. Layer-by-Layer Manipulation of Polyaniline via Hydrogen-Bonding Interactions, Macromolecules. 30 (1997) 2717–2725. doi:10.1021/ma9700486.

[11]   Y.Y. Sung, M.F. Rubner, Micropatterning of polymer thin films with pH-sensitive and cross-linkable hydrogen-bonded polyelectrolyte multilayers, J. Am. Chem. Soc. 124 (2002) 2100–2101. doi:10.1021/ja017681y.

[12]   X. Tuo, D. Chen, H. Cheng, X. Wang, Fabricating water-insoluble polyelectrolyte into multilayers with layer-by-layer self-assembly, Polym. Bull. 54 (2005) 427–433. doi:10.1007/s00289-005-0387-0.

[13]   S. Beyer, W.C. Mak, D. Trau, Reverse-phase LbL-encapsulation of highly water soluble materials by layer-by-layer polyelectrolyte self-assembly, Langmuir. 23 (2007) 8827–8832. doi:10.1021/la7011777.

[14]   P. Lavalle, C. Gergely, F.J.G. Cuisinier, G. Decher, P. Schaaf, J.C. Voegel, C. Picart, Comparison of the Structure of Polyelectrolyte Multilayer Films Exhibiting a Linear and an Exponential Growth Regime: An in Situ Atomic Force Microscopy Study, Macromolecules. 35 (2002) 4458–4465. doi:10.1021/ma0119833.

[15]   C. Picart, J. Mutterer, L. Richert, Y. Luo, G.D. Prestwich, P. Schaaf, J.-C. Voegel, P. Lavalle, Molecular basis for the explanation of the exponential growth of polyelectrolyte multilayers, Proc. Natl. Acad. Sci. 99 (2002) 12531–12535. doi:10.1073/pnas.202486099.

[16]   L. Richert, P. Lavalle, E. Payan, X.Z. Shu, G.D. Prestwich, J.F. Stoltz, P. Schaaf, J.C. Voegel, C. Picart, Layer by Layer Buildup of Polysaccharide

Films: Physical Chemistry and Cellular Adhesion Aspects, Langmuir. 20 (2004) 448–458. doi:10.1021/la035415n.

[17]   J. Ruths, F. Essler, G. Decher, H. Riegler, Polyelectrolytes. I: Polyanion/polycation multilayers at the air/monolayer/water interface as elements for quantitative polymer adsorption studies and preparation of hetero-superlattices on solid surfaces, Langmuir. 16 (2000) 8871–8878. doi:10.1021/la000257a.

[18]   D.L. Elbert, C.B. Herbert, J.A. Hubbell, Thin polymer layers formed by polyelectrolyte multilayer techniques on biological surfaces, Langmuir. 15 (1999) 5355–5362. doi:10.1021/la9815749.

[19]   C. Picart, P. Lavalle, P. Hubert, F.J.G. Cuisinier, G. Decher, P. Schaaf, J.C. Voegel, Buildup mechanism for poly(L-lysine)/hyaluronic acid films onto a solid surface, Langmuir. 17 (2001) 7414–7424. doi:10.1021/la010848g.

[20]   C. Picart, J. Mutterer, L. Richert, Y. Luo, G.D. Prestwich, P. Schaaf, J.-C. Voegel, P. Lavalle, Molecular basis for the explanation of the exponential growth of polyelectrolyte multilayers, Proc. Natl. Acad. Sci. 99 (2002) 12531–12535. doi:10.1073/pnas.202486099.

[21]   E. Pefferkorn, A.C. Jeanchronberg, R. Varoqui, Conformational Relaxation of Polyelectrolytes at A Solid Liquid Interface, Macromolecules. 23 (1990) 1735–1741. http://pubs.acs.org/doi/pdf/10.1021/ma00208a030 (accessed July 30, 2017).

[22]   S.T. Dubas, J.B. Schlenoff, Factors controlling the growth of polyelectrolyte multilayers, Macromolecules. 32 (1999) 8153–8160. doi:10.1021/ma981927a.

[23]   S.S. Lee, J.D. Hong, C.H. Kim, K. Kim, J.P. Koo, K.B. Lee, Layer-by-layer deposited multilayer assemblies of ionene-type polyelectrolytes based on the spin-coating method [2], Macromolecules. 34 (2001) 5358–5360. doi:10.1021/ma0022304.

[24]   J.B. Schlenoff, S.T. Dubas, T. Farhat, Sprayed polyelectrolyte multilayers,

Langmuir. 16 (2000) 9968–9969. doi:10.1021/la001312i.

[25] M. Ferreira, M.F. Rubner, Molecular-Level Processing of Conjugated Polymers. 1. Layer-by-Layer Manipulation of Conjugated Polyions, Macromolecules. 28 (1995) 7107–7114. doi:10.1021/ma00125a012.

[26] Y. Lvov, G. Decher, M. Mohwald, Assembly, Structural Characterization, and Thermal Behavior of Layer-by-Layer Deposited Ultrathin Films of Poly(vinyl sulfate) and Poly(allylamine), Langmuir. 9 (1993) 481–486. doi:10.1021/la00026a020.

[27] K. Ariga, Y. Lvov, T. Kunitake, Assembling alternate dye-polyion molecular films by electrostatic layer-by-layer adsorption, J. Am. Chem. Soc. 119 (1997) 2224–2231. doi:10.1021/ja963442c.

[28] D. Yoo, S.S. Shiratori, M.F. Rubner, Controlling bilayer composition and surface wettability of sequentially adsorbed multilayers of weak polyelectrolytes, Macromolecules. 31 (1998) 4309–4318. doi:10.1021/ma9800360.

[29] S.S. Shiratori, M.F. Rubner, pH-dependent thickness behavior of sequentially adsorbed layers of weak polyelectrolytes, Macromolecules. 33 (2000) 4213–4219. doi:10.1021/ma991645q.

[30] J.D. Mendelsohn, C.J. Barrett, V. V. Chan, A.J. Pal, A.M. Mayes, M.F. Rubner, Fabrication of microporous thin films from polyelectrolyte multilayers, Langmuir. 16 (2000) 5017–5023. doi:10.1021/la000075g.

[31] S.A.S. Sukhishvili, S. Granick, Layered, Erasable, Ultrathin Polymer Films, J. Am. Chem. Soc. 122 (2000) 9550–9551. doi:10.1021/ja002410t.

[32] D. Kovacevic, S. Van der Burgh, A. De Keizer, M.A. Cohen Stuart, Kinetics of formation and dissolution of weak polyelectrolyte multilayers: Role of salt and free polyions, Langmuir. 18 (2002) 5607–5612. doi:10.1021/la025639q.

[33] S.L. Clark, M.F. Montague, P.T. Hammond, Ionic Effects of Sodium Chloride on the Templated Deposition of Polyelectrolytes Using Layer-by-Layer Ionic

Assembly, Macromolecules. 30 (1997) 7237–7244. doi:10.1021/ma970610s.

[34] M. Heskins, J.E. Guillet, Solution Properties of Poly(N-isopropylacrylamide), J. Macromol. Sci. Part A - Chem. 2 (1968) 1441–1455. doi:10.1080/10601326808051910.

[35] J. Shi, F. Hua, T. Cui, Y.M. Lvov, Temperature Effect on Layer-by-Layer Self-assembly of Linear Polyions and Silica Multilayers, Chem. Lett. 32 (2003) 316–317. doi:10.1246/cl.2003.316.

[36] H.L. Tan, M.J. McMurdo, G. Pan, P.G. Van Patten, Temperature Dependence of Polyelectrolyte Multilayer Assembly, Langmuir. 19 (2003) 9311–9314. doi:10.1021/la035094f.

[37] S. Ye, C. Wang, X. Liu, Z. Tong, Deposition temperature effect on release rate of indomethacin microcrystals from microcapsules of layer-by-layer assembled chitosan and alginate multilayer films, J. Control. Release. 106 (2005) 319–328. doi:10.1016/j.jconrel.2005.05.006.

[38] C.D. Jones, L.A. Lyon, Dependence of Shell Thickness on Core Compression in Acrylic Acid Modified Poly(N -isopropylacrylamide) Core/Shell Microgels, Langmuir. 19 (2003) 4544–4547. doi:10.1021/la034392+.

[39] B.M. Wohl, J.F.J. Engbersen, Responsive layer-by-layer materials for drug delivery, J. Control. Release. 158 (2012) 2–14. doi:10.1016/j.jconrel.2011.08.035.

[40] A. Chan, R.P. Orme, R.A. Fricker, P. Roach, Remote and local control of stimuli responsive materials for therapeutic applications, Adv. Drug Deliv. Rev. 65 (2013) 497–514. doi:10.1016/j.addr.2012.07.007.

[41] J. Hiller, M.F. Rubner, Reversible molecular memory and pH-switchable swelling transitions in polyelectrolyte multilayers, Macromolecules. 36 (2003) 4078–4083. doi:10.1021/ma025837o.

[42] E. Kharlampieva, S.A. Sukhishvili, Ionization and pH stability of multilayers formed by self-assembly of weak polyelectrolytes, Langmuir. 19 (2003) 1235–

1243. doi:10.1021/la026546b.

[43] M. Delcea, H. Möhwald, A.G. Skirtach, Stimuli-responsive LbL capsules and nanoshells for drug delivery, Adv. Drug Deliv. Rev. 63 (2011) 730–747. doi:10.1016/j.addr.2011.03.010.

[44] A.A. Antipov, G.B. Sukhorukov, S. Leporatti, I.L. Radtchenko, E. Donath, H. Möhwald, Polyelectrolyte multilayer capsule permeability control, in: Colloids Surfaces A Physicochem. Eng. Asp., (2002) 535–541. doi:10.1016/S0927-7757(01)00956-6.

[45] A.A. Antipov, G.B. Sukhorukov, Polyelectrolyte multilayer capsules as vehicles with tunable permeability, in: Adv. Colloid Interface Sci., (2004) 49–61. doi:10.1016/j.cis.2004.07.006.

[46] G.B. Sukhorukov, A.A. Antipov, A. Voigt, E. Donath, H. M??hwald, pH-controlled macromolecule encapsulation in and release from polyelectrolyte multilayer nanocapsules, Macromol. Rapid Commun. 22 (2001) 44–46. doi:10.1002/1521-3927(20010101)22:1<44::AID-MARC44>3.0.CO;2-U.

[47] T. Serizawa, D. Matsukuma, M. Akashi, Loading and release of charged dyes using ultrathin hydrogels, Langmuir. 21 (2005) 7739–7742. doi:10.1021/la0505263.

[48] E. Kharlampieva, V.A. Izumrudov, S.A. Sukhishvili, Electrostatic layer-by-layer self-assembly of poly(carboxybetaine)s: Role of zwitterions in film growth, Macromolecules. 40 (2007) 3663–3668. doi:10.1021/ma062811e.

[49] E. Vázquez, D.M. Dewitt, P.T. Hammond, D.M. Lynn, Construction of hydrolytically-degradable thin films via layer-by-layer deposition of degradable polyelectrolytes, J. Am. Chem. Soc. 124 (2002) 13992–13993. doi:10.1021/ja026405w.

[50] K.C. Wood, J.Q. Boedicker, D.M. Lynn, P.T. Hammond, Tunable drug release from hydrolytically degradable layer-by-layer thin films, Langmuir. 21 (2005) 1603–1609. doi:10.1021/la0476480.

[51]   B. Onat, V. Bütün, S. Banerjee, I. Erel-Goktepe, Bacterial anti-adhesive and pH-induced antibacterial agent releasing ultra-thin films of zwitterionic copolymer micelles, Acta Biomater. 40 (2016) 293–309. doi:http://dx.doi.org/10.1016/j.actbio.2016.04.033.

[52]   V. Kozlovskaya, E. Kharlampieva, I. Drachuk, D. Cheng, V. V. Tsukruk, Responsive microcapsule reactors based on hydrogen-bonded tannic acid layer-by-layer assemblies, Soft Matter. 6 (2010) 3596. doi:10.1039/b927369g.

[53]   V. Kozlovskaya, S. Harbaugh, I. Drachuk, O. Shchepelina, N. Kelley-Loughnane, M. Stone, V. V. Tsukruk, Hydrogen-bonded LbL shells for living cell surface engineering, Soft Matter. 7 (2011) 2364–2372. doi:10.1039/C0SM01070G.

[54]   K. Kataoka, G.S. Kwon, M. Yokoyama, T. Okano, S. Sakurai, Block copolymer micelles as vehicles for drug delivery, J. Control. Release. 24 (1993) 119–132. doi:10.1016/j.addr.2012.09.016.

[55]   M. Moffitt, K. Khougaz, a Eisenberg, Micellization of ionic block copolymers, Acc. Chem. Res. 29 (1996) 95–102. doi:10.1021/AR940080.

[56]   G.S. Kwon, K. Kataoka, Block copolymer micelles as long-circulating drug vehicles, Adv. Drug Deliv. Rev. 64 (2012) 237–245. doi:10.1016/j.addr.2012.09.016.

[57]   N. Ma, H. Zhang, B. Song, Z. Wang, X. Zhang, Polymer micelles as building blocks for layer-by-layer assembly: An approach for incorporation and controlled release of water-insoluble dyes, Chem. Mater. 17 (2005) 5065–5069. doi:10.1021/cm051221c.

[58]   B.S. Kim, S.W. Park, P.T. Hammond, Hydrogen-bonding layer-by-layer-assembled biodegradable polymeric micelles as drug delivery vehicles from surfaces, ACS Nano. 2 (2008) 386–392. doi:10.1021/nn700408z.

[59]   J. Hong, L.M. Alvarez, N.J. Shah, Y. Cho, B.S. Kim, L.G. Griffith, K. Char, P.T. Hammond, Multilayer thin-film coatings capable of extended

programmable drug release: Application to human mesenchymal stem cell differentiation, Drug Deliv. Transl. Res. 2 (2012) 375–383. doi:10.1007/s13346-012-0093-z.

[60] P.M. Nguyen, N.S. Zacharia, E. Verploegen, P.T. Hammond, Extended release antibacterial layer-by-layer films incorporating linear-dendritic block copolymer micelles, Chem. Mater. 19 (2007) 5524–5530. doi:10.1021/cm070981f.

[61] Y. Masayuki, M. Mizue, Y. Noriko, O. Teruo, S. Yasuhisa, K. Kazunori, I. Shohei, Polymer micelles as novel drug carrier: Adriamycin-conjugated poly(ethylene glycol)-poly(aspartic acid) block copolymer, J. Control. Release. 11 (1990) 269–278. doi:10.1016/0168-3659(90)90139-K.

[62] M. Yokoyama, S. Inoue, K. Kataoka, N. Yui, Y. Sakurai, Preparation of adriamycin-conjugated poly(ethylene glycol)-poly(aspartic acid) block copolymer. A new type of polymeric anticancer agent, Die Makromol. Chemie, Rapid Commun. 8 (1987) 431–435. doi:10.1002/marc.1987.030080903.

[63] M. Yokoyama, M. Miyauchi, N. Yamada, T. Okano, Y. Sakurai, K. Kataoka, S. Inoue, Characterization and Anticancer Activity of the Micelle-forming Polymeric Anticancer Drug Adriamycin-conjugated Poly(ethylene glycol)-Poly(aspartic acid) Block Copolymer, Cancer Res. 50 (1990) 1693–1700. doi:10.1016/j.ijpharm.2008.08.011.

[64] B.-S. Kim, H.-I. Lee, Y. Min, Z. Poon, P.T. Hammond, Hydrogen-bonded multilayer of pH-responsive polymeric micelles with tannic acid for surface drug delivery., Chem. Commun. (Camb). (2009) 4194–4196. doi:10.1039/b908688a.

[65] C. Park, M. Rhue, M. Im, C. Kim, Hydrogen-bonding induced alternating thin films of dendrimer and block copolymer micelle, Macromol. Res. 15 (2007) 688–692. doi:10.1007/BF03218951.

[66] T. Addison, O.J. Cayre, S. Biggs, S.P. Armes, D. York, Incorporation of block copolymer micelles into multilayer films for use as nanodelivery systems,

Langmuir. 24 (2008) 13328–13333. doi:10.1021/la802396g.

[67]   S. Biggs, K. Sakai, T. Addison, A. Schmid, S.P. Armes, M. Vamvakaki, V. Bütün, G. Webber, Layer-by-layer formation of smart particle coatings using oppositely charged block copolymer micelles, Adv. Mater. 19 (2007) 247–250. doi:10.1002/adma.200601553.

[68]   T. Addison, O.J. Cayre, S. Biggs, S.P. Armes, D. York, Polymeric microcapsules assembled from a cationic/zwitterionic pair of responsive block copolymer micelles, Langmuir. 26 (2010) 6281–6286. doi:10.1021/la904064d.

[69]   T. Addison, O.J. Cayre, S. Biggs, S.P. Armes, D. York, Multi-layer films of block copolymer micelles adsorbed to colloidal templates., Philos. Trans. A. Math. Phys. Eng. Sci. 368 (2010) 4293–4311. doi:10.1098/rsta.2010.0151.

[70]   J. Hong, J. Cho, K. Char, Hollow capsules prepared from all block copolymer micelle multilayers, J. Colloid Interface Sci. 364 (2011) 112–117. doi:10.1016/j.jcis.2011.08.012.

[71]   I. Erel, H.E. Karahan, C. Tuncer, V. Bütün, A.L. Demirel, Hydrogen-bonded multilayers of micelles of a dually responsive dicationic block copolymer, Soft Matter. 8 (2012) 827. doi:10.1039/c1sm06248d.

[72]   A. Khademhosseini, K.Y. Suh, J.M. Yang, G. Eng, J. Yeh, S. Levenberg, R. Langer, Layer-by-layer deposition of hyaluronic acid and poly-L-lysine for patterned cell co-cultures, Biomaterials. 25 (2004) 3583–3592. doi:10.1016/j.biomaterials.2003.10.033.

[73]   J. Zhang, B. Senger, D. Vautier, C. Picart, P. Schaaf, J.C. Voegel, P. Lavalle, Natural polyelectrolyte films based on layer-by layer deposition of collagen and hyaluronic acid, Biomaterials. 26 (2005) 3353–3361. doi:10.1016/j.biomaterials.2004.08.019.

[74]   T.I. Croll, A.J. O'Connor, G.W. Stevens, J.J. Cooper-White, A blank slate? Layer-by-layer deposition of hyaluronic acid and chitosan onto various surfaces, Biomacromolecules. 7 (2006) 1610–1622. doi:10.1021/bm060044l.

[75]   T. Levy, C. D??jugnat, G.B. Sukhorukov, Polymer microcapsules with carbohydrate-sensitive properties, Adv. Funct. Mater. 18 (2008) 1586–1594. doi:10.1002/adfm.200701291.

[76]   Z. Ding, Y. Guan, Y. Zhang, X.X. Zhu, Layer-by-layer multilayer films linked with reversible boronate ester bonds with glucose-sensitivity under physiological conditions, Soft Matter. 5 (2009) 2302. doi:10.1039/b901910c.

[77]   R. Watahiki, K. Sato, K. Suwa, S. Niina, Y. Egawa, T. Seki, J. Anzai, Multilayer films composed of phenylboronic acid-modified dendrimers sensitive to glucose under physiological conditions, J. Mater. Chem. B. 0 (2014) 1–9. doi:10.1039/C4TB00676C.

[78]   B.G. De Geest, R.E. Vandenbroucke, A.M. Guenther, G.B. Sukhorukov, W.E. Hennink, N.N. Sanders, J. Demeester, S.C. De Smedt, Intracellularly degradable polyelectrolyte microcapsules, Adv. Mater. 18 (2006) 1005–1009. doi:10.1002/adma.200502128.

[79]   T. Borodina, E. Markvicheva, S. Kunizhev, H. Möhwald, G.B. Sukhorukov, O. Kreft, Controlled release of DNA from self-degrading microcapsules, Macromol. Rapid Commun. 28 (2007) 1894–1899. doi:10.1002/marc.200700409.

[80]   L. Sun, X. Xiong, Q. Zou, P. Ouyang, R. Krastev, Controlled heparinase-catalyzed degradation of polyelectrolyte multilayer capsules with heparin as responsive layer, J. Appl. Polym. Sci. 134 (2017) 44916. doi:10.1002/app.44916.

[81]   D.M. Munnecke, Hydrolysis of organophosphate insecticides by an immobilized enzyme system, Biotechnol. Bioeng. 21 (1979) 2247–2261. doi:10.1002/bit.260211207.

[82]   C.A. Constantine, S. V. Mello, A. Dupont, X. Cao, D. Santos, O.N. Oliveira, F.T. Strixino, E.C. Pereira, T.C. Cheng, J.J. Defrank, R.M. Leblanc, Layer-by-layer self-assembled chitosan/poly(thiophene-3-acetic acid) and organophosphorus hydrolase multilayers, J. Am. Chem. Soc. 125 (2003) 1805–

1809. doi:10.1021/ja028691h.

[83]   L. V. Sigolaeva, D. V. Pergushov, C. V. Synatschke, A. Wolf, I. Dewald, I.N. Kurochkin, A. Fery, A.H.E. Müller, Co-assemblies of micelle-forming diblock copolymers and enzymes on graphite substrate for an improved design of biosensor systems, Soft Matter. 9 (2013) 2858–2868. doi:10.1039/c2sm27298a.

[84]   R. Qu, L. Shen, Z. Chai, C. Jing, Y. Zhang, Y. An, L. Shi, Hemin-block copolymer micelle as an artificial peroxidase and its applications in chromogenic detection and biocatalysis, ACS Appl. Mater. Interfaces. 6 (2014) 19207–19216. doi:10.1021/am505232h.

[85]   S. Cosnier, Biomolecule immobilization on electrode surfaces by entrapment or attachment to electrochemically polymerized films. A review, Biosens. Bioelectron. 14 (1999) 443–456. doi:10.1016/S0956-5663(99)00024-X.

[86]   H. Inoue, K. Sato, J.I. Anzai, Disintegration of layer-by-layer assemblies composed of 2-iminobiotin-labeled poly(ethyleneimine) and avidin, Biomacromolecules. 6 (2005) 27–29. doi:10.1021/bm0495856.

[87]   S. Takahashi, K. Sato, J.I. Anzai, Layer-by-layer construction of protein architectures through avidin-biotin and lectin-sugar interactions for biosensor applications, Anal. Bioanal. Chem. 402 (2012) 1749–1758. doi:10.1007/s00216-011-5317-4.

[88]   I. Zhuk, F. Jariwala, A.B. Attygalle, Y. Wu, M.R. Libera, S.A. Sukhishvili, Self-defensive layer-by-layer films with bacteria-triggered antibiotic release, ACS Nano. 8 (2014) 7733–7745. doi:10.1021/nn500674g.

[89]   V. Albright, I. Zhuk, Y. Wang, V. Selin, B. van de Belt-Gritter, H.J. Busscher, H.C. van der Mei, S.A. Sukhishvili, Self-defensive antibiotic-loaded layer-by-layer coatings: Imaging of localized bacterial acidification and pH-triggering of antibiotic release, Acta Biomater. 61 (2017) 66–74. doi:10.1016/j.actbio.2017.08.012.

[90]   R. Steitz, V. Leiner, K. Tauer, V. Khrenov, R. V. Klitzing, Temperature-

induced changes in polyelectrolyte films at the solid-liquid interface, Appl. Phys. A Mater. Sci. Process. 74 (2002) s519–s521. doi:10.1007/s003390201782.

[91]   K. Glinel, G.B. Sukhorukov, H. Möhwald, V. Khrenov, K. Tauer, Thermosensitive Hollow Capsules Based on Thermoresponsive Polyelectrolytes, Macromol. Chem. Phys. 204 (2003) 1784–1790. doi:10.1002/macp.200350033.

[92]   D.J. Phillips, M.I. Gibson, Towards being genuinely smart: "isothermally-responsive" polymers as versatile, programmable scaffolds for biologically-adaptable materials, Polym. Chem. 6 (2015) 1033–1043. doi:10.1039/C4PY01539H.

[93]   N. Adams, U.S. Schubert, Poly(2-oxazolines) in biological and biomedical application contexts, Adv. Drug Deliv. Rev. 59 (2007) 1504–1520. doi:10.1016/j.addr.2007.08.018.

[94]   R. Hoogenboom, H. Schlaad, Bioinspired Poly(2-oxazoline)s, Polymers (Basel). 3 (2011) 467–488. doi:10.3390/polym3010467.

[95]   C. Weber, R. Hoogenboom, U.S. Schubert, Temperature responsive bio-compatible polymers based on poly(ethylene oxide) and poly(2-oxazoline)s, Prog. Polym. Sci. 37 (2012) 686–714. doi:10.1016/j.progpolymsci.2011.10.002.

[96]   N. Zhang, T. Pompe, I. Amin, R. Luxenhofer, C. Werner, R. Jordan, Tailored Poly(2-oxazoline) Polymer Brushes to Control Protein Adsorption and Cell Adhesion, Macromol. Biosci. 12 (2012) 926–936. doi:10.1002/mabi.201200026.

[97]   I. Haktaniyan, M.; Atilla, S.; Cagli, E.; Erel-Goktepe, pH- and Temperature-Induced Release of Doxorubicin from Multilayers of Poly(2-isopropyl-2-oxazoline) and Tannic Acid, Polym. Int. (2017).

[98]   J.F. Quinn, F. Caruso, Facile Tailoring of Film Morphology and Release

Properties Using Layer-by-Layer Assembly of Thermoresponsive Materials, Langmuir. 20 (2004) 20–22. doi:10.1021/la0360310.

[99] E. Bag, O. Begik, P. Yusan, Erel-goktepe, Hydrogen-Bonded Multilayers With Controllable pH-Induced Disintegration Kinetics for Controlled Release Applications From Surfaces, J. Macromol. Sci. Part A Pure Appl. Chem. ISSN. 52 (2015) 286–298. doi:10.1080/10601325.2015.1007274.

[100] E. Kharlampieva, V. Kozlovskaya, J. Tyutina, S.A. Sukhishvili, Hydrogen-bonded multilayers of thermoresponsive polymers, Macromolecules. 38 (2005) 10523–10531. doi:10.1021/ma0516891.

[101] A. Vidyasagar, C. Sung, R. Gamble, J.L. Lutkenhaus, Thermal transitions in dry and hydrated layer-by-layer assemblies exhibiting linear and exponential growth, ACS Nano. 6 (2012) 6174–6184. doi:10.1021/nn301526b.

[102] A. Vidyasagar, C. Sung, K. Losensky, J.L. Lutkenhaus, PH-dependent thermal transitions in hydrated layer-by-layer assemblies containing weak polyelectrolytes, Macromolecules. 45 (2012) 9169–9176. doi:10.1021/ma3020454.

[103] H. Sasase, T. Aoki, H. Katono, K. Sanui, N. Ogata, R. Ohta, T. Kondo, Y. Sakurai, Regulation of temperature-response swelling behavior of interpenetrating polymer networks composed of hydrogen bonding polymers, Die Makromol. Chemie, Rapid Commun. 581 (1992) 577–581. doi:10.1002/marc.1992.030131208.

[104] F. Kohori, K. Sakai, T. Aoyagi, M. Yokoyama, Y. Sakurai, T. Okano, Preparation and characterization of thermally responsive block copolymer micelles comprising poly(N-isopropylacrylamide-b-DL-lactide), J. Control. Release. 55 (1998) 87–98. doi:10.1016/S0168-3659(98)00023-6.

[105] S.Q. Liu, Y.W. Tong, Y.Y. Yang, Incorporation and in vitro release of doxorubicin in thermally sensitive micelles made from poly(N-isopropylacrylamide-co-N,N-dimethylacrylamide)-b- poly(D,L-lactide-co-glycolide) with varying compositions, Biomaterials. 26 (2005) 5064–5074.

doi:10.1016/j.biomaterials.2005.01.030.

[106] M.D. Determan, J.P. Cox, S. Seifert, P. Thiyagarajan, S.K. Mallapragada, Synthesis and characterization of temperature and pH-responsive pentablock copolymers, Polymer (Guildf). 46 (2005) 6933–6946. doi:10.1016/j.polymer.2005.05.138.

[107] S. Chen, Y. Li, C. Guo, J. Wang, J. Ma, X. Liang, L.R. Yang, H.Zh. Liu, Temperature-Responsive Magnetite/PEO−PPO−PEO Block Copolymer Nanoparticles for Controlled Drug Targeting Delivery, (2007) 12669-12676. doi:10.1021/LA702049D.

[108] M.J. Serpe, C.D. Jones, L.A. Lyon, Layer-by-Layer Deposition of Thermoresponsive Microgel Thin Films, Langmuir. 19 (2003) 8759–8764. doi:10.1021/la034391h.

[109] B.P. Timko, T. Dvir, D.S. Kohane, Remotely triggerable drug delivery systems, Adv. Mater. 22 (2010) 4925–4943. doi:10.1002/adma.201002072.

[110] S. Link, M.A. El-Sayed, Shape and size dependence of radiative, non-radiative and photothermal properties of gold nanocrystals, Int. Rev. Phys. Chem. 19 (2000) 409–453. doi:10.1080/01442350050034180.

[111] R. Palankar, A.G. Skirtach, O. Kreft, M. Bédard, M. Garstka, K. Gould, H. Möhwald, G.B. Sukhorukov, M. Winterhalter, S. Springer, Controlled intracellular release of peptides from microcapsules enhances antigen presentation on MHC class I molecules, Small. 5 (2009) 2168–2176. doi:10.1002/smll.200900809.

[112] M. Bédard, A.G. Skirtach, G.B. Sukhorukov, Optically driven encapsulation using novel polymeric hollow shells containing an azobenzene polymer, Macromol. Rapid Commun. 28 (2007) 1517–1521. doi:10.1002/marc.200700257.

[113] Y. Wang, Z. Tang, M.A. Correa-Duarte, L.M. Liz-Marzán, N.A. Kotov, Multicolor luminescence patterning by photoactivation of semiconductor

nanoparticle films, J. Am. Chem. Soc. 125 (2003) 2830–2831. doi:10.1021/ja029231r.

[114] H. Zhu, M.J. McShane, Macromolecule encapsulation in diazoresin-based hollow polyelectrolyte microcapsules, Langmuir. 21 (2005) 424–430. doi:10.1021/la048093b.

[115] A.S. Angelatos, B. Radt, F. Caruso, Light-responsive polyelectrolyte/gold nanoparticle microcapsules, J. Phys. Chem. B. 109 (2005) 3071–3076. doi:10.1021/jp045070x.

[116] X. Tao, J. Li, H. Möhwald, Self-assembly, optical behavior, and permeability of a novel capsule based on an azo dye and polyelectrolytes, Chem. - A Eur. J. 10 (2004) 3397–3403. doi:10.1002/chem.200400024.

[117] J.-F. Gohy, Y. Zhao, Photo-responsive block copolymer micelles: design and behavior., Chem. Soc. Rev. 42 (2013) 7117–7129. doi:10.1039/c3cs35469e.

[118] J. Jiang, X. Tong, Y. Zhao, A new design for light-breakable polymer micelles, J. Am. Chem. Soc. 127 (2005) 8290–8291. doi:10.1021/ja0521019.

[119] G. Wang, X. Tong, Y. Zhao, Preparation of azobenzene-containing amphiphilic diblock copolymers for light-responsive micellar aggregates, Macromolecules. 37 (2004) 8911–8917. doi:10.1021/ma048416a.

[120] S. Kurzhals, R. Zirbs, E. Reimhult, Synthesis and Magneto-Thermal Actuation of Iron Oxide Core-PNIPAM Shell Nanoparticles, ACS Appl. Mater. Interfaces. 7 (2015) 19342–19352. doi:10.1021/acsami.5b05459.

[121] L.L. Lao, R. V. Ramanujan, Magnetic and hydrogel composite materials for hyperthermia applications, J. Mater. Sci. Mater. Med. 15 (2004) 1061–1064. doi:10.1023/B:JMSM.0000046386.78633.e5.

[122] K. Katagiri, M. Nakamura, K. Koumoto, Magnetoresponsive smart capsules formed with polyelectrolytes, lipid bilayers and magnetic nanoparticles, ACS Appl. Mater. Interfaces. 2 (2010) 768–773. doi:10.1021/am900784a.

[123]   Z. Lu, M.D. Prouty, Z. Quo, V.O. Golub, C.S.S.R. Kumar, Y.M. Lvov, Magnetic switch of permeability for polyelectrolyte microcapsules embedded with Co@Aunanoparticles, Langmuir. 21 (2005) 2042–2050. doi:10.1021/la047629q.

[124]   H. Lomas, A.P.R. Johnston, G.K. Such, Z. Zhu, K. Liang, M.P. Van Koeverden, S. Alongkornchotikul, F. Caruso, Polymersome-loaded capsules for controlled release of DNA, Small. 7 (2011) 2109–2119. doi:10.1002/smll.201100744.

[125]   S. Dobretsov, M. Teplitski, V. Paul, Mini-review: quorum sensing in the marine environment and its relationship to biofouling., Biofouling. 25 (2009) 413–27. doi:10.1080/08927010902853516.

[126]   J. Wang, Z. Wang, Y. Liu, J. Wang, S. Wang, Surface modification of NF membrane with zwitterionic polymer to improve anti-biofouling property, J. Memb. Sci. 514 (2016) 407–417. doi:10.1016/j.memsci.2016.05.014.

[127]   J. Min, R.D. Braatz, P.T. Hammond, Tunable staged release of therapeutics from layer-by-layer coatings with clay interlayer barrier, Biomaterials. 35 (2014) 2507–2517. doi:10.1016/j.biomaterials.2013.12.009.

[128]   J. Fu, J. Ji, W. Yuan, J. Shen, Construction of anti-adhesive and antibacterial multilayer films via layer-by-layer assembly of heparin and chitosan, Biomaterials. 26 (2005) 6684–6692. doi:10.1016/j.biomaterials.2005.04.034.

[129]   Z. Li, D. Lee, X. Sheng, R.E. Cohen, M.F. Rubner, Two-level antibacterial coating with both release-killing and contact-killing capabilities, Langmuir. 22 (2006) 9820–9823. doi:10.1021/la0622166.

[130]   S. Krishnan, C.J. Weinman, C.K. Ober, Advances in polymers for anti-biofouling surfaces, J. Mater. Chem. 18 (2008) 3405. doi:10.1039/b801491d.

[131]   C. Hippius, V. Butun, I. Erel-Goktepe, Bacterial anti-adhesive properties of a monolayer of zwitterionic block copolymer micelles, Mater. Sci. Eng. C. 41 (2014) 354–362. doi:10.1016/j.msec.2014.04.023.

[132]   P. Yusan, I. Tuncel, V. Bütün, A.L. Demirel, I. Erel-Goktepe, pH-responsive

layer-by-layer films of zwitterionic block copolymer micelles, Polym. Chem. 5 (2014) 3777–3787.

[133] J. Fukuda, A. Khademhosseini, J. Yeh, G. Eng, J. Cheng, O.C. Farokhzad, R. Langer, Micropatterned cell co-cultures using layer-by-layer deposition of extracellular matrix components, Biomaterials. 27 (2006) 1479–1486. doi:10.1016/j.biomaterials.2005.09.015.

[134] N.J. Shah, J. Hong, M.N. Hyder, P.T. Hammond, Osteophilic multilayer coatings for accelerated bone tissue growth, Adv. Mater. 24 (2012) 1445–1450. doi:10.1002/adma.201104475.

[135] Z. Mao, L. Ma, J. Zhou, C. Gao, J. Shen, Bioactive thin film of acidic fibroblast growth factor fabricated by layer-by-layer assembly, Bioconjug. Chem. 16 (2005) 1316–1322. doi:10.1021/bc049755b.

[136] M.L. Macdonald, R.E. Samuel, N.J. Shah, R.F. Padera, Y.M. Beben, P.T. Hammond, Tissue integration of growth factor-eluting layer-by-layer polyelectrolyte multilayer coated implants, Biomaterials. 32 (2011) 1446–1453. doi:10.1016/j.biomaterials.2010.10.052.

[137] N.J. Shah, M.L. Macdonald, Y.M. Beben, R.F. Padera, R.E. Samuel, P.T. Hammond, Tunable dual growth factor delivery from polyelectrolyte multilayer films, Biomaterials. 32 (2011) 6183–6193. doi:10.1016/j.biomaterials.2011.04.036.

[138] D.F. Williams, On the mechanisms of biocompatibility, Biomaterials. 29 (2008) 2941–2953. doi:10.1016/j.biomaterials.2008.04.023.

[139] D.P. Layman, Physiology demystified, 2004. doi:10.1036/0071438289.

[140] K. Deligkaris, T.S. Tadele, W. Olthuis, A. van den Berg, Hydrogel-based devices for biomedical applications, Sensors Actuators, B Chem. 147 (2010) 765–774. doi:10.1016/j.snb.2010.03.083.

[141] A.S. Hoffman, Hydrogels for biomedical applications, Adv. Drug Deliv. Rev. 64 (2012) 18–23. doi:10.1016/j.addr.2012.09.010.

[142] D. Campoccia, P. Doherty, M. Radice, P. Brun, G. Abatangelo, D.F. Williams, Semisynthetic resorbable materials from hyaluronan esterification, Biomaterials. 19 (1998) 2101–2127. doi:10.1016/S0142-9612(98)00042-8.

[143] G.D. Prestwich, D.M. Marecak, J.F. Marecek, K.P. Vercruysse, M.R. Ziebell, Controlled chemical modification of hyaluronic acid: Synthesis, applications, and biodegradation of hydrazide derivatives, in: J. Control. Release, (1998) 93–103. doi:10.1016/S0168-3659(97)00242-3.

[144] O. Wichterle, D. Lím, Hydrophilic Gels for Biological Use, Nature. 185 (1960) 117–118. doi:10.1038/185117a0.

[145] X. Wu, L. Black, G. Santacana-Laffitte, C.W. Patrick, Preparation and assessment of glutaraldehyde-crosslinked collagen-chitosan hydrogels for adipose tissue engineering, J. Biomed. Mater. Res. - Part A. 81 (2007) 59–65. doi:10.1002/jbm.a.31003.

[146] B. Balakrishnan, M. Mohanty, P.R. Umashankar, A. Jayakrishnan, Evaluation of an in situ forming hydrogel wound dressing based on oxidized alginate and gelatin, Biomaterials. 26 (2005) 6335–6342. doi:10.1016/j.biomaterials.2005.04.012.

[147] F. Lim, a. Sun, Microencapsulated islets as bioartificial endocrine pancreas, Science (80-.). 210 (1980) 908–910. doi:10.1126/science.6776628.

[148] I. V Yannas, E. Lee, D.P. Orgill, E.M. Skrabut, G.F. Murphy, Synthesis and characterization of a model extracellular matrix that induces partial regeneration of adult mammalian skin., Proc. Natl. Acad. Sci. U. S. A. 86 (1989) 933–7. doi:10.1073/pnas.86.3.933.

[149] E.A. Kamoun, E.R.S. Kenawy, X. Chen, A review on polymeric hydrogel membranes for wound dressing applications: PVA-based hydrogel dressings, J. Adv. Res. 8 (2017) 217–233. doi:10.1016/j.jare.2017.01.005.

[150] M. Kokabi, M. Sirousazar, Z.M. Hassan, PVA-clay nanocomposite hydrogels for wound dressing, Eur. Polym. J. 43 (2007) 773–781.

doi:10.1016/j.eurpolymj.2006.11.030.

[151] B. Jeong, Y.H. Bae, S.W. Kim, Thermoreversible gelation of PEG-PLGA-PEG triblock copolymer aqueous solutions, Macromolecules. 32 (1999) 7064–7069. doi:10.1021/ma9908999.

[152] B. Jeong, Y.H. Bae, S.W. Kim, Drug release from biodegradable injectable thermosensitive hydrogel of PEG-PLGA-PEG triblock copolymers, J. Control. Release. 63 (2000) 155–163. doi:10.1016/S0168-3659(99)00194-7.

[153] T.A. Holland, Y. Tabata, A.G. Mikos, In vitro release of transforming growth factor-β1 from gelatin microparticles encapsulated in biodegradable, injectable oligo(poly(ethylene glycol) fumarate) hydrogels, J. Control. Release. 91 (2003) 299–313. doi:10.1016/S0168-3659(03)00258-X.

[154] J.L. Drury, D.J. Mooney, Hydrogels for tissue engineering: Scaffold design variables and applications, Biomaterials. 24 (2003) 4337–4351. doi:10.1016/S0142-9612(03)00340-5.

[155] Y. Takahashi, M. Yamamoto, Y. Tabata, Enhanced osteoinduction by controlled release of bone morphogenetic protein-2 from biodegradable sponge composed of gelatin and β-tricalcium phosphate, Biomaterials. 26 (2005) 4856–4865. doi:10.1016/j.biomaterials.2005.01.012.

[156] H.W. Kim, J.C. Knowles, H.E. Kim, Hydroxyapatite and gelatin composite foams processed via novel freeze-drying and crosslinking for use as temporary hard tissue scaffolds, J. Biomed. Mater. Res. - Part A. 72 (2005) 136–145. doi:10.1002/jbm.a.30168.

[157] Y. Shibata, H. Yamamoto, T. Miyazaki, Colloidal beta-tricalcium phosphate prepared by discharge in a modified body fluid facilitates synthesis of collagen composites., J. Dent. Res. 84 (2005) 827–31. doi:10.1177/154405910508400909.

[158] S. Sotome, T. Uemura, M. Kikuchi, J. Chen, S. Itoh, J. Tanaka, T. Tateishi, K. Shinomiya, Synthesis and in vivo evaluation of a novel

hydroxyapatite/collagen–alginate as a bone filler and a drug delivery carrier of bone morphogenetic protein, Mater. Sci. Eng. C. 24 (2004) 341–347. doi:10.1016/j.msec.2003.12.003.

[159] R.H. Schmedlen, K.S. Masters, J.L. West, Photocrosslinkable polyvinyl alcohol hydrogels that can be modified with cell adhesion peptides for use in tissue engineering, Biomaterials. 23 (2002) 4325–4332. doi:10.1016/S0142-9612(02)00177-1.

[160] J.A. Burdick, K.S. Anseth, Photoencapsulation of osteoblasts in injectable RGD-modified PEG hydrogels for bone tissue engineering, Biomaterials. 23 (2002) 4315–4323. doi:10.1016/S0142-9612(02)00176-X.

[161] N.O. Enemchukwu, R. Cruz-Acuña, T. Bongiorno, C.T. Johnson, J.R. García, T. Sulchek, A.J. García, Synthetic matrices reveal contributions of ECM biophysical and biochemical properties to epithelial morphogenesis, J. Cell Biol. 212 (2016) 113–124. doi:10.1083/jcb.201506055.

[162] K. V. Ranga Rao, K. Padmalatha Devi, Swelling controlled-release systems: recent developments and applications, Int. J. Pharm. 48 (1988) 1–13. doi:10.1016/0378-5173(88)90245-1.

[163] M. Şen, C. Uzun, O. Güven, Controlled release of terbinafine hydrochloride from pH sensitive poly(acrylamide/maleic acid) hydrogels, Int. J. Pharm. 203 (2000) 149–157. doi:10.1016/S0378-5173(00)00449-X.

[164] V.R. Patel, M.M. Amiji, Preparation and characterization of freeze-dried chitosan-poly(ethylene oxide) hydrogels for site-specific antibiotic delivery in the stomach, Pharm. Res. 13 (1996) 588–593. doi:10.1023/A:1016054306763.

[165] A. Gutowska, Y.H. Bae, J. Feijen, S.W. Kim, Heparin release from thermosensitive hydrogels, J. Control. Release. 22 (1992) 95–104. doi:10.1016/0168-3659(92)90194-V.

[166] C. Payne, E.B. Dolan, J. O'Sullivan, S.-A. Cryan, H.M. Kelly, A methylcellulose and collagen based temperature responsive hydrogel promotes

encapsulated stem cell viability and proliferation in vitro, Drug Deliv. Transl. Res. 7 (2017) 132–146. doi:10.1007/s13346-016-0347-2.

[167] K.L. Fujimoto, Z. Ma, D.M. Nelson, R. Hashizume, J. Guan, K. Tobita, W.R. Wagner, Synthesis, characterization and therapeutic efficacy of a biodegradable, thermoresponsive hydrogel designed for application in chronic infarcted myocardium, Biomaterials. 30 (2009) 4357–4368. doi:10.1016/j.biomaterials.2009.04.055.

[168] S. Kurihara, S. Sakamaki, S. Mogi, T. Ogata, T. Nonaka, Crosslinking of poly(vinyl alcohol)-graft-N-isopropylacrylamide copolymer membranes with glutaraldehyde and permeation of solutes through the membranes, Polymer (Guildf). 37 (1996) 1123–1128. doi:10.1016/0032-3861(96)80838-X.

[169] Y.L. Zhao, J. Fraser Stoddart, Azobenzene-based light-responsive hydrogel system, Langmuir. 25 (2009) 8442–8446. doi:10.1021/la804316u.

[170] S. Bhattacharya, F. Eckert, V. Boyko, A. Pich, Temperature-, pH-, and magnetic-field-sensitive hybrid microgels, Small. 3 (2007) 650–657. doi:10.1002/smll.200600590.

[171] V. Yesilyurt, O. Veiseh, J.C. Doloff, J. Li, S. Bose, X. Xie, A.R. Bader, M. Chen, M.J. Webber, A.J. Vegas, R. Langer, D.G. Anderson, A Facile and Versatile Method to Endow Biomaterial Devices with Zwitterionic Surface Coatings, Adv. Healthc. Mater. 6 (2017). doi:10.1002/adhm.201601091.

[172] S. Sanyasi, S. Kumar, A. Ghosh, R.K. Majhi, N. Kaur, P. Choudhury, U.P. Singh, C. Goswami, L. Goswami, A Modified Polysaccharide-Based Hydrogel for Enhanced Osteogenic Maturation and Mineralization Independent of Differentiation Factors, Macromol. Biosci. 17 (2017). doi:10.1002/mabi.201600268.

[173] M. Grossutti, R. Seenath, J. Lipkowski, Infrared and Fluorescence Spectroscopic Investigations of the Acyl Surface Modification of Hydrogel Beads for the Deposition of a Phospholipid Coating, Langmuir. 31 (2015) 11598–11604. doi:10.1021/acs.langmuir.5b02813.

[174] H. Sakaguchi, T. Serizawa, M. Akashi, Layer-by-Layer Assembly on Hydrogel Surfaces and Control of Human Whole Blood Coagulation, Chem. Lett. 32 (2003) 174–175. http://www.journal.csj.jp/doi/pdf/10.1246/cl.2003.174 (accessed August 28, 2017).

[175] L. Grossin, D. Cortial, B. Saulnier, O. Félix, A. Chassepot, G. Decher, P. Netter, P. Schaaf, P. Gillet, D. Mainard, J.C. Voegel, N. Benkirane-Jessel, Step-by-step build-up of biologically active cell-containing stratified films aimed at tissue engineering, Adv. Mater. 21 (2009) 650–655. doi:10.1002/adma.200801541.

[176] S. Mehrotra, D. Lynam, R. Maloney, K.M. Pawelec, M.H. Tuszynski, I. Lee, C. Chan, J. Sakamoto, Time controlled protein release from layer-by-layer assembled multilayer functionalized agarose hydrogels, Adv. Funct. Mater. 20 (2010) 247–258. doi:10.1002/adfm.200901172.

[177] D. Choi, J. Heo, J.H. Park, Y. Jo, H. Jeong, M. Chang, J. Choi, J. Hong, Nano-film coatings onto collagen hydrogels with desired drug release, J. Ind. Eng. Chem. 36 (2016) 326–333. doi:10.1016/j.jiec.2016.02.023.

[178] P. Gentile, C. Ghione, A.M. Ferreira, A. Crawford, P.V. Hatton, Alginate-based hydrogels functionalised at the nanoscale using layer-by-layer assembly for potential cartilage repair, Biomater. Sci. 5 (2017) 1922–1931. doi:10.1039/c7bm00525c.

CHAPTER 2

BACTERIAL ANTI-ADHESIVE AND PH-INDUCED ANTIBACTERIAL AGENT RELEASING ULTRA-THIN FILMS OF ZWITTERIONIC COPOLYMER MICELLES*

2.1. Chapter Summary

We report on preparation of substrates with dual function coatings, i.e. bacterial anti-adhesive and antibacterial agent releasing polymer films of zwitterionic BCMs. BCMs were obtained by pH-induced self-assembly of poly[3-dimethyl (methacryloyloxyethyl) ammonium propane sulfonate-*b*-2-(diisopropylamino)ethyl methacrylate] (βPDMA-*b*-PDPA), resulting in BCMs with zwitterionic βPDMA-coronae and pH-responsive PDPA-core. These zwitterionic BCMs were then used as building blocks to construct mono- and multi-layer films. We found that the number of layers in the film was critical for the anti-adhesive property and 3-layer films were the most anti-adhesive against a model Gram-positive bacterium, *Staphylococcus aureus*. Antibacterial activity could be introduced to the films by loading Triclosan into βPDMA-*b*-PDPA micelles. Triclosan containing films were effective against Triclosan-sensitive *Staphylococcus aureus* specifically at moderately acidic conditions due to pH-induced disintegration of the micellar core blocks and release of Triclosan from the surface. Three-layer films also exhibited anti-adhesive property at physiological pH against a model Gram-negative bacterium, *Escherichia coli*.

At moderately acidic pH, the coatings showed a contact antibacterial effect against an isolate of *Escherichia coli* with low sensitivity to Triclosan only when micellar cores were loaded with Triclosan. Such dual function films can be promising to combat biofouling at the non-homogeneous and/or defective parts of an anti-adhesive coating. Moreover, considering the moderately acidic conditions around an infection site, these multilayers can be advantageous due to their property of pH-induced antibacterial agent release.

2.2. Introduction

Hospital-acquired pathogenic bacteria that may cause severe illness and mortality have been a major medical concern both in developed and developing countries causing extra healthcare-related economic burden. In the United States alone, ~ 1.7 million Hospital Acquired Infections (HAIs) were observed in 2002, including the bacteria-derived ones [1]. Antibiotics and some antibacterial agents have been very commonly used on patients for the treatment of bacterial infections with limited success due to the development of resistance against these drugs. Bacteria that develop resistance against multiple drugs are known as Multiple Drug Resistant (MDR) bacteria. They are all observed as isolates of Gram-positive and Gram-negative bacteria, and are the most common reasons for the onset of hospital-acquired infections [2]. There is no standard-of-care therapy for some MDR *S. aureus* infections. For instance, one significant Gram-positive MDR bacterium is Methicillin-resistant *S. aureus* (MRSA), which is encountered predominantly in the intensive care units of hospitals, with no globally known antibiotic treatment [3]. Gram-negative MDR isolates of *E. coli* cause community and hospital-acquired bloodstream or urinary tract infections [4]. For example, MDR *E. coli* ST131, which produces extended-spectrum β-lactamase is currently the dominant extraintestinal pathogenic *E. coli* worldwide [5]. Both Gram-positive *S. aureus* and Gram-negative *E. coli* could cause biofouling through biofilm development. Bacteria develop biofilms in a two-step process: adherence on the surface and maturation. If adherence is delayed or prevented, biofilm formation could either be delayed or completely eliminated [6]. Biofilm-associated bacteria are 100 – 1000 times more resistant to antibiotics than the planktonic bacteria [7], so the

elimination of biofilm development would lead to greater success with antibiotic treatment.

Polymers have been used extensively to modify surfaces to prevent biofilm formation. Polymer coated substrates kill the bacteria either on contact [8] or by releasing antibiotics and other antibacterial compounds [9,10] (antibacterial coatings) or polymer coated substrates intrinsically possess bacterial anti-adhesive properties [11] due to their chemical nature (anti-adhesive coatings). Recently, polymer nanostructures that intrinsically show antibacterial property due to their chemical nature or possess antibacterial activity without loaded antibacterial agents have been reported to show great efficacy against bacteria [12–16]. Both antibacterial and anti-adhesive coatings prevent biofilm formation on medical devices. The major concern with releasing bactericidal agents from surfaces is the long term elimination of the biofilm formation due to depletion of the active agent. As an alternative approach, surfaces were modified by covalent attachment of antibiotics [17], however, limitations include efficacy against antibiotic-sensitive bacteria, biofilm formation from layers of dead bacteria on the surface and development of resistance to the drug molecules. Coating surfaces with anti-infective peptides have shown efficacy against antibiotic resistant bacteria [18,19], though they are disadvantageous in being sensitive to degradation by proteases in the serum.

To date, despite the recent progress in the development of anti-bacterial surfaces using stimuli-responsive polymers, only few of them have achieved long-term elimination of biofilm formation [19–21]. The drawbacks of drug-releasing and contact-killing surfaces have increased the need for development of bacterial anti-adhesive surfaces. Using polymers to prepare bacterial anti-adhesive surfaces has specifically become a promising approach in recent years due to a wide range of functional chemical groups that polymers provide to modify the properties of a surface. PEG has been extensively used to modify surfaces due to its biocompatibility, low toxicity, low immunogenicity [22,23] and anti-adhesive properties. However, PEG, especially when its molar mass is below 400 Da, has the disadvantage of being prone to oxidative degradation into

toxic diacid and hydroxyacid metabolites by alcohol and aldehyde dehydrogenases in the body [24].

Recently, zwitterionic polymers have proven to be anti-adhesive against protein adsorption, platelet adhesion, and bacteria adhesion [25–27]. Zwitterionic polymers endue their anti-adhesive property by interacting with water molecules through ionic solvation and H-bonding [28] and formation of a network of water molecules at the film-water interface. In contrast to ordinary polyelectrolytes, small disruptions of the network of hydrogen-bonded water molecules at the film-water interface were observed on polyzwitterion coated films, which was reported to be the reason for their anti-adhesive property [29]. Betainized polymers such as poly(phosphobetaine methacrylate) (pPBMA), poly(carboxybetainemethacrylate) (pCBMA), and poly(sulfobetainemethacrylate) (pSBMA), possess biocompatibility [30] and have been used to prepare bacterial anti-adhesive biointerfaces [31–33]. Recently, our group has reported on the bacterial anti-adhesive properties of monolayer films of zwitterionic micelles with polysulfobetain coronal chains [34].

LbL self-assembly of polymers at surfaces is a powerful technique for modification and functionalization of surfaces. LbL deposition of polymers has found application in developing films with antibacterial properties [35–45]. Silver nanoparticles have also been incorporated into polymer multilayers to impart antibacterial properties to LbL films [35,46,47]. LbL films with both anti-adhesive and antibacterial properties have also been reported [48–50].

In this study, we developed substrates with dual function ultra-thin polymer coatings which show bacterial anti-adhesive properties as well as release hydrophobic antibacterial compounds in response to pH changes. Different from our previous work on bacterial anti-adhesive properties of a monolayer of zwitterionic βPDMA-b-PDPA micelles [34], this study examined the effect of number of layers on the bacterial anti-adhesive properties of the films and also reports on the preparation of dual function ultra-thin coatings of zwitterionic BCMs, i.e. bacterial anti-adhesive and pH-induced antibacterial properties. This study is the first, demonstrating the use of zwitterionic

BCMs with pH-responsive cores as building blocks in the construction of dual function surfaces. Such films hold promise to control the bacterial adhesion on the surface of medical implants/devices.

2.3. Experimental Part

2.3.1. Materials

Sodium dihydrogenphosphate dehydrate and Luria Bertani (LB) broth (MILLER) were purchased from Merck Chemicals (Darmstadt, Germany). Pharmaceutical secondary standard 5-Chloro-2-(2,4-dichlorophenoxy)phenol (Triclosan), poly(sodium 4-styrene sulfonate) (PSS) (M_W 70,000), Mueller-Hinton (MH) broth, Phosphate Buffered Saline (PBS), Gram Staining Kit and Bovine Serum Albumin (BSA) were purchased from Sigma-Aldrich (USA). Agar bacteriological (Agar No.1, Oxoid) and Micro BCA protein assay kit were purchased from Thermo Scientific (USA). Sterile PTFE syringe filters (0.22 μm and 0.45 μm) were purchased from Sartorius AG (Goettingen, Germany). Cell culture plates were purchased from Sarstedt (Nibrecht, Germeny). C_{12}-Resazurin was purchased from Life Sciences (USA). The deionized (DI) H_2O was purified by passage through a Milli-Q system (Millipore). *Staphylococcus aureus* ATCC 29213 strain and *Escherichia coli* ATCC 8739 were kindly provided by Dr. Emel Uzunoglu (Microbiology Laboratory, Giresun Medical Faculty) and Prof. Dr. Aysegul Cetin Gozen (Department of Biology, Middle East Technical University), respectively.

2.3.2. Synthesis of poly[3-dimethyl (methacryloyloxyethyl) ammonium propane sulfonate]-*block*-poly[2-(diisopropylamino) ethyl methacrylate] (βPDMA-*b*-PDPA)

Poly[2-(dimethylamino)ethylmethacrylate]-*block*-poly[2-(diisopropylamino)ethyl methacrylate] (PDMA-*b*-PDPA) with 61 mol % PDMA content and a molecular weight of 15,800 g.mol^{-1} (M_w/M_n: 1.10) was synthesized by group transfer polymerization technique as described before [51]. DMA residues of PDMA-*b*-PDPA

(2 g) were selectively betainized in THF (100 mL) in the presence of 10 mol % excess (based on DMA residues) of 1,3-propane sultone at room temperature [52]. The solution was stirred for 48 hours and gelation was observed within 20 hours. The resulting βPDMA-*b*-PDPA was purified by Soxhlet extraction with THF and dried in a vacuum oven at 55 °C for at least 2 days. The extent of betainisation of PDMA block was assessed by ^{1}H NMR spectroscopy. Molecular weight of βPDMA-*b*-PDPA was calculated as 22,360 g.mol^{-1} assuming 100 % betainization.

2.3.3. Preparation of βPDMA-*b*-PDPA Micelles

βPDMA-*b*-PDPA was dissolved in 0.001 M NaH$_2$PO$_4$ buffer at pH 3.0 at a concentration of 0.1 mg.mL^{-1}. Micellization was triggered by gradually increasing the solution pH up to 7.5. The pH was adjusted using 0.1 M NaOH or 0.1 M HCl solutions. The solution was filtered through 0.22 μm syringe filter prior to use.

2.3.4. Triclosan Loading into βPDMA-*b*-PDPA Micelles

Triclosan was used as a model hydrophobic antibacterial agent. First, a solution of Triclosan in ethanol (> 99.8 %) with a concentration of 2.5 mg.mL^{-1} was prepared. 1 mL of this solution was added drop-wise into 200 mL of 0.001 M NaH$_2$PO$_4$ buffer, resulting in a solution of Triclosan with a concentration of 0.0125 mg.mL^{-1}. βPDMA-*b*-PDPA was dissolved in this Triclosan solution at pH 3.0 at a concentration of 0.1 mg.mL^{-1}. Micellization was triggered by gradually increasing the solution pH up to 7.5. The solution was stirred overnight for efficient loading of Triclosan molecules into the micellar cores. The solution was filtered through 0.22 μm syringe filter prior to use.

2.3.5. Dynamic Light Scattering and Zeta-Potential Measurements of βPDMA-*b*-PDPA

Hydrodynamic size and zeta-potential measurements were performed using Zetasizer Nano-ZS equipment (Malvern Instruments Ltd., U.K.). Particle sizes and zeta-potential values were obtained by cumulants analysis of the autocorrelation data and from electrophoretic mobility values using the Smoluchowski approximation, respectively.

2.3.6. Deposition of Multilayers for Ellipsometry, AFM Imaging, TEM Imaging and Bacterial Adhesion Experiments

Silicon wafers or glass slides were immersed into concentrated sulfuric acid for approximately 1 hour, and then rinsed with deionized (DI) water. After drying under a flow of nitrogen, wafers were immersed into 0.25 M NaOH solution for 10 minutes, thoroughly rinsed with DI water and dried again under nitrogen flow. Monolayer films were self-assembled at the surface by immersing the silicon wafers or glass slides for 30 minutes into 0.1 mg.mL^{-1} solution of βPDMA-*b*-PDPA micelles at pH 7.5. Multilayers were prepared at pH 7.5, by immersing the silicon wafers or glass slides alternatingly into 0.1 mg.mL^{-1} solutions of βPDMA-*b*-PDPA micelles and PSS for 30 minutes each with 2 intermediate rinsing steps in between. The first layer was always βPDMA-*b*-PDPA micelles. For the preparation of Triclosan containing films, 0.1 mg.mL^{-1} solution of Triclosan loaded βPDMA-*b*-PDPA micelles at pH 7.5 was used during film assembly. For microbiology experiments, each side of the coated wafers or glass slides were UV-sterilized for 1 hour. Film deposition was carried out under sterile conditions in a Class II Biosafety Cabinet. Film growth and pH-stability were monitored by measuring the dry film thickness using a spectroscopic ellipsometer of Optosense, USA (OPT-S6000). AFM imaging of the films was performed using an NT-MDT Solver P47 AFM in tapping mode using Si cantilevers. Roughness values were obtained from images with 2 x 2 μm scan size. TEM images were obtained using an FEI Tecnai G2 Spirit Bio-Twin CTEM operating at an acceleration voltage of 20 – 120 kV. A drop of either βPDMA-*b*-PDPA at pH 3.0, or Triclosan-loaded βPDMA-*b*-

PDPA micelles or unloaded βPDMA-*b*-PDPA micelles at pH 7.5 was placed on the surface of a copper grid coated with a carbon substrate with 3 mm diameter. After deposition of the βPDMA-*b*-PDPA unimers or micelles at the surface, samples were air-dried.

2.3.7. Preparation of Bacteria Growth Media

LB broth was used for the overnight cultivation of *S. aureus* ATCC 29213 and *E. coli* ATCC 8739. Mueller Hinton (MH) broth was used for the incubation of the blank and coated glass slides in the assays examining the antibacterial and anti-adhesive properties. Both of the media were autoclaved for sterilization prior to use. The pH of the MH broth was adjusted to either 5.5 or 7.5 after autoclaving. MH broth was filtered in a 0.45μm syringe filter to remove any bacterial contamination.

2.3.8. Viable Cell Counting of Surface-Adherent Bacteria

Cultures of *S. aureus* ATCC 29213 and *E. coli* ATCC 8739 in LB broth were adjusted to $OD_{600} \geq 0.2$ which corresponds to ~ 1.2×10^7 $CFU.mL^{-1}$ of bacteria. In a 24-well cell culture plate, mono- or multi-layer coated 1 cm x 1 cm glass slides were immersed into 1 mL MH Broth containing 25 μL of the above bacterial cultures or their 100x dilutions specifically for the assay with initial 10^5 $CFU.mL^{-1}$ bacteria concentration, and incubated at 37°C for 1 hour, 24 hours, or 48 hours. Each slide was washed three times in 1 mL sterile PBS (0.01 M phosphate buffer salts, 0.0027 M KCl, 0.137 M NaCl at pH 7.4). The slides were then removed from the wells and immersed in 5 mL of PBS (pH 7.4). The slides were vortexed at 2000 rpm for 1 minute, sonicated in a bath sonicator for 5 minutes, and vortexed at 2000 rpm for 1 minute. 100 μL of the sample was 100x diluted in PBS (pH 7.4) and 80 μL of this solution was spread-plated on LB agar. After an overnight incubation at 37°C, colonies of viable bacteria were counted.

2.3.9. Fluorescence Spectroscopy Assay

Multilayer coated or blank glass slides (1 cm x 1 cm) were incubated at pH either 7.5 or 5.5 for 1 hour in 1 mL MH broth containing 50 μL of a *S. aureus* ATCC 29213 culture. The glass slides were then washed 3 times with PBS (pH 7.4) and immersed into 2 mL PBS. After vortexing and sonication as mentioned in section II.VIII, each solution was pipetted into Eppendorf tubes and centrifuged at 8800 rpm for 10 minutes (Sigma 1-14 centrifuge, Germany) to increase the number of viable bacteria in the medium per unit volume. First, 300 μL of the pellet was pipetted into each well of the 96-well plate. Then, 1 μL of 1 mg.mL^{-1} C$_{12}$-Resazurin solution was added into each well. PBS was added into another well as a control for this step. The samples were incubated at 37°C for 45 minutes and fluorescence emission spectrum was recorded between 570 – 800 nm from 9 different points in each well of the 96-well plate using a Spectramax M5 Fluorescence Microplate Spectrophotometer (Molecular Devices, USA). C$_{12}$-Resazurin gets reduced to C$_{12}$-Resorufin in live cells, emitting fluorescence.

2.3.10. Light Microscopy

25 μL of *S. aureus* ATCC 29213 or *E. coli* ATCC 8739 cultures (from a broth containing ~ 1.2 x 10^7 CFU.mL^{-1}) were added onto coated and blank glass slides (control) which were already immersed into MH broth. Samples were incubated for 1 hour at 37°C in an incubator. The glass slides were then washed three times with PBS. The slides containing *S. aureus* ATCC 29213 were fixed under a flame and stained with Gram's crystal violet. Then, Gram's iodine solution and decolorizer were sequentially applied on the slides. The slides containing *E. coli* ATCC 8739 were fixed and stained with safranin only. All slides were examined under a 40X inverted light microscope (Leica, Germany).

2.3.11. Minimum Inhibitory Concentration (MIC) Analysis

25 mg.mL^{-1} Triclosan solution was prepared in ethanol (> 99.8 %). Different volumes of this Triclosan solution was added into 4 mL LB broth containing 50 μL of *S. aureus* ATCC 29213 culture (OD$_{600}$ = 0.4) or *E. coli* ATCC 8739 (OD$_{600}$ = 0.7) culture. The final Triclosan concentration in these mediums were 20, 10, 2, 1, 0.625, 0.2, 0.1 μg.mL^{-1} for the MIC determination of *S. aureus* and 60, 50, 40, 30, 20, 10, 2 μg.mL^{-1} for the MIC determination of *E. coli*. Medium without Triclosan was prepared as a control. All culture media were incubated in a shaker incubator at 37°C, 180 rpm until OD$_{600}$ of the control culture medium reached 0.4.

2.3.12. Kirby-Bauer Test

Agar plates containing MH broth at pH 7.5 or 5.5 were prepared. 80 μL of *S. aureus* ATCC 29213 or *E. coli* ATCC 8739 cultures (grown in LB medium up to OD$_{600}$ = 0.15) was spread-plated on MH agar. Mono- or multi-layer coated glass substrates were placed onto MH agar such that the uncoated sides of the glass slides touched the MH agar. The plates were incubated overnight at 37ºC and photographed.

2.3.13. Grams's Crystal Violet Staining Assay

Each coated or blank glass slide (1 cm x 1 cm) was placed in each well of a 24-well plate containing 1 mL of MH broth including 25 μL of *S. aureus* ATCC 29213 or *E. coli* ATCC 8739 cultures (from a broth of ~ 1.2 x 10^7 CFU.mL^{-1}) and incubated at 37°C for 1 hour, 24 hours, or 48 hours. Each slide was washed three times with 1 mL PBS (pH 7.4) and placed into 1 mL of 1 % Gram's crystal violet solution (diluted in PBS) and incubated at room temperature for 1 hour. Each slide was washed twice with 1 mL of PBS (pH 7.4) and then transferred into 400 μL of Gram's decolorizer solution. 300 μL of this solution was transferred into individual wells of a 96-well plate and the UV absorbance of each sample at 590 nm was recorded in a Multiscan Go Microplate Spectrophotometer (Thermo, USA). The value for the control was adjusted to 100%

and the experimental values were normalized accordingly. Gram's crystal violet is a positively-charged dye that can bind to negatively-charged components of a cell, such as the cell wall and DNA. However, it can also bind to negatively-charged surfaces. To eliminate the contribution of negatively-charged film components to the absorbance readings, mono- or multi-layer coated substrates which were not incubated in bacteria-containing growth media were also dipped into 1% Gram's crystal violet solution for 1 hour and the absorbance values were subtracted from that of the samples which were previously incubated in bacteria-containing growth media.

2.3.14. Protein Adsorption Assay

Bovine Serum Albumin adsorption on film coated and blank (control) glass slides was evaluated by microBCA assay. First, 1 cm x 1 cm glass slides were cut and cleaned as described in Section II.VI. Mono- and multi-layer films were deposited onto cleaned and sterilized 1 cm x 1 cm glass slides. Each glass slide (blank or coated) was placed in each well of a 24-well containing 1 mL of BSA solution (50 mg.mL^{-1} prepared in PBS). After 1 hour of incubation at 37°C, each substrate was carefully removed from the wells and washed three times with PBS. Then, the wafers were placed in 300 μL of PBS containing 0.5 M NaCl and 1% SDS and vortexed for 1 minute each to remove proteins from the substrate surface. Lastly, microBCA assay was carried out as described in the protocol. UV-Vis absorption spectra of these solutions were recorded using Multiscan Go Microplate Spectrophotometer (Thermo, USA). The absorbance values at 562 nm were recorded. The amount of BSA was determined using a calibration curve.

2.3.15. Statistical Analysis

Film thickness measurements were expressed as the means of three different measurements and the standard deviation (SD) of means. Results obtained in microbiology experiments were expressed as the means and standard error of means (SE) of at least three independent experiments, performed on separate days. Each set of experiment was analyzed by one-way Analysis of Variance (ANOVA). Holm-

Sidak's test was also performed as a multiple-comparisons test following ANOVA. Analysis between pair of groups was performed by unpaired one-tailed t-test with Welch's correction. Levels of significance were as follows: (*) $P<0.05$, (**) $P<0.01$, (***) $P<0.001$, (****) $P<0.0001$.

2.4. Results and Discussion

2.4.1. Preparation of βPDMA-b-PDPA Micelles

βPDMA-b-PDPA micelles were obtained by pH-induced self-assembly of βPDMA-b-PDPA in an aqueous environment above pH 6.5. First, βPDMA-b-PDPA was dissolved at pH 3 and the pH of the solution was increased gradually. Micellization occurred above pH 6.5 due to unprotonation of the amino groups resulting in loss of water solubility and enhanced hydrophobic-hydrophobic association among the PDPA blocks, triggering the self-assembly of βPDMA-b-PDPA. Micellization was followed by measuring the hydrodynamic size of the βPDMA-b-PDPA using dynamic light scattering technique. The significant increase in hydrodynamic size above pH 6.5 indicated the formation of micellar aggregates. The hydrodynamic size of βPDMA-b-PDPA was recorded as ~ 5.5 nm and ~ 16 nm at pH 3 and pH 7.5, respectively. Fig. 2.1A and 1B shows the number (%) versus size distributions of βPDMA-b-PDPA at pH 3 and pH 7.5. To prepare Triclosan-loaded βPDMA-b-PDPA micelles, βPDMA-b-PDPA was dissolved in Triclosan solution at pH 3. The pH of the solution was increased gradually to pH 7.5 and stirred at room temperature overnight. Considering the hydrophobic-hydrophobic interactions among Triclosan molecules and hydrophobic PDPA core blocks, we speculate that Triclosan was loaded mainly in the micellar cores. It is worthy of note that some of the Triclosan molecules could have also adsorbed onto the βPDMA coronal chains through either dipole-dipole interaction among the pendant groups of βPDMA and Triclosan or hydrophobic-hydrophobic interactions among βPDMA backbone and Triclosan. Triclosan loaded βPDMA-b-PDPA micelles had slightly higher hydrodynamic size (~ 20 nm) after an overnight loading period at room temperature than that of the unloaded BCMs (Fig. 2.1C). The chemical structure of βPDMA-b-PDPA and the graphical representation of a

Triclosan-loaded βPDMA-*b*-PDPA micelle are presented in Scheme 2.1. Figure 2.2. presents the TEM images of βPDMA-*b*-PDPA unimers at pH 3 (Fig. 2.2A), βPDMA-*b*-PDPA micelles at pH 7.5 (Fig. 2.2B) and Triclosan loaded βPDMA-*b*-PDPA micelles at pH 7.5 (Fig. 2.2C) and demonstrates the spherical morphology of the βPDMA-*b*-PDPA micellar aggregates after micellization. Both βPDMA-*b*-PDPA micelles and Triclosan loaded βPDMA-*b*-PDPA micelles carried positive charge at pH 7.5. The zeta potential values of βPDMA-*b*-PDPA micelles and Triclosan loaded βPDMA-*b*-PDPA micelles were recorded as ~ 6 mV and ~ 4 mV, respectively. Considering the fact that the zwitterionic coronae of βPDMA-*b*-PDPA micelles are electrically neutral, the positive zeta potential at pH 7.5 should arise from the positive charges which remained at the surface of the PDPA core (pK_a of PDPA is ~6 [51]). We have previously reported on the pH-responsive behavior of βPDMA-*b*-PDPA in detail [53].
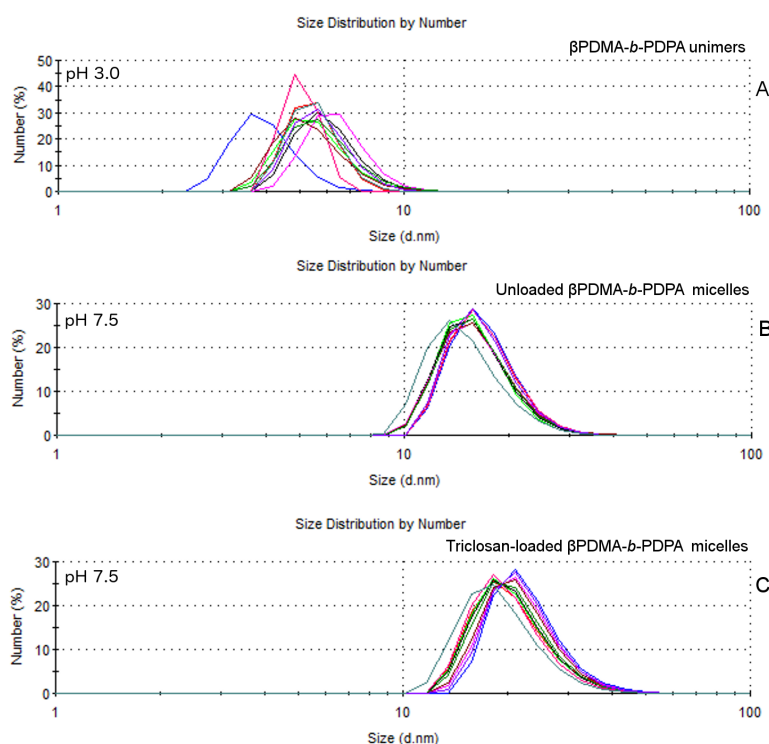
Fig. 2. 1. Number (%) versus size distributions of βPDMA-*b*-PDPA unimer at pH 3.0 (A), unloaded βPDMA-*b*-PDPA micelle at pH 7.5 (B), and Triclosan-loaded βPDMA-*b*-PDPA micelle at pH 7.5 (C) (acquired from [54]).
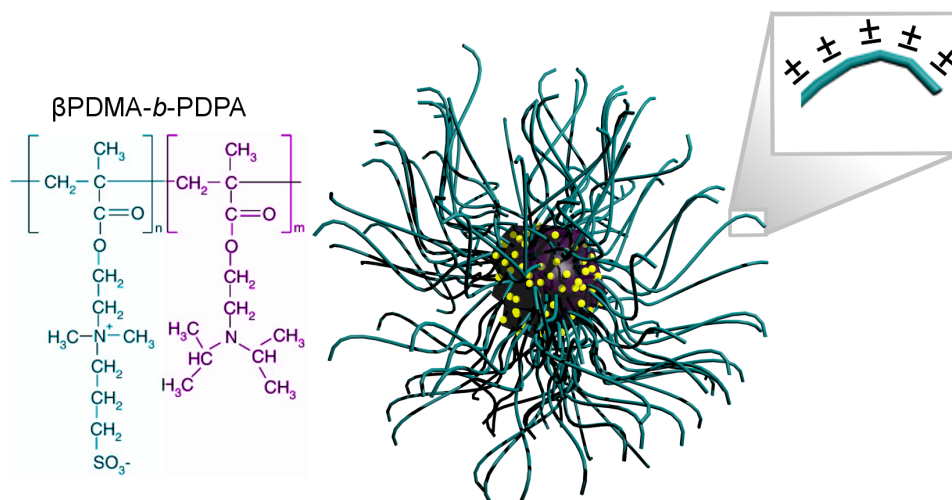
Scheme 2. 1. The chemical structure of βPDMA-*b*-PDPA and the graphical representation of a Triclosan-loaded βPDMA-*b*-PDPA micelle. Yellow spots represent the Triclosan molecules (acquired from [54]).
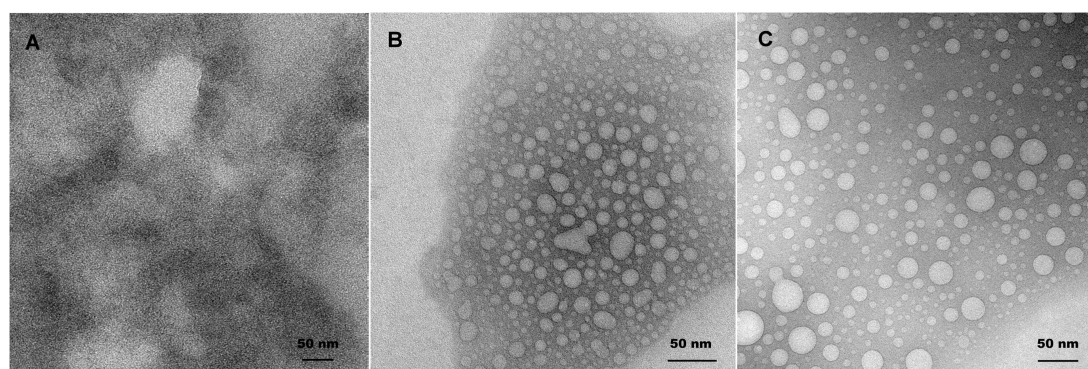
Fig. 2. 2. TEM images of βPDMA-*b*-PDPA unimers at pH 3 (Fig. 2.2A), βPDMA-*b*-PDPA micelles at pH 7.5 (Fig. 2.2B) and Triclosan loaded βPDMA-*b*-PDPA micelles at pH 7.5 (Fig. 2.2C) (acquired from [54]).

2.4.2. Preparation of Mono- and Multi-Layer Films

Monolayer films were prepared by self-assembly of βPDMA-*b*-PDPA micelles at the surface at pH 7.5. The driving force for monolayer deposition of βPDMA-*b*-PDPA micelles was the electrostatic interactions among the partially negatively charged silanol groups of the glass/silicon wafer substrates and quaternized amino groups of the zwitterionic βPDMA-coronal chains as well as the positively charged PDPA micellar cores.

Multilayer films were constructed by LbL deposition of βPDMA-*b*-PDPA micelles and PSS at pH 7.5. The primary driving force for LbL growth was electrostatic interactions among positively charged PDPA core surfaces of βPDMA-*b*-PDPA micelles and the negatively charged PSS. Recently, we reported that when βPDMA-*b*-PDPA micelles were completely neutral, e.g. at pH 8.5, LbL films of βPDMA-*b*-PDPA micelles and PSS could not be formed through electrostatic interactions among quaternized ammonium groups of βPDMA coronae and sulfonate groups of PSS. Multilayers could be constructed at pH 8.5 only if the negative charges of the zwitterionic units were screened through complexation of the βPDMA coronal chains with poly(allyl amine hydrochloride) (PAH) [53]. Therefore, we suggest that the main driving force for LbL growth at pH 7.5 was the electrostatic interaction among the positively charged PDPA core surface and sulfonate groups of PSS rather than the electrostatic interaction among quaternized ammonium groups of βPDMA coronae and sulfonate groups of PSS.

As seen in Figure 2.3., multilayer growth showed an exponential growth profile when the thickness was plotted as a function of every βPDMA-*b*-PDPA micellar layer. However, when film thickness is monitored for every βPDMA-*b*-PDPA micelle and PSS layers, the growth profile deviates from exponential growth (Fig. 2.3., inset). This can be explained by the higher increment in thickness upon deposition of βPDMA-*b*-PDPA micelles than that of PSS. βPDMA-*b*-PDPA micellar layers formed ~ 77% of the total film thickness. Of note, the initial irregular growth (the first four data point in the inset) is attributed to weak binding of the polymers at the substrate which was

73

overcome after deposition of the first couple of layers at the surface. Figure 2.4. shows the AFM images of mono- and multi-layer films of βPDMA-*b*-PDPA micelles with 0.5 x 0.5 μm scan size as well as the roughness values obtained from images with 2 x 2 μm scan size.
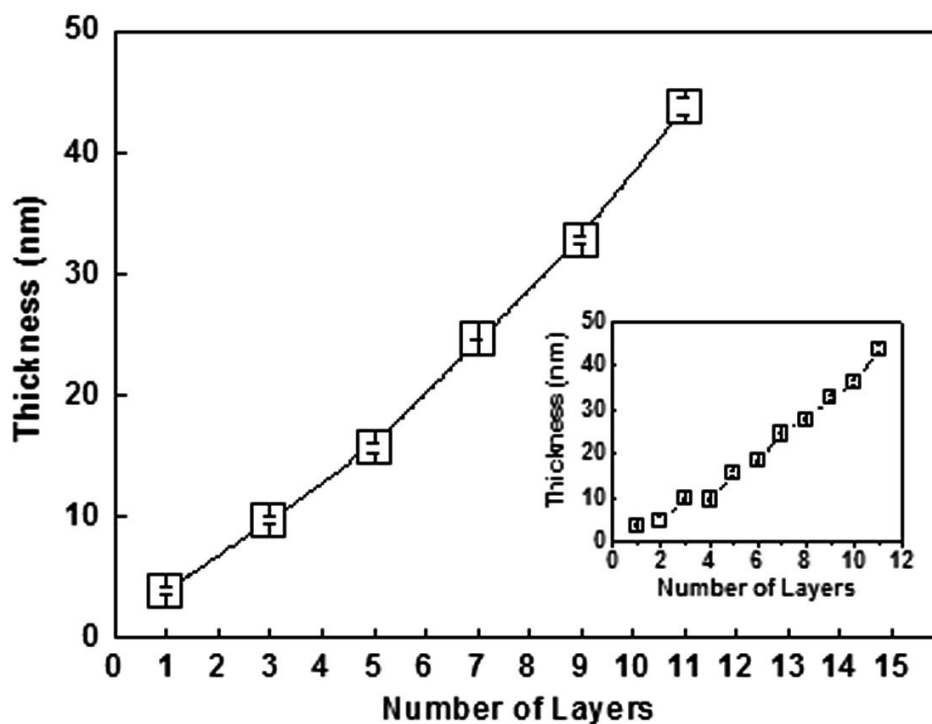
Fig. 2. 3. LbL growth of βPDMA-*b*-PDPA micelles and PSS films at pH 7.5 (acquired from [54]).

1-layer film (Roughness = 0.54 nm)

3-layer film (Roughness = 1.36 nm)

5-layer film (Roughness = 1.48 nm)
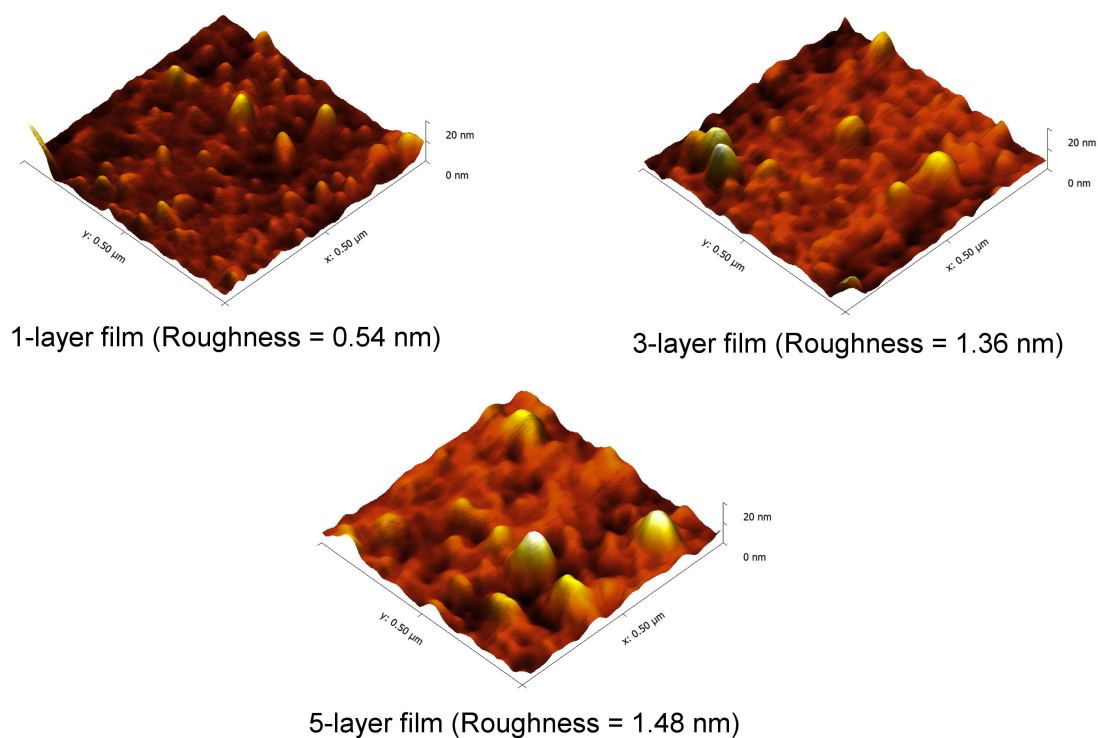
Fig. 2. 4. AFM images (0.5 x 0.5 µm scan size) and rms roughness values of 1-, 3-, 5-layer films of βPDMA-*b*-PDPA micelles (acquired from [54]).

2.4.3. pH-stability of βPDMA-*b*-PDPA Micelles and PSS Films

We examined the pH-stability of the films prior to bacterial anti-adhesive tests by immersing the 5-layer films of βPDMA-*b*-PDPA micelles and PSS into PBS at either pH 7.5 or pH 5.5 at 25°C for 1 hour. The coated substrates were then removed and dried under N_2 flow. Same experiments were also performed at 37°C. Figure 5.5. shows the fraction retained at the surface after 1 hour at 25°C or 37°C at pH 7.5 or pH 5.5.

5-layer βPDMA-*b*-PDPA micelles and PSS films were completely stable within 1 hour time period at pH 7.5 at both 25°C and 37°C. Of note, ~ 25% of the film was removed from the surface at pH 7.5 when multilayers were constructed using Triclosan-loaded βPDMA-*b*-PDPA micelles (data not shown). The loss in film thickness can be correlated with the self-diffusion of Triclosan molecules, which may have also

dislodged any loosely bound macromolecules from the surface. Despite the disintegration of βPDMA-*b*-PDPA micelles below pH 6.5, only ~ 20% of the film was released from the surface within 1 hour when the multilayers were immersed into PBS solution at pH 5.5 and 25°C. The decrease in film thickness was only 5% after exposure to PBS at pH 5.5 and 37°C for 1 hour. These results indicated a restructuring within the multilayers due to reassociation among negatively charged PSS and positively charged PDPA blocks or quaternized ammonium groups of βPDMA blocks of the βPDMA-*b*-PDPA unimers. The loss can be correlated with the partial release of macromolecules from the surface due to formation of a charge imbalance within the multilayers upon protonation of the PDPA core blocks at pH 5.5. The disintegration of LbL films arising from the charge imbalance within the multilayers has been previously reported by Sukhorukov [55] and Schlenoff [56]. We did not record any loss in film thickness at pH 5.5 in 1 hour when multilayers were constructed using Triclosan loaded βPDMA-*b*-PDPA micelles (data not shown).
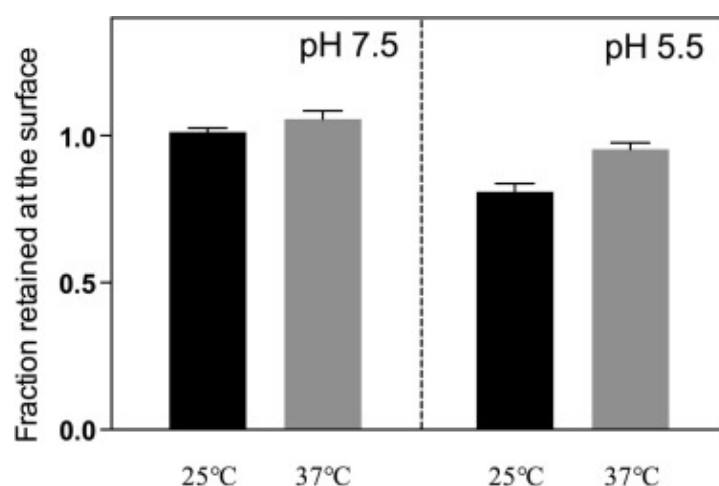
Fig. 2. 5. Fraction retained at the surface of 5-layer films of βPDMA-*b*-PDPA micelles/PSS after exposure to PBS at pH 7.5 (Panel A) or pH 5.5 at 25°C or 37°C (Panel B) for 1 hour (acquired from [54]).

2.4.4. Bacterial Anti-Adhesive Properties of Mono- and Multi-Layers of βDMA-*b*-PDPA Micelles Against *S. aureus*

Agar plating method was used to examine the anti-adhesive properties of the mono- and multi-layer films of βPDMA-*b*-PDPA micelles using lag-phase cultures of *Staphylococcus aureus* ATCC 29213. The results were supported by light microscopy images. MH broth, commonly used for antibiotic susceptibility tests, was used as the medium in order to limit rapid bacterial growth and allow the observation of the viability of bacteria with minimal error.

As seen in Figure 2.6A, the most anti-adhesive property (lowest number of adhered bacteria) was observed on glass substrates coated with 3 layers of βPDMA-*b*-PDPA micelles and PSS. The number of bacteria on a monolayer coated substrate was ~ 28% higher than that detected on the 3-layer coated substrate. The enhanced anti-adhesive property of 3-layer film can be attributed to higher surface coverage by βPDMA-*b*-PDPA micelles as the layer number increased. However, the number of adhered bacteria increased by ~ 190% when layer number was increased from 3 to 5. Light microscopy images (Figure 2.6B-E) illustrate the difference in the amount of bacteria adhered onto bare glass slide, and glass slides coated with 1-, 3- and 5-layer films of βPDMA-*b*-PDPA micelles.

It was previously reported that rough surfaces were better sites for bacterial accumulation [57], although different strains of bacteria have different preferences of surface roughness [58]. Considering the fact that the difference in surface roughness was not significant between 3- and 5- layer films (1.36 nm and 1.48 nm for 3- and 5-layer films, respectively, Fig. 2.4.), we correlate the decrease in the anti-adhesive property of 5-layer films with the decrease in the number of free zwitterionic units rather than an increase in surface roughness. Of note, interpenetration between the layers increases as the substrate effect diminishes with increasing number of layers. Therefore, we speculate that the extent of interpenetration at the outermost part of a 5-layer film is higher than that of a 3-layer film resulting in lower number of free zwitterionic units and a decrease in anti-adhesive property.
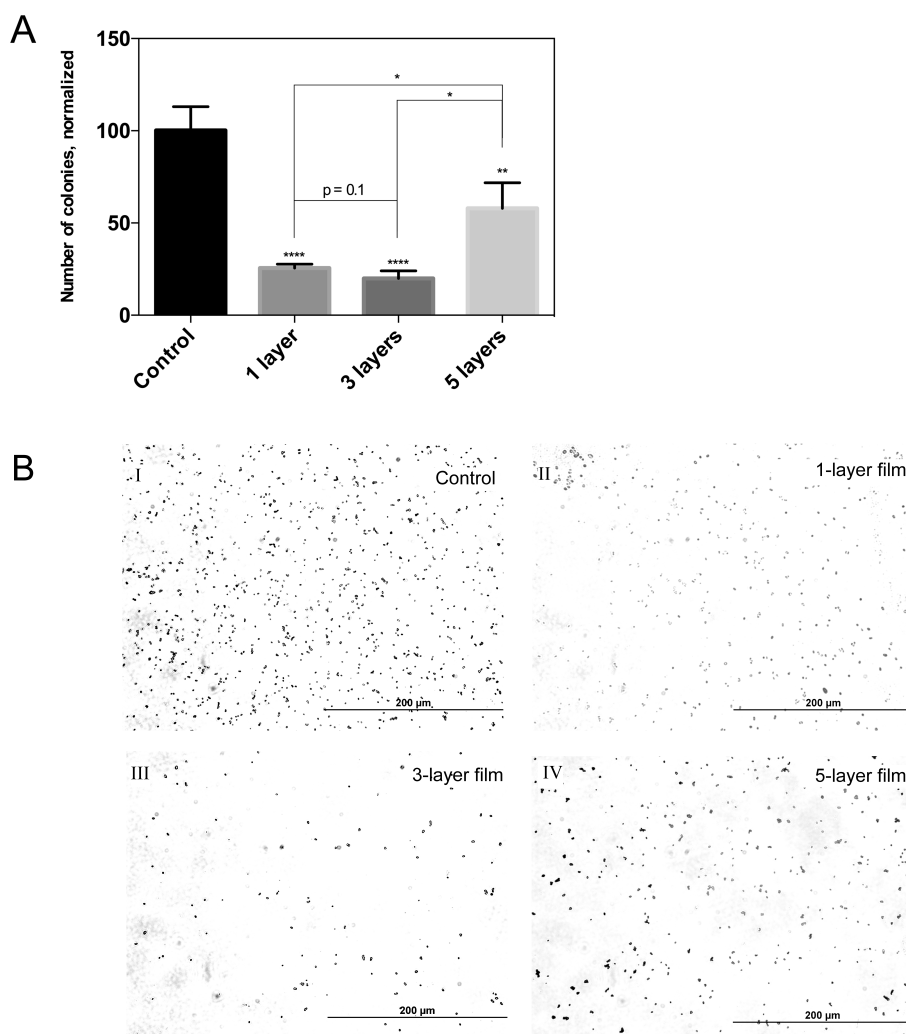
Fig. 2. 6. Panel A: Number of colonies on 1-, 3- and 5- layer films of βPDMA-*b*-PDPA micelles after 1 hour incubation at pH 7.5 with *S. aureus*. Number of colonies for each control group is normalized to 100. *t*-test comparison for the values are significant *$P < 0.05$*, unless otherwise stated. Error bars represent standard error (SE) of mean. **Panel B:** Light microscopy images of the blank substrate (I) and the substrates coated with 1- (II), 3- (III); 5- (IV) layer films of βPDMA-*b*-PDPA micelles after 1 hour incubation with *S. aureus* (acquired from [54]).

2.4.5. Effect of Triclosan Release from The Surface on The Antibacterial Properties of The Multilayers Against *S. aureus*

Our previous study reported that βPDMA-*b*-PDPA did not exhibit antibacterial effect towards *S. aureus* in PBS at pH 3.0 and pH 7.5 when βPDMA-*b*-PDPA was in the unimer and micellar form, respectively [34]. In this study, we aimed to introduce dual functionality to mono- and multi- layer films of βPDMA-*b*-PDPA micelles, i.e. anti-adhesive and pH-induced antibacterial agent release properties at moderately acidic conditions. In this way, additional antibacterial functionality can compensate for the anti-adhesive property at defective or non-homogeneous sites and/or deliver antibacterial agents to moderately acidic locations in the body, e.g. the site of infection.

Triclosan was chosen as a model hydrophobic antibacterial agent that is bacteriostatic at low doses, but bactericidal once the dose is elevated. It is known to inhibit cell wall and membrane synthesis of MRSA [59]. Minimum inhibitory concentration (MIC) of Triclosan was found to be 2 −10 $\mu g.mL^{-1}$ for *S. aureus* ATCC 29213 that could reach $\sim 2 \times 10^7$ $CFU.mL^{-1}$ concentration after overnight incubation. Prior to film assembly, Triclosan was loaded within the BCMs, which were then used as building blocks to prepare mono- and multi-layer films. Effect of Triclosan release on the number of bacteria adhered on the surface was examined at pH 7.5 and pH 5.5 using fluorescence staining, Kirby-Bauer test and agar plating techniques.

2.4.5.1. Fluorescence Staining

We carried out fluorescence staining of bacteria using the C_{12}-Resazurin dye to determine the amount of living bacteria that adhered onto the films. This technique is based on the fact that the intensity of fluorescence emission of reduced C_{12}-Resazurin (C_{12}-Resorufin) is proportional to the number of live bacterial cells. Figure 2.7A contrasts the normalized intensity of C_{12}-Resorufin for bare glass substrate, 1-, 3- and 5- layer films at pH 7.5 and pH 5.5. For each pH value, the result obtained for control

substrate (bare glass) was assumed as 100 % and the results obtained for 1-, 3- and 5-layers films were normalized accordingly.

As seen in Figure 2.7A, the number of living bacteria decreased when films containing Triclosan loaded micelles were incubated in medium at pH 5.5. The difference in the number of bacteria between pH 7.5 and pH 5.5 was more distinct with increasing number of layers due to release of higher amount of Triclosan from the surface. The decrease in the number of bacteria at pH 5.5 can be correlated with the protonation of PDPA blocks and disintegration of the micellar cores resulting in release of Triclosan molecules and initiation of the antibacterial effect. It is important to emphasize that we did not record loss in film thickness for 2 hours at pH 5.5 despite the pH-induced disintegration of βPDMA-*b*-PDPA micelles. This indicates a restructuring among βPDMA-*b*-PDPA unimers and PSS chains within the multilayers rather than a complete destruction of the films even after disintegration of the micelles. Scheme 2 illustrates the changes in film structure when films were exposed to media at pH 5.5. Of note, in contrast to results obtained from mono- and multi-layer films of Triclosan loaded βPDMA-*b*-PDPA micelles, we found that the number of bacterial colonies that adhered onto mono- and multi-layer films of unloaded βPDMA-*b*-PDPA micelles at pH 5.5 was higher than that at pH 7.5 (Figure 2.8.). This can be explained by the increased amount of positive charge at the outermost part of the films due to protonation of the 3° amino groups on the PDPA blocks at pH 5.5, enhancing the interaction between the surface and negatively charged bacteria cell wall and adherence of organisms at the surface. Thus, a comparison of the results obtained from films of unloaded and Triclosan loaded βPDMA-*b*-PDPA micelles at pH 7.5 and pH 5.5 also confirmed the effect of Triclosan release and initiation of the antibacterial effect at moderately acidic conditions.
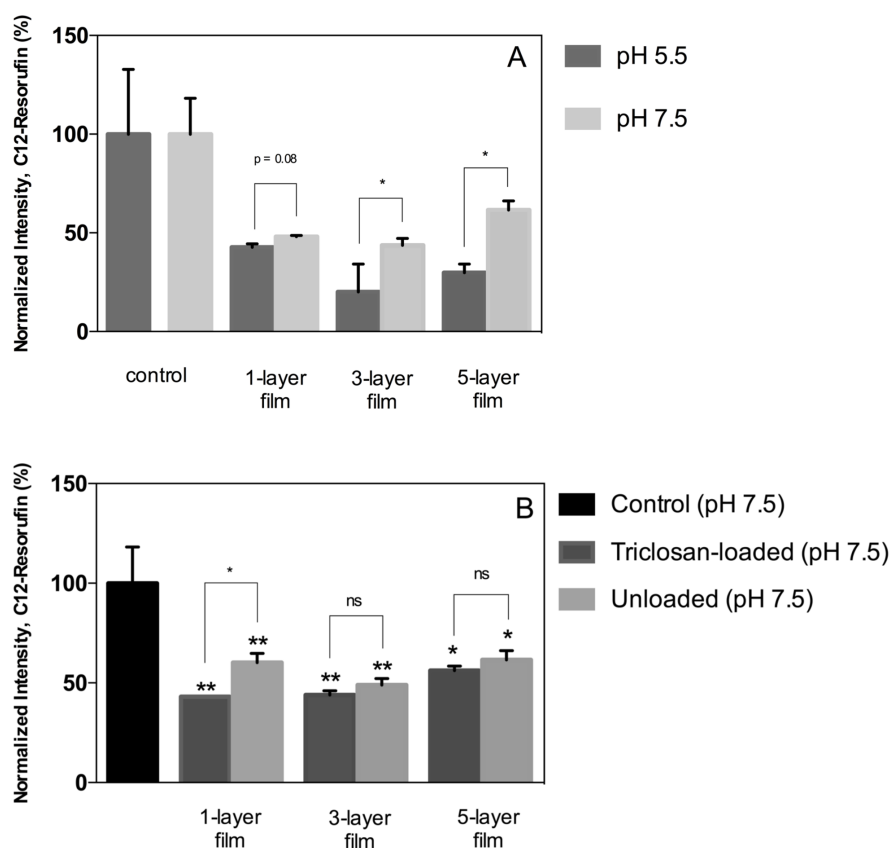
Fig. 2. 7. Panel A: Normalized intensity of C_{12}-Resorufin for bare glass substrates (control) and glass substrates coated with 1-,3-, 5- layers of Triclosan loaded βPDMA-*b*-PDPA micelles, at pH 7.5 and pH 5.5. For each pH value, the intensity of C_{12}-Resorufinfor the control was assumed as 100% and the intensities for 1-, 3- and 5-layer films were normalized accordingly. Error bars represent the standard error (SE) of mean. **Panel B:** Normalized intensity of C_{12}-Resorufin for bare glass substrates (control) and glass substrates coated with 1-,3-, 5- layers of unloaded and Triclosan loaded βPDMA-*b*-PDPA micelles at pH 7.5 (acquired from [54]).
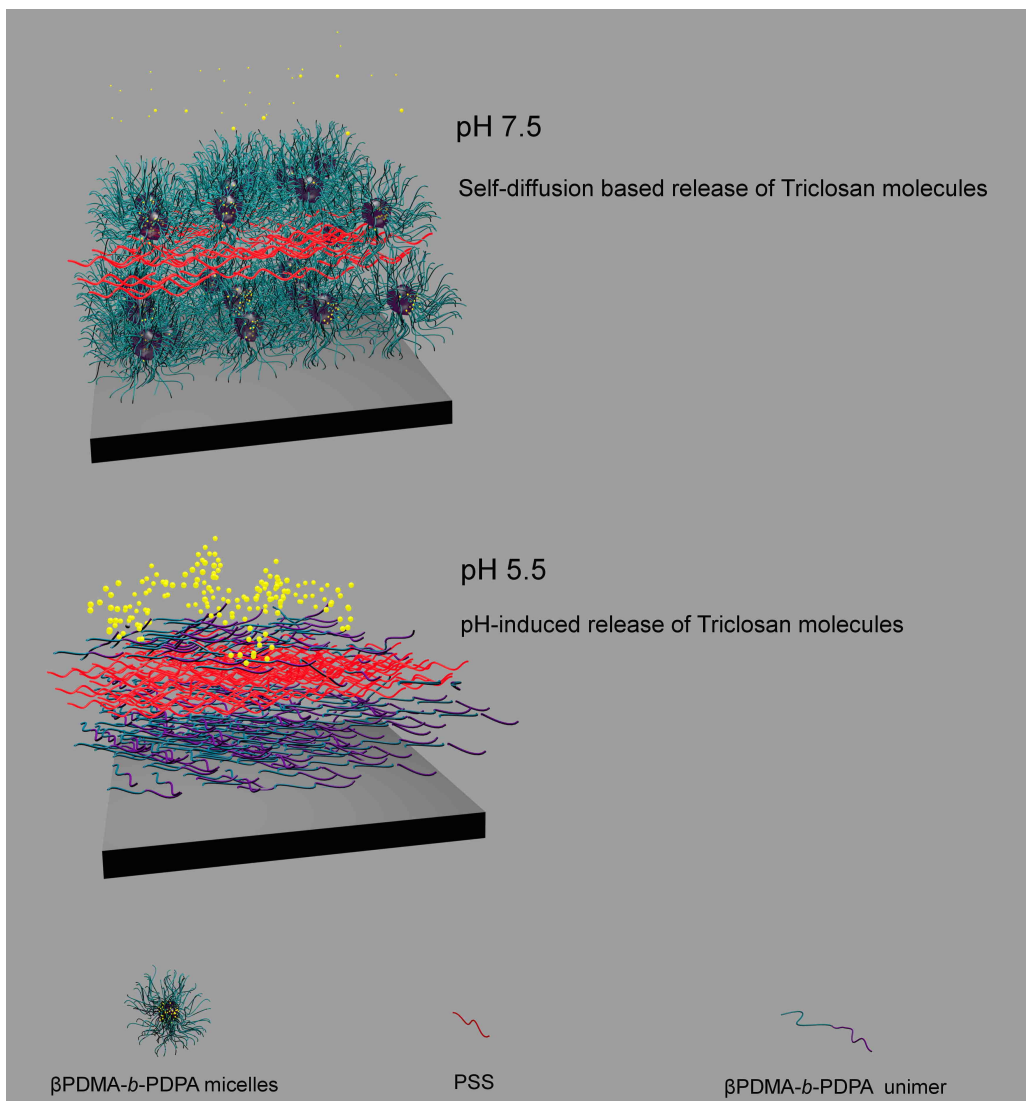
Scheme 2. 2. Graphical representation of a 3-layer film of βPDMA-*b*-PDPA micelles and PSS at physiological conditions (pH 7.5) and moderately acidic conditions (pH 5.5) (acquired from [54]).
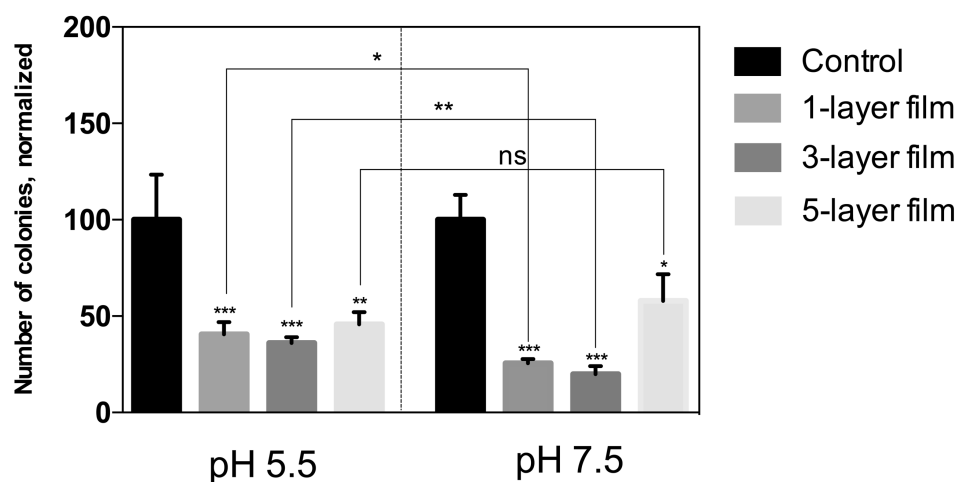
Fig. 2. 8. The difference between the number of colonies on a monolayer of βPDMA-*b*-PDPA micelles; 3- and 5- layer films of βPDMA-*b*-PDPA micelles and PSS after a 1 hour incubation at pH 5.5 and 7.5 with *Staphylococcus aureus*. The assay is carried out by agar plating. Number of colonies for each control group is normalized to 100 (acquired from [54]).

To further confirm the pH-induced release of Triclosan at pH 5.5 and its effect on the number of adhered bacteria, we have also contrasted the fluorescence intensity of C_{12}-Resazurin obtained from mono- and multi- layer films of unloaded and Triclosan loaded βPDMA-*b*-PDPA micelles at pH 7.5 as a control experiment (Fig. 2.7B). In contrast to pH-triggered release of Triclosan at pH 5.5, βPDMA-*b*-PDPA micelles remains intact at pH 7.5 and Triclosan release from the βPDMA-*b*-PDPA micelles is expected to occur only through self-diffusion, thus the total amount released should be smaller than that at pH 5.5. As seen in Figure 2.7B, Triclosan loading into βPDMA-*b*-PDPA micelles did not make a significant difference on the number of bacteria adhered onto the surface at pH 7.5.

2.4.5.2. Kirby-Bauer Test

Kirby-Bauer test is an antibiotic susceptibility test designed to determine the susceptibility of a strain of bacterium towards one or more antibiotics. We have carried out a modified version of the Kirby-Bauer test where we could reduce the amount of Triclosan that is released from film-coated glass substrates, by comparing the diameters of the "zone of inhibition" around the substrates placed on agar.

We found that monolayer film of Triclosan loaded βPDMA-*b*-PDPA micelles had the minimal antibacterial effect on *S. aureus* ATCC 29213. A clear zone of inhibition of bacterial growth was not observed both at pH 7.5 and pH 5.5 (Fig. 2.9A and 2.9B). In contrast, 3- and 5-layer films of Triclosan loaded βPDMA-*b*-PDPA micelles showed a clear zone of inhibition of bacterial growth on MH agar at both pH values. At pH 7.5, 3.0 cm and 3.3 cm of inhibition zones were recorded for the 3- and 5-layer films, respectively (Fig. 2.9C and 2.9E). However, a larger zone with clear edges was observed at pH 5.5 (3.2 cm and 3.5 cm of inhibition zones for 3- and 5-layer films, respectively) due to pH-induced release of Triclosan at moderately acidic conditions (Fig. 2.9D and 2.9F). The difference in the images is more obvious for 5-layer films due to higher amount of Triclosan release from multilayers with higher number of layers. To further confirm the effect of Triclosan release on antibacterial activity, we performed a control experiment in which we carried out the Kirby-Bauer Test on the MH agar plate with the 5-layer film of unloaded βPDMA-*b*-PDPA micelles at pH 7.5 and pH 5.5. As seen in Figure 2.9G and 2.9H, no antibacterial activity was observed when multilayers were constructed using unloaded βPDMA-*b*-PDPA micelles.
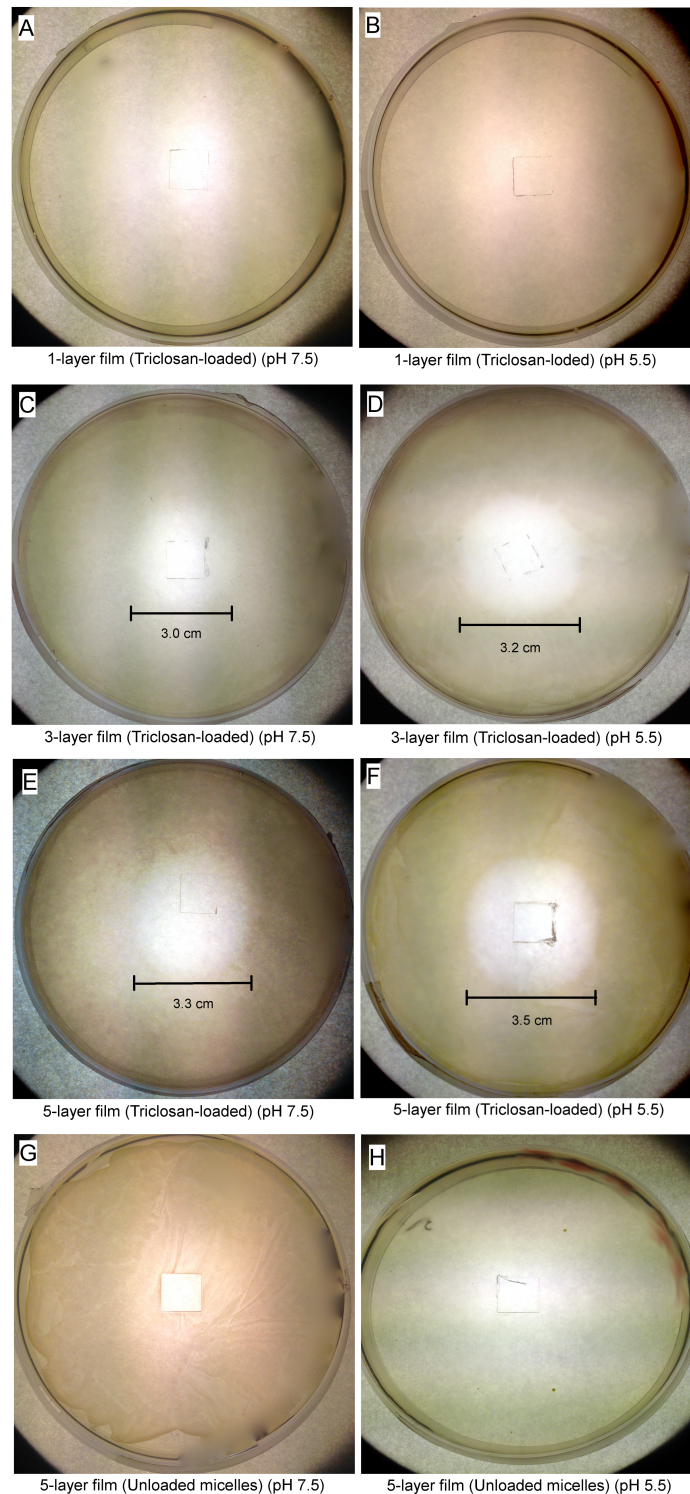
Fig. 2. 9. Kirby-Bauer test from 1-; 3- and 5- layer films of βPDMA-*b*-PDPA micelles. 5-layer films of unloaded βPDMA-*b*-PDPA micelles and PSS at pH 7.5 and pH 5.5 were used as control (acquired from [54]).

2.4.5.3. Agar-Plating Method

The antibacterial activity of the films was also studied by the agar plating method. Agar-plating method is used to determine the viability of bacteria and the number of viable, colony-forming bacteria. Results obtained from agar plating method were in good agreement with the trends observed in fluorescence staining and Kirby-Bauer tests. The effect of pH-induced Triclosan release on the number of viable bacteria was remarkable especially for 3-layer films and the number of viable bacteria was even less at pH 5.5 (Fig. 2.10.). Importantly, the difference in the number of bacteria between the control substrates and 5-layer films was distinct at both pH 5.5 and 7.5, most likely due to greater amounts of Triclosan molecules released from the surface.
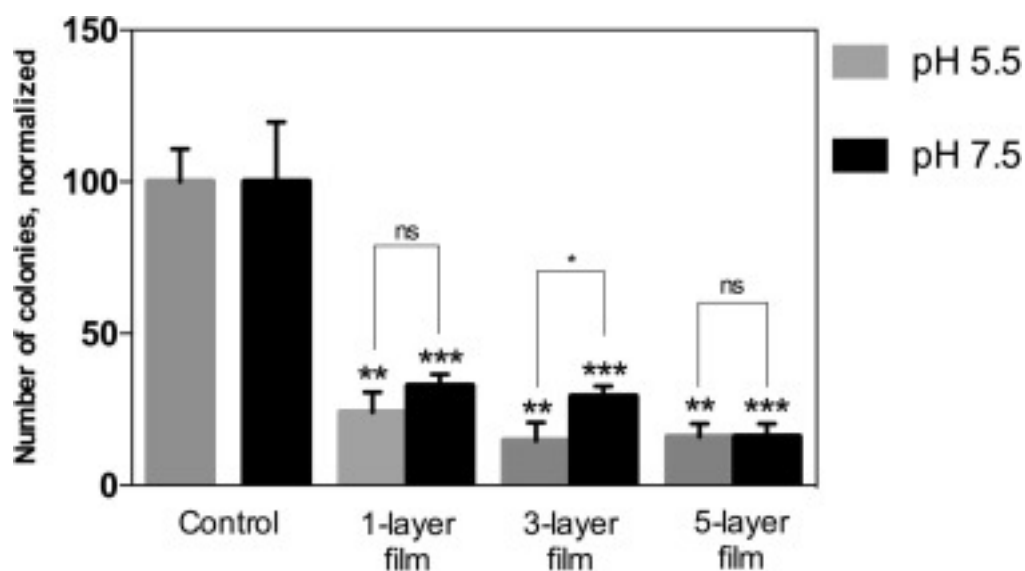
Fig. 2. 10. Number of colonies on 1-, 3- and 5- layer films of Triclosan-loaded βPDMA-*b*-PDPA micelles after 1-hour incubation with *S. aureus*. Control results for each pH are normalized to 100. Error bars represent standard error (SE) of mean (acquired from [54]).

Although a similar trend with the results of fluorescent staining technique was obtained, the effect of Triclosan release on the antibacterial activity did not reach statistical significance at pH 5.5 and 7.5 when the bacterial concentration was 10^7 CFU.mL^{-1} (Fig. 2.11.). This is probably because of the error-prone nature of the agar-

plating method and the large standard deviation of the values. To circumvent the effect of the large standard deviation and attain statistically significant results, we lowered the initial concentration of bacteria containing medium to 10^5 CFU.mL^{-1}, so that the amount of Triclosan acting on bacteria was increased by 100 fold. As more Triclosan molecules acted on each bacterium, the number of viable bacteria adhering on Triclosan-releasing films diminished significantly compared to the control values.
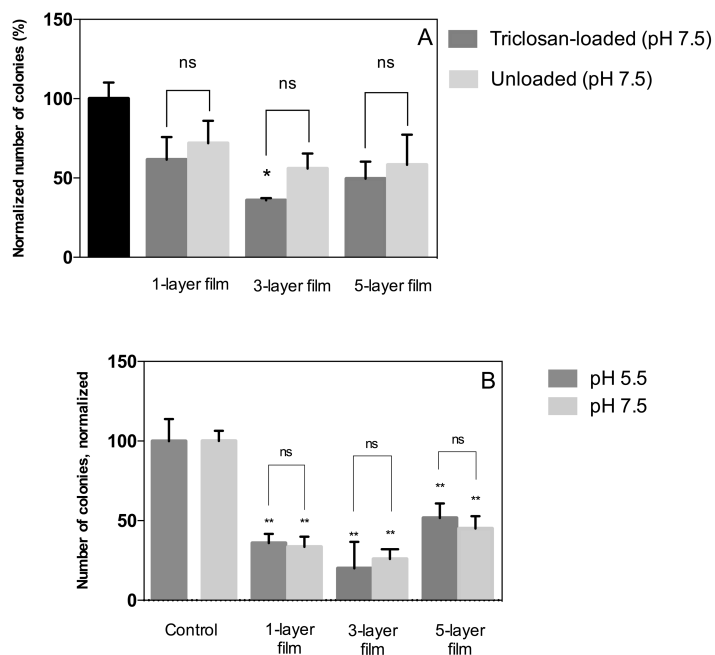
Fig. 2. 11. Panel A: Number of colonies on a monolayer of Triclosan-loaded βPDMA-*b*-PDPA micelles, 3- and 5- layer films of unloaded and Triclosan-loaded βPDMA-*b*-PDPA micelles and PSS after 1-hour incubation with *Staphylococcus aureus* at pH 7.5 **Panel B:** Films of Triclosan-loaded βPDMA-*b*-PDPA micelles and PSS after 1-hour incubation with *Staphylococcus aureus* at pH 5.5 and 7.5. Control results for each pH are normalized to 100 (acquired from [54]).

2.4.5.4. Gram's Crystal Violet Staining Assay

Considering the fact that a surface with lower amount of adhered biomass would have less tendency to cause biofilm formation, we carried out Gram's crystal violet staining

assay to determine the total amount of biomass (including the bacteria and the components of biofilms) adsorbed onto film-coated substrates. Crystal violet is a positively-charged reagent which stains the living and dead cells as well as any negatively-charged film and matrix components. Thus, to eliminate the contribution of negatively-charged film components to the absorbance readings, mono- or multi-layer coated substrates that were not incubated in bacteria-containing growth media were also immersed in 1% Gram's crystal violet solution for the same time period and the absorbance values were subtracted from that of the samples which were previously incubated in bacteria-containing growth media. Figure 2.12. shows biomass formation at the surface after 1 hour incubation with bacteria. Higher normalized UV absorbance (%) corresponded to stronger staining and thereby more accumulated biomass. We found that the absorbance values obtained from mono- and multi-layer films of Triclosan loaded βPDMA-*b*-PDPA micelles were lower than that of the films including unloaded βPDMA-*b*-PDPA micelles both at pH 7.5 and pH 5.5, indicating an effect of pH-induced release of Triclosan on eliminating bacterial growth and thereby the development of biofilms. Similar to the trends observed in the fluorescence staining and the agar-plating methods, 3-layer films of Triclosan loaded βPDMA-*b*-PDPA micelles exhibited the lowest amount of biomass accumulation at pH 7.5, whereas the amount of accumulated biomass onto 3- and 5- layer films of βPDMA-*b*-PDPA micelles was remarkably low at pH 5.5 due to pH-induced release of Triclosan from the surface. Similar to our observations in the fluorescence staining and the agar-plating methods, 3-layer film of Triclosan-loaded βPDMA-*b*-PDPA micelles exhibited minimal bacterial adherence and accumulation of biomass.
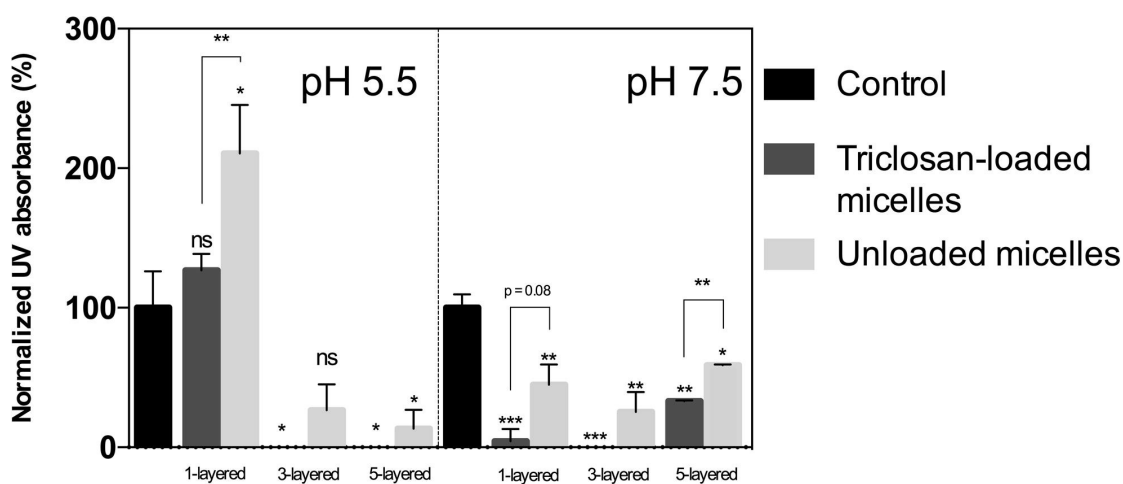
Fig. 2. 12. Normalized UV-Visible Absorbance (%) data for 1-, 3- and 5- layer films of Triclosan-loaded and unloaded βPDMA-*b*-PDPA micelles at pH 7.5 and pH 5.5, determined by crystal violet staining assay. UV•Vis absorbance (OD_{590}) of crystal violet was normalized to 100% for control values at pH 5.5 and 7.5. Error bars represent the standard error (SE) of mean. (ns = not significant) (acquired from [54]).

2.4.6. Protein Adsorption Assay

In addition to Van der Walls forces, electrostatic interactions and hydrophobic interactions, there are proteinaceous adhesins responsible for the adherence of bacteria on surfaces [60]. Thus, if protein based adherence of bacteria is reduced, biofilm development can be postponed. Albumin is the dominant protein in the human serum and comprises about 60-65% of all serum protein pool [61].

We examined the anti-adhesive property of the mono- and multi-layers of unloaded βPDMA-*b*-PDPA micelles against albumin to determine any correlation between protein adsorption and bacterial anti-adhesive properties of the coatings. The concentration of albumin is approximately 25 $mg.mL^{-1}$ in human blood plasma, considering an average blood volume of 5 L. Only 42% of all albumin in the body is held by the plasma [62]. To mimic the conditions of the biointerface where the substrate interacts the blood in the body, we immersed the mono- or multi-layer coated substrates in PBS (pH 7.4) containing 50 $mg.mL^{-1}$ BSA. Using a microBCA assay, the

UV absorbance values from 3 replicates of each film were recorded. The amount of BSA adsorbed on each film was calculated using a calibration curve.

As shown in Fig. 2.13., BSA adsorption on 3-layer films was lower than that on mono- and 5-layer films. These results are in good agreement with the results obtained using fluorescence staining and agar-plating methods indicating both bacteria and protein-repelling properties, especially for 3-layer films. These results suggest that the interaction of cell wall anchored proteinaceous adhesins of *S. aureus* with coated substrates could be a mechanism of bacterial adherence. Cheng et al. also indicated a correlation between protein resistance and bacterial anti-adhesive properties of zwitterionic poly (sulfobetaine methacrylate) surfaces [27,33]. However, it is worth to note that bacterial adherence is not always directly dependent on protein adsorption. Ostuni et al. reported that self-assembled monolayers of materials that were known to have protein resistance property did not always exhibit anti-adhesive property against *S. aureus* and *Staphylococcus epidermidis* strains of bacteria [63].
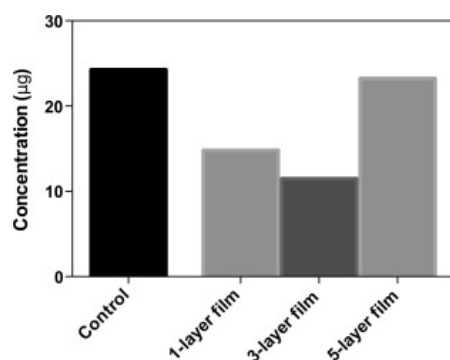
Fig. 2. 13. Amount of BSA adsorbed onto 1-, 3- and 5- layer films of βPDMA-*b*-PDPA micelles. Results are the corresponding best-fit value of 3 different values collected for each type of substrate ($^{*}P< 0.05$) (acquired from [54]).

2.4.7. Bacterial Anti-Adhesive and Antibacterial Properties of 3-layer Films of ßDMA-PDPA Micelles Against *E. coli*

The organization of the cell wall of a Gram-negative bacterium is distinctly different than that of a Gram-positive bacterium, which might lead to a different nature of

adherence and propagation at the surfaces. Therefore, we also tested the bacterial anti-adhesive and antibacterial properties of the films against a model Gram-negative bacterium *E. coli*. *E. coli* is a Gram-negative facultative anaerobic bacterium and is one of the predominant pathogens causing community-onset and hospital-acquired infections. Non-pathogenic *E. coli* is commonly found in the intestines of warm-blooded organisms, but some subtypes of *E. coli* are pathogenic and cause infections through association with medical devices and catheters [64]. We tested the multilayer films against an isolate of *E. coli* that has low sensitivity to Triclosan and determined the bacterial anti-adhesive or antibacterial behaviour of the coatings with or without Triclosan loaded BCMs. The minimum inhibitory concentration (MIC) of the *E. coli* isolate was found to be > 30 μg.mL^{-1} for a culture that could reach a bacterial concentration of ~ 1.3 x 10^7 CFU.mL^{-1} after overnight incubation. The maximum concentration of Triclosan solution that we could prepare was 30 μg.mL^{-1} due to hydrophobic nature of Triclosan and its low solubility in an aqueous medium. Thus, the Triclosan-sensitivity of the *E. coli* strain used in this study was much lower than that of *S. aureus*.

Guided by the results obtained with *S. aureus*, we chose 3-layer films of βPDMA-*b*-PDPA micelles and PSS to be tested against the *E. coli* isolate due to: i) higher surface coverage of 3-layer films than that of a monolayer film; ii) higher number of free zwitterionic units of 3-layer films than that of 5-layer films.

Kirby-Bauer test on 3-layer films showed that, in contrast to results obtained using *S. aureus,* 3-layer films of Triclosan loaded βPDMA-*b*-PDPA micelles did not show a clear zone of inhibition of bacterial growth on MH agar at both pH 7.5 and pH 5.5 (Fig. 14). This could be due to the relatively low sensitivity of the *E. coli* isolate to Triclosan.

3-layer film (Triclosan-loaded) (pH 7.5)

3-layer film (Triclosan-loaded) (pH 5.5)

3-layer film (unloaded micelles) (pH 7.5)

3-layer film (unloaded micelles) (pH 5.5)
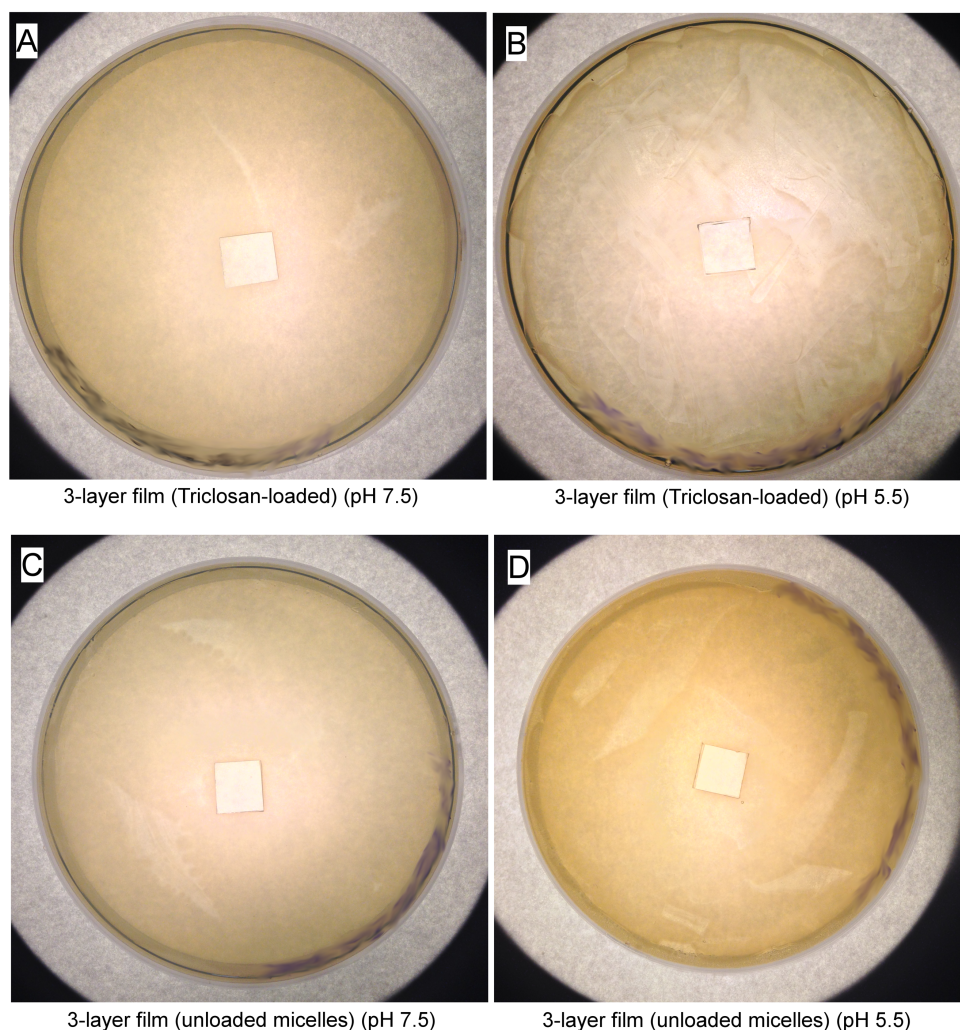
Fig. 2. 14. Kirby-Bauer test from 3-layer films of Triclosan loaded or unloaded βPDMA-*b*-PDPA micelles at pH 5.5 and pH 7.5 (acquired from [54]).

To determine the number of viable bacteria (as CFU) on substrates, we carried out an agar-plating assay. Similar to the results obtained against *S. aureus*, at pH 7.5 we found that 3-layer films of βPDMA-*b*-PDPA micelles and PSS exhibited anti-adhesive behaviour against *E. coli* in 1 hour (Fig. 2.15A). Triclosan loading into the micellar cores at pH 7.5 did not make a significant difference in the number of viable bacteria that adhered at the surface of the coating (Fig. 2.15A). At pH 5.5, the substrates with unloaded BCMs were not only no longer anti-adhesive to *E. coli*; rather, bacterial adherence was higher on these surfaces. This behavior was not observed with *S. aureus*. We reported for *S. aureus* that at pH 5.5 the anti-adhesive behaviour of 3-layer

films with unloaded zwitterionic BCMs had significantly diminished compared to the behaviour of the similar film at pH 7.5. Though both at pH 7.5 and 5.5 the films were anti-adhesive against *S. aureus*, compared to the control (Fig. 2.8.). Nonetheless, with the Triclosan loaded BCMs we observed a modest decrease in the number of viable adhered *E. coli* most likely because of the release of Triclosan from the micellar core at pH 5.5. We hypothesize that the sensitivity to Triclosan of the *E. coli* isolate that adhered to the surface may have increased when the Triclosan was released from the micellar cores. This may be explained with the phenomenon of "catch-and-kill" reported by Cao et al. [65] and Cheng et al. [66]. Cao and Cheng reported on polycationic coatings which promoted bacterial adherence and killed the bacteria in contact with the surface (so called "catch-and-kill state") and then released the bacteria when the coating transformed from cationic to zwitterionic state either by pH trigger [65] or hydrolysis [66] by taking advantage of the anti-adhesive behaviour of the polyzwitterions.
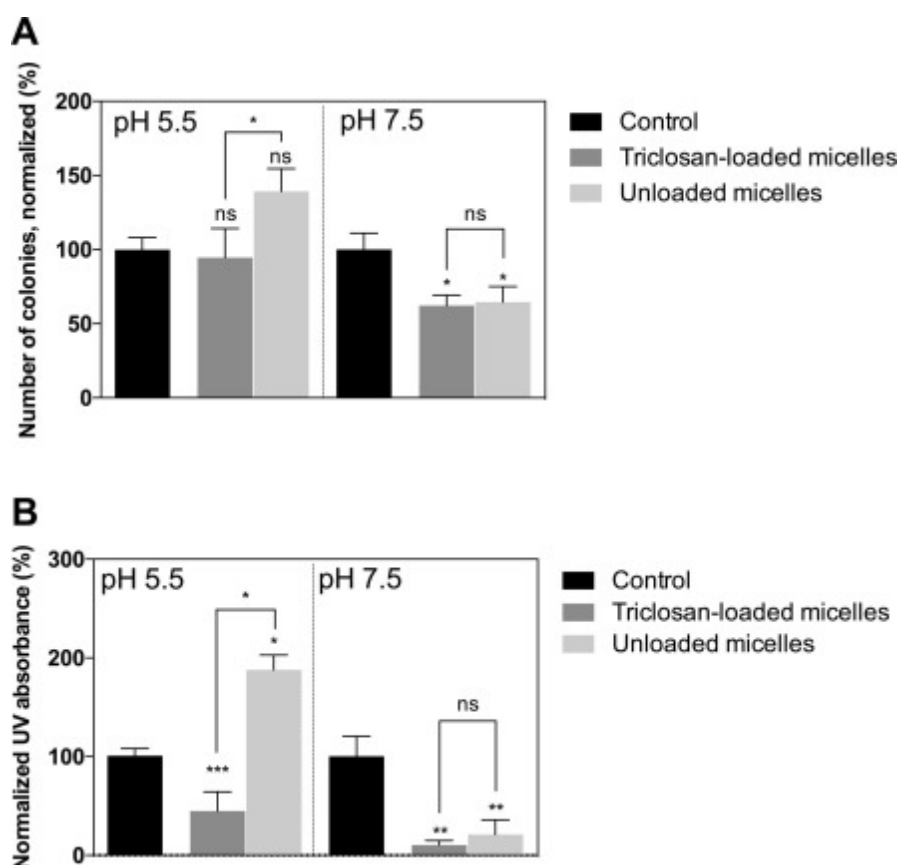
Fig. 2. 15. Panel A: Number of colonies on 3-layer films of Triclosan-loaded and unloaded βPDMA-*b*-PDPA micelles after 1-hour incubation with *E. coli*. Control

93

results for each pH are normalized to 100. **Panel B:** Normalized UV-Visible absorbance (%) data for 3-layer films of Triclosan-loaded and unloaded βPDMA-*b*-PDPA micelles at pH 7.5 and pH 5.5, determined by crystal violet staining assay. UV•Vis absorbance (OD_{590}) of crystal violet was normalized to 100% for control values at pH 5.5 and 7.5. Error bars represent the standard error (SE) of mean. (ns = not significant) (acquired from [54]).

In our study, this similar contact antimicrobial effect that is observed at pH 5.5, may have been provided by the pH-induced release of Triclosan from the coatings due to the pH-responsive behaviour of the βPDMA-*b*-PDPA polymer micelles (Fig. 2.15A).

Additionally, we carried out Gram's crystal violet staining assay to determine the total amount of biomass adsorbed onto the substrates coated with 3-layer βPDMA-*b*-PDPA micelles and PSS in 1 hour at pH 7.5 and pH 5.5 (Fig. 2.15B). We found that the *E. coli* biomass on the 3-layer films of unloaded and Triclosan-loaded BCMs were similar (but lower than the control) at pH 7.5, indicating that self-diffusion of Triclosan from the micellar cores did not make a significant difference. The highest biomass was observed at pH 5.5 for 3-layer films of unloaded BCMs. Very similar to our observations with the agar-plating assay (Fig. 2.15A), biomass formation with Triclosan-loaded BCMs was slightly lower than that of the unloaded BCMs at pH 5.5. This supports our hypothesis that contact antibacterial effect against *E. coli* may be present on films containing Triclosan loaded BCMs. Therefore, the coatings can reduce the biomass even of bacterial strains that are less sensitive to Triclosan, once such bacteria are "caught" by the films under mildly acidic conditions. The anti-adhesive effect of the 3-layer films with unloaded BCMs under physiological pH is further supported by the microscopy images (Fig. 2.16.).
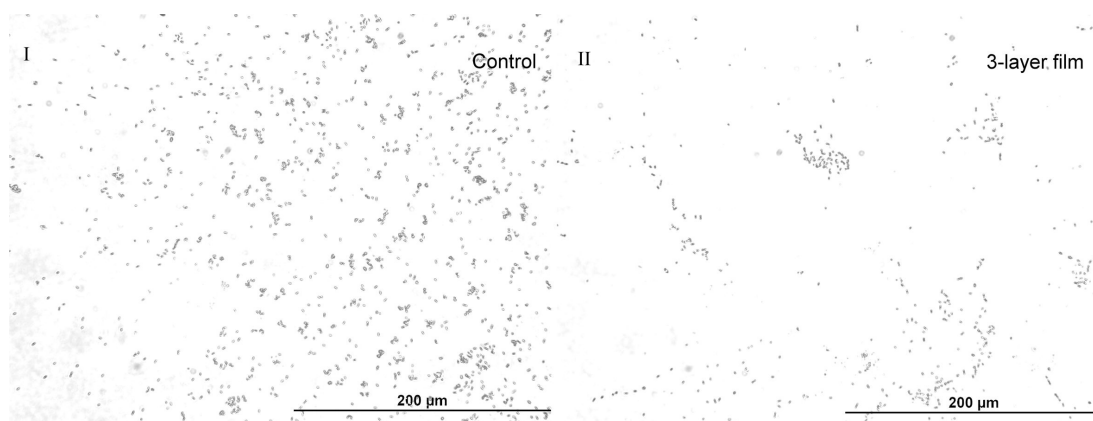
Fig. 2. 16. Light microscopy images of the blank substrate and the substrate coated with 3-layer films of unloaded βPDMA-*b*-PDPA micelles after 1 hour incubation with *E. coli*. Light microscopy images gathered at 40X magnification (acquired from [54]).

2.4.8. Long Term Testing of 3-layer Films of βPDMA-*b*-PDPA Micelles Against *S. aureus and E. coli*

We tested 3-layer films for 24 hours and 48 hours at pH 7.5 against *Staphylococcus aureus and E. coli* using agar plating and crystal violet staining techniques. Here, we focused on the anti-biofilm effect of the coatings since the biofilm formation by *S. aureus* or *E. coli* is initiated in less than 24 hours. As seen in results obtained using agar plating method (Fig. 2.17A), the βPDMA-*b*-PDPA micelles exhibited significant anti-biofilm behavior against *S. aureus* for 24 hours, which continued 48 hours. Triclosan loading in the micellar cores further decreased the number of *S. aureus* colonies as well as the amount of biofilm at the surface. Results obtained using crystal violet staining method (Fig. 2.17B) were in good agreement with the results obtained using agar plating technique, confirming the anti-biofilm behaviour of the 3-layer films against *S. aureus*. The images of crystal violet-stained substrates incubated with *S. aureus* for 48 hours are shown in Fig. 2.19A.
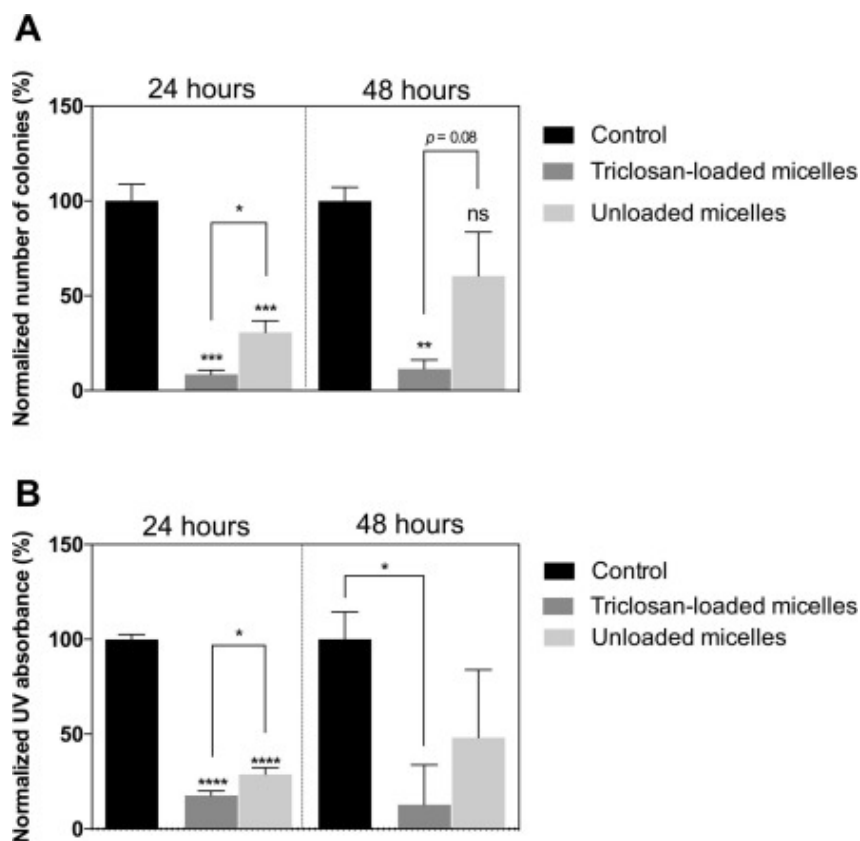
Fig. 2. 17. Panel A: Number of colonies on 3-layer films of Triclosan loaded and unloaded βPDMA-*b*-PDPA micelles after 24 hours and 48 hours incubation at pH 7.5 with *S. aureus*. Number of colonies for each control group is normalized to 100. **Panel B:** Normalized UV-Visible Absorbance (%) data for 3-layer films of Triclosan-loaded and unloaded βPDMA-*b*-PDPA micelles at pH 7.5 after 24 hours and 48 hours incubation with *S. aureus,* determined by crystal violet staining assay. UV•Vis absorbance (OD_{590}) of crystal violet was normalized to 100 % for control values of the 24-hour and 48-hour experiments. Error bars represent the standard error (SE) of mean. (ns = not significant) (acquired from [54]).

In contrast, the unloaded βPDMA-*b*-PDPA micelles exhibited a slight decrease in biofilm formation by *E. coli* that did not reach statistical significance when the substrates were incubated with the bacteria for 24 hours and 48 hours (Fig. 2.18A). Interestingly, when the micellar cores were loaded with Triclosan, the coatings showed a significant anti-biofilm activity compared to unloaded micelles. Results obtained using crystal violet staining method (Fig. 2.18B) also shows that the Triclosan loading

in the films significantly reduced the *E. coli* biofilm formation at the surfaces, even though the *E. coli* strain we used was relatively less sensitive to Triclosan. The images of crystal violet stained substrates incubated with *E. coli* for 48 hours are shown in Figure 2.19B. Thus, at pH 7.5, when Triclosan is likely to diffuse out from loaded BCMs, enhanced susceptibility was observed even against a bacterial strain that has relatively low Triclosan sensitivity.
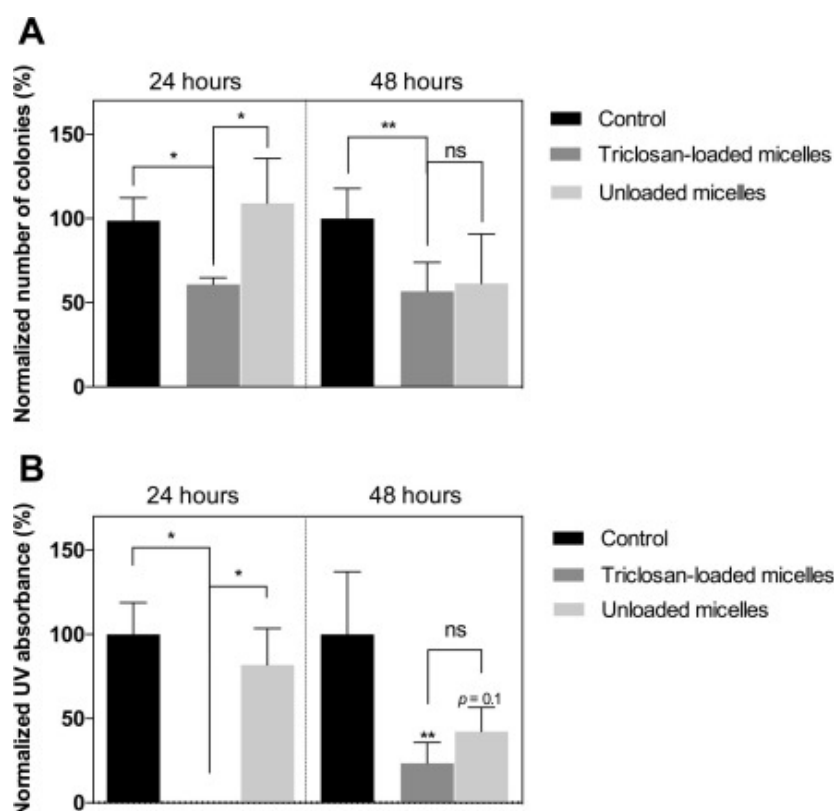
Fig. 2. 18. Panel A: Number of colonies on 3-layer films of Triclosan loaded and unloaded βPDMA-*b*-PDPA micelles after 24 hours and 48 hours incubation at pH 7.5 with *E. coli*. Number of colonies for each control group is normalized to 100. **Panel B:** Normalized UV-Visible Absorbance (%) data for 3-layer films of Triclosan-loaded and unloaded βPDMA-*b*-PDPA micelles at pH 7.5 after 24 hours and 48 hours incubation with *E. coli,* determined by crystal violet staining assay. UV•Vis absorbance (OD_{590}) of crystal violet was normalized to 100 % for control values of the 24-hour and 48-hour experiments. Error bars represent the standard error (SE) of mean. (ns = not significant) (acquired from [54]).

A

Crystal violet-staining of *S. aureus* biofilms

Films with
Triclosan-loaded
micelles

Films with
unloaded micelles

Control substrates
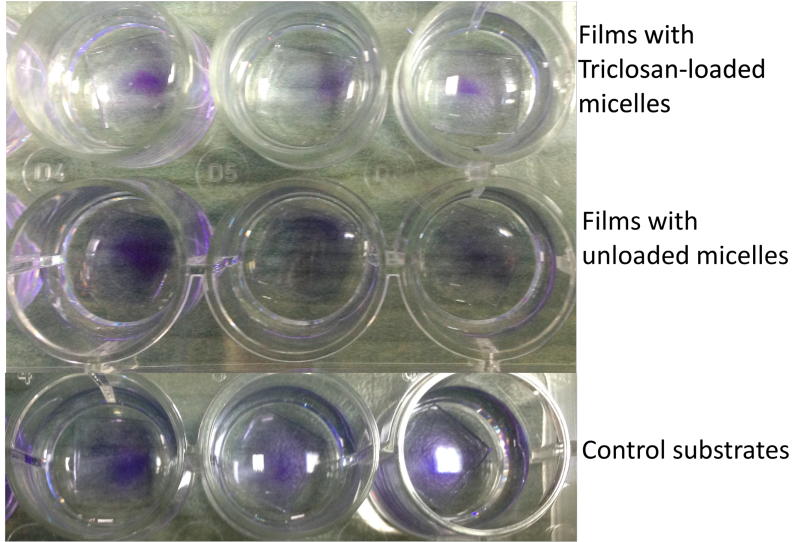
B

Crystal violet-staining of *E. coli* biofilms

Films with
Triclosan-loaded
micelles

Films with
unloaded micelles

Control substrates
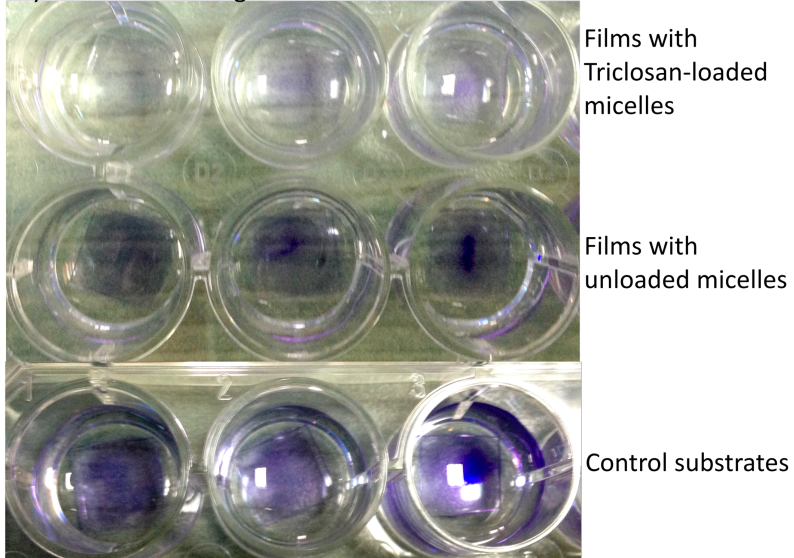
Fig. 2. 19. Images of crystal-violet stained wafers with or without film coting, after a 48-hour assay. The purple crystal violet indicates the biomass on the wafers. For both *S. aureus* **(Panel A)** and *E. coli* **(Panel B)**, we can observe the low amount of biomass on wafers with Triclosan-loaded BCMs (acquired from [54]).

2.5. Conclusion

We developed substrates with dual function coatings in which both bacterial anti-adhesive property and antibacterial activity were achieved. The anti-adhesive property was provided by the zwitterionic coronae of the BCMs, which were used as building blocks to construct the multilayers, whereas the antibacterial activity was ensured by Triclosan, an antibacterial agent, loaded in the micellar cores.

We found that the number of layers deposited at the surface affected the anti-adhesive property and 3-layer films were the most anti-adhesive coating against a *S. aureus* isolate with high sensitivity to Triclosan. The number of *S. aureus* colonies at the surface further decreased when the micellar cores were loaded with Triclosan. The antibacterial effect of Triclosan was more remarkable in acidic conditions due to pH-induced disintegration of the micellar cores and release of Triclosan from the surface. Long-term (1 day and 2 days) testing against *S. aureus* confirmed the anti-biofilm properties of the coatings. 3-layer films of zwitterionic BCMs also showed initial anti-adhesive behaviour against an *E. coli* isolate with low sensitivity to Triclosan at physiological pH. Although the coatings with unloaded BCMs were not anti-adhesive at moderately acidic pH against this strain, a significant contact antibacterial effect was observed when Triclosan was released from the coatings. Similarly, results obtained from long term testing showed anti-biofilm effect when the *E. coli* were in direct contact with the substrates coated with Triclosan loaded BCMs. Therefore, these films hold promise in combatting long term biofilm development.

By releasing antibacterial agents from the surface, these films can be useful not only to compensate for the anti-biofilm effect at non-homogeneous or defective parts of the coating but also combat bacteria at moderately acidic infection site. These results also provide a potential strategy of delivering hydrophobic drugs to moderately acidic locations in the body (i.e. tumors, sites of infection) via circulating zwitterionic BCMs without any adsorption of blood/plasma proteins until their accumulation at the target site.

2.6. References

[1] R.M. Klevens, J.R. Edwards, C.L. Richards, T.C. Horan, R.P. Gaynes, D.A. Pollock, D.M. Cardo, Estimating Health Care-Associated Infections and Deaths in U.S. Hospitals, 2002, Public Health Rep. 122 (2007) 160–166.

[2] J.E. McGowan, Antimicrobial Resistance in Hospital Organisms and Its Relation to Antibiotic Use, Rev. Infect. Dis. 5 (1983) 1033–1048. http://cid.oxfordjournals.org/content/5/6/1033.abstract.

[3] J.A. Cepeda, T. Whitehouse, B. Cooper, J. Hails, K. Jones, F. Kwaku, L. Taylor, S. Hayman, B. Cookson, S. Shaw, C. Kibbler, M. Singer, G. Bellingan, A.P.R. Wilson, Isolation of patients in single rooms or cohorts to reduce spread of MRSA in intensive-care units: Prospective two-centre study, Lancet. 365 (2005) 295–304. doi:10.1016/S0140-6736(05)17783-6.

[4] N.K. Petty, N.L. Ben Zakour, M. Stanton-Cook, E. Skippington, M. Totsika, B.M. Forde, M.-D. Phan, D. Gomes Moriel, K.M. Peters, M. Davies, B. a Rogers, G. Dougan, J. Rodriguez-Baño, A. Pascual, J.D.D. Pitout, M. Upton, D.L. Paterson, T.R. Walsh, M. a Schembri, S. a Beatson, Global dissemination of a multidrug resistant Escherichia coli clone., Proc. Natl. Acad. Sci. U. S. A. 111 (2014) 5694–9. doi:10.1073/pnas.1322678111.

[5] J.R. Johnson, V. Tchesnokova, B. Johnston, C. Clabots, P.L. Roberts, M. Billig, K. Riddell, P. Rogers, X. Qin, S. Butler-Wu, L.B. Price, M. Aziz, M.H. Nicolas-Chanoine, C. Debroy, A. Robicsek, G. Hansen, C. Urban, J. Platell, D.J. Trott, G. Zhanel, S.J. Weissman, B.T. Cookson, F.C. Fang, A.P. Limaye, D. Scholes, S. Chattopadhyay, D.C. Hooper, E. V. Sokurenko, Abrupt emergence of a single dominant multidrug-resistant strain of Escherichia coli, J. Infect. Dis. 207 (2013) 919–928. doi:10.1093/infdis/jis933.

[6] C.C. Goller, T. Romeo, Environmental influences on biofilm development., Curr. Top. Microbiol. Immunol. 322 (2008) 37–66.

[7] R. Saginur, M. St. Denis, W. Ferris, S.D. Aaron, F. Chan, C. Lee, K. Ramotar,

Multiple combination bactericidal testing of staphylococcal biofilms from implant-associated infections, Antimicrob. Agents Chemother. 50 (2006) 55–61. doi:10.1128/AAC.50.1.55-61.2006.

[8]   P. Kurt, L. Wood, D.E. Ohman, K.J. Wynne, Highly effective contact antimicrobial surfaces via polymer surface modifiers, Langmuir. 23 (2007) 4719–4723. doi:10.1021/la063718m.

[9]   R. Kumar, H. Münstedt, Silver ion release from antimicrobial polyamide/silver composites, Biomaterials. 26 (2005) 2081–2088. doi:10.1016/j.biomaterials.2004.05.030.

[10]   S. Pavlukhina, Y. Lu, A. Patimetha, M. Libera, S. Sukhishvili, Polymer multilayers with pH-triggered release of antibacterial agents, Biomacromolecules. 11 (2010) 3448–3456. doi:10.1021/bm100975w.

[11]   M.J. Bridgett, M.C. Davies, S.P. Denyer, Control of staphylococcal adhesion to polystyrene surfaces by polymer surface modification with surfactants., Biomaterials. 13 (1992) 411–416. doi:10.1016/0142-9612(92)90159-L.

[12]   Y. Li, X. Hu, S. Tian, Y. Li, G. Zhang, G. Zhang, S. Liu, Polyion complex micellar nanoparticles for integrated fluorometric detection and bacteria inhibition in aqueous media, Biomaterials. 35 (2014) 1618–1626. doi:10.1016/j.biomaterials.2013.10.077.

[13]   C. Zhang, Y. Zhu, C. Zhou, W. Yuan, J. Du, Antibacterial vesicles by direct dissolution of a block copolymer in water, Polym. Chem. (2013) 255–259. doi:10.1039/c2py20719b.

[14]   W. Yuan, J. Wei, H. Lu, L. Fan, J. Du, Water-dispersible and biodegradable polymer micelles with good antibacterial efficacy, Chem. Commun. 48 (2012) 6857. doi:10.1039/c2cc31529g.

[15]   Y. Qiao, C. Yang, D.J. Coady, Z.Y. Ong, J.L. Hedrick, Y.Y. Yang, Highly dynamic biodegradable micelles capable of lysing Gram-positive and Gram-negative bacterial membrane, Biomaterials. 33 (2012) 1146–1153.

doi:10.1016/j.biomaterials.2011.10.020.

[16]   F. Nederberg, Y. Zhang, J.P.K. Tan, K. Xu, H. Wang, C. Yang, S. Gao, X.D. Guo, K. Fukushima, L. Li, J.L. Hedrick, Y.-Y. Yang, Biodegradable nanostructures with selective lysis of microbial membranes., Nat. Chem. 3 (2011) 409–414. doi:10.1038/nchem.1012.

[17]   B. Jose, V. Antoci, A.R. Zeiger, E. Wickstrom, N.J. Hickok, Vancomycin covalently bonded to titanium beads kills Staphylococcus aureus, Chem. Biol. 12 (2005) 1041–1048. doi:10.1016/j.chembiol.2005.06.013.

[18]   F. Costa, I.F. Carvalho, R.C. Montelaro, P. Gomes, M.C.L. Martins, Covalent immobilization of antimicrobial peptides (AMPs) onto biomaterial surfaces, Acta Biomater. 7 (2011) 1431–1440. doi:10.1016/j.actbio.2010.11.005.

[19]   A.F. Radovic-Moreno, T.K. Lu, V.A. Puscasu, C.J. Yoon, R. Langer, O.C. Farokhzad, Surface charge-switching polymeric nanoparticles for bacterial cell wall-targeted delivery of antibiotics, ACS Nano. 6 (2012) 4279–4287. doi:10.1021/nn3008383.

[20]   I. Zhuk, F. Jariwala, A.B. Attygalle, Y. Wu, M.R. Libera, S. a Sukhishvili, Self-Defensive Layer-by-Layer Films with Bacteria-Triggered Antibiotic Release., ACS Nano. (2014) 7733–7745. doi:10.1021/nn500674g.

[21]   B. Horev, M.I. Klein, G. Hwang, Y. Li, D. Kim, H. Koo, D.S.W. Benoit, pH-Activated Nanoparticles for Controlled Topical Delivery of Farnesol To Disrupt Oral Biofilm Virulence, ACS Nano. 9 (2015) 2390–2404. doi:10.1021/nn507170s.

[22]   S. Pasche, S.M. De Paul, J. Vörös, N.D. Spencer, M. Textor, Poly(l-lysine)-graft-poly(ethylene glycol) Assembled Monolayers on Niobium Oxide Surfaces: A Quantitative Study of the Influence of Polymer Interfacial Architecture on Resistance to Protein Adsorption by ToF-SIMS and in Situ OWLS, Langmuir. 19 (2003) 9216–9225. doi:10.1021/la034111y.

[23]   J.M. Harris, R.B. Chess, Effect of pegylation on pharmaceuticals., Nat. Rev.

Drug Discov. 2 (2003) 214–221. doi:10.1038/nrd1033.

[24]   K. Knop, R. Hoogenboom, D. Fischer, U.S. Schubert, Poly(ethylene glycol) in drug delivery: Pros and cons as well as potential alternatives, Angew. Chemie - Int. Ed. 49 (2010) 6288–6308. doi:10.1002/anie.200902672.

[25]   I. Izquierdo-Barba, S. Sánchez-Salcedo, M. Colilla, M.J. Feito, C. Ramírez-Santillán, M.T. Portolés, M. Vallet-Regí, Inhibition of bacterial adhesion on biocompatible zwitterionic SBA-15 mesoporous materials, Acta Biomater. 7 (2011) 2977–2985. doi:10.1016/j.actbio.2011.03.005.

[26]   P.S. Liu, Q. Chen, S.S. Wu, J. Shen, S.C. Lin, Surface modification of cellulose membranes with zwitterionic polymers for resistance to protein adsorption and platelet   adhesion,   J.   Memb.   Sci.   350   (2010)   387–394. doi:10.1016/j.memsci.2010.01.015.

[27]   Y. Chang, S. Chen, Z. Zhang, S. Jiang, Highly protein-resistant coatings from well-defined diblock copolymers containing sulfobetaines, Langmuir. 22 (2006) 2222–2226. doi:10.1021/la052962v.

[28]   Y. He, J. Hower, S. Chen, M.T. Bernards, Y. Chang, S. Jiang, Molecular simulation studies of protein interactions with zwitterionic phosphorylcholine self-assembled monolayers in the presence of water, Langmuir. 24 (2008) 10358–10364. doi:10.1021/la8013046.

[29]   H. Kitano, M. Imai, K. Sudo, M. Ide, Hydrogen-bonded network structure of water in aqueous solution of sulfobetaine polymers, J. Phys. Chem. B. 106 (2002) 11391–11396. doi:10.1021/jp020185r.

[30]   S.L. West, J.P. Salvage, E.J. Lobb, S.P. Armes, N.C. Billingham, A.L. Lewis, G.W. Hanlon, A.W. Lloyd, The biocompatibility of crosslinkable copolymer coatings containing sulfobetaines and phosphobetaines, Biomaterials. 25 (2004) 1195–1204. doi:10.1016/j.biomaterials.2003.08.010.

[31]   Z. Zhang, H. Vaisocherová, G. Cheng, W. Yang, H. Xue, S. Jiang, Nonfouling behavior of polycarboxybetaine-grafted surfaces: Structural and environmental

effects, Biomacromolecules. 9 (2008) 2686–2692. doi:10.1021/bm800407r.

[32] G. Li, G. Cheng, H. Xue, S. Chen, F. Zhang, S. Jiang, Ultra low fouling zwitterionic polymers with a biomimetic adhesive group, Biomaterials. 29 (2008) 4592–4597. doi:10.1016/j.biomaterials.2008.08.021.

[33] G. Cheng, Z. Zhang, S. Chen, J.D. Bryers, S. Jiang, Inhibition of bacterial adhesion and biofilm formation on zwitterionic surfaces, Biomaterials. 28 (2007) 4192–4199. doi:10.1016/j.biomaterials.2007.05.041.

[34] C. Hippius, V. Bütün, I. Erel-Goktepe, Bacterial anti-adhesive properties of a monolayer of zwitterionic block copolymer micelles, Mater. Sci. Eng. C. 41 (2014) 354–362. doi:10.1016/j.msec.2014.04.023.

[35] L. Shen, B. Wang, J. Wang, J. Fu, C. Picart, J. Ji, Asymmetric free-standing film with multifunctional anti-bacterial and self-cleaning properties., ACS Appl. Mater. Interfaces. 4 (2012) 4476–83. doi:10.1021/am301118f.

[36] D. Cui, A. Szarpak, I. Pignot-Paintrand, A. Varrot, T. Boudou, C. Detrembleur, C. Jérôme, C. Picart, R. Auzély-Velty, Contact-killing polyelectrolyte microcapsules based on chitosan derivatives, Adv. Funct. Mater. 20 (2010) 3303–3312. doi:10.1002/adfm.201000601.

[37] F. Boulmedais, B. Frisch, O. Etienne, P. Lavalle, C. Picart, J. Ogier, J.C. Voegel, P. Schaaf, C. Egles, Polyelectrolyte multilayer films with pegylated polypeptides as a new type of anti-microbial protection for biomaterials, Biomaterials. 25 (2004) 2003–2011. doi:10.1016/j.biomaterials.2003.08.039.

[38] J. a. Lichter, M.F. Rubner, Polyelectrolyte multilayers with intrinsic antimicrobial functionality: The importance of mobile polycations, Langmuir. 25 (2009) 7686–7694. doi:10.1021/la900349c.

[39] P.H. Chua, K.G. Neoh, E.T. Kang, W. Wang, Surface functionalization of titanium with hyaluronic acid/chitosan polyelectrolyte multilayers and RGD for promoting osteoblast functions and inhibiting bacterial adhesion, Biomaterials. 29 (2008) 1412–1421. doi:10.1016/j.biomaterials.2007.12.019.

[40] A. Agarwal, T.L. Weis, M.J. Schurr, N.G. Faith, C.J. Czuprynski, J.F. McAnulty, C.J. Murphy, N.L. Abbott, Surfaces modified with nanometer-thick silver-impregnated polymeric films that kill bacteria but support growth of mammalian cells, Biomaterials. 31 (2010) 680–690. doi:10.1016/j.biomaterials.2009.09.092.

[41] A. Shukla, S.N. Avadhany, J.C. Fang, P.T. Hammond, Tunable vancomycin releasing surfaces for biomedical applications., Small. 6 (2010) 2392–2404. doi:10.1002/smll.201001150.

[42] J.S. Moskowitz, M.R. Blaisse, R.E. Samuel, H.-P. Hsu, M.B. Harris, S.D. Martin, J.C. Lee, M. Spector, P.T. Hammond, The effectiveness of the controlled release of gentamicin from polyelectrolyte multilayers in the treatment of Staphylococcus aureus infection in a rabbit bone model., Biomaterials. 31 (2010) 6019–30. doi:10.1016/j.biomaterials.2010.04.011.

[43] P.M. Nguyen, N.S. Zacharia, E. Verploegen, P.T. Hammond, Extended release antibacterial layer-by-layer films incorporating linear-dendritic block copolymer micelles, Chem. Mater. 19 (2007) 5524–5530. doi:10.1021/cm070981f.

[44] S.Y. Wong, J.S. Moskowitz, J. Veselinovic, R. a. Rosario, K. Timachova, M.R. Blaisse, R.C. Fuller, A.M. Klibanov, P.T. Hammond, Dual functional polyelectrolyte multilayer coatings for implants: Permanent microbicidal base with controlled release of therapeutic agents, J. Am. Chem. Soc. 132 (2010) 17840–17848. doi:10.1021/ja106288c.

[45] I. Zhuk, F. Jariwala, A.B. Attygalle, Y. Wu, M.R. Libera, S. a Sukhishvili, Self-defensive layer-by-layer films with bacteria-triggered antibiotic release., ACS Nano. 8 (2014) 7733–45. doi:10.1021/nn500674g.

[46] D. Lee, R.E. Cohen, M.F. Rubner, Antibacterial properties of Ag nanoparticle loaded multilayers and formation of magnetically directed antibacterial microparticles, Langmuir. 21 (2005) 9651–9659. doi:10.1021/la0513306.

[47] D.-G. Yu, W.-C. Lin, M.-C. Yang, Surface modification of poly(L-lactic acid)

membrane via layer-by-layer assembly of silver nanoparticle-embedded polyelectrolyte multilayer., Bioconjug. Chem. 18 (2007) 1521–1529. doi:10.1021/bc060098s.

[48]   J. Fu, J. Ji, W. Yuan, J. Shen, Construction of anti-adhesive and antibacterial multilayer films via layer-by-layer assembly of heparin and chitosan, Biomaterials. 26 (2005) 6684–6692. doi:10.1016/j.biomaterials.2005.04.034.

[49]   J. Fu, J. Ji, D. Fan, J. Shen, Construction of antibacterial multilayer films containing nanosilver via layer-by-layer assembly of heparin and chitosan-silver ions complex., J. Biomed. Mater. Res. A. 79 (2006) 665–74. doi:10.1002/jbm.a.30819.

[50]   B.L. Wang, K.F. Ren, H. Chang, J.L. Wang, J. Ji, Construction of degradable multilayer films for enhanced antibacterial properties, ACS Appl. Mater. Interfaces. 5 (2013) 4136–4143. doi:10.1021/am4000547.

[51]   V. Bütün, S.P. Armes, N.C. Billingham, Synthesis and aqueous solution properties of near-monodisperse tertiary amine methacrylate homopolymers and diblock copolymers, Polymer (Guildf). 42 (2001) 5993–6008. doi:10.1016/S0032-3861(01)00066-0.

[52]   V. Bütün, Selective betainization of 2-(dimethylamino)ethyl methacrylate residues in tertiary amine methacrylate diblock copolymers and their aqueous solution properties, Polymer (Guildf). 44 (2003) 7321–7334. doi:10.1016/j.polymer.2003.09.027.

[53]   P. Yusan, I. Tuncel, V. Bütün, A.L. Demirel, I. Erel-Goktepe, pH-responsive layer-by-layer films of zwitterionic block copolymer micelles, Polym. Chem. 5 (2014) 3777–3787.

[54]   B. Onat, V. Bütün, S. Banerjee, I. Erel-Goktepe, Bacterial anti-adhesive and pH-induced antibacterial agent releasing ultra-thin films of zwitterionic copolymer micelles, Acta Biomater. 40 (2016) 293–309. doi:http://dx.doi.org/10.1016/j.actbio.2016.04.033.

106

[55]   T. Mauser, C. Déjugnat, H. Möhwald, G.B. Sukhorukov, Microcapsules made of weak polyelectrolytes: Templating and stimuli-responsive properties, Langmuir. 22 (2006) 5888–5893. doi:10.1021/la060088f.

[56]   Z. Sui, J.B. Schlenoff, Phase separations in pH-responsive polyelectrolyte multilayers: Charge extrusion versus charge expulsion, Langmuir. 20 (2004) 6026–6031. doi:10.1021/la0495985.

[57]   T. Scheuerman, A. Camper, M. Hamilton, Effects of Substratum Topography on Bacterial Adhesion., J. Colloid Interface Sci. 208 (1998) 23–33. doi:10.1006/jcis.1998.5717.

[58]   V.K. Truong, R. Lapovok, Y.S. Estrin, S. Rundell, J.Y. Wang, C.J. Fluke, R.J. Crawford, E.P. Ivanova, The influence of nano-scale surface roughness on bacterial adhesion to ultrafine-grained titanium, Biomaterials. 31 (2010) 3674–3683. doi:10.1016/j.biomaterials.2010.01.071.

[59]   A.D. Russell, Whither triclosan?, J. Antimicrob. Chemother. 53 (2004) 693–695. doi:10.1093/jac/dkh171.

[60]   M. Habash, G. Reid, Microbial biofilms: their development and significance for medical device-related infections., J. Clin. Pharmacol. 39 (1999) 887–898. doi:10.1177/00912709922008506.

[61]   R.A. Kekwick, The serum proteins in multiple myelomatosis, Biochem. J. 34 (1940) 1248–1257. http://www.ncbi.nlm.nih.gov/pmc/articles/PMC1265407/.

[62]   J.P. Nicholson, M.R. Wolmarans, G.R. Park, The role of albumin in critical illness., Br. J. Anaesth. 85 (2000) 599–610. doi:10.1093/bja/85.4.599.

[63]   E. Ostuni, R.G. Chapman, M.N. Liang, G. Meluleni, G. Pier, D.E. Ingber, G.M. Whitesides, Self-assembled monolayers that resist the adsorption of proteins and the adhesion of bacterial and mammalian cells, Langmuir. 17 (2001) 6336–6343. doi:10.1021/la010552a.

[64]   J. Rodríguez-Baño, M.D. Navarro, L. Romero, M. a Muniain, E.J. Perea, R. Pérez-Cano, J.R. Hernández, A. Pascual, Clinical and molecular epidemiology

of extended-spectrum beta-lactamase-producing Escherichia coli as a cause of nosocomial infection or colonization: implications for control., Clin. Infect. Dis. 42 (2006) 37–45. doi:10.1086/498519.

[65] B. Cao, Q. Tang, L. Li, J. Humble, H. Wu, L. Liu, G. Cheng, Switchable antimicrobial and antifouling hydrogels with enhanced mechanical properties, Adv. Healthc. Mater. 2 (2013) 1096–1102. doi:10.1002/adhm.201200359.

[66] G. Cheng, H. Xue, Z. Zhang, S. Chen, S. Jiang, A switchable biocompatible polymer surface with self-sterilizing and nonfouling capabilities, Angew. Chemie - Int. Ed. 47 (2008) 8831–8834. doi:10.1002/anie.200803570.

CHAPTER 3

LAYER-BY-LAYER FILMS OF BIODEGRADABLE POLY(4-HYDROXY-L-PROLINE ESTER) (PHPE) AND ANTIBACTERIAL TANNIC ACID (TA)

3.1. Chapter Summary

We report on the osteoinductivity of poly(4-hydroxy-L-proline ester) (PHPE) and the inductive effect of PHPE on collagen synthesis of osteoblast-like cells (SaOS-2). Treatment of these cells with PHPE induced mineralization of the extracellular matrix even when mineralization activators were absent in the growth medium. Moreover, we report on preparation of water-soluble complexes of PHPE and the antibacterial polymer TA, and LbL self-assembly of PHPE-TA complexes at the surface without using a polymer counterpart. Surfaces coated with PHPE-TA complexes showed osteoconductive property confirmed with enhanced adherence for osteoblast-like cells, increased collagen deposition and mineralization in their extracellular matrix. Our results indicate that PHPE is a potential osteoinductive agent which can favor bone regeneration at defect sites. Additionally, PHPE-based LbL films are promising for coating bioimplants/scaffolds to overcome cytotoxicity-based complications of the bulk biomaterial, to facilitate cell adherence at the surface, and conduct bone regeneration.

3.2. Introduction

The current principle of bone regenerative medicine is to provide regeneration of the native bone tissue in a timely manner without causing any cytotoxicity or complications. Traditionally, autografts are used in orthopedic surgery, as they are the

sources of viable cells, osteoinductive growth factors, and osteoconductive scaffold for bone regeneration, all in one [1]. On the other hand, autografts carry limitations, such as confined size and limited availability, and morbidity at the harvest site [2]. To overcome these limitations, *in vitro* engineering of bone constructs has gained attention as a potential strategy. The major challenge in designing such constructs is to balance the harmony of the agents that provide osteoconductivity, osteoinductivity, or osseointegration to the construct [3]. In engineered bone constructs, biodegradable polymers are used either as the bulk material of the scaffold or to deposit as thin films onto the scaffolds for surface modification. For example, synthetic biodegradable polymers such as PLLA [4], PGA [5], PLGA [6], PCL [7] and natural materials such as collagen [8], elastin [9], chitosan [10], and alginate [11] have found applications in the development and manufacturing of biodegradable constructs in both forms of use. Even though biodegradable polymers generally provide osteoconductivity to biomaterials [12,13], osteoinductivity could only be imparted by doping them with growth factors [14,15], or minerals such as calcium phosphate and derivatives [16]. Extensive research has been carried out on using recombinant growth factors, such as human recombinant bone morphogenetic protein-2 (hrBMP-2) to provide osteoinductivity, though complications such as off-target bone formation and even cancer have been reported [17]. Natural minerals such as hydroxyapatite and tricalcium phosphate have shown great promise in providing osteoinductivity to engineered constructs, though these minerals are only used as a component of composites which are tedious and time-consuming to assemble [18].

Surface modification of biomaterials is commonly carried out using water-soluble, biodegradable polymers [19,20]. Some polymers are known to display biomimetic assembly in aqueous environment similar to the native ECM of osteoblasts [15]. The primary component of osteoblast ECM is collagen, therefore collagen-based surface modifications have been commonly used for bone regeneration [21,22]. A common amino acid present in mature collagen is *trans*-4-hydroxy-L-proline (Hyp). Hyp is the product of post-translational modification of collagen by hydroxylation on proline residues [23]. Such modifications are mandatory for the quaternary structure and function of the mature collagen [24]. Cell-collagen interactions regulate osteoblast

110

proliferation, differentiation, and ECM deposition [25]. The high-affinity binding site of $\alpha_2\beta_1$ and $\alpha_1\beta_1$ integrins of osteoblasts is the GxOGER amino acid sequence in collagen and it is important in the regulation of osteogenic differentiation [25–27]. This sequence possesses a Hyp residue (O). Studies carried out with recombinant collagen showed that hydroxylation of proline was necessary to enable the binding of $\alpha_1\beta_1$ integrin to the peptide sequence GFOGER [28].

Inspired by the outcomes of previous research on the importance of Hyp in integrin binding and the advantages of biodegradable and biomimetic polymers in bone tissue engineering, we synthesized poly(4-hydroxy-L-proline ester) (PHPE), which is a cationic biodegradable polymer possessing (4-hydroxy-L-proline ester) at every repeating unit. Putnam and Langer were the first to report on PHPE as an alternative to poly L-lysine (PLL) and poly ethylene imine (PEI), two commonly used polymers for complexation of DNA. PHPE was reported to have very low cytotoxicity on COS-7 cells compared to other commonly used cationic polymers [29]. Following their work, Li et al. reported on preparation of poly(D,L-lactide-*co*-4-hydroxy-L-proline)-based microspheres for DNA complexation and gene therapy [30]. In this study, PHPE was found to be potentially osteoinductive, through a series of experiments indicating the osteogenic differentiation of osteoblast-like SaOS-2 cells. To the best of our knowledge, this is the first study demonstrating the use of a biodegradable synthetic polymer as a supplement to induce collagen deposition and osteogenic differentiation of osteoblast-like cells. Designer peptides are the closest to PHPE in terms of osteoinductive properties [31]. However, there are no studies in the literature reporting the release of amino acid components from peptides by hydrolytic degradation. Peptides were reported to degrade only if they were designed to possess cleavage sites for ECM remodeling enzymes, such as matrix metalloproteinases (MMPs) [32].

LbL self-assembly of water-soluble biodegradable polymers is a practical method for surface modification of biomaterials [19,20]. In this study, we also aimed to functionalize surfaces using PHPE to impart osteoconductive properties to a material. Water-soluble complexes of PHPE and TA were prepared and then used as building blocks to construct LbL films. Importantly, LbL assembly of PHPE-TA complexes did

not require use of an oppositely charged counter polymer. PHPE-TA complexes were sequentially deposited at the surface during multilayer formation. Osteoblast-like cells exhibited good adherence onto substrates coated with multilayers of PHPE-TA complexes and these multilayers provided a non-cytotoxic osteoconductive environment for osteoblast-like cells. Apart from osteoinductive properties of PHPE, this study demonstrated the first example of PHPE based biodegradable LbL films and their stabilization via periodate-mediated cross-linking to obtain osteoconductive surfaces. The enhanced adherence of osteoblast-like cells to multilayers of PHPE-TA complexes together with the non-cytotoxic behavior of the films make such multilayers promising structures to functionalize the surface of bioimplants or scaffolds and promote bone regeneration at bone defects.

3.3. Materials And Methods

3.3.1. Synthesis of poly(4-hydroxy-L-proline ester) (PHPE)

3.3.1.1. Synthesis of poly(4-hydroxy-N-cbz-L-proline ester) (PHCP)

Poly(4-hydroxy-L-proline ester) (PHPE) was synthesized by a two-step condensation polymerization by slightly modifying the procedures described by Putnam and Langer [29] and Lim, Choi, and Park [33]. 1 g of N-cbz-4-hydroxy-L-proline (Sigma-Aldrich, St. Louis, USA) was melted and stirred under high vacuum (1×10^{-6}) bar at 120°C. In three hours, the temperature was gradually increased to 180°C and the reaction mixture was stirred for 4.5 days (including the first three hours). The crude polymer was dissolved in 200 μL chloroform and precipitated in 100 mL of methanol. The precipitate, poly(4-hydroxy-N-cbz-L-proline ester) (PHCP), was dried in a vacuum oven at 25°C for 16 hours. ^{1}H-NMR spectra of the polymer was recorded using Brucker Electrospin Avance DPX-400 Ultra Shield instrument operating at 400 MHz. ^{1}H-NMR (CDCl$_3$, 400 MHz): δ (ppm) = 7.23-7.36(5H, m, Ph), 5.34(1H, br s, CH), 4.94-5.18(2H, br m, CH$_2$), 4.29-4.58(1H, br m; CH), 3.55-3.78(2H, br m, CH$_2$), 2.12-2.34(2H, br m, CH$_2$).

The number average (M_n) and weight average (M_w) molecular weights of PHCP were determined by gel permeation chromatography (GPC). Shimadzu LC-20AT instrument, with a refractive index detector, RID 20A was calibrated with polystyrene standards and the polymer was dissolved in $CHCl_3$ at 2 mg/mL concentration. The solution was passed through a column, PSS SDV analytical linear M. (Eluent: $CHCl_3$, M_n = 4687 Da, M_w = 8049 Da, PDI= 1.71).

3.3.1.2. Deprotection of Carboxybenzyl (cbz) Group of PHCP

300 mg of PHCP was dissolved in 4 mL DMF. 1 g Pd/C (10% Pd basis) catalyst was added to this solution under a nitrogen atmosphere. Following this, formic acid (14 mL) was added dropwise in a 15 min period under vigorous stirring. The reaction mixture was continued stirring at room temperature for 16 h, followed by filtering through Celite. Celite was washed with 20 mL of 1 N HCl. The filtrates were rotoevaporated to a volume of 5 mL using a water bath at 45°C. Then, 10 mL of 1 N HCl was added onto the filtrates to dissolve the precipitate. The solution was rotoevaporated to a volume of ~1 mL and then added dropwise to 125 mL of acetone under stirring. The precipitate (PHPE) was filtered out and freeze-dried for 3 days to remove any residual water or organic solvents remaining from the polymerization. The percent yield was calculated as 68%. ^{1}H-NMR spectra of the polymer was recorded using Brucker Electrospin Avance DPX-400 Ultra Shield instrument operating at 400 MHz. ^{1}H-NMR (D_2O, 400 MHz): δ (ppm) = 5.58-5.60(1H, br s, CH), 4.26-4.65(1H, br s, CH), 3.35-3.63(2H, m, CH_2), 2.52-2.60(2H, br m, CH_2).

The number average (M_n) and weight average (M_w) molecular weights of PHPE were determined by matrix assisted laser desorption/ionization – time of flight (MALDI-TOF) analysis with slight modifications of the protocol reported by Lim et al. [33] by using a Bruker Daltonics Microflex LT instrument (Figure 3.4.). Basically, 10 mg/mL of sinapinic acid was dissolved in water/3% trifluoroacetic acid (TFA)/acetonitrile (4:1:5, v/v). 10 mg/mL KCl was dissolved in methanol and 5 mg/mL PHPE was dissolved in water. Polymer solution was mixed with the sinapinic acid solution and

the KCl solution (1:1:2, v/v) prior to measurements. M_n = 2330, M_w = 2900, PDI= 1.24.

3.3.2. Preparation of Water Soluble Complexes of PHPE and TA

0.5 mg/mL PHPE was added onto 0.5 mg/mL TA solution with a volume to volume ratio of 20:1 (v/v). This corresponds to a molar ratio of 1:27 for PHPE:TA. Molar ratio is calculated by taking the molecular weight of PHPE and TA as 2330 Da and 1701 Da, respectively. Hydrodynamic size and zeta-potential measurements were performed using a Zetasizer Nano-ZS equipment (Malvern Instruments Ltd.). Particle sizes were obtained by cumulants analysis of the autocorrelation data. Zeta-potential values were obtained from electrophoretic mobility values using the Smoluchowski approximation.

3.3.3. LbL Deposition of PHPE-TA Complexes

Silicon wafers or glass slides were immersed in concentrated sulphuric acid for 1 h and 25 min, and then rinsed with deionized water (18.2 MΩ·cm). After drying under a flow of nitrogen, wafers were immersed into 0.25 M NaOH solution for 10 min, thoroughly rinsed with deionized water and dried again under nitrogen flow. LbL films were deposited at the surface by immersing the substrate into solutions of PHPE-TA complexes for 15 minutes for each layer. Importantly, drying after each layer of PHPE-TA complexes was crucial for successful film growth. Of note, in contrast to traditional LbL process, an oppositely charged polymer counterpart was not used during construction of multilayers. Multilayer growth and film stability were followed by monitoring the thickness of the dried films using a spectroscopic ellipsometer (Optosense, USA). Each side of the multilayer coated substrates were sterilized under UV light for 1 h prior to biological experiments.

3.3.4. Crosslinking of Multilayers of PHPE-TA Complexes

Multilayers of PHPE-TA complexes were crosslinked using the procedure described by Ball [34] with slight modifications. Briefly, multilayers were immersed into 10 mM $NaIO_4$ solution (prepared using 0.001 M monobasic phosphate buffer at pH 4) for 5 min. To assure complete removal of $NaIO_4$ residuals from the surface, substrates were immersed in excess amount of 0.001 M monobasic phosphate buffer at pH 4 for 1 h. The substrates were then rinsed thoroughly with a pisette using 0.001 M monobasic phosphate buffer. Finally, coated substrates were immersed into 0.001 M monobasic phosphate buffer at pH 4 overnight and then dried under a flow of N_2. Each side of the multilayer coated substrates were sterilized under UV light for 1 h prior to biological experiments.

3.3.5. Cell Culture and Treatments

The SaOS-2 human osteoblastic cell line (ATCC) was used for all biological experiments. Cells were cultivated in high-glucose DMEM (Sigma) supplemented with 4 mM L-glutamine, 10% Fetal Bovine Serum (FBS), 100 U/mL penicillin, and 100 µg/mL streptomycin (standard medium). After thawing the stocks, cells were cultivated in T25 flasks and the medium was renewed every two or three days. All cell culture flasks were maintained in a humidified atmosphere at 37°C in 95% air and 5% CO_2. To harvest cells from the flasks, 0.5 mg/mL porcine trypsin with 0.2 mg/mL EDTA·4Na solution was used. To isolate protein or RNA, cells were harvested by gentle scraping with a sterile cell scraper. Where indicated, the growth medium was supplemented with the Mineralization Activation Cocktail (MAC). The MAC medium was composed of 5 mM β-glycerophosphate, 50 µg/mL L-ascorbic acid, and 100 nM dexamethasone [35,36]. 5 mM of β-glycerophosphate was used in this research, as higher concentrations are reported to cause non-specific mineralization in the culture medium. PHPE was dissolved in sterile Dulbecco's Phosphate Buffered Saline (D-PBS) in a concentration of 2 mg/mL and filtered through 0.2 µm sterile PES filters before addition in the growth medium. For experiments based on the direct addition of PHPE into the growth medium, 75,000 SaOS-2 cells were seeded in the wells of a

48-well plate, cultivated in standard medium for two days. For some of the wells, the medium was replaced with MAC medium; others were cultivated in standard medium. For all the wells, the medium (MAC or standard) were replaced every two days. PHPE supplementation was carried out every two days including the first day of cell seeding. For experiments carried out with coated surfaces, 150,000 SaOS-2 cells were initially seeded in the wells of a 24-well plate. For 7-day experiments, the medium was renewed twice in total. For 15-day experiments, the medium was renewed five times in total. MAC medium was replaced with the standard medium where indicated, but just 3 days after the initial seeding of cells in wells.

3.3.6. Cell Viability Analysis

The viability of cells grown on LbL films of PHPE-TA complexes was determined by the 3-(4,5-dimethylthiazolyl-2)-2,5-diphenyltetrazolium bromide (MTT) protocol. For the experiments that are related with the direct addition of PHPE, cell viability was determined after cultivation of SaOS-2 cells for 2 days and 4 days. Treatments of samples with a final PHPE concentration of 0.01 mg/mL, 0.05 mg/mL or 0.2 mg/mL were compared with samples where no PHPE was added. 5 mg/mL of stock MTT solution was prepared in D-PBS. This solution was diluted by 10 times using standard DMEM with 10% FBS, to reach a final concentration of 0.5 mg/mL. 500 μL of the diluted MTT medium was added into each cell-seeded well of a 24-well plate. After incubating the plate for 4 hours in a cell culture incubator, 500 μL of detergent reagent (0.01 N HCl with 100 mg/mL SDS prepared in deionized water) was added into each well and the plate was kept in the cell culture incubator for overnight duration. Three different samples were taken from each well and reading of OD_{570nm} was obtained with a microplate reader and analyzed for comparisons.

3.3.7. Determination of the Cell Adherence and Propagation on Surfaces

SaOS-2 cells (30,000) were seeded on each of the following: 1) 1 cm x 1 cm glass substrates; 2) 1 cm x 1 cm glass substrates coated with collagen; 3) 1 cm x 1 cm glass

substrates coated with non-crosslinked multilayers of PHPE-TA complexes; 4) 1 cm x 1 cm glass substrates coated with crosslinked multilayers of PHPE-TA complexes; and 5) 1 cm x 1 cm glass substrates coated with non-crosslinked multilayers of PHPE-TA complexes placed in 24-well tissue culture plate. As a control, cells were directly seeded into tissue culture plate wells. The cells were cultivated in high glucose-DMEM with 10% FBS for 2 h or 24 h, the surfaces were washed twice with sterile PBS and cells were fixed in 10% parafolmaldehyde for 20 min. After rinsing the surfaces twice with deionized water, cells were permeabilized in 10 mM Tris-HCl containing 2 mM $MgCl_2$ and 0.5% Triton X-100 in PBS and the surfaces were rinsed 4 times with deionized water. The cells were treated with 3,3′-dioctadecyl-5,5′-di(4-sulfophenyl) oxacarbocyanine sodium salt (SP-DiOC$_{18}$(3)) with a final concentration of 5 μg/mL in the culture medium for 5 min in a cell culture incubator at 37˚C and subsequently for 15 min on ice. The cells were observed under a FloID fluorescent microscope (Life Sciences, USA) in the green channel. Images from 6 random sites for each well were recorded.

3.3.8. Determination of Total Collagen Amount

Total collagen amount was determined by staining the layer of cells with Direct Red 80 (Sirius Red F3B) according to Tullberg-Reinert and Jundt [37] with slight modifications. This anionic dye binds to the [Gly-X-Y] triple helical structure found in collagen fibrils where X is most commonly proline and Y is either hydroxyproline or hydroxylysine [38]. Cell layers grown on glass substrates were rinsed twice with D-PBS and fixed with Bruin's fluid (15 mL saturated aqueous picric acid mixed with 5 mL 35% formaldehyde and 1 mL glacial acetic acid) for 1 h. The cell layers were extensively washed with D-PBS and then 100 mg/mL Direct Red 80 (dissolved in saturated aqueous picric acid) was added into each well and the cell culture plate was shaken slowly at room temperature in a microplate shaker for 1 h. To remove all non-bound dye, the cells were rinsed with 0.01 N HCl until no dye released from the surface. Every stained cell layer was observed under a light microscope and images from 5 different points were recorded under 4x lenses of a light microscope equipped

with a CCD camera (Leica, Wechsler, Germany). The images were analyzed with ImageJ software. The dark-red areas on the surface were indicative of collagen amount.

3.3.9. Determination of The Amount of Mineralized ECM

SaOS-2 cells were cultured in growth medium with varying concentrations of PHPE for 8 days. As a control group, cells were cultured in a growth medium containing no PHPE under the same conditions. Substrates coated with crosslinked multilayers of PHPE-TA complexes, substrates coated with collagen, and blank tissue culture plate as the control were cultured with cells for 15 days. To determine hydroxyapatite deposition in the extracellular matrix of SaOS-2 cells, Alizarin Red S staining of the cell layer was carried out, with slight modifications of the protocol described by Gregory et al. [39] Cell layers were rinsed twice with D-PBS and were fixed with 10% paraformaldehyde solution (prepared in DI water) for 15 min at room temperature. 40 mM Alizarin Red S was dissolved in deionized water and the pH of the solution was adjusted to 4.1. Paraformaldehyde-fixed cell sheets were rinsed 5 times using deionized water. Alizarin Red S solution was added into each well and the plate was shaken slowly in a microplate shaker for 20 min. Stained cell sheets were rinsed 5 times with deionized water and observed under a light microscope under a 4x objective. 5 different images from random points on the well were recorded with the CCD camera of the light microscope (Leica, Wechsler, Germany) and analyzed with ImageJ software. Bright red areas corresponded to mineralization of the ECM.

3.3.10. Analysis of Gene Expression by Reverse Transcriptase Quantitative Polymerase Chain Reaction (RT-qPCR)

75,000 SaOS-2 cells were seeded in 48-well TC-treated tissue culture plates using a culture medium containing PHPE with a final concentration of 0.01 mg/mL, 0.05 mg/mL, or 0.2 mg/mL. As a control group, cells were seeded using a culture medium containing no PHPE under the same conditions. Every 2 days, culture medium was replaced and PHPE supplementation was continued. After 8 days, total RNA isolation

from cells was carried out with the RNeasy® Mini Kit (Qiagen, Hilden, Germany), according to the manufacturer's protocol. 1000 ng of RNA was reverse transcribed with Revert-Aid first strand cDNA synthesis kit (Thermo Fisher Scientific, Boston, MA, USA). The following *GAPDH*, *COL1A1*, *VEGFA*, and *BMP2* primers were used for the PCR of the cDNA and qPCR reactions (Table 3.1.). *COL1A1*, *VEGFA*, and *BMP2* represent early osteogenic marker genes.

Table 3. 1. PCR primers sequences designed for human *GAPDH*, *COL1A1*, *VEGFA*, and *BMP2* genes. T_m stands for the primer melting temperature, *F* is the forward primer, *R* is the reverse primer

Gene specific primer		Accession number	Primer sequence	Product length (bp)	T_m (°C)
GAPDH	F	NM_001289746	5' – CGACCACTTTGTCAAGCTCA – 3'	238	58.42
	R		5' – CCCCTCTTCAAGGGGTCTAC – 3'		58.79
COL1A1	F	XM_005257059	5' – TCTGACTGGAAGAGTGGAG – 3'	214	55.36
	R		5' – ACTCGAACTGGAATCCATCGG – 3'		59.86
VEGFA	F	NM_001287044	5' – ATCACGAAGTGGTGAAGTTC – 3'	265	55.71
	R		5' – TGCTGTAGGAAGCTCATCTC – 3'		56.73
BMP2	F	NM_001200	5' – TCCATGTGGACGCTCTTTCA – 3'	80	59.32
	R		5' – ACCATGGTCGACCTTTAGGAGA – 3'		60.56

SYBR Green master mix with ROX reference dye (Bio-Rad Laboratories Inc., Berkeley, CA, USA) was used to determine the relative amounts of *GAPDH*, *COL1A1*, *VEGFA*, and *BMP2* expression after 45 cycles of qPCR. Relative expression of these

119

genes were evaluated by the Pfaffl method [40]. The results were normalized respect to *GAPDH* expression in every sample and given as "fold increase".

3.3.11. Determination of Alkaline Phosphatase Activity of Cells on Coated Substrates

To determine the differentiation of SaOS-2 cells grown on coated glass substrates, alkaline phosphatase activity was determined. Cells were lysed in PBS containing 10 mM Tris-HCl, 2 mM $MgCl_2$ and 0.5% Triton X-100 and the pH was adjusted to 8.2. Cell lysates were scraped into an Eppendorf tube and frozen in liquid nitrogen and thawed twice. All samples were sonicated on ice for 2 min and centrifuged at 14,000 rpm for 10 min at 4°C. 5 μL aliquots from the supernatants were incubated with 50 μL of 50 mM pNPP solution at room temperature for 1 hour and 1 mL of 50% EDTA was added into each sample to stop the reaction. The absorbance of the samples was recorded at 405 nm with a microplate reader.

3.3.12 Isolation of Total DNA from Cells

Genomic DNA of cells growing on different type of surfaces was isolated as described previously [41]. Simply, cells were washed twice with sterile PBS, and lysed with 200 μL of 100 mM Tris-HCl, 0.5 M EDTA, 2% SDS, and 5 M NaCl for 15 min at pH 8.5. The cells were always kept on ice during this protocol. Lysed cells were scraped and moved to an Eppendorf tube. 1 mL isopropanol was added into this lysate and the samples were centrifuged at 4 °C for 5 min at 10,000x *g*. The organic phase was transferred to a new tube and 1 mL of absolute ethanol was added to this mixture. The samples were centrifuged at 4 °C for 5 min at 10,000x *g*. Samples were heated at 65ºC until the organic solvents were evaporated. The precipitate was dissolved overnight in 70 μL of Tris-EDTA buffer and DNA concentration of aliquots were measured with a NanoDrop Microvolume Spectrophotometer (Thermo Fisher Scientific, Boston, MA, USA).

3.3.13. Statistical Analysis

Statistical analysis was carried out by GraphPad Prism 7 software. The level of significance was determined at the level of $p \leq 0.05$. Results obtained in experiments were expressed as the means and standard error of means (SE) of at least three independent experiments, performed on separate days. Column graphs were statistically analyzed by one-way Analysis of Variance (ANOVA) and if ANOVA was significant, column values were compared with the control values with the Holm-Sidak multiple-comparisons test. Analysis between pairs of groups other than the control values was performed by one-tailed or two-tailed *t*-test with Welch's correction. Levels of significance were as follows: (*) $P < 0.05$, (**) $P < 0.005$, (***) $P < 0.0005$, (****) $P < 0.0001$.

3.4. Results and Discussion

Poly(4-hydroxy-L-proline ester) (Figure 3.1.) is a polyester with *trans*-4-hydroxy-L-proline ester repeating units. PHPE was synthesized via polycondensation of *N*-cbz-4-hydroxy-L-proline, followed by deprotection of carboxybenzy (cbz) groups of poly(4-hydroxy-N-cbz-L-proline ester) (PHCP). ^{1}H-NMR graphic of PHCP can be seen in Figure 2. ^{1}H-NMR and MALDI-TOF analysis of PHPE can be found in Figure 3.3. and Figure 3.4. PHPE is cationic at physiological pH. PHPE was reported to be hydrolytically degradable in HEPES buffer at pH 7 and 37°C with a half-life of ~2 hours by Lim et al. The rate of degradation of PHPE was found to increase as the pH of the solution increased [33]. High rate of polymer degradation was correlated with the nucleophilic attack of the secondary amine groups of PHPE to its backbone, at neutral and basic pH. Degredation is lower at acidic pH, as the hydronium ion concentration in the buffer increased and the amine group is protonated [33].
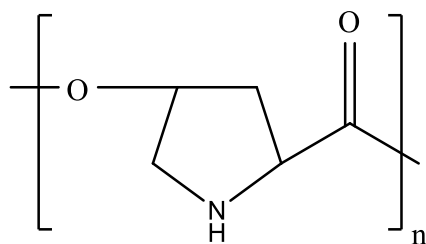
Fig. 3. 1. The chemical structure of the repating unit of poly(4-hydroxy-L-proline ester) (PHPE)
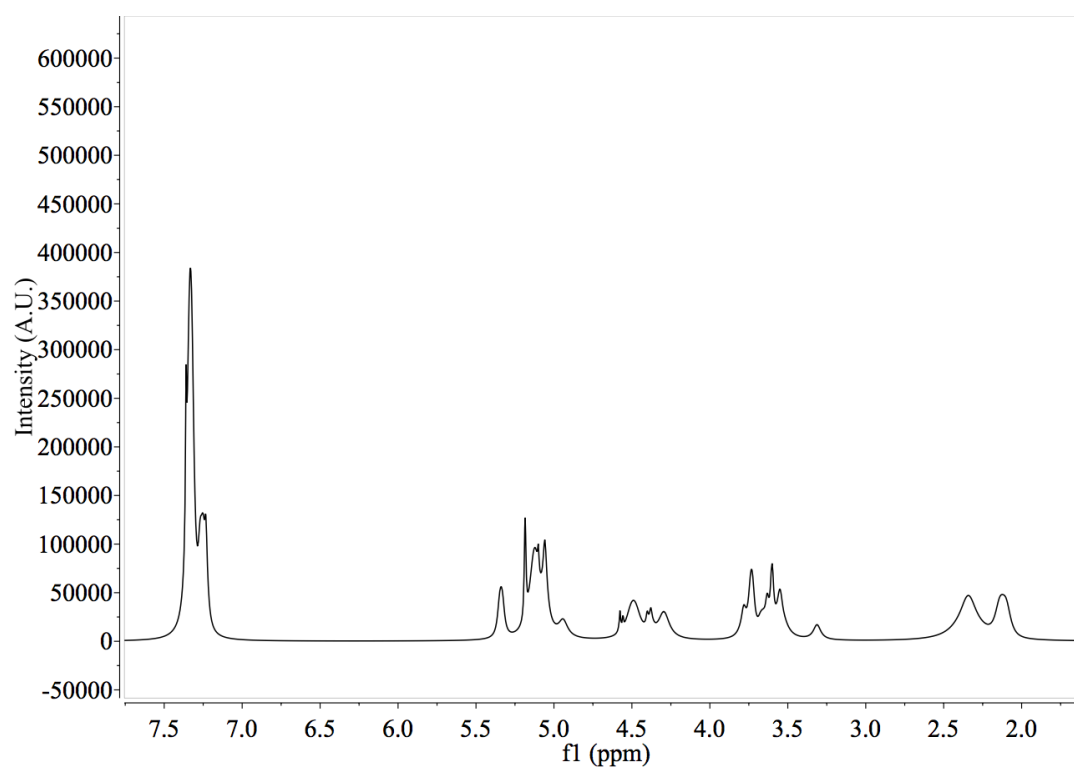
Fig. 3. 2. ^{1}H-NMR spectrum of poly(4-hydroxy-*N*-cbz-L-proline ester) in CDCl$_3$. ^{1}H-NMR (CDCl$_3$, 400 MHz): δ (ppm) = 7.23-7.36(5H, m, Ph), 5.34(1H, br s, CH), 4.94-5.18(2H, br m, CH$_2$), 4.29-4.58(1H, br m; CH), 3.55-3.78(2H, br m, CH$_2$), 2.12-2.34(2H, br m, CH$_2$).

122
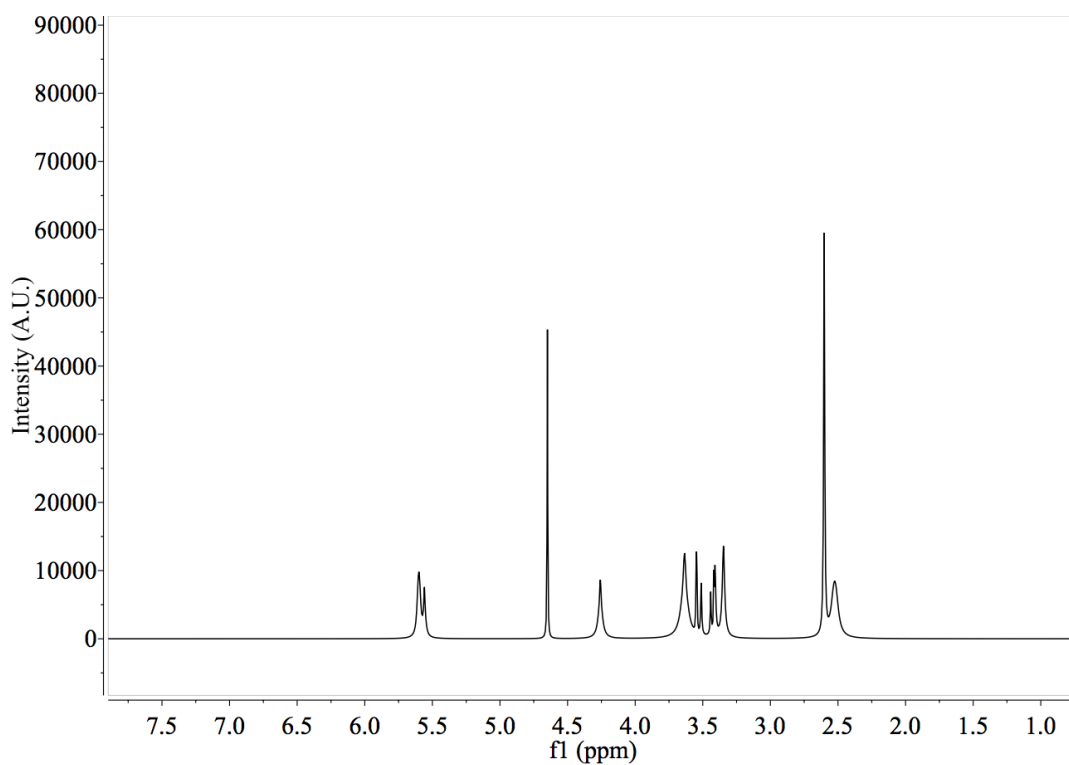
Fig. 3. 3. ^{1}H-NMR spectrum of poly(4-hydroxy-L-proline ester) in D_2O. ^{1}H-NMR (D_2O, 400 MHz): δ (ppm) = 5.58-5.60(1H, br s, CH), 4.26-4.65(1H, br s, CH), 3.35-3.63(2H, m, CH_2), 2.52-2.60(2H, br m, CH_2).

123
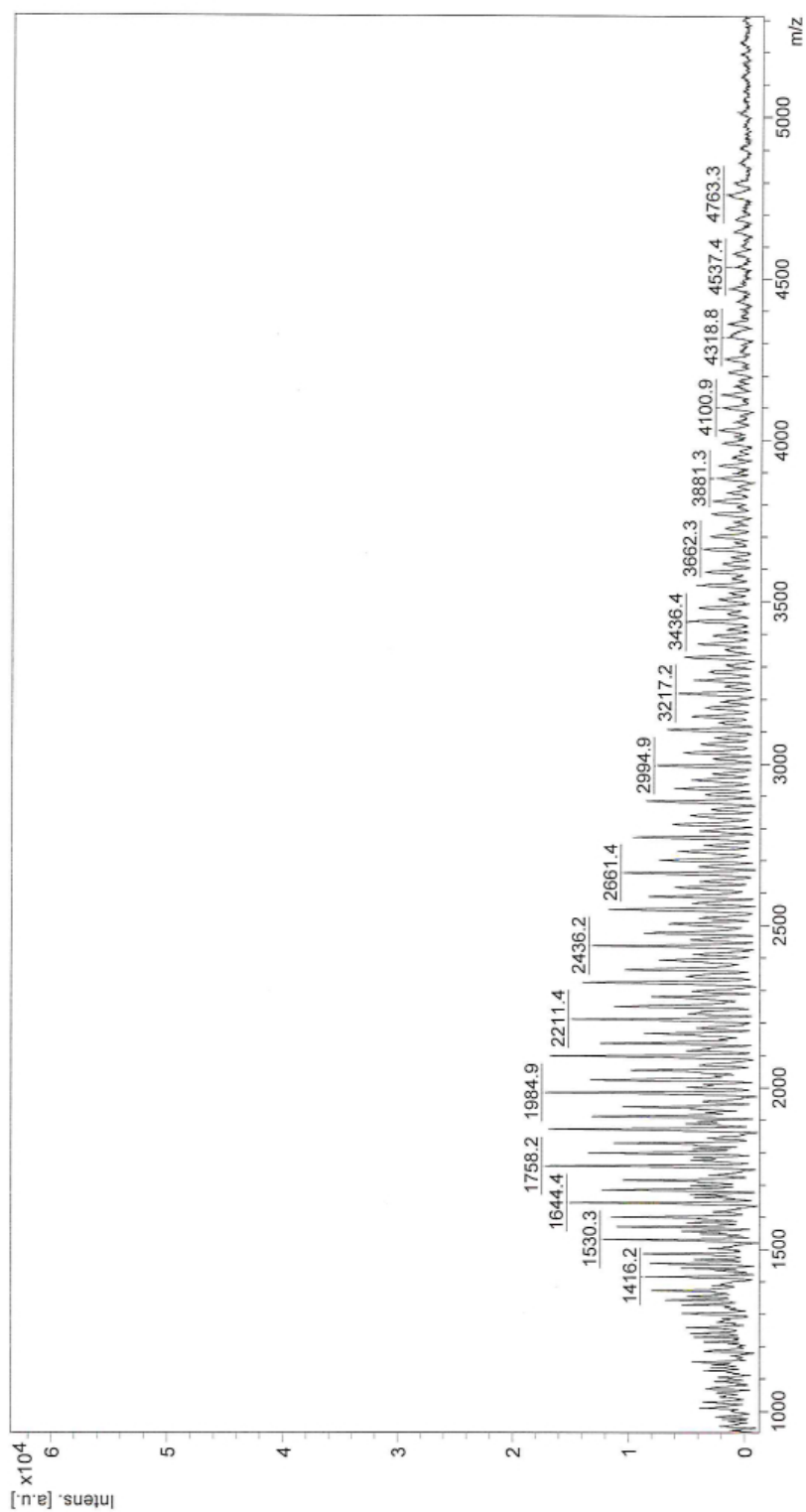
Fig. 3. 4. MALDI-TOF spectrum of poly(4-hydroxy-L-proline ester). x axis represents the molecular weight in g/mol. $M_n = 2330$, $M_w = 2900$.

124

Under physiological conditions, PHPE can rapidly degrade to Hyp [33], a non-coded amino acid that possesses many unique functions in the human body such as collagen helix formation [42], calcium binding [43], glucose metabolism [44] and neurotransmission [45]. Hyp is the product of post translational hydroxylation of proline in procollagen and is primarily responsible for the formation of the triple helical structure of collagen, imparting enhanced water binding property to collagen [46]. Collagens, have distinctive Gly-Xaa-Yaa repeating sequence, where Xaa is often proline and Yaa is Hyp, and disruptions of this sequence suppresses the formation of collagen helix, thus osteogenesis [47]. The lack of proline hydroxylation *in vivo* leads to dysfunctional collagen extracellular matrix assembly by changing its hydration properties [46] and increasing its melting temperature. Thereby, providing stability to collagen [48].

3.4.1. Cytotoxicity of PHPE

The cytotoxicity of PHPE on the SaOS-2 cell line was determined by an MTT assay using different concentrations of the PHPE. SaOS-2 cells were cultivated in the standard growth medium with or without PHPE treatment. The treatment did not lead to any loss in cell viability after 48 and 96 hours from cell seeding. Importantly, the cell viability was determined to be higher for most of the samples with PHPE supplementation, compared to the control samples (Figure 3.5.). At 96 h, cell viability was significantly higher for the samples treated with 0.05 mg/mL PHPE than the control (Figure 5B). Although cationic polymers generally cause cytotoxicity in mammalian cells [49], the reason for higher cell viability could be related with the degradation product of PHPE, Hyp [33]. This amino acid metabolizes to pyruvate and glyoxylate, thus providing a source of energy for the mitochondria [50,51]. Perret et al. reported that $\alpha_1\beta_1$ integrins on cells can interact with the GFOGER sequence in collagen [42]. Therefore, it is possible that integrin-Hyp interaction enhanced cell adherence and propagation on surfaces, leading to an increase in cell proliferation. However, on the contrary, Seo et al. reported that hydroxylation of proline was not necessary for mammalian collagen-α_1 integrin binding [52].
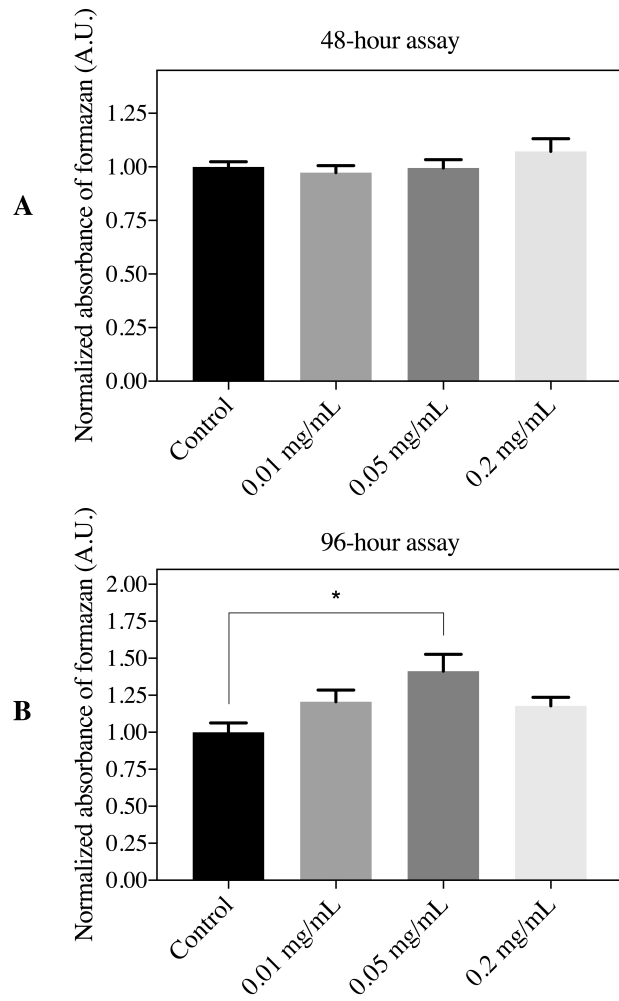
Fig. 3. 5. MTT assay showing the viability of cells supplemented with PHPE with a final concentration of 0.01 mg/mL, 0.05 mg/mL, or 0.2 mg/mL in the standard medium or without PHPE (control), after 48 hours (Panel A) and 96 hours (Panel B). Results are given as the means and the their standard errors (SE). Statistical variance is analyzed with one-way ANOVA and results are further compared with the Control through Holm-Sidak's multiple comparisons test (*$P<0.05$)

3.4.2. PHPE-Induced Collagen Type I Expression of SaOS-2 Cells

Human *COL1A1* gene codes for the enzymes necessary for the synthesis of procollagen type I, which is then post-translationally modified and secreted outside the cells and form collagen type I in the extracellular matrix. In their course of differentiation to mature cells, osteoblasts are known to express *COL1A1* [53]. To determine the effect of PHPE treatment on the *COL1A1* expression and collagen synthesis in SaOS-2 cells, we divided the treatment groups into two: **i**) treatment of cells cultivated in the standard medium or **ii**) cultivated in MAC. In groups **i** and **ii**, the cells were treated with different concentrations of PHPE every two days, including the day cells were seeded. Control cells were treated with the vehicle. In group **ii**, the standard medium was replaced with MAC, only after cell monolayer formation. Replacement of the medium with MAC was carried out to see if PHPE would have an inductive effect on collagen expression and synthesis even when osteogenic differentiation was induced with the supplemented ingredients of MAC.

In groups **i** and **ii**, the formation of small collagenous nodules of the extracellular matrix was observed in the wells and the nodules belonging to the samples with higher concentration of PHPE treatment appeared darker under a phase contrast microscope (Figure 6A). This was most likely because of the high absorbance of light passing through the specimen at denser regions. We cultured the cells for 8 days, and the cells with PHPE treatment showed nodules with higher collagen deposition at the end of this duration, as determined by Direct Red 80-staining. 0.05 mg/mL and 0.2 mg/mL PHPE supplementation into the medium significantly increased the amount of collagen in the ECM, compared to the control (Figure 6B). Direct Red 80 binds to collagen type I and III primarily, and possesses a red color, thus the observed darker shade of red represents denser collagen-rich nodules [37]. Once the cell culture medium was replaced with MAC after the cell monolayer formation, and the cell monolayer was stained with Direct Red 80, we observed collagen-rich nodules in every well. However, the nodules were larger and more localized in samples treated with PHPE. In group **ii**, we observed significant increase in the sample with 0.2 mg/mL PHPE treatment only, compared to the control (Figure 3.6C). To support our claims

regarding collagen synthesis, *COL1A1* expression of SaOS-2 cells was examined via qRT-PCR method. qRT-PCR analysis from total RNA extracts of each group showed that the *COL1A1* expression of the cells treated for 8 days with 0.2 mg/mL PHPE was ~2.4 fold higher while the same samples treated with 0.01 mg/mL PHPE was ~1.5 fold higher when compared to the control group (Figure 3.6D).
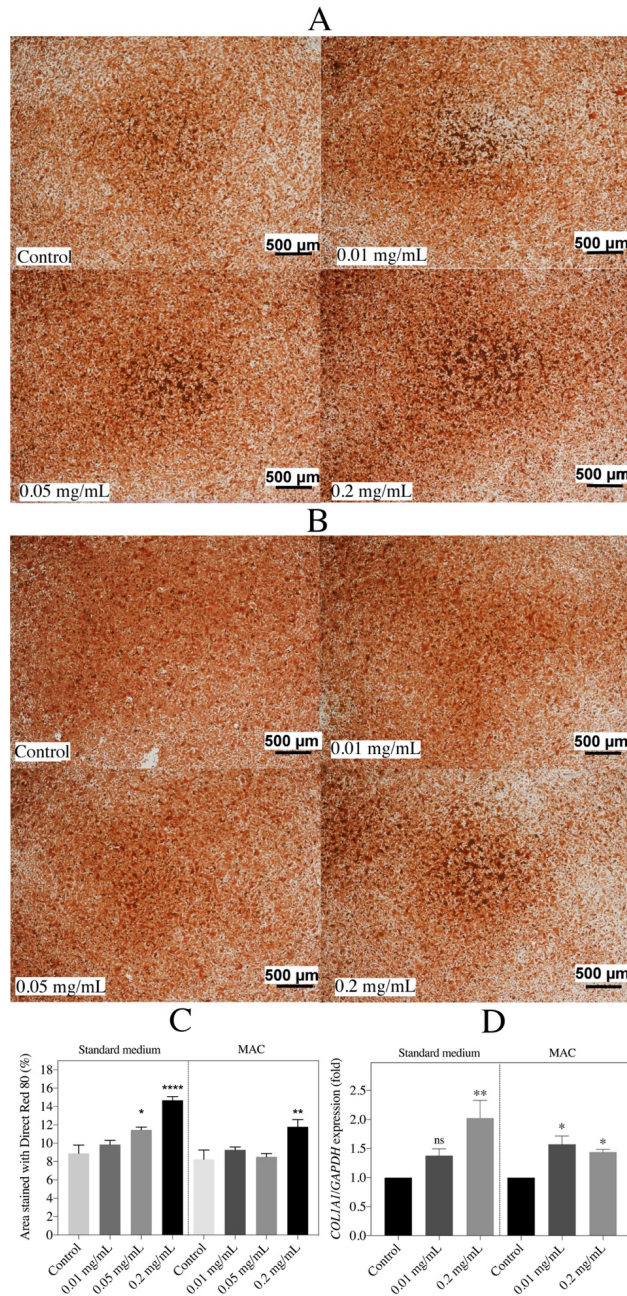
Fig. 3. 6. Panel A: 4x magnified phase contrast microscopy images of Direct Red 80-stained SaOS-2 cell monolayers that were cultivated for 8 days using standard

medium, without PHPE or with 0.01 mg/mL, 0.05 mg/mL, 0.2 mg/mL PHPE supplementation. Dark red nodules represent collagen-rich segments in the extracellular matrix. **Panel B:** 4x magnified phase contrast microscopy images of Direct Red 80-stained SaOS-2 cell monolayers which were cultivated for 8 days using MAC, without PHPE or with 0.01 mg/mL, 0.05 mg/mL, 0.2 mg/mL PHPE supplementation. **Panel C:** Amount of collagen in the extracellular matrix of SaOS-2 cell monolayers as determined by the percentage of the total cell monolayer area stained with Direct Red 80. Total area of the surface is expressed as 100% and the stained area is calculated accordingly. **Panel D:** *GAPDH*-normalized relative expression of *COL1A1* gene of SaOS-2 cells without PHPE or with 0.01 mg/mL, 0.2 mg/mL PHPE supplementation in standard medium or MAC. Gene expression of the control groups was normalized to 1 and expression values are shown as fold change, accordingly. All results are given as means and the their standard errors (SE) of means. Statistical variance was analyzed with one-way ANOVA and results were further compared with the control group through Holm-Sidak's multiple comparisons test (*$P<0.05$, **$P<0.005$, ***$P<0.0005$ and ns= not significant).

Expression of *COL1A1* was also induced by PHPE treatment of SaOS-2 cells when cells were cultivated in MAC. 0.2 mg/mL of PHPE treatment of cells every two days increased the level of expression of *COL1A1* by 1.5 fold compared to the control without PHPE treatment. As indicated in Section 3.2.5., MAC is a cell culture medium containing dexamethasone, L-ascorbic acid, and β-glycerophosphate supplementation. Dexamethasone can induce the expression of *RUNX2*, a master regulator of osteogenic differentiation, through the transcriptional activity of FHL2/β-catenin, whereas L-ascorbic acid may facilitate osteogenic differentiation by increasing collagen type I secretion. β-glycerophosphate serves as a phosphate source for ECM mineralization and induces osteogenic gene expression by extracellular related kinase phosphorylation [54]. Our data indicate that mechanistically, PHPE may upregulate *COL1A1* through signaling pathways independent of those induced by dexamethasone, L-ascorbic acid, and β-glycerophosphate.

3.4.3. Osteoinductivity of PHPE in SaOS-2 cells

Similar to the conditions described in Section 3.2., SaOS-2 cells were treated with or without PHPE up to 8 days. This time, cell monolayers were fixed, and then stained with Alizarin Red S. Alizarin Red S interacts with calcium phosphate-mineralized nodules and is indicative of the amount of calcium phosphate (predominantly hydroxyapatite) secreted from cells. In Section 3.2., we described that the supplementation of the standard medium with 0.2 mg/mL of PHPE significantly induced collagen type I expression and synthesis. Similarly, PHPE supplementation of 0.2 mg/mL in the standard medium caused a significant amount of mineralization in the ECM (Figure 3.7A). This finding supports the study of Salasznyk et al. on the requirement of matrix collagen-cell contact for the induction of osteogenic differentiation [55]. Samples with PHPE treatment of 0.01 mg/mL, 0.05 mg/mL and the samples with no PHPE treatment did not exhibit any visible mineralization, although nodules of collagen-rich extracellular matrix were present in all samples. ECM mineralization was limited solely to the sample with 0.2 mg/mL PHPE supplementation in the standard medium, either due to the significant upregulation in *COL1A1* gene, or due to the induction of a different pathway of osteogenic differentiation by PHPE at high concentrations. Presence of collagen in the ECM of osteoblasts is crucial for differentiation. α2β1 integrin, when in contact with the GFOGER peptide sequence on collagen, where 'O' stands for Hyp, has been shown to induce osteogenic differentiation of mesenchymal stem cells by regulating the expression of important osteogenic marker genes [35]. In the current study, once the standard medium was replaced with MAC, we observed that cells treated with 0.01 mg/mL and 0.05 mg/mL PHPE exhibited significantly higher amount of mineralization compared to the control sample. In contrast, 0.2 mg/mL PHPE supplementation in D-PBS in the standard culture medium did not significantly affect mineralization compared with the control (Figure 3.7B). Our results further support that the effect of PHPE in the induction of osteogenic differentiation is independent of the signaling pathways induced by dexamethasone, L-ascorbic acid, and β-glycerophosphate.

130

Bone formation and remodeling are complex processes where cytokines, growth factors, and hormones play significant roles. RUNX2 is an activator of a range of genes such as osteopontin (*SPP1*) and osteocalcin (*BGLAP*) that play essential roles in osteogenic differentiation [56]. This activator is highly expressed in preosteoblasts and is down-regulated after the osteoblasts mature [57]. *RUNX2* expression is regulated by bone morphogenetic proteins (BMPs) and BMP-2 signalling activates a cascade where *RUNX2* expression is induced in primary rat osteoblasts [58] and human bone marrow mesenchymal stem cells (hMSCs) [59]. BMP-2 release from cells has major importance in bone repair and remodelling and lack of BMP-2 has catastrophic effects on bone growth. For example, *Bmp2$^{-/-}$* knockout mice show major delay in bone maturation. Lack of femur fracture healing was reported to be observed in *Bmp2* knockout mice compared to the wild-type [60]. Collagen type I have been reported to induce osteogenic differentiation by enhancing the effects of TGF-β and BMPs. Inhibition of interaction of α1β1 and α2β1 integrins with collagen type I was reported to block the osteogenic differentiation of 2T3 cells induced by human recombinant BMP-2 [61]. We observed a significant upregulation in both *COL1A1* (Figure 3.6D) and *BMP2* expression (Figure 3.7D) in cells treated with 0.01 and 0.2 mg/mL PHPE in the standard medium, respectively which may indicate the differentiation of SaOS-2 cells into osteoblasts. In line with these findings, enhanced expression of *BMP2* in SaOS-2 cells under the treatment with PHPE could also explain the upregulated expression of *COL1A1* gene, and thus the deposition of denser collagen-rich nodules. These results also support the presence of denser collagen-rich nodules and the presence of mineralized nodules in samples treated with 0.2 mg/mL PHPE.

Another marker gene for osteogenic differentiation is *VEGFA*. *VEGFA* codes for vascular endothelial growth factor (VEGF), a growth factor that stimulates tissue neovascularization and angiogenesis [62]. The vascularization of bone tissue is necessary for healthy bone regeneration [63]. There have been several reports on the induction of *VEGFA* expression during osteogenic differentiation of stem cells [64,65] and SaOS-2 cells [66]. Parallel to the findings in these reports, we observed 1.8-2 fold induction of *VEGFA* expression in SaOS-2 cells treated with PHPE compared to untreated cells (Figure 3.7E), which could indicate induced osteogenic differentiation.

These findings further support osteogenic differentiation of the cells and indicate that PHPE may also promote tissue vascularization. As an upregulation of the *VEGFA* gene of SaOS-2 cells under PHPE treatment was observed, we can conclude that the vascular endothelial growth factor (VEGF) was secreted in higher amounts from cells. VEGF is a growth factor which recruitsendothelial cells and mural cells to form blood capillaries in tissues. As previously reported, Ciclopirox, a drug that inhibited the synthesis of two non-coded amino acids, hypusine and hydroxyproline, also inhibited angiogenesis of HUVECs, which are endothelial cancer cells [67]. These outcomes could support our findings on induced *VEGFA* expression with PHPE treatment.
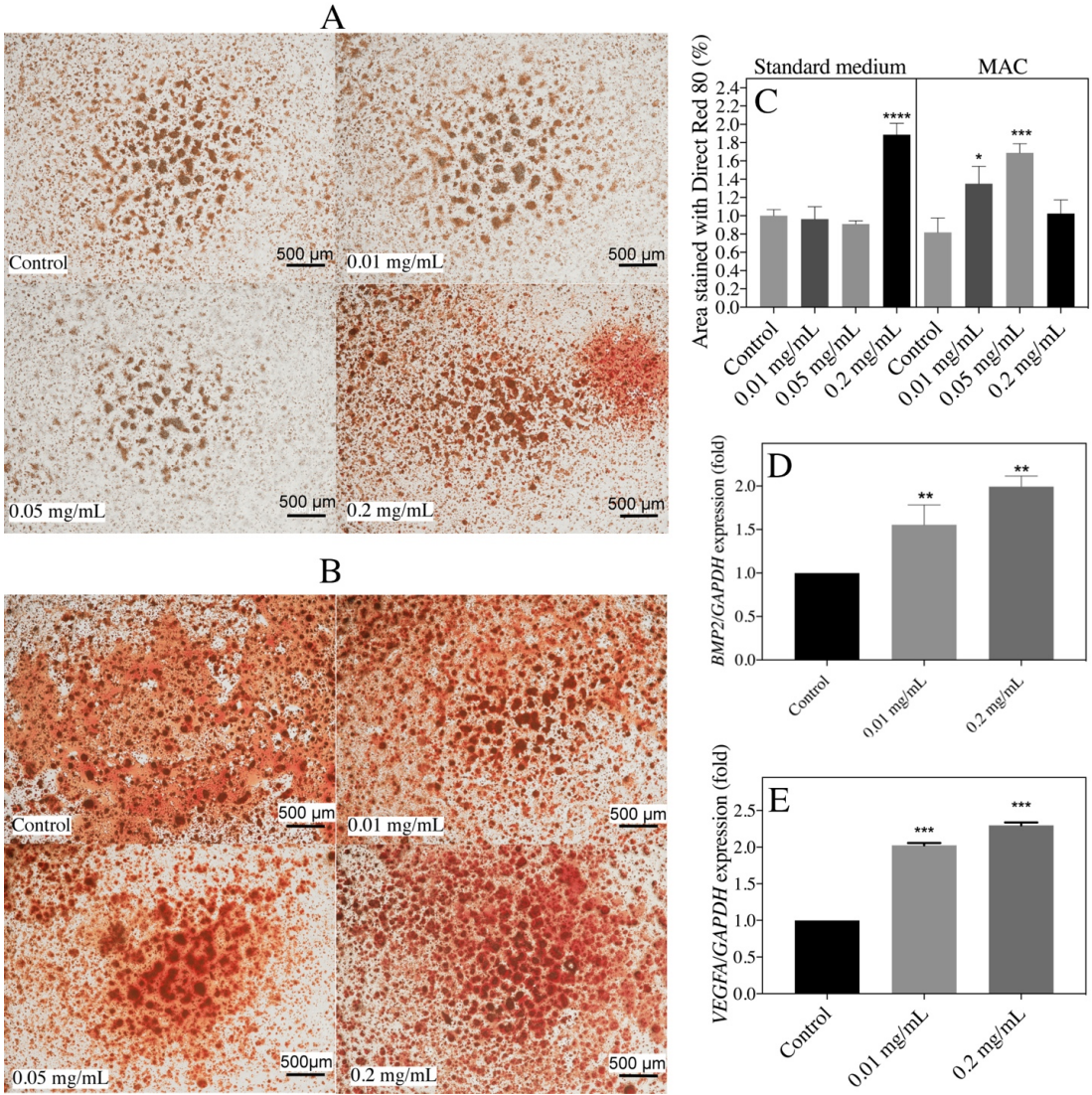
Fig. 3. 7. Panel A: 4x magnified phase contrast microscopy images of Alizarin Red S-stained SaOS-2 cell sheets which were cultivated for 8 days with standard DMEM

medium, without PHPE or with 0.01, 0.05, 0.2 mg/mL PHPE supplementation. **Panel B:** 4x magnified light microscopy images of Direct Red 80-stained SaOS-2 cell sheets which were cultivated for 8 days with MAC medium, without PHPE or with 0.01, 0.05, 0.2 mg/mL PHPE supplementation. **Panel C:** Fraction of Alizarin Red S-stained areas in wells supplemented with 0.01, 0.05, and 0.5 mg/mL PHPE or no supplementation in standard medium or MAC. Total area of the surface is expressed as 100% and the stained area is calculated accordingly. **Panel D:** *GAPDH*-normalized relative expression of *BMP2* gene of SaOS-2 cells under the supplementation of PHPE in the standard medium. **Panel E:** *GAPDH*-normalized relative expression of *VEGFA* gene in SaOS-2 cells under the supplementation of PHPE in the standard medium. All results are given as the means and the their standard errors (SE) of means. Statistical variance is analyzed with one-way ANOVA and results are further compared with the Control through Holm-Sidak's multiple comparisons test (*$P<0.05$, **$P<0.005$, ***$P<0.0005$, ****$P<0.0001$ and ns= not significant).

3.4.4. LbL Films of Water-Soluble Complexes of PHPE and TA

3.4.4.1. Preparation of Water Soluble Complexes of PHPE and TA

Water soluble complexes of PHPE and TA were prepared at pH 4 with a PHPE:TA molar ratio of 1:27. TA is a polyphenol and pK_a of TA varies in the literature due to use of different TA sources. One of our recent study showed that TA used in this study has two pK_a values. p$K_{a,1}$ and p$K_{a,2}$ were approximated as 6.5 and 8.5, respectively [68]. pK_a (amine) of trans-4-hydroxy-L-proline was reported as 9.47 [69] thus amino groups of PHPE were expected to be protonated at pH 4. The driving force for complexation was attributed to both hydrogen bonding and electrostatic interactions among PHPE and TA. PHPE has carbonyl units which could act as hydrogen acceptors, whereas TA has phenolic hydroxyl groups which could act as hydrogen donors. On the other hand, PHPE is positively charged at pH 4 and TA is expected to have phenolate groups at pH 4. p$K_{a,1}$ of TA was estimated as 6.5, however ionization of TA could have been enhanced in the presence of positively charged PHPE.

Enhanced ionization of polyacids in the presence of polycations has been reported earlier [70]. Complexation was followed by measuring the hydrodynamic size of PHPE-TA complexes using dynamic light scattering technique. PHPE-TA complexes precipitated as the amount of PHPE was increased during complexation. Therefore, PHPE:TA mol ratio was limited to 1:27. Figure 3.8. shows the size distribution by number of PHPE-TA complexes. The average hydrodynamic size of TA at pH 4 was 1.6 ± 0.2 nm and zeta potential was -26.1 ± 1.5 mV prior to complexation. The average hydrodynamic size (Figure 3.8.) and Zeta-potential of PHPE-TA complexes were recorded as 93.0 ± 8.0 nm and 21.0 ± 0.9 mV, respectively.
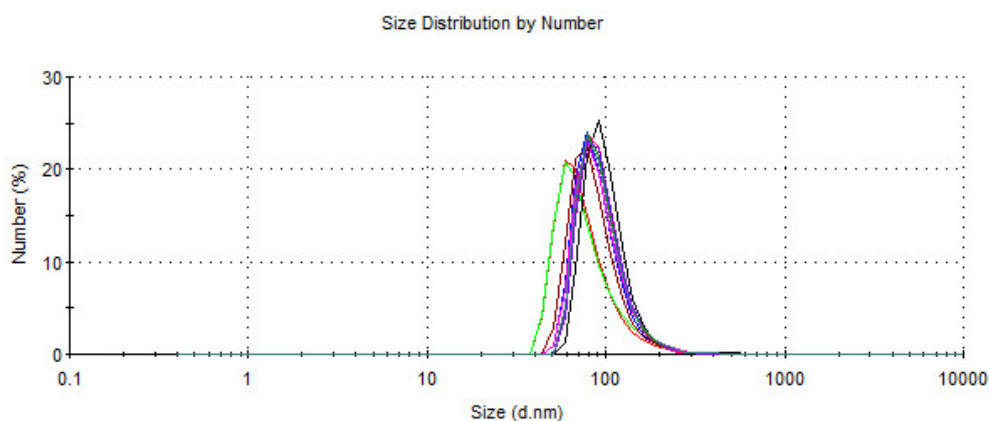
Fig. 3. 8. Hydrodynamic size distribution by number of PHPE-TA complexes in 0.001 M buffer at pH 4. Hydrodynamic sizes were determined by dynamic light scattering.

3.4.4.2. LbL Deposition of PHPE-TA Complexes

As mentioned in the previous section, PHPE:TA molar ratio was 1:27 in PHPE:TA complexes. The greater amount of TA in the complexes provided free hydroxyl/phenolate groups on TA which could be further used for LbL self-assembly at the surface. PHPE-TA complexes were LbL deposited at the surface without using a polymer counterpart. Traditional LbL deposition requires deposition of interacting polymers of two different kinds. De Saint-Aubin et al. was the first demonstrating construction of LbL films through an untraditional way, i.e. multilayer films had only one component and a polymer counterpart was not used [71]. Figure 3.9. shows the

evolution of ellipsometric thickness after deposition of every three layers of PHPE-TA complexes at the surface. Inset shows LbL growth of PHPE-TA complexes up to eight layers. The driving force for LbL assembly was hydrogen bonding interactions among carbonyl groups of PHPE and protonated hydroxyl groups of TA as well as electrostatic interactions among free secondary amino groups of PHPE and free phenolate groups of TA. Note that, drying after deposition of each layer was crucial for LbL deposition of PHPE-TA complexes. Effect of drying and orientation of the molecules at the surface on LbL film growth has been reported before [72,73]. Also, for successful multilayer growth of PHPE-TA complexes, deposition solution had to be refreshed every 3 layers to avoid aggregation of PHPE-TA complexes and the decrease in the number of free functional groups with time. Refreshing of deposition solutions provided higher increment per layer of PHPE-TA complexes. For example, refreshing deposition solution after every layer resulted in 0.91 ± 0.41 nm increase in thickness, whereas refreshing after every 3 layers led to 0.49 ± 0.13 nm increase per layer (Figure 3.9.). It is important to mention that we have also tried LbL deposition of PHPE and TA, rather than PHPE-TA complexes. However, we could not achieve successful growth of layers at the surface possibly due to the highly hydrophilic nature of PHPE and desorption of the film to the solution during PHPE deposition.
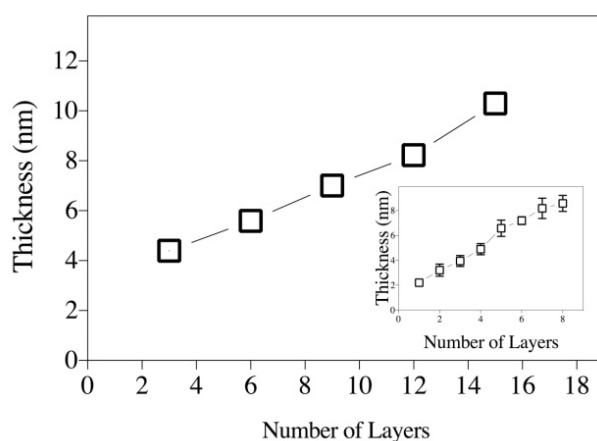
Fig. 3. 9. Evolution of ellipsometric thickness after deposition of every three layers of PHPE-TA complexes at the surface. Inset shows LbL growth of PHPE-TA complexes up to eight layers. Results are given as the averages of three thickness values and their standard deviation (SD).

3.4.4.3. Crosslinking of Multilayers of PHPE-TA Complexes

Multilayers of PHPE-TA complexes did not display long term stability (stable up to 4 days) in PBS at pH 7.4 and 37°C possibly due to the ionization of TA as the pH was increased and loss of hydrogen bonding interactions among the layers. Additionally, PBS contains various salt ions at different concentrations, resulting in enhanced ionization of TA. Enhanced ionization of polyacids at high ionic strength has been reported earlier [74]. Therefore, prior to performing bioassay experiments, multilayers were partially crosslinked using $NaIO_4$ to avoid desorption of the films from the surface. Ball reported that $IO4^-$ anions facilitated the oxidation of TA to yield quinone groups and formed covalent bonds between the quinone groups of TA and amino groups of poly(allylamine) (PAH) [34]. Using the procedure reported in this study, multilayers of PHPE-TA complexes were crosslinked using $NaIO_4$. For FTIR analysis, two samples were prepared: i) a solution of PHPE-TA complexes and ii) a solution of PHPE-TA complexes with $NaIO_4$ at a final molar concentration of 10 mM. Both solutions were examined with a NicoletTM ATR-FTIR instrument. As shown in Figure 3.10., FTIR spectra of crosslinked and non-crosslinked PHPE-TA complexes showed differences in some of the vibrational bands. Crosslinked PHPE-TA complexes, compared to the non-crosslinked complexes showed reduced absorbance at 1450 cm^{-1}, 1338 cm^{-1} and 1216 cm^{-1}. Our observations are in good agreement with the findings reported in Ball et al. [34]. Reduced absorbance may indicate the formation of quinone groups on TA. The secondary amine groups of PHPE might have reacted with these quinone groups, resulting in covalent bond formation.

To examine the effect of crosslinking on the stability of multilayers of PHPE-TA complexes, stability of crosslinked and non-crosslinked 15-layer PHPE-TA complexes was followed in PBS buffer at pH 7.4 at 37°C using UV-Vis Spectroscopy. The change in intensity of the peak at 205 nm, associated with protonated hydroxyl groups of TA was followed and the percent change in the intensity was correlated with the amount of TA retained at the surface. Figure 3.11. represents the normalized intensity at 205 nm as a function of time. In the case of non-crosslinked films, only ~20% of TA

remanied at the surface after 6 days of incubation. In the case of crosslinked films, ~70% of TA remained at the surface even after 15 days.
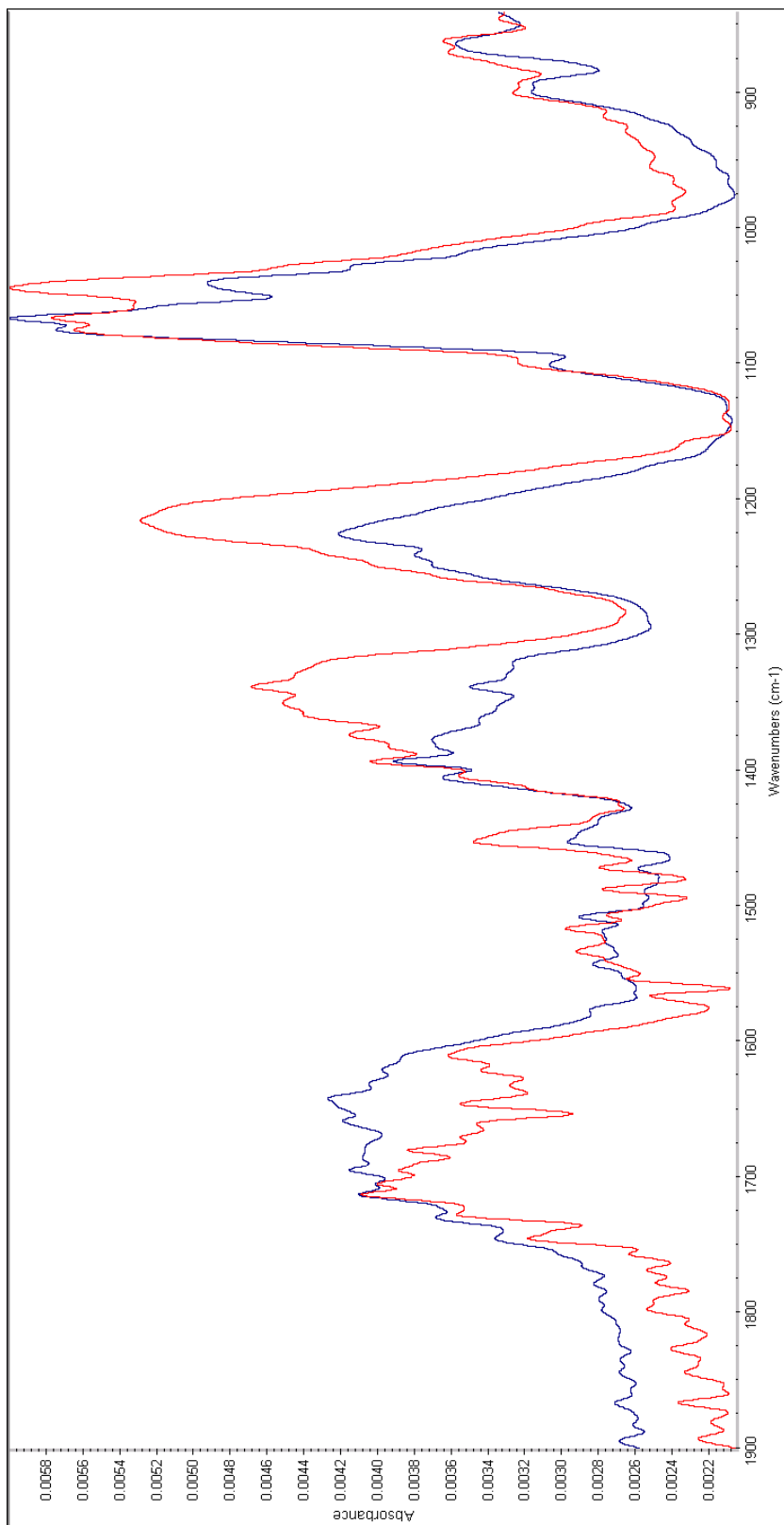
Fig. 3. 10. ATR-FTIR absorbance spectrum of non-crosslinked PHPE-TA complexes (red line) and crosslinked PHPE-TA complexes (blue line).

138
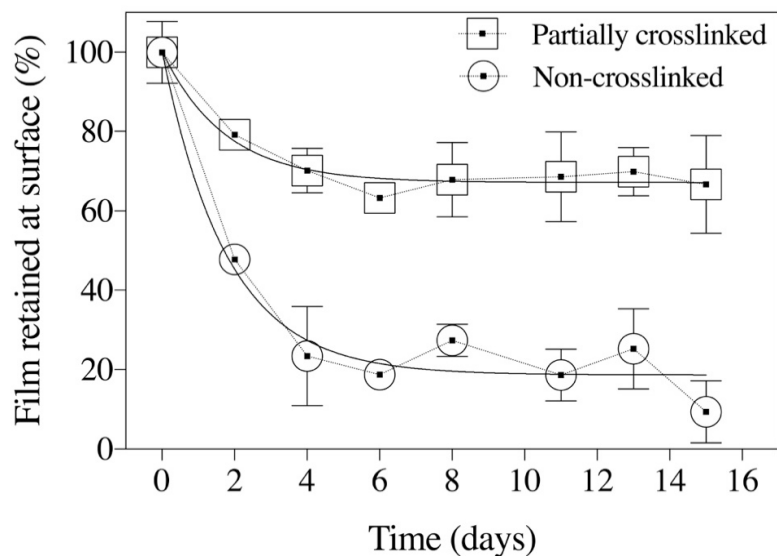
Fig. 3. 11. Normalized absorbance at 205 nm of 15-layer partially crosslinked (squares) and non-crosslinked (circles) PHPE-TA complexes as a function of time. Both multilayers were exposed to PBS solution at pH 7.5 and 37.5°C. Films were dried prior to collection of the spectra. The thickness of the film at day 0 was given as 100%, and the remaining film thicknesses are given as the percentage of the day 0 value. Results are given as the averages of three thickness values and their standard deviation (SD).

Of note, we have further confirmed the effect of crosslinking on the stability of multilayers of PHPE-TA complexes by exposing both crosslinked and non-crosslinked multilayers to highly acidic and basic conditions and comparing the stability of both types of films through ellipsometric thickness measurements, as suggested by Ball [34]. The difference in the fraction retained at surface between non-crosslinked and crosslinked films before and after exposure to 0.1 M HCl was distinct (Figure 3.12.).

139
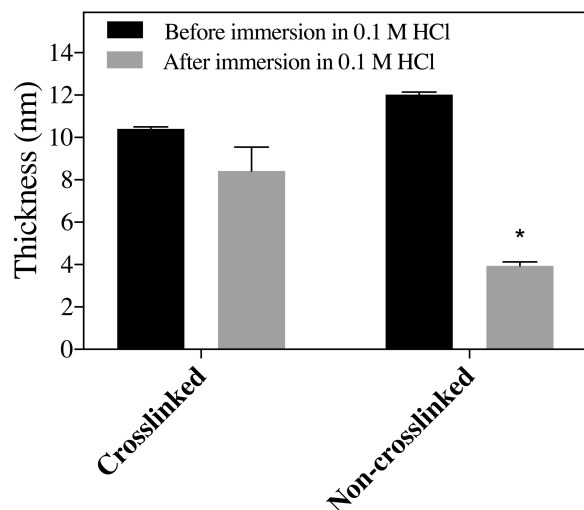
Fig. 3. **12.** Ellipsometric thickness of partially crosslinked and non-crosslinked LbL films of PHPE-TA complexes before and after immersion into 0.1 M HCl and solution for 5 min. Statistical analysis is carried with two-tailed student's *t*-test with Welch's correction, *$P<0.05$

3.4.4.5. Cytotoxicity and Adherence Properties of Substrates Coated With Multilayers of PHPE-TA Complexes

SaOS-2 cells were seeded in either: **i)** cell culture plate containing glass substrates coated with partially crosslinked multilayers of PHPE-TA complexes or **ii)** tissue culture treated plate containing glass substrates coated with collagen (positive control) or **iii)** cell culture plate (control). Of note, 1 layer of collagen deposition (~2.5 nm) at the surface was confirmed using ellipsometry. Two days after seeding, we observed that viability of cells grown on multilayers of PHPE-TA complexes was significantly higher than the viability of the control cells (Figure 3.13.). This data supports our previous findings on high cell viability of samples with the direct addition of PHPE. We suggest that degradation of PHPE and release of Hyp from the multilayers may have enhanced cell viability or the rate of cell division, as described previously in Section 3.1. (Figure 3.5.). As previously discussed by Lim et al., PHPE degrades to Hyp under physiological conditions [33].

140
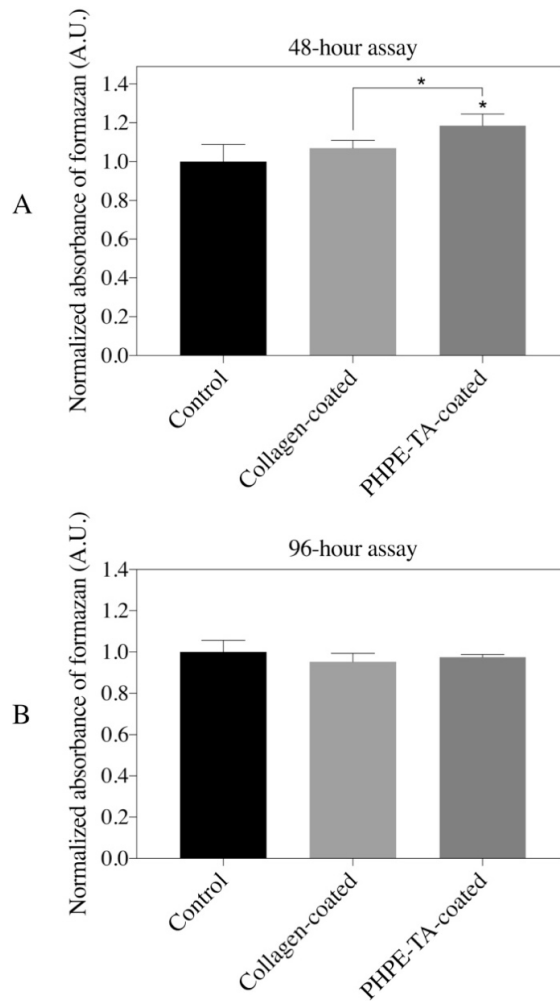
Fig. 3. 13. Viability of SaOS-2 cells in empty tissue culture treated plate (control), in tissue culture treated plate containing glass substrates coated with partially crosslinked 15-layer PHPE-TA complexes or tissue culture treated plate containing glass substrates coated with collagen (positive control) after 48 hours (Panel A) and 96 hours (Panel B) from cell seeding. All results are given as the means and the their standard errors (SE). Statistical variance is analyzed with one-way ANOVA and results are further compared with the Control through Holm-Sidak's multiple comparisons test. Two-tailed t-test with Welch's correction is applied for the comparisons of samples other than the Control (*$P<0.05$).

SaOS-2 cells, like osteoblasts, are adherent cells that possess cell-cell and cell-ECM interactions. Cell surface receptors and molecules such as integrins, I-CAMS, selectins, cadherins and proteoglycans are required for cell adhesion, movement and development [75]. Electrostatic interactions between functional chemical groups of the substrate and negatively-charged cell-surface proteoglycans are commonly preferred while designing biomaterial surfaces [76]. Adherent cells do not adhere properly on bare glass surfaces, which were used as substrate for LbL self-assembly in this study. Like many other adherent cell lines, SaOS-2 cell adherence can be affected by the surface chemistry; these cells prefer to adhere to biological molecules. Bioactivity of a surface can be determined by determining surface adhesion and rate of spreading of cells on a surface. In our case, osteoconductivity of multilayer films of PHPE-TA complexes was our primary focus and cell adherence, spreading, and proliferation of cells on these surfaces were the primary indicators of the surface osteoconductivity. We stained SaOS-2 cells with a lipid-binding fluorescent molecule, SP-DiOC$_{18}$ (Molecular Probes^{TM}, Oregon, USA) to determine the cellular morphology after adherence to the different substrates under study. SP-DiOC$_{18}$ can interact with the lipid membranes on cells and help determine the total area that cells covered on the seeded surfaces. SaOS-2 cells were cultivated in the standard medium and seeded on **i**) cell culture plate surface, **ii**) bare glass substrate, **iii**) collagen type I coated substrate, and **iv**) both partially crosslinked and non-crosslinked 15-layer films of PHPE-TA complexes. Two hours after seeding, bare glass substrate surfaces showed reduced cell adherence compared to all other groups (Figure 3.14.). After 24 h, cells grown on all surfaces showed spindle-like morphology and enhanced propagation (Figure 3.14.). Here, non-crosslinked films of PHPE-TA complexes showed significantly enhanced adherence compared to bare glass substrates and partially crosslinked films of PHPE-TA complexes. Glass surfaces also lack functional groups that can engage with cell surface receptors. This could be the reason of reduced surface binding of cells to plain glass substrates. After 24 h of cell seeding, we observed a significant difference between surface adherence property of partially crosslinked and non-crosslinked films of PHPE-TA complexes.
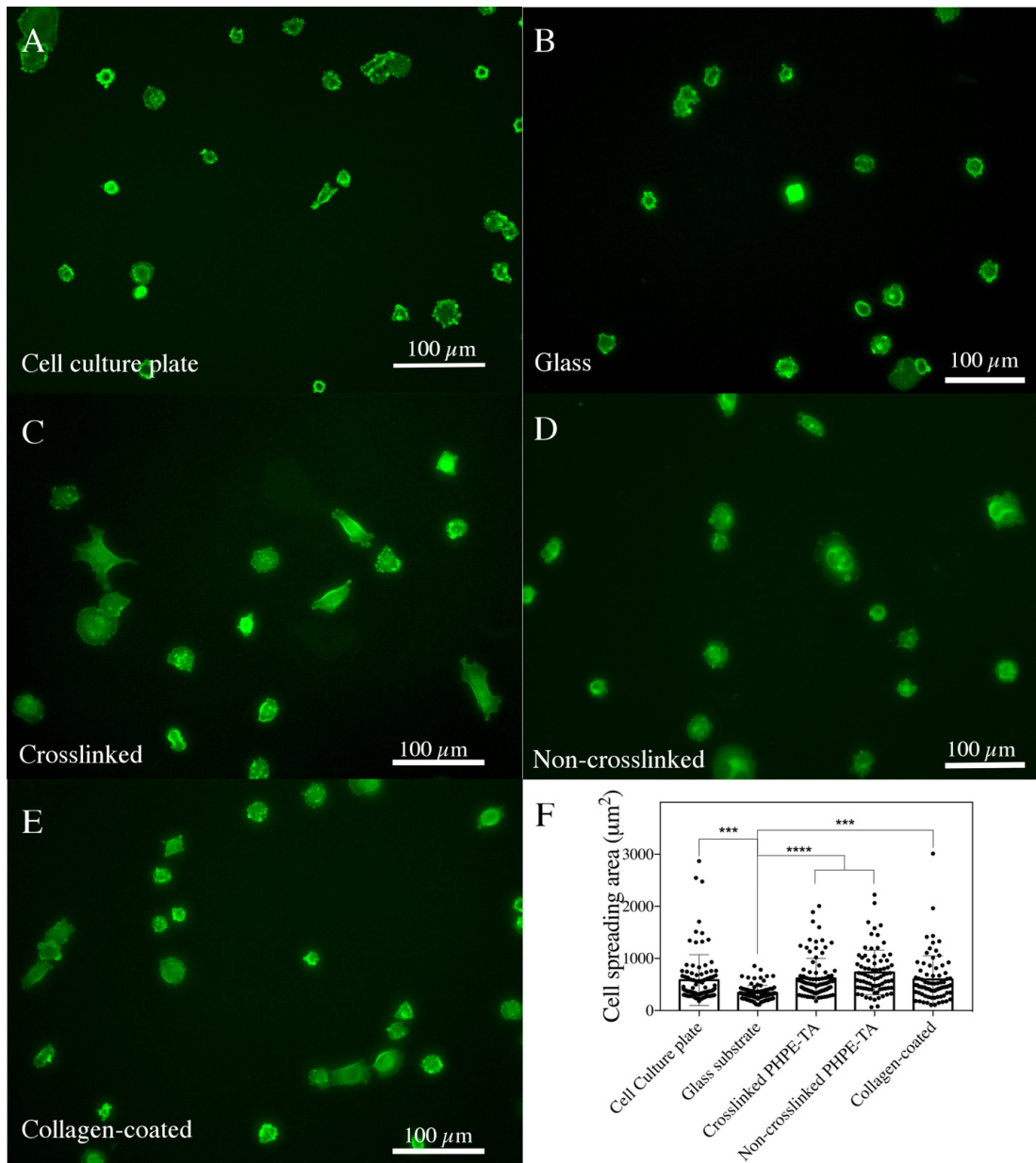
Fig. 3. 14. Fluorescent images and the cell area graph comparing the cell spreading areas 2 hours after seeding cells on surfaces. The cells were stained with SP-DiOC$_{18}$ fluorescent dye to determine the positions of the cell membrane. SaOS-2 were cultivated in the standard medium and seeded on (A) cell culture plate surface, (B) bare glass substrate, (C) collagen type I coated substrate, (D) partially crosslinked and (E) non-crosslinked 15-layer films of PHPE-TA complexes. Panel F shows total cell spreading area of each cell and their mean value. All results are given as the means and the their standard errors (SE) of means, along with the specific values as dots. Statistical variance is analyzed with one-way ANOVA and columns are further

compared with each other through Tukey's test (*P<0.05, **P<0.005, ***P<0.0005, ****P<0.0001).
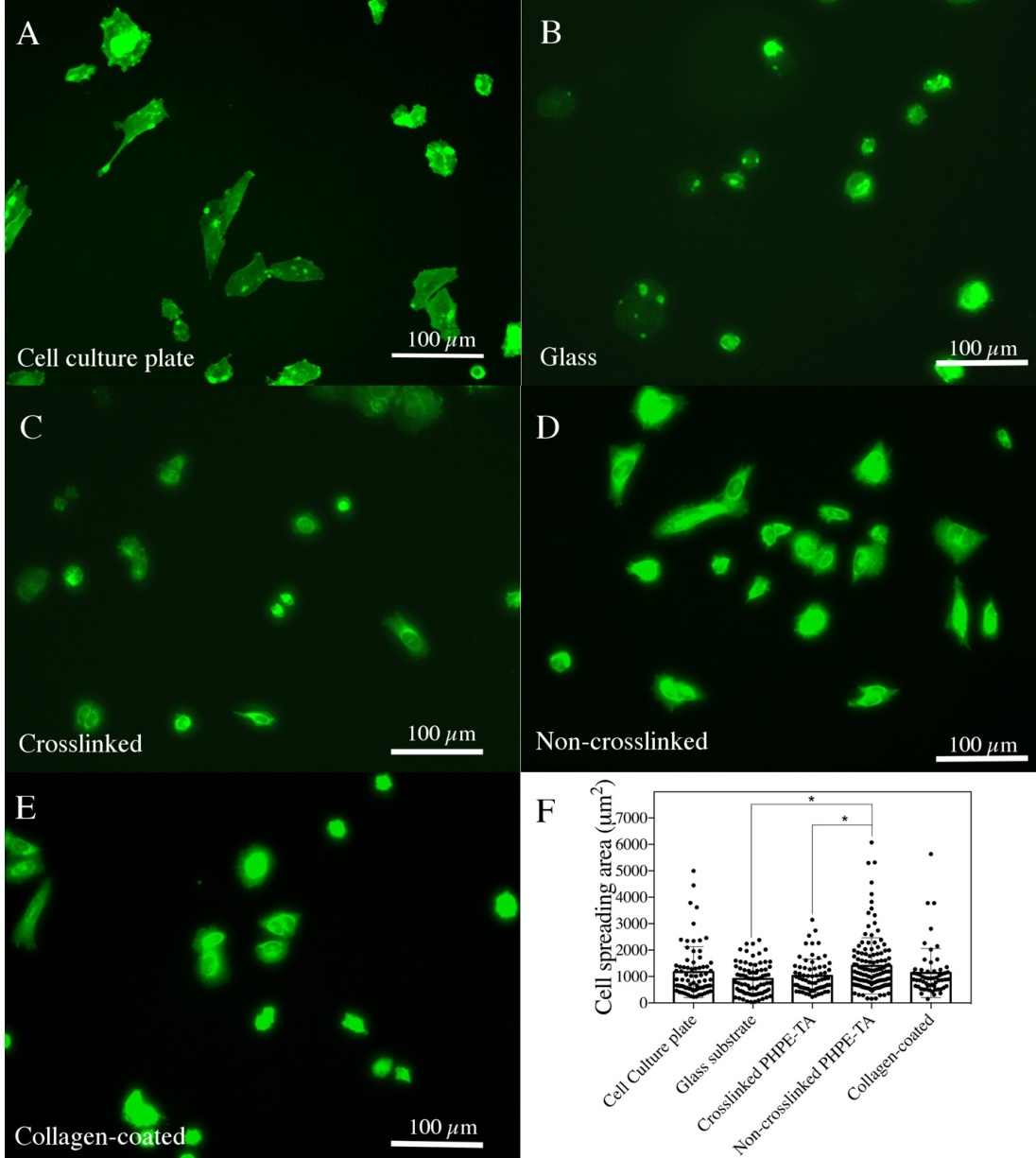
Fig. 3. 15. Fluorescent images and the cell area graph comparing the cell spreading areas 24 hours after seeding cells on surfaces. The cells were stained with SP-DiOC$_{18}$ fluorescent dye to determine the positions of the cell membrane. SaOS-2 cells were cultivated in the standard medium and seeded on (A) cell culture plate surface, (B) bare glass substrate, (C) collagen type I coated substrate, (D) partially crosslinked and

144

(E) non-crosslinked 15-layer films of PHPE-TA complexes. Panel F shows the total cell spreading area of each cell and their mean value. All results are shown as the means and the their standard errors (SE) of means, along with the specific values as dots. Statistical variance was analyzed with one-way ANOVA and columns were further compared with by Tukey's post hoc test (*P<0.05)

TA is partially ionized at physiological pH, thus it has both hydroxyl and phenolate groups. On the other hand, PHPE has a secondary amine group on every repeating unit and is positively charged under the same conditions. It was previously reported that surface modifications can change the adherence property of surfaces to mammalian cells. Even though amino-functionalized surfaces are adhesive towards cells, a balanced mixture of hydroxyl and methyl groups on surfaces can also modify the surface to have high adhesiveness [77]. Considering the negative charge of the cell membrane, PHPE can be attributed to be the main reason for the good adherence of SaOS-2 cells on surfaces coated with multilayers of PHPE-TA complexes. It was reported earlier that surfaces coated with monolayers of alkylsilanes containing terminal amino groups created adherent surfaces for cell attachment [78]. Interestingly, non-crosslinked and partially crosslinked multilayers of PHPE-TA complexes behaved differently for the adherence of SaOS-2 cells. Cells spread to a larger (albeit statistically non-significant) area on surfaces containing non-crosslinked multilayers compared to partially crosslinked films at 2 h or 24 h after seeding. This could be explained with the decrease in the number of free secondary amino groups of PHPE upon crosslinking, resulting in a lower extent of interaction between the film surface and surface proteoglycans on cells. Crosslinking multilayer films of PHPE-TA complexes was crucial in our experiments to obtain long-term stability. However, unfortunately, it decreased the adhesion property of SaOS-2 cells onto the multilayers.

3.4.5. Osteoconductivity of Multilayers of Partially Crosslinked PHPE-TA Complexes

3.4.5.1. Determination of The Collagen Amount Released into The Extracellular Matrix

SaOS-2 cells were seeded on three different groups of surfaces: **i**) cell culture plate (control), **ii**) collagen type I coated glass substrate, **iii**)15 layers of partially crosslinked multilayers of PHPE-TA complexes on glass substrate, and cultivated for 15 days in the standard culture medium. In all three groups, Direct Red 80 stained large areas were full of collagen-rich nodules. We observed significantly higher amount of collagen in nodules on surfaces of groups **ii** and **iii**, compared to the control (**i**) (Figure 3.15D). Figure 15A - C show phase contrast microscopy images of Direct Red 80-stained nodules deposited by cells, cultivated in the standard medium on the indicated surfaces. When we replaced the standard medium with MAC after cell monolayer formation (Figure 3.16A - C), we again observed increased amount of collagen in the nodules in groups **ii** and **iii**, compared to the control (**i**), though the results did not reach statistical significance (Figure 3.16D). In either case, the results were not statistically significant between groups **ii** and **iii**. These results support our hypothesis that PHPE-containing surfaces could regulate collagen synthesis and secretion by cells in a similar way that collagen type I-coated surfaces do.
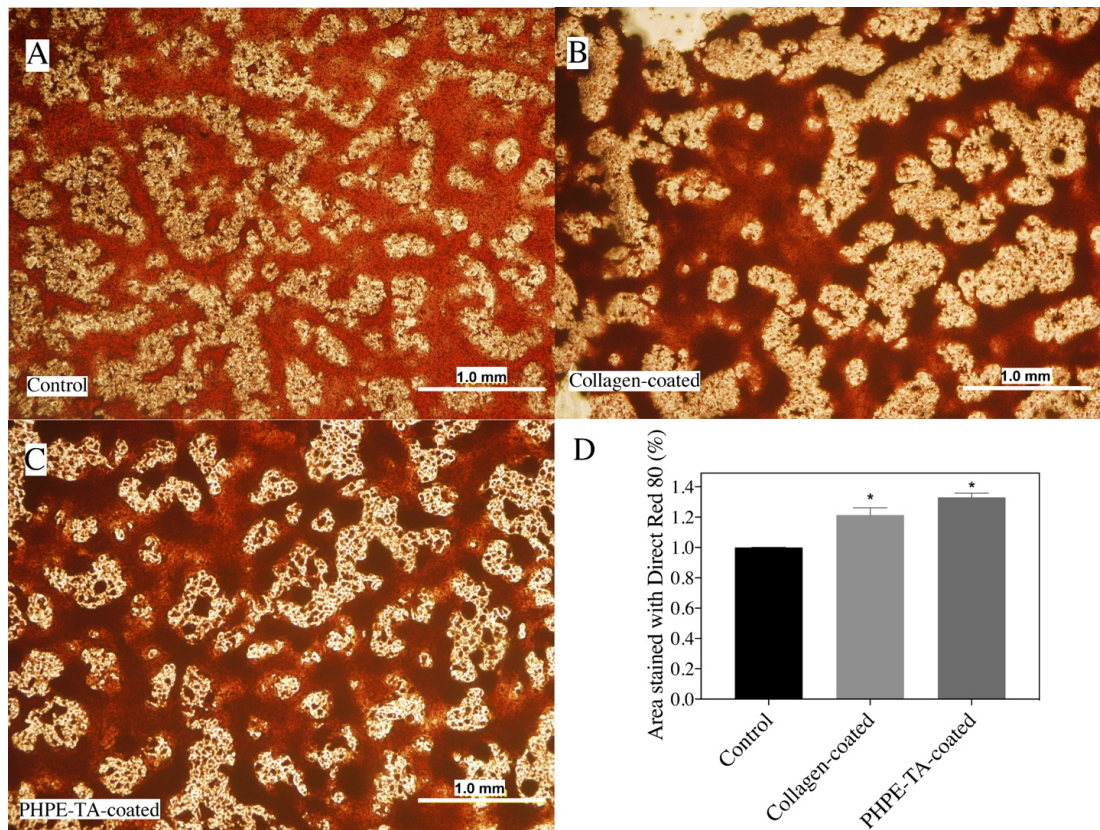
Fig. 3. 16. Phase contrast microscopy images of Direct Red 80-stained collagen-rich nodules deposited by cells cultivated in the standard medium onto surfaces of (A) tissue culture plate, glass substrates coated with (B) collagen type I , or (C) partially crosslinked 15-layers of PHPE-TA complexes in standard medium for 15 days; in MAC medium for 15 days. (D) Quantitative comparison of the percent area of cell monolayers which are stained with Direct Red 80, which shows the collagen amount. Total area of the surface was expressed as 100% and the stained area was calculated accordingly. All results are given as means and their standard errors (SE) of means. Statistical variance was analyzed with one-way ANOVA and results were further compared with the Control using the Holm-Sidak's multiple comparisons test (*P<0.05).
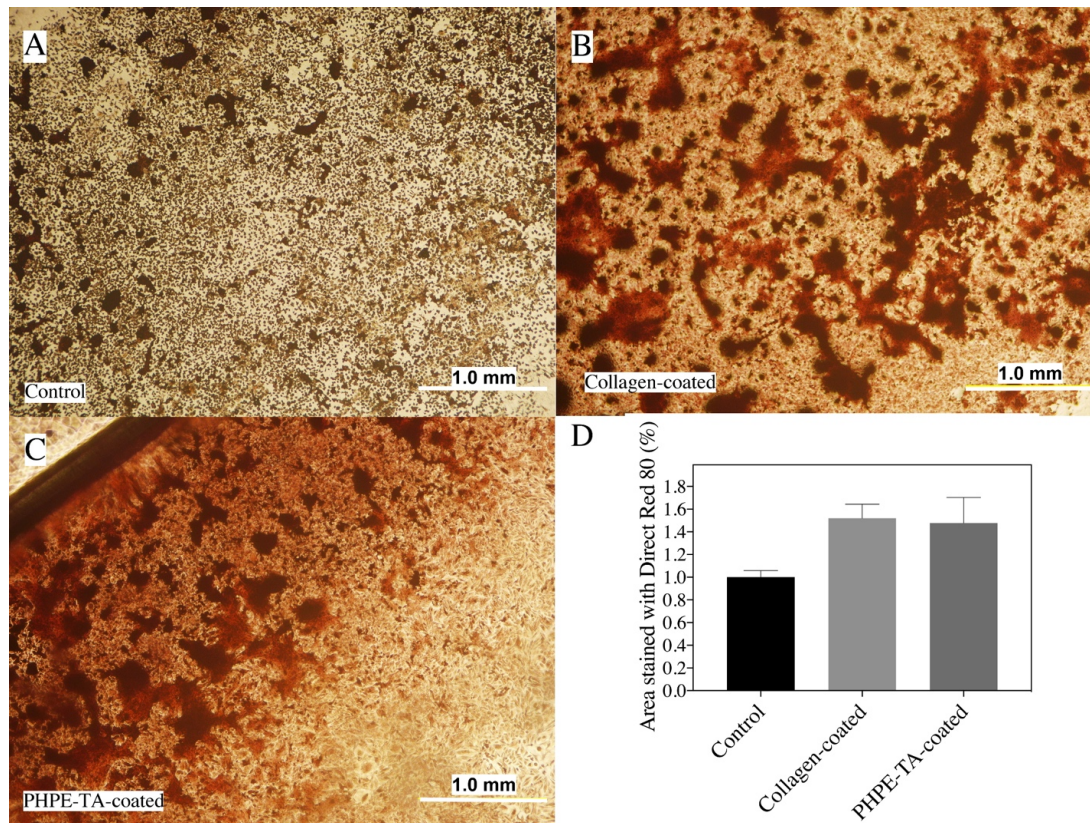
Fig. 3. 17. Phase contrast microscopy images of Direct Red 80-stained collagen-rich nodules deposited by cells cultivated in MAC onto surfaces of (A) tissue culture plate, glass substrates coated with (B) collagen type I , or (C) partially crosslinked 15-layer films of PHPE-TA complexes in standard medium for 15 days or in MAC medium for 15 days. (D) Quantitative comparison of the percent area of cell monolayers that were stained with Direct Red 80, indicating the the collagen amount. Total area of the surface was expressed as 100% and the stained area was calculated accordingly. All results are given as the means and the their standard errors (SE) of means. Statistical variance was analyzed with one-way ANOVA and results were further compared with the control using Holm-Sidak's multiple comparisons test (*P<0.05).

3.4.5.2 Determination of The Amount of Mineralization in The Extracellular Matrix on Substrates

SaOS-2 cells were cultivated either on cell culture plate wells, collagen type I-coated glass substrates, or partially crosslinked 15-layer films of PHPE-TA complexes for 15 days. After this, the cells were fixed with 10% paraformaldehyde solution and stained with Alizarin Red-S to determine the mineralization in the extracellular matrix of the cell monolayer. Initially, cells were seeded on surfaces and cell medium was replaced with the standard medium regularly. After Alizarin Red S-staining of these cell monolayers, we observed that the collagen-rich nodules of extracellular matrix were faintly stained red (Figure 3.17A, 3.17B, and 3.17C) and the difference between stained areas of the substrates coated with collagen type I and multilayers of PHPE-TA complexes was not significant (Figure 3.17D). Images from 5 different locations on the well indicated that the cells on substrates coated with either collagen type I or multilayers of PHPE-TA complexes exhibited collagen-rich nodules at the very center of the substrate. This was contrary to the cell culture plate wells where the collagen nodules were observed to be equally distributed throughout the well. The reason for this phenomenon could be the contact-inhibition of cells and their interaction with each other. When the cells were seeded on coated glass substrates (either with collagen type I or multilayers of PHPE-TA complexes) and placed in tissue culture wells, the adherence of cells to the substrate margins was limited due to non-homogeneous deposition of the films at the edges of the surface. This reduced the cell-cell and cell-surface interaction in those locations. For the SaOS-2 cell line, formation of a monolayer was necessary for osteogenic differentiation, thus differentiation was unsuccessful at corners of glass substrates. This may have resulted in similar levels of Alizarin Red S staining on the different surfaces (Figure 3.17. and 3.18.). The difference between the staining of substrates coated with collagen and multilayers of PHPE-TA complexes did not reach statistical significance, supporting that both surfaces behaved similarly in terms of osteoconductivity.
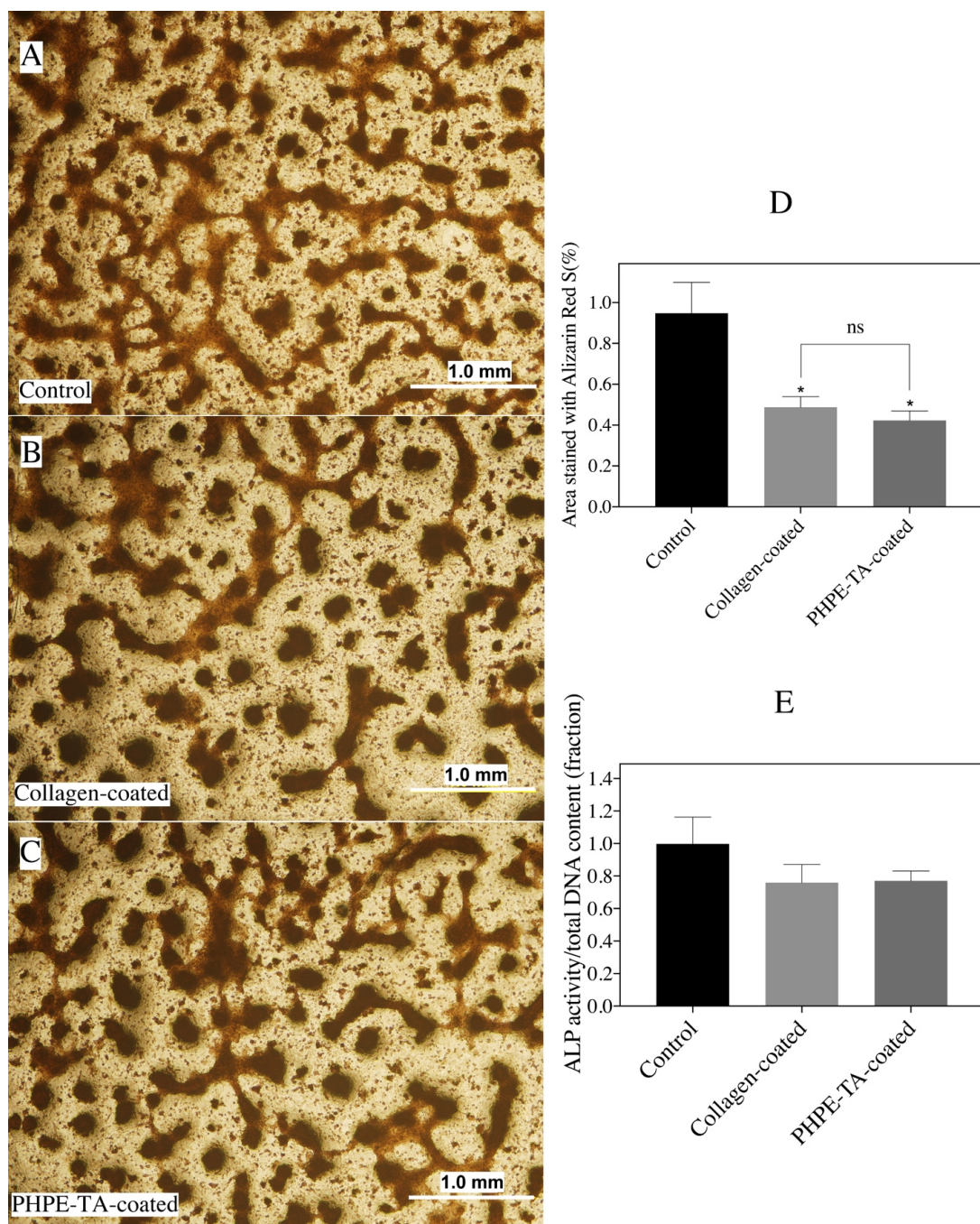
Fig. 3. 18. Phase contrast microscopy images of Alizarin Red S-stained SaOS-2 cell monolayers on surfaces of (A) cell culture plate, substrates coated with collagen (B) and partially crosslinked 15-layer films of PHPE-TA complexes (C) cultivated in standard medium for 15 days. (D) Quantitative comparison of the percent area of cell monolayers which were stained with Alizarin Red S, indicating the collagen amount. Total area of the surface was expressed as 100% and the stained area was calculated

accordingly. (E) Alkaline phosphatase (ALP) activity of the cells seeded on surfaces after 15 days of cultivation. All results are given as the means and the their standard errors (SE) of means. Statistical variance was analyzed with one-way ANOVA and results were further compared with the Control through Holm-Sidak's multiple comparisons test (*P<0.05). Statistical comparison of treatment columns was carried out with two-tailed t-test with Welch's correction (ns= not-significant).

To further establish the differentiation of SaOS-2 cells into an osteogenic phenotype, we determined the alkaline phosphatase (ALP) activity of these cells. ALP is an early biomarker for bone formation and biological mineralization is associated with elevated levels of ALP in SaOS-2 cells [79]. ALP activity was measured in SaOS-2 cell lysates and the UV-Vis absorbance values were normalized to the total DNA amount from cells of the same treatment group. We observed that ALP activity of SaOS-2 cells was similar irrespective of whether they were cultivated for 15 days on substrates coated with collagen type I or multilayers of PHPE-TA complexes. This again supports our hypothesis that Hyp, degradation product of PHPE, could induce osteogenic differentiation and shorten the duration of differentiation of SaOS-2 cells, as described before (Figure 3.6. and 3.7.). ALP activity of cells seeded on different types of surfaces showed different characteristics when we normalized the results with total DNA isolated from the cells seeded on each surface. For the samples cultured in standard medium for 15 days, we observed that the difference between ALP activity of surfaces coated with collagen or multilayers of PHPE-TA complexes did not reach statistical significance (Figure 3.13E), which may support our hypothesis that both surfaces were osteoconductive. Total ALP activity was higher when normalized to total DNA from lysed cells on control surfaces, although this was most likely observed because of better survival signals provided by uninterrupted tissue culture coated plates. The other coated glass slides inside the wells might have limited cell-cell interactions and survival. However, this phenomenon was not observed for the cells cultured in MAC. Cells on substrates coated with collagen type I or multilayers of PHPE-TA complexes exhibited significantly higher ALP activity, compared to the control (cell culture plate

151

surface) and surfaces of multilayers of PHPE-TA complexes significantly facilitated osteoconduction, compared to the control.

As an additional set of experiments, SaOS-2 cells were seeded on substrates in standard medium, which was replaced with MAC after formation of the cell monolayer. The cell monolayers were fixed and then stained with Alizarin Red-S. Both the control and the films with PHPE-TA complexes exhibited significant mineralization (Figure 3.18A - C). The areas stained with Alizarin Red-S on the surface of multilayers of PHPE-TA complexes were significantly higher than the areas stained on collagen type I-coated substrates (Figure 3.18D). As described in Section 3.3., although collagen-cell receptor interaction is known to induce osteogenic differentiation and collagen should allow for enhanced mineralization, cells on multilayer films of PHPE-TA complexes released more collagen compared to the cells on collagen type I-coated surfaces. This could be the reason why multilayer films of PHPE-TA complexes provided significantly enhanced ECM mineralization, compared to collagen type I-coated surfaces. As discussed previously, cell monolayer formed at a shorter time in culture plate wells (control) than coated substrates. Therefore, it is possible that the cells on these surfaces differentiated into mature osteoblast-like cells in a shorter time and released more minerals. This resulted in significantly higher Alizarin Red S-staining on the control surface than that on substrates coated with collagen type I or multilayer films of PHPE-TA complexes. Supporting these results, ALP activity of cells seeded on multilayer films of PHPE-TA complexes exhibited significant enhancement compared to the control and the collagen type I-coated surface (Figure 3.18E). This further supports our hypothesis that Hyp induced mineralization through a different pathway than the MAC components.

152

Fig. 3. 19. Phase contrast microscopy images of Alizarin Red S-stained cell monolayers on surfaces of (A) cell culture plate, substrates coated with collagen (B) and partially crosslinked 15-layer films of PHPE-TA complexes (C) cultivated in standard medium for 15 days. SaOS-2 cells were cultivated in MAC. (D) Quantitative comparison of the percent area of cell monolayers which are stained with Alizarin Red S, which shows the collagen amount. Total area of the surface was expressed as 100% and the stained area was calculated accordingly. (E) Alkaline phosphatase (ALP)
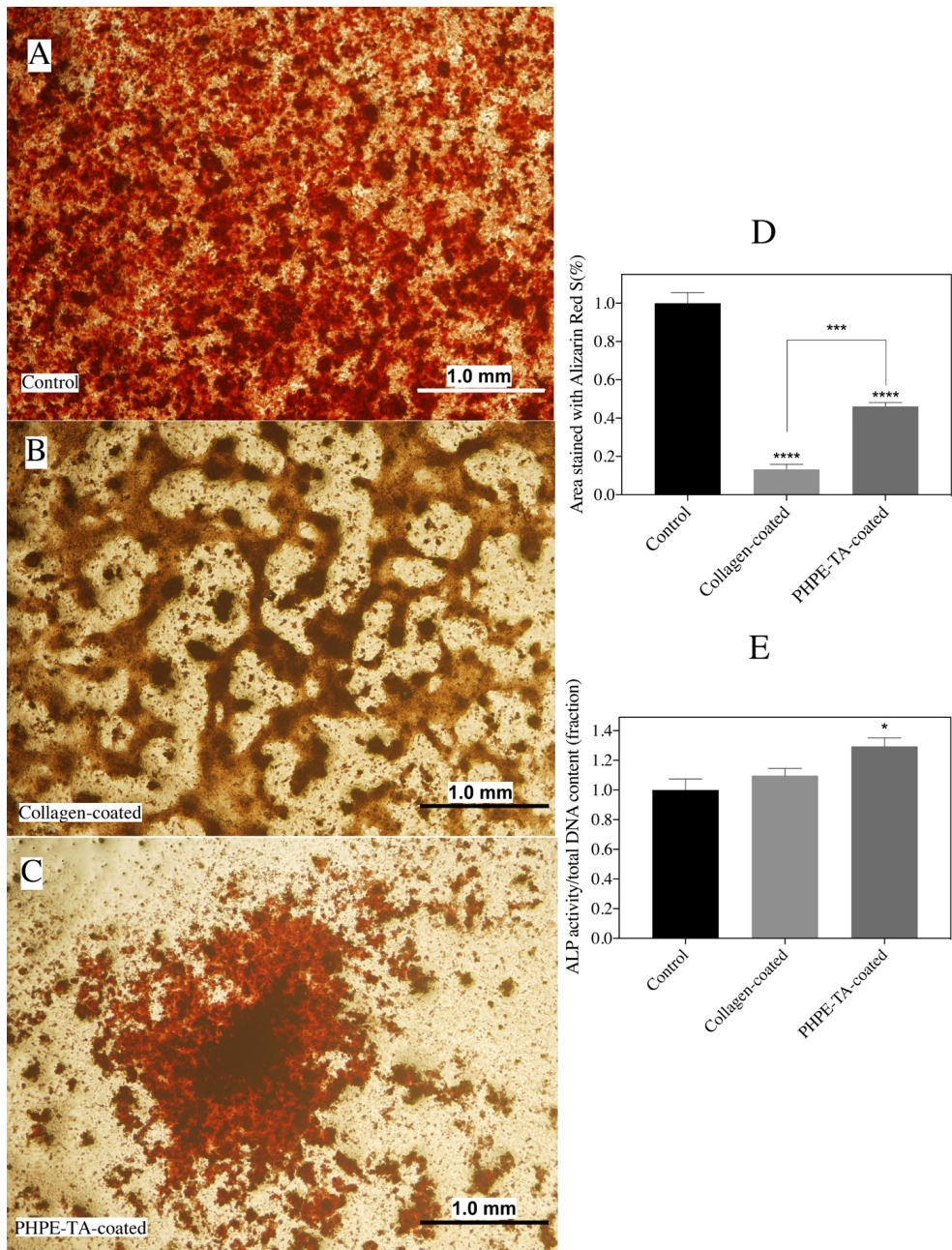
153

activity of the cells seeded on surfaces after 15 days of cultivation. All results are given as the means and the their standard errors (SE) of means. Statistical variance was analyzed with one-way ANOVA and results were further compared with the control using the Holm-Sidak's multiple comparisons test (*P<0.05, **P<0.005, ***P<0.0005, ****P<0.0001). Statistical comparison of treatment columns was carried out with one-tailed t-test with Welch's correction (*P<0.05).

3.5. Conclusion

Even though the bone tissue can repair itself, if the bone defect is non-repairable, organic bone grafts (e.g. allografts, autografts) or synthetic bone grafts (e.g. metallic or composite implants) are required to replace a particular segment of the bone or the whole bone [80]. Shortening the time required for osteoblasts to induce new bone formation would decrease the periods of hospitalization and vastly reduce the socioeconomical effects of orthopedic therapies. Current clinical techniques depend on direct injection of growth hormones (such as hrBMP-2) to the sites of bone defect. However, these techniques may cause several complications [17]. Therefore, alternative osteoinductive agents that would not cause any side effects on patients are needed. In this study, we showed that direct supplementation of a cationic biodegradable polymer poly(4-hydroxy-L-proline ester) and its degradation product *trans*-4-hydroxy-L- proline (Hyp) in the growth medium of SaOS-2 osteosarcoma cell line could induce collagen expression and synthesis in these cells. PHPE is suggested to be a potential osteoinductive agent and may be used as a direct supplementation to induce *COL1A1*, *BMP2*, and *VEGFA* gene expressions. Moreover, we showed that when PHPE was complexed with TA and deposited at the surface in a LbL fashion, osteoblast-like cells adhered, surived and displayed enhanced adherence towards the multilayers. Stability of multilayers in PBS at pH 7.5 was improved by crosslinking using NaIO$_4$. Although adherence property of cells towards non-crosslinked substrates was higher than that towards crosslinked films, SaOS-2 cells still showed good adherence onto crosslinked multilayer films. A comparison between surfaces coated with collagen type I and multilayers of PHPE-TA complexes showed that LbL films

154

of PHPE-TA complexes exhibited enhanced osteoconduction, as SaOS-2 cells released higher amount of collagen and minerals in their extracellular matrices.

To the best of our knowledge, this study is the first reporting on the osteoinductive property of a hydrolytically-degradable polymer that can degrade and release a non-coded amino acid [33]. Moreover, for the first time, we show that surfaces could be modified by PHPE via LbL deposition of water-soluble complexes of PHPE and TA and osteoblast-like cells seeded on these surfaces showed enhanced adherence, high cell viability, increased collagen secretion and ECM mineralization. These results suggest that PHPE based multilayers are promising for coating bone implants, other biomaterials such as bone screws and knobs, or scaffolds designed specifically for bone tissue engineering. In bone regenerative medicine, directly treating the defect site with PHPE may enhance tissue integration or regeneration. PHPE could be potentially used as an osteoinductive agent and may be a safer alternative to hrBMP-2 since the degradation product of PHPE. As an amino acid, Hyp can be metabolized and thereby may not cause any off-target effects like ectopic bone formation. Proof of concept studies of the effects of Hyp on osteogenic differentiation and regenerative medicine for the purpose of bone regeneration in animal models need to be conducted in the future.

3.6. References

[1]   A. Oryan, S. Alidadi, A. Moshiri, N. Maffulli, Bone regenerative medicine: classic options, novel strategies, and future directions, J. Orthop. Surg. Res. 9 (2014) 18. doi:10.1186/1749-799X-9-18.

[2]   R. Dimitriou, E. Jones, D. McGonagle, P. V Giannoudis, Bone regeneration: current concepts and future directions, BMC Med. 9 (2011) 66. doi:10.1186/1741-7015-9-66.

[3]   F.R.A.J. Rose, R.O.C. Oreffo, Bone Tissue Engineering: Hope vs Hype, Biochem. Biophys. Res. Commun. 292 (2002) 1–7. doi:10.1006/bbrc.2002.6519.

[4]   W.Y. Zhou, S.H. Lee, M. Wang, W.L. Cheung, W.Y. Ip, Selective laser sintering of porous tissue engineering scaffolds from poly(L-lactide)/carbonated hydroxyapatite nanocomposite microspheres, in: J. Mater. Sci. Mater. Med., (2008) 2535–2540. doi:10.1007/s10856-007-3089-3.

[5]   H. Cao, N. Kuboyama, A biodegradable porous composite scaffold of PGA/beta-TCP for bone tissue engineering, Bone. 46 (2010) 386–395. doi:10.1016/j.bone.2009.09.031.

[6]   P. Gentile, V. Chiono, I. Carmagnola, P. V. Hatton, An overview of poly(lactic-co-glycolic) Acid (PLGA)-based biomaterials for bone tissue engineering, Int. J. Mol. Sci. 15 (2014) 3640–3659. doi:10.3390/ijms15033640.

[7]   V. Guarino, F. Causa, P.A. Netti, G. Ciapetti, S. Pagani, D. Martini, N. Baldini, L. Ambrosio, The role of hydroxyapatite as solid signal on performance of PCL porous scaffolds for bone tissue regeneration, J. Biomed. Mater. Res. - Part B Appl. Biomater. 86 (2008) 548–557. doi:10.1002/jbm.b.31055.

[8]   Y.S. Pek, S. Gao, M.S.M. Arshad, K.J. Leck, J.Y. Ying, Porous collagen-apatite nanocomposite foams as bone regeneration scaffolds, Biomaterials. 29 (2008) 4300–4305. doi:10.1016/j.biomaterials.2008.07.030.

[9]   L.B. Rocha, R.L. Adam, N.J. Leite, K. Metze, M.A. Rossi, Biomineralization of polyanionic collagen-elastin matrices during cavarial bone repair, J. Biomed. Mater. Res. - Part A. 79 (2006) 237–245. doi:10.1002/jbm.a.30782.

[10]   A. Fakhry, G.B. Schneider, R. Zaharias, S. Şenel, Chitosan supports the initial attachment and spreading of osteoblasts preferentially over fibroblasts, Biomaterials. 25 (2004) 2075–2079. doi:10.1016/j.biomaterials.2003.08.068.

[11]   E.A. Bayer, J. Jordan, R. Gottardi, M. Fedorchak, P.N. Kumta, S. Little, Programmed Platelet Derived Growth Factor-ββ and Bone Morphogenetic Protein-2 Delivery from a Hybrid Calcium Phosphate/Alginate Scaffold, Tissue Eng. Part A. (2017) ten.TEA.2017.0027. doi:10.1089/ten.TEA.2017.0027.

[12]   S.C. Rizzi, D.J. Heath, A.G.A. Coombes, N. Bock, M. Textor, S. Downes,

Biodegradable polymer/hydroxyapatite composites: Surface analysis and initial attachment of human osteoblasts, J. Biomed. Mater. Res. 55 (2001) 475–486. doi:10.1002/1097-4636(20010615)55:4<475::AID-JBM1039>3.0.CO;2-Q.

[13]   A. Oyane, M. Uchida, Y. Yokoyama, C. Choong, J. Triffitt, A. Ito, Simple surface modification of poly(ε-caprolactone) to induce its apatite-forming ability, J. Biomed. Mater. Res. - Part A. 75 (2005) 138–145. doi:10.1002/jbm.a.30397.

[14]   Y. Liu, E.B. Hunziker, P. Layrolle, J.D. De Bruijn, K. De Groot, Bone Morphogenetic Protein 2 Incorporated into Biomimetic Coatings Retains Its Biological   Activity,   Tissue   Eng.   10   (2004)   101–108. doi:10.1089/107632704322791745.

[15]   M.L. Macdonald, R.E. Samuel, N.J. Shah, R.F. Padera, Y.M. Beben, P.T. Hammond, Tissue integration of growth factor-eluting layer-by-layer polyelectrolyte multilayer coated implants, Biomaterials. 32 (2011) 1446–1453. doi:10.1016/j.biomaterials.2010.10.052.

[16]   S.B. Goodman, Z. Yao, M. Keeney, F. Yang, The future of biologic coatings for   orthopaedic   implants,   Biomaterials.   34   (2013)   3174–3183. doi:10.1016/j.biomaterials.2013.01.074.

[17]   N. Epstein, Complications due to the use of BMP/INFUSE in spine surgery: The evidence continues to mount, Surg. Neurol. Int. 4 (2013) 343. doi:10.4103/2152-7806.114813.

[18]   K. Rezwan, Q.Z. Chen, J.J. Blaker, A.R. Boccaccini, Biodegradable and bioactive porous polymer/inorganic composite scaffolds for bone tissue engineering,   Biomaterials.   27   (2006)   3413–3431. doi:10.1016/j.biomaterials.2006.01.039.

[19]   K.C. Wood, J.Q. Boedicker, D.M. Lynn, P.T. Hammond, Tunable drug release from hydrolytically degradable layer-by-layer thin films, Langmuir. 21 (2005) 1603–1609. doi:10.1021/la0476480.

[20] V.H. Orozco, V. Kozlovskaya, E. Kharlampieva, B.L. López, V. V. Tsukruk, Biodegradable self-reporting nanocomposite films of poly(lactic acid) nanoparticles engineered by layer-by-layer assembly, Polymer (Guildf). 51 (2010) 4127–4139. doi:10.1016/j.polymer.2010.06.060.

[21] A.J. García, C.D. Reyes, Bio-adhesive Surfaces to Promote Osteoblast Differentiation and Bone Formation, J. Dent. Res. 84 (2005) 407–413. doi:10.1177/154405910508400502.

[22] M. Morra, C. Cassinelli, G. Cascardo, L. Mazzucco, P. Borzini, M. Fini, G. Giavaresi, R. Giardino, Collagen I-coated titanium surfaces: mesenchymal cell adhesion and in vivo evaluation in trabecular bone implants, J Biomed Mater Res. 78 (2006) 449–458. http://infoprovider.library.bbraun.com/bbmlit/docs/AA02305.pdf.

[23] R.A. Berg, D.J. Prockop, The thermal transition of a non-hydroxylated form of collagen. Evidence for a role for hydroxyproline in stabilizing the triple-helix of collagen, Biochem. Biophys. Res. Commun. 52 (1973) 115–120. doi:10.1016/0006-291X(73)90961-3.

[24] E. Pokidysheva, S. Boudko, J. Vranka, K. Zientek, K. Maddox, M. Moser, R. Fässler, J. Ware, H.P. Bächinger, Biological role of prolyl 3-hydroxylation in type IV collagen., Proc. Natl. Acad. Sci. U. S. A. 111 (2014) 161–6. doi:10.1073/pnas.1307597111.

[25] A. Jikko, S.E. Harris, D. Chen, D.L. Mendrick, C.H. Damsky, Collagen Integrin Receptors Regulate Early Osteoblast Differentiation Induced by BMP-2, J. Bone Miner. Res. 14 (1999) 1075–1083. doi:10.1359/jbmr.1999.14.7.1075.

[26] L.-H. Chiu, T.-S. Yeh, H.-M. Huang, S.-J. Leu, C.-B. Yang, Y.-H. Tsai, Diverse effects of type II collagen on osteogenic and adipogenic differentiation of mesenchymal stem cells., J. Cell. Physiol. 227 (2012) 2412–20. doi:10.1002/jcp.22976.

[27] K. Sipilä, S. Haag, K. Denessiouk, J. Käpylä, E.C. Peters, A. Denesyuk, U. Hansen, Y. Konttinen, M.S. Johnson, R. Holmdahl, J. Heino, Citrullination of

158

collagen II affects integrin-mediated cell adhesion in a receptor-specific manner, FASEB J. 28 (2014) 3758–3768. doi:10.1096/fj.13-247767.

[28] S. Perret, J.A. Eble, P.R.M. Siljander, C. Merle, R.W. Farndale, M. Theisen, F. Ruggiero, Prolyl hydroxylation of collagen type I is required for efficient binding to integrin α1β1 and platelet glycoprotein VI but not to α2β1, J. Biol. Chem. 278 (2003) 29873–29879. doi:10.1074/jbc.M304073200.

[29] D. Putnam, R. Langer, Poly(4-hydroxy-L-proline ester): low-temperature polycondensation and plasmid DNA complexation, Macromolecules. 32 (1999) 3658–3662. doi:10.1021/ma982004i.

[30] Z. Li, L. Huang, Sustained delivery and expression of plasmid DNA based on biodegradable polyester, poly(D,L-lactide-co-4-hydroxy-L-proline), J. Control. Release. 98 (2004) 437–446. doi:10.1016/j.jconrel.2004.05.013.

[31] F.R. Maia, M. Barbosa, D.B. Gomes, N. Vale, P. Gomes, P.L. Granja, C.C. Barrias, Hydrogel depots for local co-delivery of osteoinductive peptides and mesenchymal stem cells, J. Control. Release. 189 (2014) 158–168. doi:10.1016/j.jconrel.2014.06.030.

[32] K.M. Galler, L. Aulisa, K.R. Regan, R.N. D'Souza, J.D. Hartgerink, Self-assembling multidomain peptide hydrogels: Designed susceptibility to enzymatic cleavage allows enhanced cell migration and spreading, J. Am. Chem. Soc. 132 (2010) 3217–3223. doi:10.1021/ja910481t.

[33] Y.B. Lim, Y.H. Choi, J.S. Park, A self-destroying polycationic polymer: Biodegradable poly(4-hydroxy-L- proline ester), J. Am. Chem. Soc. 121 (1999) 5633–5639. doi:10.1021/ja984012k.

[34] V. Ball, Stabilization of [poly(allylamine)–tannic acid] n multilayer films in acidic and basic conditions after crosslinking with NaIO 4, (n.d.). doi:10.1039/c5ra06783a.

[35] F. Langenbach, J. Handschel, Effects of dexamethasone, ascorbic acid and β-glycerophosphate on the osteogenic differentiation of stem cells in vitro., Stem

Cell Res. {&} Ther. 4 (2013) 117. doi:10.1186/scrt328.

[36]   I.R. Orriss, M.O.R. Hajjawi, C. Huesa, V.E. MacRae, T.R. Arnett, Optimisation of the differing conditions required for bone formation in vitro by primary osteoblasts from mice and rats., Int J Mol Med. 34 (2014) 1201–1208. doi:10.3892/ijmm.2014.1926.

[37]   H. Tullberg-Reinert, G. Jundt, In situ measurement of collagen synthesis by human bone cells with a sirius red-based colorimetric microassay: effects of transforming growth factor beta2 and ascorbic acid 2-phosphate., Histochem. Cell Biol. 112 (1999) 271–76.

[38]   L.C.U. Junqueira, G. Bignolas, R.R. Brentani, Picrosirius staining plus polarization microscopy, a specific method for collagen detection in tissue sections, Histochem. J. 11 (1979) 447–455. doi:10.1007/BF01002772.

[39]   C.A. Gregory, W.G. Gunn, A. Peister, D.J. Prockop, An Alizarin red-based assay of mineralization by adherent cells in culture: Comparison with cetylpyridinium chloride extraction, Anal. Biochem. 329 (2004) 77–84. doi:10.1016/j.ab.2004.02.002.

[40]   M. Pfaffl, Quantification strategies in real-time PCR Michael W . Pfaffl, A-Z Quant. PCR. (2004) 87–112. doi:http://dx.doi.org/10.1007/s10551-011-0963-1.

[41]   N. Shojaie, M.S. Ghaffari, Z. Safari, Simultaneous Extraction of DNA and RNA from Animal Cells by a Modified Laemmli Buffer, (n.d.). https://www.nature.com/protocolexchange/system/uploads/3299/original/Full_text_and_figures.pdf?1410873763 (accessed April 17, 2017).

[42]   S. Perret, C. Merle, S. Bernocco, P. Berland, R. Garrone, D.J.S. Hulmes, M. Theisen, F. Ruggiero, Unhydroxylated Triple Helical Collagen I Produced in Transgenic Plants Provides New Clues on the Role of Hydroxyproline in Collagen Folding and Fibril Formation, J. Biol. Chem. 276 (2001) 43693–43698. doi:10.1074/jbc.M105507200.

[43]   K. Azuma, S. Shiba, T. Hasegawa, K. Ikeda, T. Urano, K. Horie-Inoue, Y.

Ouchi, N. Amizuka, S. Inoue, Osteoblast-Specific ??-Glutamyl Carboxylase-Deficient Mice Display Enhanced Bone Formation with Aberrant Mineralization, J. Bone Miner. Res. 30 (2015) 1245–1254. doi:10.1002/jbmr.2463.

[44] S.L. Booth, A. Centi, S.R. Smith, C. Gundberg, The role of osteocalcin in human glucose metabolism: marker or mediator?, Nat. Rev. Endocrinol. 9 (2013) 43–55. doi:10.1038/nrendo.2012.201.

[45] J. Wei, J.Y. Wu, Post-translational regulation of L-glutamic acid decarboxylase in the brain, Neurochem Res. 33 (2008) 1459–1465. doi:10.1007/s11064-008-9600-5.

[46] W. Ying Chow, D. Bihan, C.J. Forman, D.A. Slatter, D.G. Reid, D.J. Wales, R.W. Farndale, M.J. Duer, Hydroxyproline Ring Pucker Causes Frustration of Helix Parameters in the Collagen Triple Helix, Sci. Rep. 5 (2015) 12556. doi:10.1038/srep12556.

[47] J.M. Pace, M. Atkinson, M.C. Willing, G. Wallis, P.H. Byers, Deletions and duplications of Gly-Xaa-Yaa triplet repeats in the triple helical domains of type I collagen chains disrupt helix formation and result in several types of osteogenesis imperfecta, Hum. Mutat. 18 (2001) 319–326. doi:10.1002/humu.1193.

[48] L.I. Fessler, J.H. Fessler, Protein assembly of procollagen and effects of hydroxylation., J Biol Chem. 249 (1974) 7637–7646.

[49] D. Fischer, Y. Li, B. Ahlemeyer, J. Krieglstein, T. Kissel, In vitro cytotoxicity testing of polycations: influence of polymer structure on cell viability and hemolysis, Biomaterials. 24 (2003) 1121–31. doi:S0142961202004453 [pii].

[50] J. Knight, R.P. Holmes, Mitochondrial hydroxyproline metabolism: Implications for primary hyperoxaluria, in: Am. J. Nephrol., (2005) 171–175. doi:10.1159/000085409.

[51] J. Knight, J. Jiang, D.G. Assimos, R.P. Holmes, Hydroxyproline ingestion and

urinary oxalate and glycolate excretion., Kidney Int. 70 (2006) 1929–1934. doi:10.1038/sj.ki.5001906.

[52] N. Seo, B.H. Russell, J.J. Rivera, X. Liang, X. Xu, V. Afshar-Kharghan, M. Höök, An engineered α1 integrin-binding collagenous sequence, J. Biol. Chem. 285 (2010) 31046–31054. doi:10.1074/jbc.M110.151357.

[53] C.G. Bellows, S.M. Reimers, J.N.M. Heersche, Expression of mRNAs for type-I collagen, bone sialoprotein, osteocalcin, and osteopontin at different stages of osteoblastic differentiation and their regulation by 1,25 dihydroxyvitamin D, Cell Tissue Res. 297 (1999) 249. doi:10.1007/s004410051353.

[54] L. F., H. J., Effects of dexamethasone, ascorbic acid and β-glycerophosphate on the osteogenic differentiation of stem cells in vitro, Stem Cell Res. Ther. 4 (2013).

[55] R.M. Salasznyk, W.A. Williams, A. Boskey, A. Batorsky, G.E. Plopper, Adhesion to Vitronectin and Collagen I Promotes Osteogenic Differentiation of Human Mesenchymal Stem Cells., J. Biomed. Biotechnol. 2004 (2004) 24–34. doi:10.1155/S1110724304306017.

[56] P. Ducy, R. Zhang, V. Geoffroy, A.L. Ridall, G. Karsenty, Osf2/Cbfa1: A Transcriptional Activator of Osteoblast Differentiation, Cell. 89 (1997) 747–754. doi:10.1016/S0092-8674(00)80257-3.

[57] Z. Maruyama, C.A. Yoshida, T. Furuichi, N. Amizuka, M. Ito, R. Fukuyama, T. Miyazaki, H. Kitaura, K. Nakamura, T. Fujita, N. Kanatani, T. Moriishi, K. Yamana, W. Liu, H. Kawaguchi, K. Nakamura, T. Komori, Runx2 determines bone maturity and turnover rate in postnatal bone development and is involved in bone loss in estrogen deficiency, Dev. Dyn. 236 (2007) 1876–1890. doi:10.1002/dvdy.21187.

[58] C. Banerjee, A. Javed, J.Y. Choi, J. Green, V. Rosen, A.J. Van Wijnen, J.L. Stein, J.B. Lian, G.S. Stein, Differential regulation of the two principal Runx2/Cbfa1 N-terminal isoforms in response to bone morphogenetic protein-2 during development of the osteoblast phenotype, Endocrinology. 142 (2001)

4026–4039. doi:10.1210/en.142.9.4026.

[59] F. Gori, T. Thomas, K.C. Hicok, T.C. Spelsberg, B.L. Riggs, Differentiation of human marrow stromal precursor cells: bone morphogenetic protein-2 increases OSF2/CBFA1, enhances osteoblast commitment, and inhibits late adipocyte maturation., J. Bone Miner. Res. 14 (1999) 1522–1535. doi:10.1359/jbmr.1999.14.9.1522.

[60] K. Tsuji, A. Bandyopadhyay, B.D. Harfe, K. Cox, S. Kakar, L. Gerstenfeld, T. Einhorn, C.J. Tabin, V. Rosen, BMP2 activity, although dispensable for bone formation, is required for the initiation of fracture healing., Nat. Genet. 38 (2006) 1424–1429. doi:10.1038/ng1916.

[61] A. Jikko, S.E. Harris, D. Chen, D.L. Mendrick, C.H. Damsky, Collagen integrin receptors regulate early osteoblast differentiation induced by BMP-2., J. Bone Miner. Res. 14 (1999) 1075–1083. doi:10.1359/jbmr.1999.14.7.1075.

[62] N. Ferrara, H.-P. Gerber, J. LeCouter, The biology of VEGF and its receptors, Nat. Med. 9 (2003) 669–676. doi:10.1038/nm0603-669.

[63] H. Yu, P.J. VandeVord, L. Mao, H.W. Matthew, P.H. Wooley, S.Y. Yang, Improved tissue-engineered bone regeneration by endothelial cell mediated vascularization, Biomaterials. 30 (2009) 508–517. doi:10.1016/j.biomaterials.2008.09.047.

[64] M.M. Deckers, M. Karperien, C. van der Bent, T. Yamashita, S.E. Papapoulos, C.W. Löwik, Expression of vascular endothelial growth factors and their receptors during osteoblast differentiation., Endocrinology. 141 (2000) 1667–1674. doi:10.1210/endo.141.5.7458.

[65] H. Mayer, H. Bertram, W. Lindenmaier, T. Korff, H. Weber, H. Weich, Vascular endothelial growth factor (VEGF-A) expression in human mesenchymal stem cells: Autocrine and paracrine role on osteoblastic and endothelial differentiation, J. Cell. Biochem. 95 (2005) 827–839. doi:10.1002/jcb.20462.

[66] D.L. Goad, J. Rubin, H. Wang, A.H. Tashjian, C. Patterson, Enhanced expression of vascular endothelial growth factor in human SaOS-2 osteoblast-like cells and murine osteoblasts induced by insulin-like growth factor I., Endocrinology. 137 (1996) 2262–2268. doi:10.1210/endo.137.6.8641174.

[67] Y. Maruo, A. Gochi, A. Kaihara, H. Shimamura, T. Yamada, N. Tanaka, K. Orita, The antifungal drug ciclopirox inhibits deoxyhypusine and proline hydroxylation, endothelial cell growth and angiogenesis in vitro, Int. J. Cancer. 100 (2002) 491–498. doi:10.1002/ijc.10515.

[68] I. Haktaniyan, M.; Atilla, S.; Cagli, E.; Erel-Goktepe, pH- and Temperature-Induced Release of Doxorubicin from Multilayers of Poly(2-isopropyl-2-oxazoline) and Tannic Acid, Polym. Int. (2017).

[69] L.N. Neumann, M.B. Baker, C.M.A. Leenders, I.K. Voets, R.P.M. Lafleur, A.R.A. Palmans, E.W. Meijer, Supramolecular polymers for organocatalysis in water, Org. Biomol. Chem. 13 (2015) 7711–7719. doi:10.1039/C5OB00937E.

[70] E. Kharlampieva, S.A. Sukhishvili, Ionization and pH stability of multilayers formed by self-assembly of weak polyelectrolytes, Langmuir. 19 (2003) 1235–1243. doi:10.1021/la026546b.

[71] C. De Saint-Aubin, J. Hemmerlé, F. Boulmedais, M.F. Vallat, M. Nardin, P. Schaaf, New 2-in-1 polyelectrolyte step-by-step film buildup without solution alternation: From PEDOT-PSS to polyelectrolyte complexes, Langmuir. 28 (2012) 8681–8691. doi:10.1021/la301254a.

[72] Y. Lvov, K. Ariga, M. Onda, I. Ichinose, T. Kunitake, A careful examination of the adsorption step in the alternate layer-by- layer assembly of linear polyanion and polycation, Colloids Surfaces A Physicochem. Eng. Asp. 146 (1999) 337–346. doi:10.1016/S0927-7757(98)00789-4.

[73] C. De Saint-Aubin, M. Hassan, P. Kunemann, T. Patois, B. Lakard, R. Fabre, J. Hemmerlé, P. Schaaf, M. Nardin, M.F. Vallat, PEDOT-PSS based 2-in-1 step-by-step films: A refined study, Synth. Met. 194 (2014) 38–46. doi:10.1016/j.synthmet.2014.04.003.

[74] K. Vermöhlen, H. Lewandowski, H.D. Narres, M.J. Schwuger, Adsorption of polyelectrolytes onto oxides - The influence of ionic strength, molar mass, and Ca2+ ions, Colloids Surfaces A Physicochem. Eng. Asp. 163 (2000) 45–53. doi:10.1016/S0927-7757(99)00429-X.

[75] K.E. Healy, C.H. Thomas, A. Rezania, J.E. Kim, P.J. Mckeownj, B. Lom$, P.E. Hockberge$, R.R. Mccormick, Kinetics of bone cell organization and mineralization on materials with patterned surface chemistry, Biomaterials. 17 (1996) 195–208. http://ac.els-cdn.com/0142961296857644/1-s2.0-0142961296857644-main.pdf?_tid=5b97cd42-5aaf-11e7-909e-00000aab0f26&acdnat=1498509666_eb01dab21fce80f6b48b6889f7d7e389 (accessed June 26, 2017).

[76] S.P. Massia, J.A. Hubbell, Immobilized amines and basic amino acids as mimetic heparin-binding domains for cell surface proteoglycan-mediated adhesion, J. Biol. Chem. 267 (1992) 10133–10141.

[77] Y. Arima, H. Iwata, Effect of wettability and surface functional groups on protein adsorption and cell adhesion using well-defined mixed self-assembled monolayers, Biomaterials. 28 (2007) 3074–3082. doi:10.1016/j.biomaterials.2007.03.013.

[78] N. Faucheux, R. Schweiss, K. Lützow, C. Werner, T. Groth, Self-assembled monolayers with different terminating groups as model substrates for cell adhesion studies, Biomaterials. 25 (2004) 2721–2730. doi:10.1016/j.biomaterials.2003.09.069.

[79] H. Orimo, T. Shimada, The role of tissue-nonspecific alkaline phosphatase in the phosphate-induced activation of alkaline phosphatase and mineralization in SaOS-2 human osteoblast-like cells, Mol. Cell. Biochem. 315 (2008) 51–60. doi:10.1007/s11010-008-9788-3.

[80] K.M. Alghazali, Z.A. Nima, R.N. Hamzah, M.S. Dhar, D.E. Anderson, A.S. Biris, Bone-tissue engineering: complex tunable structural and biological responses to injury, drug delivery, and cell-based therapies, Drug Metab. Rev.

CHAPTER 4

TEMPERATURE-INDUCED ANTIBIOTIC RELEASE FROM ANTIBACTERIAL CHITOSAN/PEG HYDROGEL MEMBRANES FUNCTIONALIZED USING LAYER-BY-LAYER TECHNOLOGY

4.1. Chapter Summary

In this chapter, we report on the LbL coating of chitosan/PEG hydrogels, either with PVCL/TA films or PVCL/TA-Ciprofloxacin films. Complexation of antibiotics, such as Ciprofloxacin supports its sustained release from surfaces. Chitosan is a polysaccharide with antibacterial property. However, with this LbL coating, we enhanced the antibacterial activity of the hydrogel membranes, by adding the property of antibiotic release to them. The antibiotic release was found to be temperature-responsive, due to the presence of a thermoresponsive polymer in the LbL coating. Coated hydrogel surfaces also showed enhanced adhesion property towards fibroblasts and supported their proliferation. Such hydrogel membranes can hold potential in uses as wound dressings for chronic wounds where bacterial proliferation is a major problem.

4.2. Abstract

There is increasing interest in the development of multifunctional hydrogels in biomedical sciences and clinical applications. Chitosan/PEG hydrogels are commonly used as wound dressings and biocompatible vehicles of drug delivery, though their controlled drug release behavior is only dependent on pH and enzymatic activity. Furthermore, hydrogel wound dressing/skin interfaces are prone to be occupied by

pathogenic or opportunistic bacteria, such as Methicillin-Resistant *Staphylococcus aureus* (MRSA), during wound regeneration. Especially in chronic skin wounds, the chances of bacterial infections at dressing/dermis interfaces is much higher. The drug-release behavior of chitosan-based hydrogels that have modified surfaces through the LbL self-assembly of polymers has not been studied before. In this publication, we report on the modification of the surface of a chitosan/PEG hydrogel membrane with PVCL, a thermoresponsive polymer, and TA, a polyphenol, as a potential wound dressing. The modified hydrogel released Ciprofloxacin, a broad-spectrum antibiotic from its polymer coating in response to the physiological temperature and enhanced the antibacterial property of the hydrogel to a broader spectrum. The modification of the hydrogel surface also enhanced the propagation of human fibroblasts on the hydrogel surface, and increased their viability, making the modified hydrogel suitable for wound healing applications. Such polymer surface modifications of chitosan-based hydrogels could be useful in conveying multiple stimuli-response to them without sacrificing their physical properties, such as the swelling behavior, and the antibacterial property and biocompatibility. Such LbL-coated chitosan/PEG hydrogels hold promise as antibacterial wound dressings and overcoming MRSA-derived infections, which is a major medical concern worldwide.

4.3. Introduction

Wound healing is a complex process in which macrophages and fibroblasts take serious roles. Once the skin is wounded, the dermal integrity is reestablished through the formation of a granulation tissue which consists of macrophages, fibroblasts, and the loose connective tissue [1]. Macrophages provide the cytokines that signal fibroblasts to ingrow to lay the extracellular matrix components. Thus, fibroblasts are the primary cells that lay the extracellular matrix in the granulation tissue and the clot. These cells are responsible for secreting collagen, fibrinogen, thrombospondin, and several polysaccharides (e.g. hyaluronan) to the defect site, during neovascularization [2]. Skin wounds could be very commonly observed in the human body, due to common injuries of the daily life. Minor wounds can be self-repaired by the body, but severe wounds that involve the loss of both epidermis and the dermis would need

serious treatment. Otherwise, imperfect scar formation could occur and the physical properties of the skin, such as elasticity and strength, would be impaired [3].

Wound dressings should be designed to aid skin regeneration at the shortest time possible. It should cover or fill the wound completely so that no small pockets which may allow the proliferation of bacteria remains. Hydrogel wound dressings provide the warm and moist environment to the tissue, and such conditions are known to induce skin regeneration [4].

Chitosan is a natural polysaccharide and can be very easily supplied and designed for forming hydrogel blends, which can be used in wound treatment, skin regeneration and tissue engineering. Chitosan-based hydrogels as wound dressings has found broad attention, because they promote wound healing and cell proliferation [5]. These hydrogels retain large amounts of water and exhibit antibacterial property [6] and biocompatibility [7]. They also can act as semi-permeable oxygen-penetrating membranes [8] and are hemostatic agents presenting antithrombogenic properties [9]. Although chitosan-based hydrogels possess antibacterial properties, this effect is limited to a level, and the effectiveness is limited within the hydrogel only. The antibacterial property of hydrogels can be divided into two categories: hydrogels that can release antibacterial agents, and hydrogels that kill on contact due to the activity of specific functional groups [10]. Unless bacteria are in contact with chitosan, it neither prevents the bacterial contamination, nor kills the bacteria [11]. On the other hand, infection of chronic soft tissue wounds with pathogenic and opportunistic bacteria, such as *Staphylococcus aureus* are often observed at wound sites where the chitosan-based hydrogel cannot be in direct contact with. Especially MRSA, a resistant substrain of *S. aureus*, is a predominant cause of wound infections and is a prevalent cause of nosocomial infections in hospitals around the world [12]. The antibacterial property of a chitosan-based wound dressing can be improved through encapsulation of broad-spectrum antibiotics, e.g. Ciprofloxacin, which is reported to be effective against MRSA [13], inside the gel to be released on-demand.

Stimuli-responsive drug release from hydrogels limits the available drug that was released from the hydrogel at the desired level, only where the stimuli is present. This limits the toxic effects of drugs and maintains the minimum inhibitory concentration at the target site [14]. Stimuli-responsive polymers undergo phase transition under a variety of physical and chemical stimuli such as pH, ionic strength, temperature, light, electrical potential, and biological stimuli [15]. Stimuli-responsive polymers on-demand drug release behavior to the hydrogels, commonly due to conformational modifications of the polymers and their swelling/deswelling properties [16]. Temperature-responsive hydrogels have specific sol/gel transition temperatures which induce swollen hydrogels to deswell above the lower critical solution temperature (LCST), if they present LCST-type behavior, or below the upper critical solution temperature (UCST), if they present UCST-type bahavior [17]. Quick release of antibiotics at higher temperatures could prevent bacterial contamination in the wound bed of chronic wounds, where the temperature is higher than the surrounding tissue [18,19]. pH and biodegradability are the only stimuli that chitosan/PEG hydrogels possess at physiological conditions [20]. To impart temperature response to chitosan-based hydrogels, researchers have used blends of thermoresponsive polymers with chitosan [21,22], or chemically modified chitosan by grafting it onto synthetic polymers [23,24]. However, blending chitosan with other polymers in high ratios may modify the physical properties of the hydrogel in an undesired way. On the other hand, chemical modification of chitosan could reduce its biocompatibility and biodegradability. Surface modification of biomaterials is a method to customize the surface properties of the bulk material. Surface modification of chitosan membranes have been reported before. These studies mostly concerned improving cell adhesion and proliferation on chitosan membranes. Of note, even though chitosan-based hydrogels are biocompatible and have broad range of applications in biomedical sciences, they are resistant to cell adhesion due to high water-binding property and lack of charged functional groups under physiological conditions.

To improve the behavior of fibroblasts in the wound bed to chitosan-based hydrogels, studies have focused on the surface modification of the hydrogel through blending [25], gamma irradiation [26], chemical reactions [27], and plasma surface

modification [28,29]. The surface modification by these methods is limited to tuning the surface roughness, porosity and the variety of functional groups at the surface.

LbL self-assembly of polymers onto hydrogel substrates is a potential approach for surface modification without sacrificing the physical properties of the hydrogel. Stimuli responsive LbL films are used as platforms to load and release cargo under a variety of stimuli, such as pH, temperature, light, ionic charge etc. [30]. Hydrogels can be made responsive to multiple stimuli by modifying their surface via LbL technique. Biomedical applications of LbL-coated hydrogels have found significant place in the literature. Sakaguchi et al. reported on the LbL deposition of dextran sulfate and chitosan on poly(vinyl alcohol) hydrogels [31]. This report was the first example of LbL coating of hydrogels with natural polymers. Later, Grossin et al. reported on preparation of fibroblast encapsulated alginate hydrogels which were then deposited onto multilayers of PLL and PGA or PLL-HA and PLL via spraying. Such multilayers with fibroblast loaded hydrogels on the top were used to investigate the biological activity of the cells in the hydrogels when they were in contact with multilayers [32]. Mehrotra et al. developed LbL-coated porous agarose hydrogels by alternating deposition of PAA and PEG as well as protein and PEG multilayers onto agarose hydrogels for time-controlled release of proteins [33]. Choi et al. reported on LbL coating of collagen hydrogels with two-story polymer coatings, first with multilayers of BPEI and TA and second with PDAC and lignin multilayers on top to improve the strength of the hydrogels and to prevent the burst release of an anti-cancer agent out of the hydrogel [34]. Very recently, Gentile et al. reported on the modification of alginate/gelatin blend hydrogels via LbL self-assembly of PSS/PAH multilayers over the hydrogel for the regeneration of the cartilage tissue [35].

Here, we report on the modification of chitosan/PEG hydrogel membranes via LbL assembly of TA and PVCL onto the surface of the hydrogels. Different strategies were applied to load Ciprofloxacin into the multilayers and the resulting hydrogels were compared in terms of Ciprofloxacin release kinetics, antibacterial acitivity and cell adhesion properties. Ciprofloxacin containing TA/PVCL coated chitosan/PEG hydrogel membranes were found to be capable of releasing Ciprofloxacin via

temperature-trigger at physiological conditions due to LCST-type phase behaviour of PVCL and conformational changes occurred within the multilayers. Moreover, our results showed that TA/PVCL coated chitosan/PEG hydrogels showed increased adherence and proliferation of fibroblasts. The surface modification technique demonstrated here to impart temperature response and enhanced cell adhesion property to chitosan/PEG hydrogels was practical and advantageous in the sense that no chemical modification or blending of the hydrogel was required. Taking advantage of LbL films in controlling the amount of drug release from a surface, such Ciprofloxacin containing LbL coated chitosan/PEG hydrogels can be used to tune the antibiotic release from membranes to a desired level, such as the minimum inhibitory concentration of MRSA, and overcoming the proliferation of bacteria at the interface of the dermis and the hydrogel.

Different from the above mentioned studies, this study is the first describing the LbL coating of a cationic hydrogel. Additionally, it is the first in showing that an antibiotic-releasing LbL-coated hydrogel can overcome the colonization of both Gram-negative and Gram-positive bacteria in infected wounds beds.

4.4. Materials and Methods

4.4.1. Materials

Chitosan (50,000 – 190,000 Da), phosphate buffered saline (PBS) (tablet), Ciprofloxacin, and trypsin/EDTA were purchased from Sigma-Aldrich Co. (Missouri, USA). Poly(ethylene oxide) (average M_V = 200,000) was purchased from Aldrich Chemical Co. (Wisconsin, USA). Sodium dihydrogen phosphate dehydrate, Tannic Acid, HCl, NaOH (pellets), and H_2SO_4 were purchased from Merck (Darstadt, Germany). Poly(N-vinyl caprolactam) (M_w = 1800, M_n = 1300) was purchased from Polymer Source Inc. (Quebec, Canada). Eagle's Minimal Essential Medium (EMEM), Fetal Bovine Serum (FBS), L-gultamine, sodium pyruvate, and MEM non-essential mino acid solution (100X) were purchased from Gibco/Life Technologies (Carlsbad, California, USA). Dulbecco's Phosphate Buffered Saline (D-PBS) was purchased

from Biowest (Nuaillé, France). Cell culture plates and T25 flasks were purchased from Greiner Bio-One (Kremsmünster, Austria). M9 minimal medium was prepared from Merck products (Darmstadt, Germany).

4.4.2. Preparation of Chitosan/PEG Hydrogel Membranes

Chitosan and PEG were dissolved in deionized H_2O (18.2 MΩ·cm) at 3% w/v and 0.5% w/v respectively, with an addition of 60 mM HCl and mixed thoroughly overnight. 1% w/v glutaraldehyde was then added into this mixture with a weight ratio of 10:1. A 250 μm-thick PDMS mold with 800 μm diameter circular wells were placed on PTFE-coated glass slide. 70 μL of the mixture was poured into each well. The mold was placed inside an oven and kept at 60°C for 1 h. Another PTFE-coated glass slide was placed on top of the gel-filled mold and left for drying for 3 hours. The dried hydrogel membranes were removed from the mold and placed inside a 2 M NaOH solution (prepared in deionized water) and waited overnight for neutralization.

For all biological experiments, the hydrogels were kept overnight in 70% ethanol solution (prepared with 18.2 MΩ·cm deionized H_2O).

4.4.3. Preparation of TA- Ciprofloxacin Complexes

0.5 mg/mL TA and 0.25 mg/mL Ciprofloxacin solutions were prepared using 0.001 M phosphate buffer (prepared in deionized H_2O). Ciprofloxacin solution's pH was adjusted to 2, and the solution was mixed for 45 minutes until the antibiotic dissolved completely. pH of both solutions were adjusted to 4 prior to complexation. 0.147 mL Ciprofloxacin solution was added dropwise into 10 mL TA solution and mixed for 30 minutes. pH adjustments were performed using 0.1 M HCl and 0.1 M NaOH solutions. Hydrodynamic size and zeta-potential measurements were performed using Zetasizer Nano-ZS equipment (Malvern Instruments Ltd., U.K.). Particle sizes were obtained by cumulants analysis of the autocorrelation data. Zeta-potential values were obtained from electrophoretic mobility values using the Smoluchowski approximation.

4.4.4. LbL Self-Assembly of TA and PVCL or TA-Ciproflaxicin and PVCL onto Hydrogel Membranes

TA-Ciproflaxocin complexes were prepared as described in Section 4.4.2. 0.5 mg/mL PVCL solution was prepared at pH 4. All solutions were filtered through a 0.2 μm PES syringe filter prior to deposition on the hydrogel membranes. Under a Class 2 Biosafety cabinet, chitosan/PEG hydrogel membranes were removed from 70% ethanol solution and immersed in sterile 0.001 M phosphate buffer for 30 minutes to remove the residual ethanol. TA-Ciproflaxicin complexes and PVCL were deposited onto the hydrogel membranes by alternatingly dipping the membranes for 5 minutes in each polymer solution. Coated membranes were rinsed twice using 0.001 M phosphate buffer solution for 1 minute after deposition of each layer. The cycle was repeated until desired number of layers are deposited.

Multilayers of PVCL and TA were deposited in the same way except 0.5 mg/mL TA solution was used instead of TA-Ciprofloxacin complex solution.

To track LbL deposition, same polymer pairs were deposited onto silicon wafers instead of chitosan/PEG hydrogel membranes. 1 cm x 1cm sized silicon wafers were immersed in concentrated H_2SO_4 for 1 h and 25 min, and then rinsed with deionized H_2O. After drying under a flow of nitrogen, wafers were immersed into 0.25 M NaOH solution for 10 min, thoroughly rinsed with deionized H_2O and dried again under nitrogen flow. LbL films were deposited at the surface by immersing the substrate into polymer solutions as described above in detail. Multilayer growth and film stability were followed by monitoring the thickness of the dried films using a spectroscopic ellipsometer [Optosense, USA (OPT-S6000)]. Thickness measurements were performed from three different regions on the substrate and averaged.

4.4.6. Atomic Force Microscopy (AFM) and Scanning Electron Microscopy (SEM) Imaging

2 cm x 1 cm glass microscope slides were cleaned using the same procedure as described above for cleaning of silicon wafers. Acetate films of 35 μm thickness were cut in 1 cm x 1 cm dimensions and were rinsed with deionized H_2O. These films were placed on each side of the glass slide, so that a 1 cm x 1 cm blank area was left on the slide. A drop of chitosan/PEG mixture containing glutaraldehyde crosslinker was poured on this empty area, and another 2 cm x 1 cm glass microscope slide was pressed on top of it. The set-up was squeezed with cantilevers and placed inside an oven at 60°C for 3 h. Then, it was disassembled slowly inside 2 M NaOH solution and placed in 0.001 M phosphate buffer solution for 30 min.

LbL-coated and bare chitosan/PEG hydrogel membranes were prepared as described in Sections 4.4.2 and 4.4.4. TA and PVCL or TA-Ciprofloxacin complexes and PVCL multilayers were coated on chitosan/PEG hydrogel membranes for SEM analysis. For cross-sectional SEM imgaes, samples were frozen in liquid nitrogen and cracked from one corner to obtain a cross-section image. SEM imaging of these samples was performed using QUANTA 400F Field Emission SEM after Au-Pd coating.

AFM imaging of the films was performed using an NT-MDT Solver P47 AFM in tapping mode using Si cantilevers. Roughness values were obtained from images with 1 x 1 μm scan size.

4.4.7. Drug Release Studies

Ciprofloxacin release was followed via fluorescence spectroscopy technique (Hitachi F2500 fluorescence spectrophotometer, Tokyo, Japan), by taking readings of sample aqueous solutions at specified time points. Simply, 10 bilayers of TA/PVCL or TA-Ciprofloxacin complexes and PVCL films were coated on chitosan/PEG hydrogel membranes. In case of TA/PVCL coated membranes, coated substrates were placed overnight in 1 mg/mL of Ciprofloxacin solution at pH 4 (prepared in 0.001 M

phosphate buffer). These drug-loaded membranes were rinsed twice with 0.001 M phosphate buffer at pH 4.

For release studies, LbL coated hydrogel membranes were immersed in 40 mL of PBS buffer (pH 7.4) at either 25°C or 37°C. Aliquots were taken from the PBS at specified time points. Ciprofloxacin was excited at 275 nm and the change in the intensity of the peak at 415 nm was followed as a function of time.

4.4.8. Antimicrobial Activity of Hydrogel Membranes

LB broth was used for the overnight cultivation of *Staphylococcus aureus* ATCC 29213 and *Escherichia coli* BL21. M9 minimal growth medium was prepared and used for the incubation of the bare and LbL coated chitosan/PEG hydrogel membranes in all assays examining the antibacterial properties. Both of the media were autoclaved for sterilization prior to use.

To determine the antibacterial activity of bare, 5- and 10-bilayer coated hydrogel membranes with either type of the multilayers, the membranes were fitted inside the wells of a 96-well plate and each well was filled with 200 μL of M9 medium. 5 μL of overnight cultures of *S. aureus* and *E. coli* were added in each well. 5 h after incubation of the plate in a microbiological incubator at 37°C, shaking at 54 rpm, 150 μL of the bacteria culture were taken from the wells and the absorbance was recorded with a UV·Vis spectrophotometer at 600 nm.

4.4.9. CCD-18Co Fibroblast Adhesion and Proliferation on Hydrogel Membranes

CCD-18Co cells (human primary fibroblast cell line from colon) were cultivated in EMEM complete medium supplemented with 20% FBS, 2 mM L-glutamine, 1 mM sodium pyruvate, 1X MEM non-essential amino acid solution, 100 U/mL penicillin, and 100 μg/mL streptomycin. After thawing the stocks, cells were cultivated in T25 flasks and the medium was renewed every two or three days. All cell culture flasks and plates were maintained in a humidified atmosphere at 37°C in 95% air and 5%

CO_2. To harvest cells from the flasks, 0.5 mg/mL porcine trypsin with 0.2 mg/mL EDTA·4Na solution was used.

5- or 10-bilayer TA/PVCL coated membranes were fitted inside the wells of a 96-well tissue culture plate. 10,000 cells were seeded in each well and the cells were left to grow and proliferate for either 48 h or 96 h.

The viability of cells grown on the membranes was determined by the 3-(4,5-dimethylthiazolyl-2)-2,5-diphenyltetrazolium bromide (MTT) protocol. 5 mg/mL of stock MTT solution was prepared in D-PBS. This solution was diluted by 10 times using the EMEM medium, to reach a final concentration of 0.5 mg/mL. 100 μL of the diluted MTT medium was added into each cell-seeded well. After incubating the plate for 4 hours in a cell culture incubator, 100 μL of detergent reagent (0.01 N HCl with 100 mg/mL SDS prepared in deionized H_2O) was added into each well and the plate was kept in the cell culture incubator overnight. Three different samples were taken from each well and the readings were obtained with a microplate reader at OD_{570nm} and analyzed for comparisons.

Additionally, to assess the adhesion property of the tissue culture plate well, bare, or coated hydrogel membranes on CCD-18Co cells, after incubation of cells for 48 h, we washed the plates twice with sterile PBS and cells were fixed in 10% parafolmaldehyde for 20 min. After rinsing the surfaces twice with deionized water, cells were permeabilized in 10 mM Tris-HCl containing 2 mM $MgCl_2$ and 0.5% Triton X-100 in PBS and the surfaces were rinsed 4 times with deionized water. The cells were treated with 3,3′-dioctadecyl-5,5′-di(4-sulfophenyl) oxacarbocyanine sodium salt (SP-DiOC$_{18}$(3)) with a final concentration of 5 μg/mL in the culture medium for 5 min in a cell culture incubator at 37°C and subsequently for 15 min on ice. The cells were observed under a FloID fluorescent microscope (Life Sciences, USA) in the green channel. Images from 6 random sites for each well were recorded.

4.4. Results

4.4.1. Preparation of Chitosan/PEG Hydrogel Membranes

Chitosan and PEG were dissolved in deionized H_2O with 60 mM HCl at 3% w/v and 0.5% w/v ratios, respectively. After mixing this polymer mixture (gel) overnight, we have poured the gel inside the 250 μm-thick PDMS mold with 800 μm diameter circular wells, which was placed on a PTFE-coated glass slide. The image for the glass slide and the mold can be seen in Figure 4.1. After letting the gel dry in an oven at 60°C, the gel was placed in 10^{-3} M $NaH_2PO_4 \cdot 2H_2O$ buffer prepared in deionized H_2O at pH 4. The gel dissolved shortly after, unable to retain its shape. Thus, we decided to add a cross-linker inside the chitosan/PEG mixture before pouring the gel in the mold. At 4°C , we mixed the polymer mixture with 1% w/v glutaraldehyde at a gel/cross-linker weight ratio of 10:1. After the drying step, the gel retained its shape for several days in 10^{-3} M $NaH_2PO_4 \cdot 2H_2O$ buffer at pH 4. The image of the swollen chitosan/PEG hydrogel can be seen in Figure 4.2. As reported by Hu et al., glutaraldehyde makes covalent bonds with the amine groups of chitosan, forming imine groups [36]. Like other interpenetrating polymer networks (IPNs), chitosan/PEG blends form networks where two different polymers are held together by permanent entanglements with no more than a few accidental covalent bonds between the chains of two different type of polymers [37]. Most probably because of the entanglements between chitosan and PEG, polymer chains hold chitosan and PEG together for couple of minutes in 10^{-3} M $NaH_2PO_4 \cdot 2H_2O$ buffer at pH 4, but to achieve more stable hydrogels cross-linking of chitosan chains with glutaraldehyde is necessary.
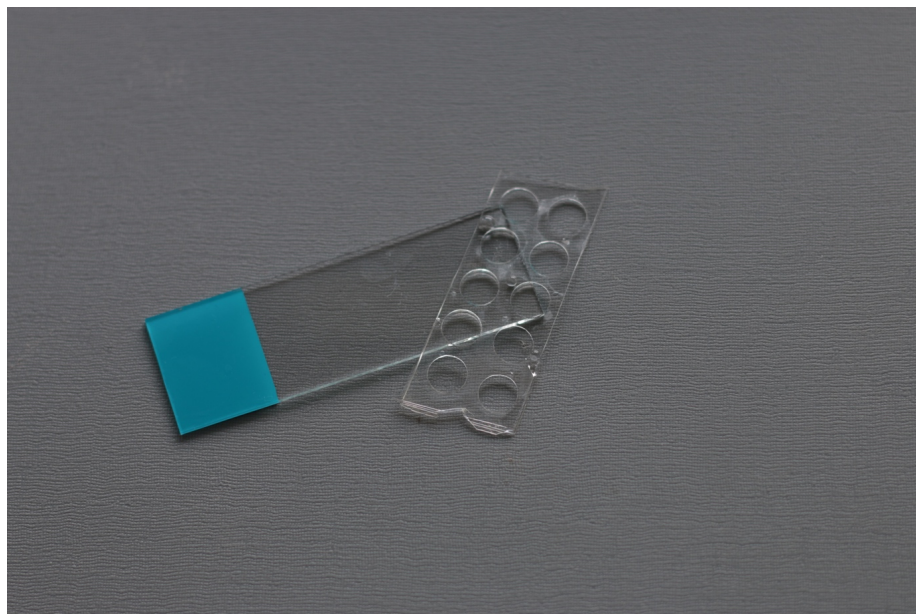
Fig. 4. 1. The photograph of the PDMS mold and the PTFE-coated glass slide that were used in experiments.
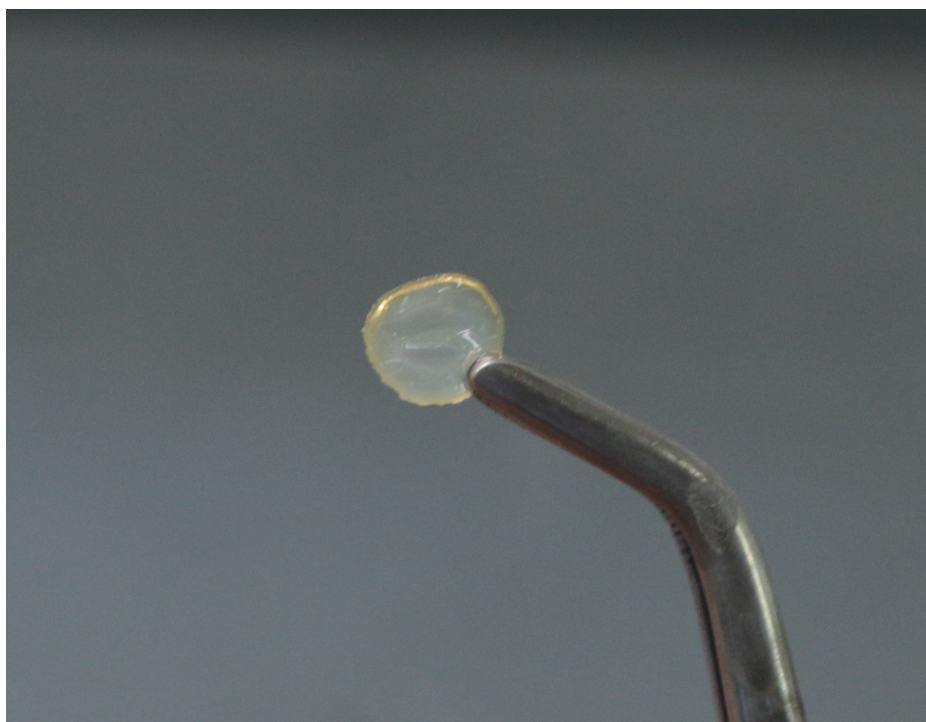
Fig. 4. 2. The photograph of a swollen glutaraldehyde-crosslinked chitosan/PEG hydrogel membrane.

To prove the cross-linking of chitosan chains via the formation of covalent bonds within the amine groups of chitosan and the aldehyde groups of glutaraldehyde, we carried out FTIR analysis under ATR mode. The FTIR spectra of non-crosslinked chitosan/PEG hydrogel and glutaraldehyde-crosslinked chitosan/PEG hydrogel is represented in Figure 4.3. After cross-linking the hydrogel, we observed the formation of a band at 1516 cm^{-1}, similar to the findings of Hu et al. [36] and Baldino et al. [36] on the FTIR peaks of non-crosslinked and glutaraldehyde-crosslinked chitosan. The shift at the band 1647 cm^{-1} towards 1629 cm^{-1} most probably corresponds to a reduction in the amide bonds after glutaraldehyde-mediated cross-linking to form new imine bonds between chitosan and glutaraldehyde [36].

After cross-linked hydrogel membranes were dried in the oven, the apparatus that is composed of the PDMS mold and the PTFE-coated glass slide was placed in 2 M NaOH solution where excess acid is neutralized to form salts. Placing these membranes in 70% ethanol overnight sterilized the membrane, but also caused the replacement of water with ethanol. To replace excess ethanol with water, we placed the membrane in 10^{-3} M $NaH_2PO_4 \cdot 2H_2O$ buffer at pH 4, till the hydrogels swelled with water again.
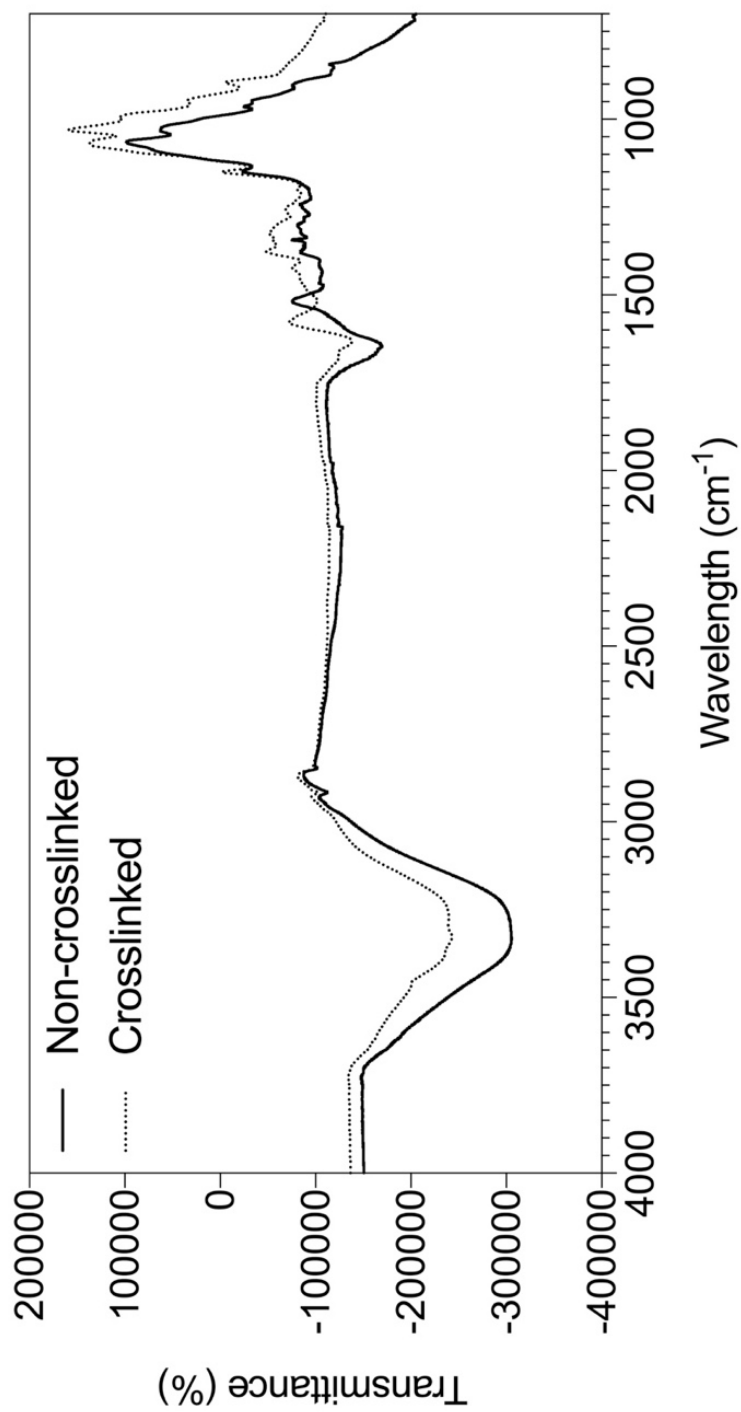
Fig. 4. 3. The FTIR spectrum of glutaraldehyde- crosslinked and non-crosslinked chitosan/PEG hydrogel membranes.

181

4.4.1. Complexation of TA and Ciprofloxacin

Non-covalent interactions, such as the electrostatic interactions and hydrogen-bonding between molecules do not involve sharing electrons, thus do not comprise very strong binding, but can influence the release of a drug from a polymer film. The complexation between antibiotics and polymers that are available on catheter surfaces had shown that the availability and the period of release of the antibiotic was doubled *in vitro* and *in vivo*, compared to antibiotic-coated catheter surfaces [38], due to the non-covalent interactions between the antibiotic and the polymer. Complexes of an anti-cancer agent (Doxorubicin) with TA has been successfully used in LbL films. In this report, the release of the anti-cancer agent was observed to be higher under mildly acidic conditions, where the hydroxyl groups of TA are not deprotonated, and to be lower at pH 7.5, due to the enhanced electrostatic interactions between the agent and TA, due to the deprotonation of the hydroxyl groups of TA [39]. 0.25 mg/mL Ciprofloxacin solution was added dropwise onto 0.5 mg/mL TA solution with a 1.47:10 volume ratio at pH 4. TA degrades hydrolytically to gallic acid and glucose in aqueous solutions and the degradation is enhanced at physiological pH, compared to the degradation rate at mildly acidic pH [40]. Therefore, to minimize the degradation of TA during complexation and later during LbL assembly, we performed complexation at pH 4.

TA is a natural polyphenol with 25 phenolic hydroxyl groups per molecule. pK_a of TA depends on its source and for the one used in this study, two pK_a values were determined, i.e. $pK_{a,1} = 6.5$ and $pK_{a,2} = 8$ [39] which were both correlated with the phenolic hydroxyl groups of TA. Ciprofloxacin is a zwitterionic molecule with a $pK_{a,1} = 6.09$ and $pK_{a,2} = 8.74$. The $pK_{a,1}$ associates with the carboxylic acid of Ciprofloxacin, whereas $pK_{a,2}$ associates with the amino groups [41]. The driving force for the formation of water-soluble TA-Ciprofloxacin complexes at pH 4 was electrostatic interactions among protonated amino groups of Ciprofloxacin and phenolate groups of TA. Enhanced ionization of TA in the presence of salt cations has been reported earlier [42]. Thus, ionization of TA could have been enhanced in the presence of positively charged Ciprofloxacin molecules at pH 4 leading to greater extent of association among TA and Ciprofloxacin. In addition to electrostatic interactions,

182

hydrogen bonding interactions among carbonyl groups of Ciprofloxacin and phenolic hydroxyl groups of TA could have also been contributed to the association of these two molecules. Scheme 4.1. shows the chemical structures of TA and Ciprofloxacin and the schematic representation of TA-Ciprofloxacin complexes. Formation of TA-Ciprofloxacin complexes were followed by monitoring the hydrodynamic size of the complexes using dynamic light scattering technique. Number average hydrodynamic size increased from ~ 1.6 ± 0.2 to ~ 120.36 ± 36.73 nm upon addition of Ciprofloxacin into TA solution. Figure 4.4. contrasts the number average size distribution of TA and TA-Ciprofloxacin complexes. In addition, zeta potential measurements were performed before and after complexation. Zeta potential became positive (switched from -26.1 ± 1.5 mV to 10.99 ± 0.57 mV) as Ciprofloxacin was added due to screening the negative charge on TA molecules by the positively charged Ciprofloxacin molecules. Figure 4.5. contrasts the Zeta potential distribution of TA and TA-Ciprofloxacin complexes.
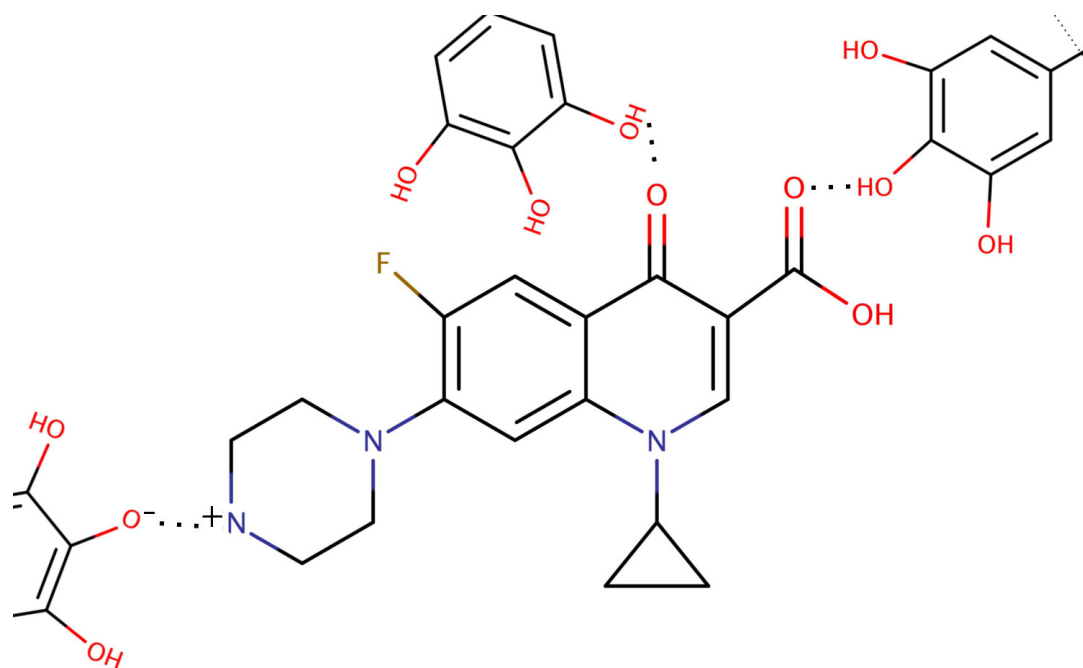
Scheme 4. 1. The chemical structure of Ciprofloxacin (center) and the gallic acid groups of tannic acid (corners).
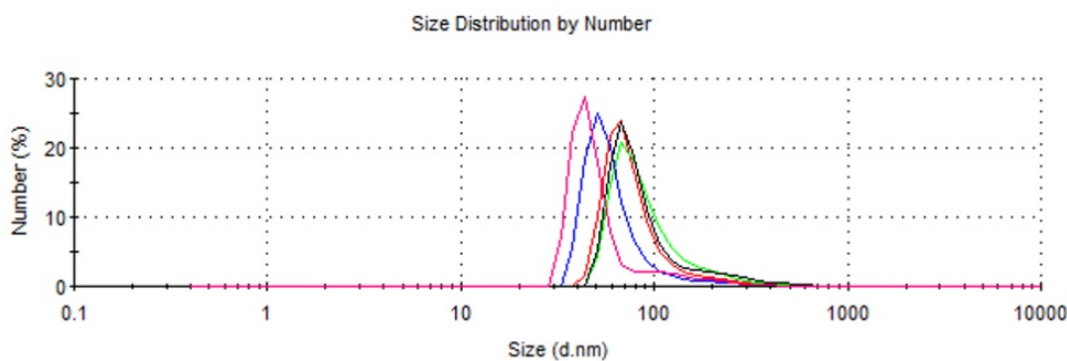
Fig. 4. 4. Hydrodynamic size distribution by number of TA-Ciprofloxacin complexes at pH 4. Size distribution curves obtained from several individual measurements of the same sample are represented with different colors.
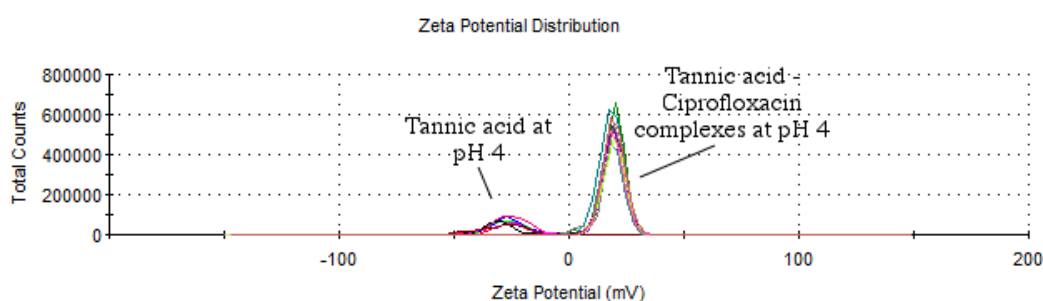
Fig. 4. 5. Zeta potential distribution of TA and TA-Ciprofloxacin complexes at pH 4. Zeta potential distribution curves obtained from several individual measurements of the same sample are represented with different colors.

4.4.2. LbL Self-Assembly of Ciprofloxacin Containing PVCL and TA Multilayers onto Chitosan/PEG Hydrogel Membranes

Prior to construction of multilayers onto chitosan/PEG hydrogels, LbL growth of PVCL and water soluble complexes of TA and Ciprofloxacin on silicon wafers was examined at pH 4 and 25°C using ellipsometry. The first layer was PVCL and adhered to the surface via Si-OH groups of the substrate and phenolic hydroxyl groups of TA. PVCL/TA-Ciprofloxacin multilayers had a linear growth profile with 3.1 nm increment per bilayer (Figure 4.6.). For comparison, LbL growth of PVCL and TA which included no Ciprofloxacin molecules was also shown in the same graph. For

both of the films, the driving force for multilayer build-up was hydrogen bonding interactions among the hydrogen accepting carbonyl groups of PVCL and hydrogen donating phenolic hydroxyl groups of TA. For PVCL/TA-Ciprofloxacin multilayers, hydrogen bonding interactions among carbonyl groups of PVCL and carboxylic acid groups of Ciprofloxacin which remained free after complexation could have also contributed to the LbL growth. Scheme 4.2. shows schematic representation of LbL films of PVCL and TA-Ciprofloxacin complexes.
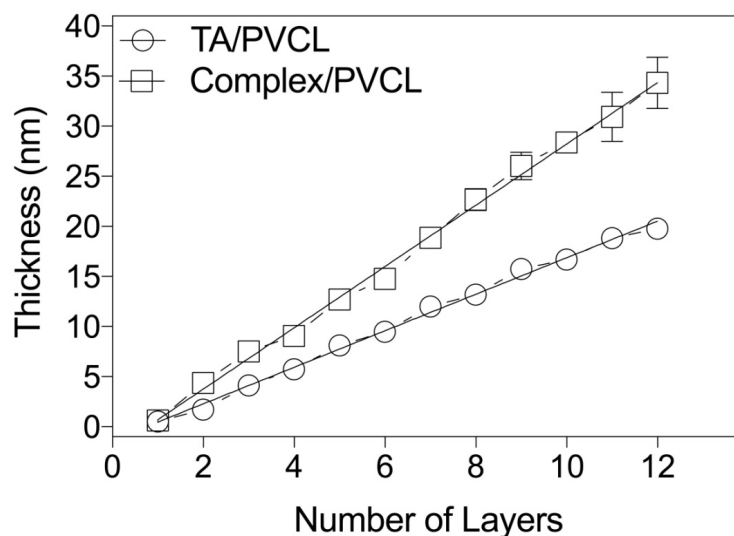
Fig. 4. 6. LbL growth of PVCL and TA-Ciprofloxacin complexes. PVCL/TA films are plotted for comparison.
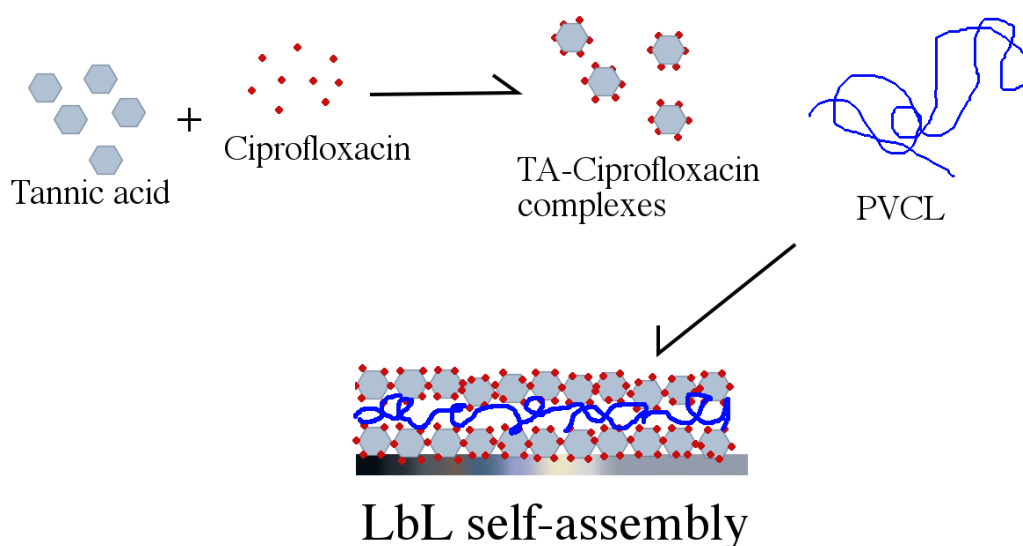
Scheme 4. 2. Schematic representation of the complexation of TA and Ciprofloxacin and the LbL assembly of PVCL with TA-Ciprofloxacin complexes on silicon surfaces.

We then constructed multilayers of PVCL and TA or TA-Ciprofloxacin complexes onto chitosan/PEG hydrogels. Different from the LbL growth of the films on silicon wafer, first layer was TA or TA-Ciprofloxacin complexes. Chitosan has a pKa of 6.5 [43], therefore it is positively charged at the deposition pH of 4 due to protonation of the amino groups. Deposition of TA or TA-Ciprofloxacin complexes onto hydrogels via electrostatic interactions was expected to be greater and provide better adhesion of the first layers than that of a PVCL layer. Therefore, first layer was chosen as TA or TA-Ciprofloxacin complexes. Deposition of multilayers onto chitosan/PEG hydrogels was followed using AFM and SEM. Figure 4.7. shows the AFM images of bare chitosan/PEG hydrogels, 5- and 10-bilayer films of PVCL/TA-Ciprofloxacin complexes and PVCL/TA. Bare chitosan/PEG hydrogels exhibited low surface roughness (~ 3.60 nm) with some globular structures on the surface which probably formed in the drying step of the hydrogel preparation. For both of the films, surface roughness changed dramatically upon deposition of multilayers. The surface roughness increased from 3.60 nm to 41.5 nm and 59.2 nm after deposition of 5-bilayer films of PVCL/TA and PVCL/TA-Ciprofloxacin complexes, respectively. The higher surface roughness of PVCL/TA-Ciprofloxacin films can be correlated with the larger

hydrodynamic size of TA-Ciprofloxacin complexes than that of TA molecules. Incomplete and irregular packing of TA-Ciprofloxacin at the surface is suggested to be the reason for the higher surface roughness of the PVCL/TA-Ciprofloxacin films than PVCL/TA films. During the deposition of PVCL chains, the adsorption on TA-Ciprofloxacin complexes are more likely when compared to deposition onto incomplete parts. This results in higher surface roughness in case of PVCL/TA-Ciprofloxacin films.

Importantly, surface roughness increased from ~1 nm to 14.1 nm and 10.5 nm when 5-bilayer PVCL/TA and PVCL/TA-Ciprofloxacin films were deposited onto silicon wafers rather than chitosan/PEG hydrogels. This significant difference in surface roughness was correlated with the absorption of TA molecules or TA-Ciprofloxacin complexes and PVCL into chitosan/PEG hydrogels. These polymers probably diffused out during multilayer deposition, followed by formation of water soluble complexes of TA and PVCL or TA-Ciprofloxacin and PVCL and deposition of polymers at the surface in the aggregated form. This affect was even enhanced in case of PVCL/TA-Ciprofloxacin films as can be recognized by the greater lateral dimensions of the surface aggregates due to larger sizes of PVCL associated TA-Ciprofloxacin complexes than that of PVCL and TA complexes.

Surface roughness increased with increasing number of layers for PVCL/TA films although the increment per 5-bilayer was lower than the increment upon the deposition of the first 5-bilayers. The surface roughness increased from 41.5 nm to 48.1 nm when additional 5-bilayers of PVCL/TA were deposited onto 5-bilayer PVCL/TA films. This result suggests that diffusing out of TA molecules from the hydrogel matrix probably completed during the deposition of the first 5-bilayers. In contrast, surface roughness remained same for PVCL/TA-Ciprofloxacin films even after additional 5-bilayer coating leaving a question mark for the successful deposition of this additional 5-bilayers of PVCL/TA-Ciprofloxacin films. Film thickness measurements could not be performed via AFM as AFM technique is built upon the tapping of the surface by a cantilever where the topography of the surface is determined, rather than its average thickness.
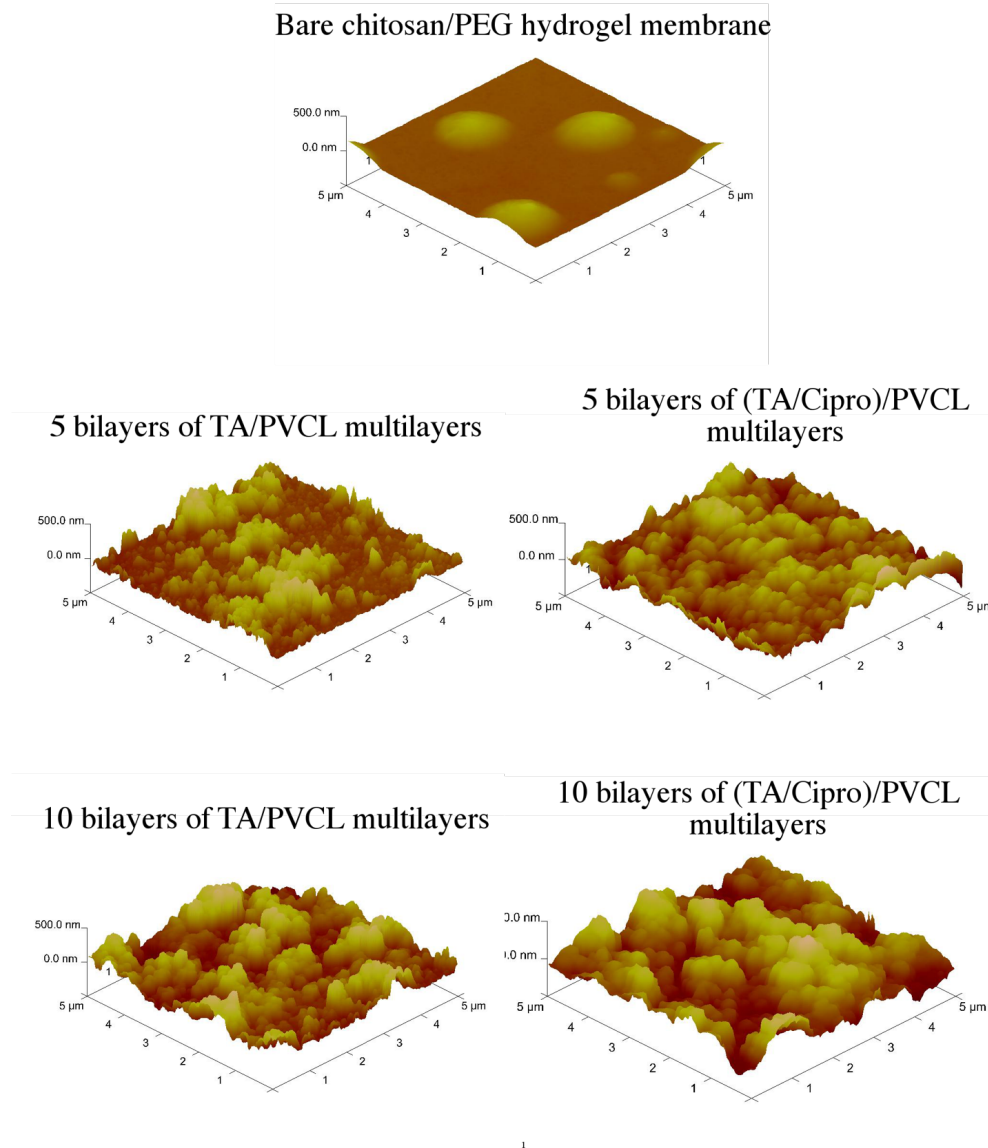
Fig. 4. 7. Atomic force microscopy images of coated or bare chitosan/PEG hydrogel membranes, obtained from 5 μm x 5 μm areas.

SEM analysis was performed on bare and 30- and 60-bilayer PVCL/TA and PVCL/TA-Ciprofloxacin coated chitosan/PEG hydrogel membranes. Figure 4.8. shows the longitudinal and cross-sectional SEM images of bare and 30- or 60-bilayer PVCL/TA or PVCL/TA-Ciprofloxacin coated chitosan/PEG hydrogel membranes. Similar to AFM images, PVCL/TA-Ciprofloxacin films exhibited large and fused

aggregates, while aggregates were smaller in case of PVCL/TA films. Thickness of 30- and 60-bilayer PVCL/TA films was recorded as 2.6 μm and 3.7 μm, respectively via cross-sectional SEM imaging. On the other hand, thickness values for 30- and 60-bilayers of PVCL/TA-Ciprofloxacin films were measured as 1.33 μm and 1.19 μm, respectively. The results for PVCL/TA-Ciprofloxacin films are in good agreement with the results obtained from AFM imaging and suggests that PVCL/TA-Ciprofloxacin films do not grow beyond a certain layer number when deposited onto chitosan/PEG hydrogel membranes. The reason can be explained by the lower number of phenolic hydroxyl groups on TA-Ciprofloxacin complexes than that on bare TA molecules and further occupation of these functional groups by the desorbed PVCL chains from the hydrogel matrix. This phenomenon results in even lower number of free phenolic hydroxyl groups on TA-Ciprofloxacin complexes than that on bare TA molecules which were not high enough to drive the LbL assembly.

Bare chitosan/PEG hydrogel membrane

30-bilayer PVCL/TA films   30-bilayer PVCL/TA-Ciprofloxacin films

60-bilayer PVCL/TA films   60-bilayer PVCL/TA-Ciprofloxacin films
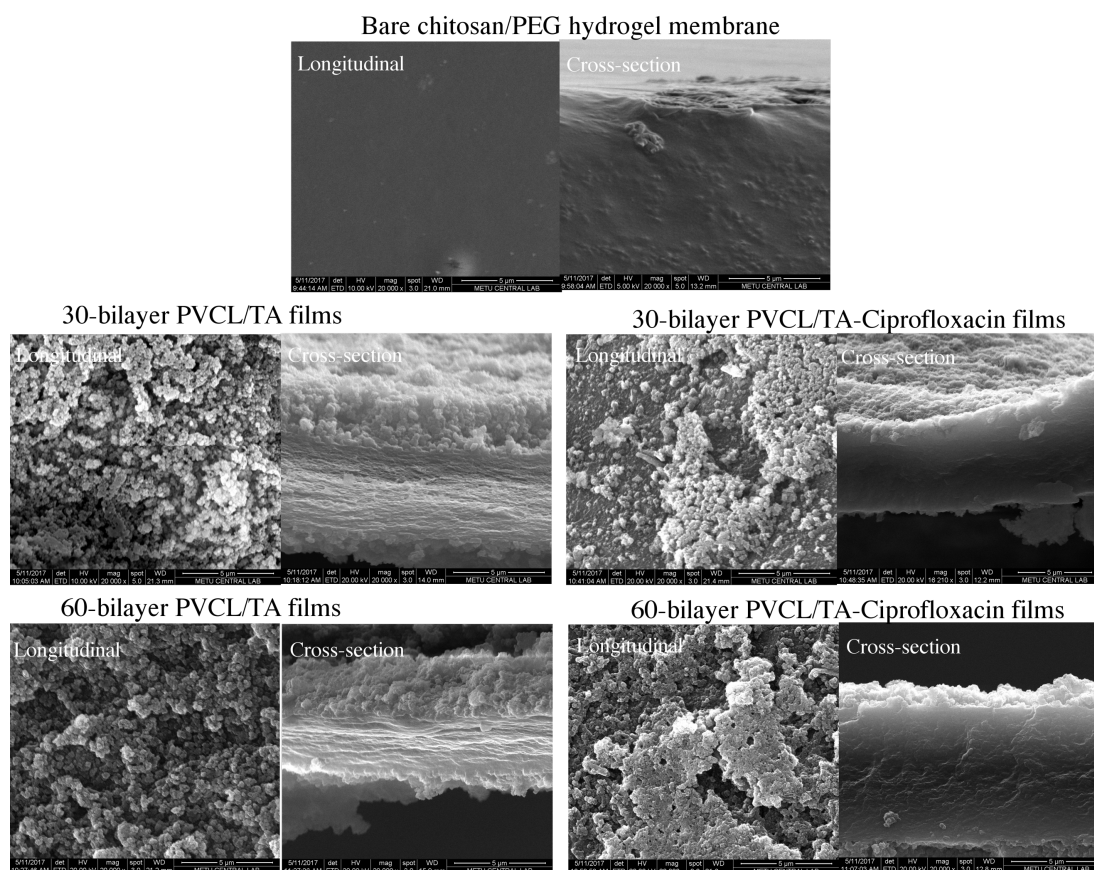
Fig. 4. 8. Longitudinal and cross-section scanning electron microscopy (SEM) images of bare coated and chitosan/PEG hydrogel membranes. Images are obtained by 20,000x magnification.

4.4.3. Ciprofloxacin Release from PVCL/TA-Ciprofloxacin and PVCL/TA Multilayers

Ciprofloxacin release from 10-bilayer PVCL/TA-Ciprofloxacin coated chitosan/PEG hydrogel membranes was performed at pH 7.4 and 25°C or 37°C (Figure 4.9.). At both temperatures, a burst release was observed in the first 1.5 hours. Then a gradual increase was observed in the total amount of drug released. The amount of Ciprofloxacin released from the surface was significantly higher at 37°C than that at 25°C. The release at 25°C was mainly due to ionization of phenolic hydroxyl groups of TA and carboxylic acid units of Ciprofloxacin, resulting in disruption of hydrogen bonding interactions among Ciprofloxacin and TA as well as Ciprofloxacin and

PVCL. In addition, self-diffusion of Ciprofloxacin molecules from LbL coated hydrogel membrane cannot be ignored. To further understand the release mechanism, we have compared the hydrodynamic sizes of TA-Ciprofloxacin complexes at pH 4 and pH 7.4 and found that the interaction among TA and Ciprofloxacin got even stronger at pH 7.4 due to ionization of phenolic hydroxyl groups and stronger electrostatic interactions among TA and Ciprofloxacin. The size increased from 115 nm to 384 nm when the pH was increased from 4 to 7.4, indicating a stronger interaction among TA and Ciprofloxacin molecules. Therefore, we correlated the release at pH 7.4 and 25°C mainly to the loss of hydrogen bonding interactions among the polymers and Ciprofloxacin.

PVCL/TA-Ciproloxacin coated
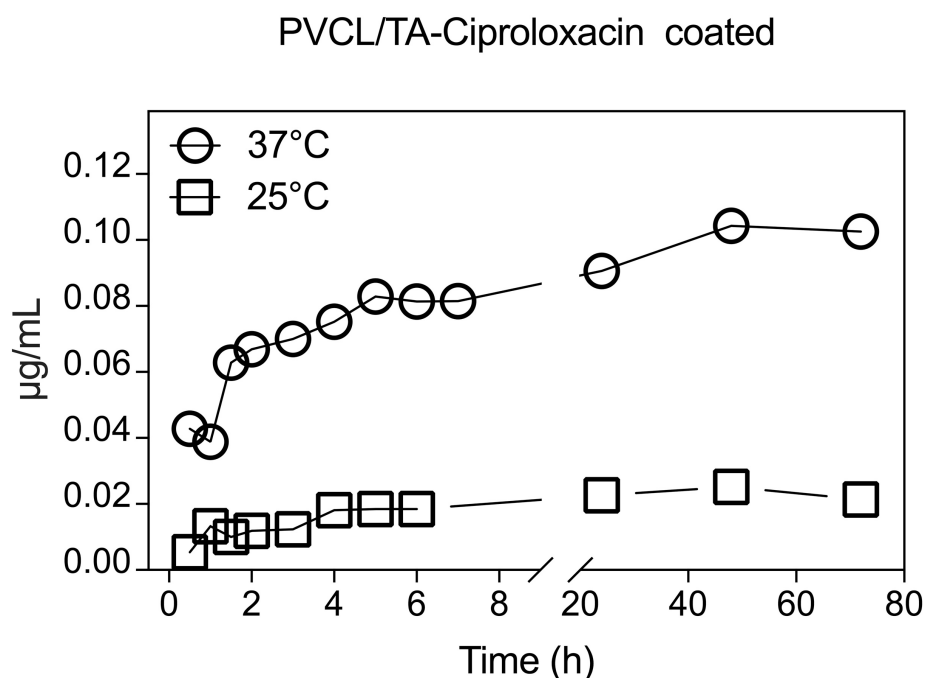
Fig. 4. 9. Ciprofloxacin release at 25°C and 37°C from 10-bilayer PVCL/TA-Ciprofloxacin coated chitosan/PEG hydrogel membranes.

At 37°C, Ciprofloxacin release was significantly higher than that at 25°C. This can be explained by the LCST-type phase behavior of PVCL. PVCL displays LCST behavior in the range of 32-35°C in aqueous solutions, depending on the polymer weight [44]. At pH 7.4, PVCL was expected to transform from extended to globular conformation within the multilayers, resulting in void-like structures in the film matrix. This

191

restructuring within the multilayers probably facilitated the Ciprofloxacin release. Enhanced kinetic energy of Ciprofloxacin molecules at increasing temperature values could have also induced greater amount of release from the hydrogels.

4.4.4. Post-Loading of Ciprofloxacin into PVCL/TA Coated Hydrogel Membranes

In case of 10-bilayer PVCL/TA coated hydrogel membranes, Ciprofloxacin was loaded at the post-assembly step. 10-bilayer PVCL/TA coated chitosan/PEG hydrogel membranes were prepared at pH 4 and immersed into 1 mg/mL Ciprofloxacin solution at pH 4 for 16 hours. Figure 4.10. shows the amount of Ciprofloxacin release from the surface as a function of time. The effect of increasing temperature on the amount of Ciprofloxacin release from the surface was obvious also for PVCL/TA coated hydrogels. The amount of Ciprofloxacin released from the surface almost quadrupled when temperature was increased from 25°C to 37°C. In both types of the films, PVCL/TA coatings introduced temperature-response to chitosan/PEG hydrogels and facilitated the release of Ciprofloxacin from the surface.
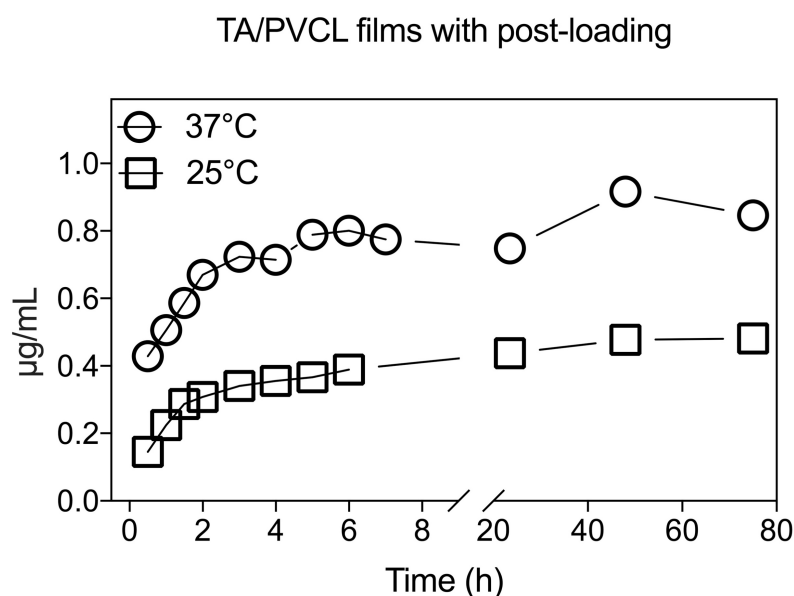

Fig. 4. 10. Ciprofloxacin release at 25°C and 37°C from 10-bilayer PVCL/TA coated chitosan/PEG hydrogel membranes with post-loading of Ciprofloxacin.

4.4.5. Comparison of Ciprofloxacin Release from Hydrogels

Release from two different hydrogels at 37°C was compared. In addition, a control experiment was conducted in which Ciprofloxacin release was tracked from bare chitosan/PEG hydrogels. Figure 4.11. contrasts the release from different hydrogels. In all hydrogels, an initial burst release was observed in the first 1.5 hours. However, different from the release of Ciprofloxacin from the surface of hydrogels coated with PVCL and TA-Ciprofloxacin complexes, sustained release was observed when Ciprofloxacin was loaded into the 10- bilayer PVCL/TA coated or bare hydrogel membranes at the post-assembly step. Interestingly, Ciprofloxacin release from bare hydrogels was greater than that from the surface of hydrogel membranes coated with 10-bilayer of PVCL and TA-Ciprofloxacin complexes.
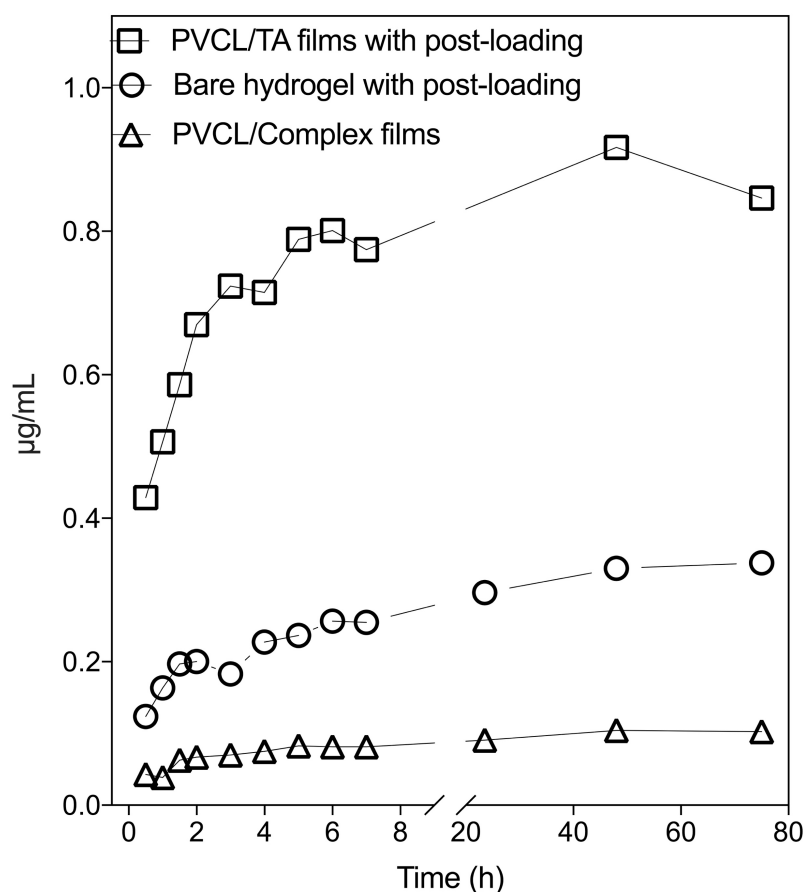
Fig. 4. 11. Ciprofloxacin release at 37°C from 10-bilayer PVCL/TA coated chitosan/PEG hydrogel membranes with post-loading of Ciprofloxacin, bare

chitosan/PEG hydrogel membranes with post-loading of Ciprofloxacin and PVCL/TA-Ciprofloxacin.

4.4.5.1. Comparison of The Amount of Ciprofloxacin Release from The Surface of Hydrogels

i) Ciprofloxacin is smaller in size than TA-Ciprofloxacin complexes. Therefore, its penetration into the hydrogel matrix is more probable than penetration of TA-Ciprofloxacin complexes. Therefore, Ciprofloxacin could have been loaded in greater amounts into bare and 10-bilayer PVCL/TA coated hydrogels at the post-assembly step.

ii) As discussed earlier, Ciprofloxacin and TA interaction gets stronger due to enhanced electrostatic interactions among the molecules at pH 7.4. In case of hydrogels coated with TA-Ciprofloxacin complexes and PVCL, Ciprofloxacin release could have been reduced since Ciprofloxacin molecules have already been associated with TA. In case of post-loading of Ciprofloxacin into either 10-bilayer PVCL/TA coated or bare hydrogels, association of Ciprofloxacin with the multilayers could be weaker so that the release from the hydrogel and multilayer matrix was easier.

iii) In case of hydrogels coated with PVCL and TA-Ciprofloxacin complexes, Ciprofloxacin molecules could have self-diffused into the solution during the multilayer deposition step with 10 cycles.

iv) Concentration of Ciprofloxacin solution in which the PVCL/TA coated hydrogel membranes were immersed into at the post-assembly step was higher than the concentration of Ciprofloxacin in the deposition solutions in case of PVCL/TA-Ciprofloxacin coated chitosan/PEG hydrogel membranes.

194

4.4.5.2. Comparison of The Release Kinetics

Release of Ciprofloxacin reached a maximum value after 48, 48, and 75 hours in case of hydrogels coated with 10-bilayers of PVCL and TA-Ciprofloxacin complexes, 10-bilayers of PVCL and TA and bare hydrogels, respectively. The sustained release from PVCL/TA coated or bare hydrogels was correlated with greater amount of Ciprofloxacin loading into chitosan/PEG hydrogel membranes which took longer to release from the surface. Although it was not obvious as much as the sustained release observed for PVCL/TA coated hydrogels, bare hydrogels also demonstrated sustained release. It was probably due to PVCL and TA multilayers which provided the maximum sustained release in case of PVCL/TA coated hydrogel membranes.

Importantly, we have further examined the sustained release after the first day for 10-bilayer PVCL/TA coated quartz wafers. The stability of TA/PVCL films was studied by monitoring the change in the fluorescence intensity of TA at 370 nm as a function of time after being immersed into PBS solution at pH 7.4 and 37°C. Figure 4.12. shows the evolution of the fluorescence intensity as arbitrary units (A.U.) at 370 nm as a function of time and shows that almost no TA remained at the surface after 24 hours. Therefore, the sustained release of Ciprofloxacin after the first day was correlated with the Ciprofloxacin molecules entrapped within the hydrogel matrix.
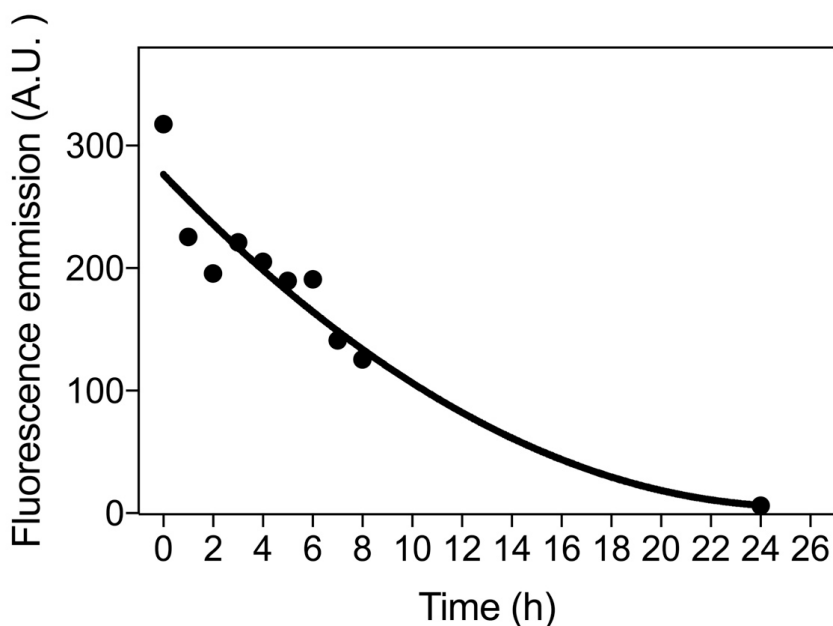
Fig. 4. 12. The evolution of fluorescence intensity of TA at 370 nm from the surface of a 30-bilayer TA/PVCL film coated chitosan/PEG hydrogel, placed in PBS at pH 7.4 and 37°C.

Several methods of loading drugs inside chitosan-based hydrogels were reported. One way of loading drugs in hydrogels is diffusion of the drug inside hydrogel for a controlled duration. Mixing the components of a hydrogel with the drug prior to crosslinking, or tethering the drug chemically to the components of the hydrogel, such as tethering through enzyme-sensitive peptides [45], or the hydrolytically-degradable linkage polymers, to induce the release [46] are two other commonly applied methods. Diffusion-based loading can allow large amounts of drug molecules to be loaded inside hydrogels, but this method has the primary disadvantage of causing the release of the drug as a burst release. Although above mentioned methods allow high amounts of drug molecules to be trapped in the hydrogel matrix, they have got several disadvantages, such as initial burst release of the drug after implantation in the case of diffusion-based loading, or deactivation of the drug due to screening of the active functional groups on drug molecules, due to cross-links [47].

196

4.4.6. Antimicrobial Properties of the Membranes

Chitosan is a commonly used antibacterial agent in biomedical sciences and the mechanism of the antibacterial property lies in the property of chitosan that facilitates membrane disruption, thus the leak of the cytoplasm out of the bacteria [11]. The antibacterial activity of chitosan increases as its deacetylation degree increases [48]. Chitosan exhibits anti-bacterial property only when the bacteria are in contact with the Chitosan-modified surface. This limits chitosan products' use in infection wound treatment, due to the resident bacteria that penetrates the wound tissue. To augment the antibacterial effect of chitosan, antibiotic release from the chitosan/PEG hydrogel would be of use. Ciprofloxacin is a broad-spectrum antibiotic with efficacy against several types of Methicillin-Resistant *Staphylococcus aureus* (MRSA) [13]. We have examined the antibacterial activity of bare and LbL coated chitosan/PEG hydrogels against *Escherichia coli* BL21 and *Staphylococcus aureus* ATCC 29213. Figure 4.11. shows the bacteria density at OD_{600}. As seen in the figure, bare chitosan/PEG hydrogel exhibits a significant bacteriostatic effect on *E. coli* against the bacteria grown in tissue culture plate wells (positive control) but the effect was insignificant on *S. aureus*, compared to the positive control.

During the experiments, the microbiology incubator was shaken at 54 rpm and it mixed the bacteria culture properly that were on each type of hydrogel membrane. In case of bare hydrogels, the bacteria were in contact with the hydrogel surface, thus chitosan showed its contact-killing property. When chitosan/PEG hydrogels were coated with 5 bilayers of TA/PVCL (no Ciprofloxacin was included), we observed higher bacteria density due to a decrease in contact-killing behavior upon coating with multilayers. However, the number of bacteria growing around the coated hydrogel membrane was still lower than that on the positive control, indicating that contact-killing behavior could still be effective even after 5-bilayers of PVCL/TA coating. It is worth to mention that TA is also known to exhibit antibacterial property with 46 μg/mL MIC on *Escherichia coli* ATCC 25922 [49]. Therefore, TA containing multilayers could have been also effective on the lower number of bacteria on 5-bilayer PVCL/TA coated hydrogel membranes when compared to the positive control. Hydrogel

membranes coated with 5-bilayers of PVCL and TA-Ciprofloxacin complexes were slightly more bacteriostatic on *E. coli* than the 5-layer PVCL/TA coated hydrogels, indicating the temperature-induced release of Cipro from the membrane. To observe the antibacterial effect of Ciprofloxacin, the antibiotic should be free in solution and should penetrate the cell wall of bacteria as its antibacterial mechanism is based on the inhibition of DNA gyrase [50]. Due to this fact, we think that Ciprofloxacin was released from the membranes and free Ciprofloxacin penetrated the bacterial cell wall.

To further examine the effect of LbL coating on the antibacterial activity of the hydrogels, chitosan/PEG hydrogel membranes coated with either 10-bilayers of PVCL and TA (no Ciprofloxacin was included) or PVCL and TA-Ciprofloxacin complexes were prepared. Both membranes were significantly antibacterial against *E. coli*. The higher antibacterial activity of 10-bilayer PVCL/TA coated hydrogels than 5-bilayer coated ones supported the discussion on the effect of TA on decreasing the number of bacteria on the LbL coated substrates due to antibacterial property of TA. The antibacterial activity was further improved when hydrogel membranes were coated with 10-bilayers of PVCL and TA-Ciprofloxacin complexes. The greatest antibacterial activity observed in case of hydrogels coated with 10-bilayers of PVCL and TA-Ciprofloxacin complexes was due to antibacterial effect of chitosan, tannic acid, and temperature-induced release of Ciprofloxacin (Figure 4.13A) combined on a single surface.

The antibacterial activity of chitosan/PEG hydrogels against *S. aureus* was lower than that observed against *E. coli*. However, chitosan/PEG hydrogels coated with 10-bilayers of PVCL and TA-Ciprofloxacin complexes showed improved efficacy against *S. aureus* (Figure 4.13B), most probably due to the release of Ciprofloxacin from the multilayers. Importantly, hydrogels coated with PVCL and TA and loaded with Ciprofloxacin at the post-assembly step exhibited lower antibacterial activity against both *E. coli* and *S. aureus*. This was against the expectations based on the Ciprofloxacin release results discussed in Section 4.4.5. Remember that Ciprofloxacin release was significantly greater in case of hydrogels coated with 10-bilayer PVCL and TA than the bare hydrogels or hydrogels coated with 10-bilayers of PVCL and

TA-Ciprofloxacin complexes. Experiments on hydrogels coated with PVCL and TA-Ciprofloxacin complexes will be re-conducted.
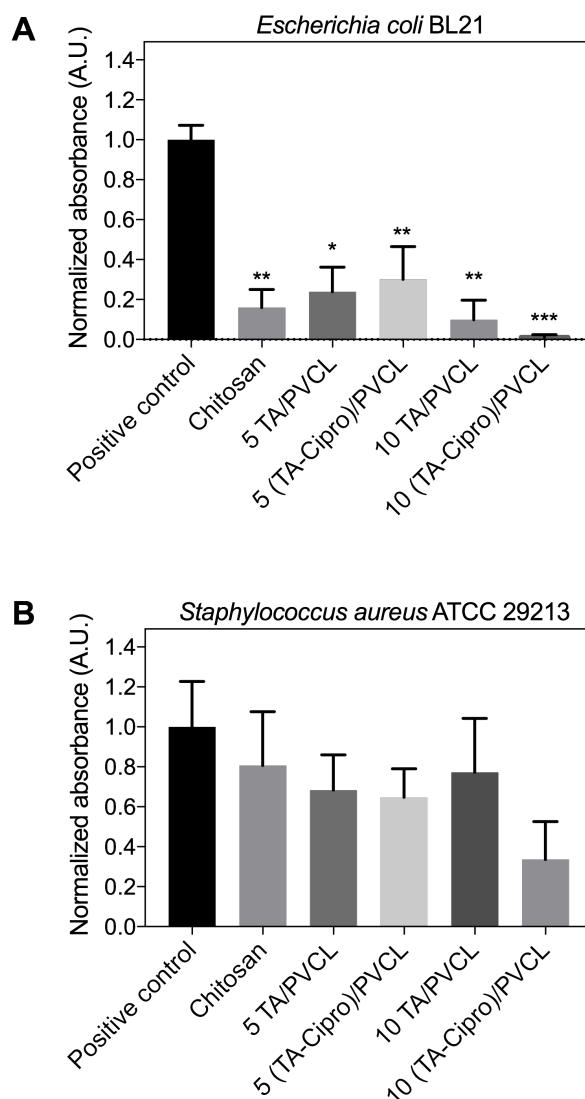
Fig. 4. 13. The antibacterial activity of bare chitosan/PEG hydrogels, hydrogels coated with 5- and 10-bilayers of TA and PVCL or PVCL and TA-Ciprofloxacin complexes, as shown by the absorbance at OD_{600nm} in M9 minimal growth medium. The measurements were taken 5 h after seeding *E. coli* and *S. aureus* bacterial cells on bare or coated hydrogel membranes. All results were significantly different for *E. coli* on membranes, compared to the positive control (cells grown in the blank well). Control column value average was normalized to 1. The columns are compared with ANOVA and further with Holm-Sidak's test (**$P<0.01$, ***$P<0.001$).

4.4.7. CCD-18Co Fibroblast Adhesion and Proliferation on Hydrogel Membranes

Fibroblast cells are the predominant cells in the skin and are the primary cells that lay the extracellular matrix present in the dermis, thus carry essential roles in wound healing [51]. They signal each other to proliferate and release the collagen-rich extracellular matrix which is mandatory for endothelial cells to promote neovascularization [52]. Due to this important regulation of fibroblasts in wound healing, we checked the adherence and viability properties of CCD-18Co primary fibroblasts on bare and LbL coated chitosan/PEG hydrogel membranes.

CCD-18Co cells adhered better on coated substrates than on bare hydrogel membranes (Figure 4.14.) and the viability of cells after 96 h was significantly higher for both 5- and 10-bilayer PVCL/TA coated hydrogel membranes (Figure 4.15.). As reported previously Silva et al. and Chatelet et al., chitosan could suppress the proliferation of fibroblasts most probably due to high electrostatic attractions between the fibroblast membrane and the chitosan-coated surface, even though chitosan possesses several favorable functions in the treatment of wounds, such as biocompatibility and promoting the regeneration at the wound bed [25,53]. To increase the surface adherence property of chitosan-based hydrogels towards fibroblasts, several techniques were applied and some were found to be successful. For example, the immobilization of RGD peptide on chitosan derivatives improved the fibroblast adherence and propagation on surfaces [54]. LbL films that are self-assembled on hydrogel surfaces tune the chemical and physical properties of the surface [31]. The properties of fibroblast cell viability on LbL film-coated chitosan-based hydrogels have not been studied before. This work, for the first time, reports on the induced fibroblast proliferation and viability through the MTT assay. The MTT assay showed that the cell viability was significantly improved for fibroblasts growing on 5- or 10-bilayer PVCL/TA coated membranes, compared to the bare membrane. The values for 5- and 10-bilayer PVCL/TA coated membranes did not reach statistical significance (Figure 4.14.). This could be explained by the diminished effect of chitosan and PEG on fibroblast adhesion through deposition of LbL films on the hydrogel membrane. As the film thickness and the amount of the material surrounding the hydrogel

increases, the effect of the base hydrogel material seems to diminish, thus cells exhibited faster proliferation. It is also common that cells adhere successfully to surfaces with high density of hydroxyl groups [55]. The free hydroxyl groups of TA which did not participate in film formation could have improved the adhesive property of the surface towards fibroblasts.
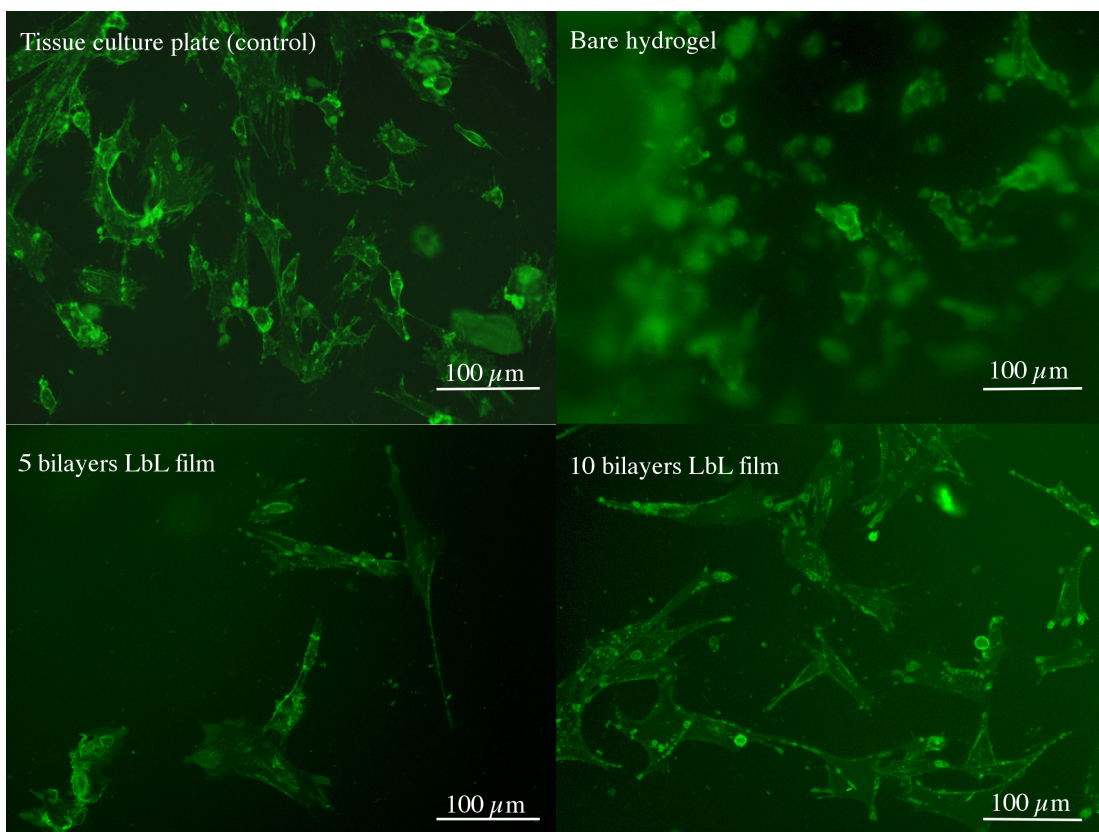
Fig. 4. 14. Fluorescence images of CCD18-Co cells cultivated on tissue culture plate surface, bare hydrogel, 5-bilayer TA/PVCL coated hydrogel, and 10-bilayer TA/PVCL coated hydrogel.
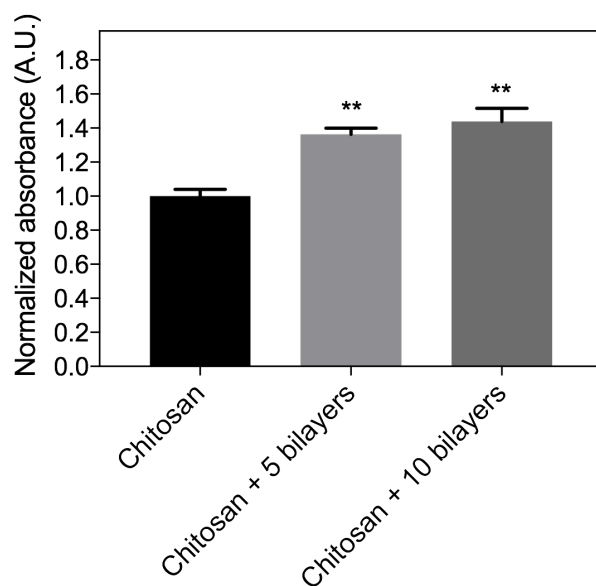
Fig. 4. 15. The viability of CCD-18Co human fibroblasts on bare chitosan/PEG hydrogel membranes and membranes coated with 5- or 10-bilayers of PVCL and TA. The cell viability was observed to be significantly higher for coated membranes. The viability was reported as the absorbance of formazan crystals at OD_{570nm}. Control column value average was normalized to 1. The columns are compared with ANOVA and further with Holm-Sidak's test (**$P<0.01$).

4.5. Conclusion

In this study, antibacterial property of chitosan/PEG hydrogel membranes was improved as potential wound dressings via LbL coating of the membranes using TA and PVCL. Ciprofloxacin, a broad spectrum antibiotic with efficacy against some multiple drug resistant bacteria, such as MRSA, was incorporated into LbL films either during film deposition (via complexation with TA), or at the post-assembly step (via diffusion). The antibacterial activity of bare chitosan/PEG hydrogel membranes, membranes with TA/PVCL coating and TA-Ciprofloxacin complexes)/PVCL coatings were assessed against *E. coli* and *S. aureus*. All types of membranes showed antibacterial activity against *E. coli*, however the lowest number of bacteria was detected on hydrogel membranes coated with PVCL and TA-Ciprofloxacin complexes due to temperature-induced release of Ciprofloxacin from the surface. Among all

hydrogels, only the ones coated with TA-Ciprofloxacin complexes and PVCL showed antibacterial activity against *S. aureus*. This indicated the need of a broad spectrum antibiotic to to overcome the proliferation of *S. aureus* on surfaces. Moreover, it was shown that modification of the hydrogel surface by LbL deposition of PVCL and TA provided better adhesion and high viability of CCD-18Co cells (human colon fibroblast cell line) on the surface.

To the best of our knowledge, this study is the first describing the surface modification of chitosan/PEG hydrogels by temperature-induced antibiotic releasing LbL films to prepare antibacterial membranes with high fibroblast cell viability. Such hydrogel membranes are promising to be used as wound dressings due to enhanced antibacterial acitivity of the hydrogel membranes and increased bioactivity against human fibroblasts cells.

4.6. References

[1]   R.A.F. Clark, The molecular and cellular biology of wound repair, 1996.

[2]   C.L. Baum, C.J. Arpey, Normal cutaneous wound healing: clinical correlation with cellular and molecular events, Dermatol. Surg. 31 (2005) 674–86; discussion 686. doi:10.1111/j.1524-4725.2005.31612.

[3]   M.B. Dreifke, A.A. Jayasuriya, A.C. Jayasuriya, Current wound healing procedures and potential care, Mater. Sci. Eng. C. 48 (2015) 651–662. doi:10.1016/j.msec.2014.12.068.

[4]   G.D. Winter, Formation of the scab and the rate of epithelisation of superficial wounds in the skin of the young domestic pig, Nature. 193 (1962) 293–294. doi:10.1038/193293a0.

[5]   C.J. Brine, P.A. Sandford, J.P. Zikakis, N.J.. International Conference on Chitin and Chitosan (5th : 1991 : Princeton, Advances in chitin and chitosan, Elsevier Applied Science, 1992.

[6]   M.P. Ribeiro, A. Espiga, D. Silva, P. Baptista, J. Henriques, C. Ferreira, J.C. Silva, J.P. Borges, E. Pires, P. Chaves, I.J. Correia, Development of a new chitosan hydrogel for wound dressing, Wound Repair Regen. 17 (2009) 817–824. doi:10.1111/j.1524-475X.2009.00538.x.

[7]   I.-Y. Kim, S.-J. Seo, H.-S. Moon, M.-K. Yoo, I.-Y. Park, B.-C. Kim, C.-S. Cho, Chitosan and its derivatives for tissue engineering applications., Biotechnol. Adv. 26 (2008) 1–21. doi:10.1016/j.biotechadv.2007.07.009.

[8]   T. Dai, M. Tanaka, Y.-Y. Huang, M.R. Hamblin, Chitosan preparations for wounds and burns: antimicrobial and wound-healing effects, Expert Rev. Anti. Infect. Ther. 9 (2011) 857–879. doi:10.1586/eri.11.59.

[9]   G. Brandenberg, L.G. Leibrock, R. Shuman, W.G. Malette, H. Quigley, Chitosan: A new topical hemostatic agent for diffuse capillary bleeding in brain tissue, Neurosurgery. 15 (1984) 9–13.

[10]   V.W.L. Ng, J.M.W. Chan, H. Sardon, R.J. Ono, J.M. García, Y.Y. Yang, J.L. Hedrick, Antimicrobial hydrogels: A new weapon in the arsenal against multidrug-resistant infections, Adv. Drug Deliv. Rev. 78 (2014) 46–62. doi:10.1016/j.addr.2014.10.028.

[11]   M. Kong, X.G. Chen, C.S. Liu, C.G. Liu, X.H. Meng, L.J. Yu, Antibacterial mechanism of chitosan microspheres in a solid dispersing system against E. coli, Colloids Surfaces B Biointerfaces. 65 (2008) 197–202. doi:10.1016/j.colsurfb.2008.04.003.

[12]   N. Desroche, C. Dropet, P. Janod, J. Guzzo, Antibacterial properties and reduction of MRSA biofilm with a dressing combining polyabsorbent fibres and a silver matrix., J. Wound Care. 25 (2016) 577–584. doi:10.12968/jowc.2016.25.10.577.

[13]   J.I. Bueso-Bordils, M.T. Perez-Gracia, B. Suay-Garcia, M.J. Duart, R.V. Martin Algarra, L. Lahuerta Zamora, G.M. Anton-Fos, P.A. Aleman Lopez, Topological pattern for the search of new active drugs against methicillin resistant Staphylococcus aureus, Eur. J. Med. Chem. 138 (2017).

doi:10.1016/j.ejmech.2017.07.010.

[14]   P. Gupta, K. Vermani, S. Garg, Hydrogels: From controlled release to pH-responsive drug delivery, Drug Discov. Today. 7 (2002) 569–579. doi:10.1016/S1359-6446(02)02255-9.

[15]   Y. Qiu, K. Park, Environment-sensitive hydrogels for drug delivery, Adv. Drug Deliv. Rev. 64 (2012) 49–60. doi:10.1016/j.addr.2012.09.024.

[16]   H. Priya James, R. John, A. Alex, K.R. Anoop, Smart polymers for the controlled delivery of drugs – a concise overview, Acta Pharm. Sin. B. 4 (2014) 120–127. doi:10.1016/j.apsb.2014.02.005.

[17]   G. Grassi, R. Farra, P. Caliceti, G. Guarnieri, S. Salmaso, M. Carenza, M. Grassi, Temperature-sensitive hydrogels: Potential therapeutic applications, Am. J. Drug Deliv. 3 (2005) 239–251. doi:10.2165/00137696-200503040-00004.

[18]   R.G. Sibbald, K. Woo, E. Ayello, Increased bacterial burden and infection: NERDS and STONES, Wounds UK. 3 (2007) 25–46. doi:10.1097/00129334-200610000-00012.

[19]   M. Fierheller, R.G. Sibbald, A clinical investigation into the relationship between increased periwound skin temperature and local wound infection in patients with chronic leg ulcers., Adv. Skin Wound Care. 23 (2010) 369-379-381. doi:10.1097/01.ASW.0000383197.28192.98.

[20]   J. Jin, M. Song, D.J. Hourston, Novel chitosan-based films cross-linked by genipin with improved physical properties, Biomacromolecules. 5 (2004) 162–168. doi:10.1021/bm034286m.

[21]   M. V. Risbud, A.A. Hardikar, S. V. Bhat, R.R. Bhonde, pH-sensitive freeze-dried chitosan-polyvinyl pyrrolidone hydrogels as controlled release system for antibiotic delivery, J. Control. Release. 68 (2000) 23–30. doi:10.1016/S0168-3659(00)00208-X.

[22]   S.Y. Kim, S.M. Cho, Y.M. Lee, S.J. Kim, Thermo- and pH-responsive

behaviors of graft copolymer and blend based on chitosan andN-isopropylacrylamide, J. Appl. Polym. Sci. 78 (2000) 1381–1391. doi:10.1002/1097-4628(20001114)78:7<1381::AID-APP90>3.0.CO;2-M.

[23]   K.L. Shantha, D.R.K. Harding, Preparation and in-vitro evaluation of poly[N-vinyl-2-pyrrolidone-polyethylene glycol diacrylate]-chitosan interpolymeric pH-responsive hydrogels for oral drug delivery, Int. J. Pharm. 207 (2000) 65–70. doi:10.1016/S0378-5173(00)00533-0.

[24]   J.-P. Chen, T.-H. Cheng, Thermo-Responsive Chitosan-graft-poly(N-isopropylacrylamide) Injectable Hydrogel for Cultivation of Chondrocytes and Meniscus Cells, Macromol. Biosci. 6 (2006) 1026–1039. doi:10.1002/mabi.200600142.

[25]   S.S. Silva, M.I. Santos, O.P. Coutinho, J.F. Mano, R.L. Reis, Physical properties and biocompatibility of chitosan/soy blended membranes, in: J. Mater. Sci. Mater. Med., 2005 (575–579). doi:10.1007/s10856-005-0534-z.

[26]   F. Yang, X. Li, M. Cheng, Y. Gong, N. Zhao, X. Zhang, Y. Yang, Performance modification of chitosan membranes induced by gamma irradiation., J. Biomater. Appl. 16 (2002) 215–226. doi:10.1177/0885328202016003176.

[27]   V. Tangpasuthadol, N. Pongchaisirikul, V.P. Hoven, Surface modification of chitosan films. Effects of hydrophobicity on protein adsorption, Carbohydr. Res. 338 (2003) 937–942. doi:10.1016/S0008-6215(03)00038-7.

[28]   H. Wang, Y.-E. Fang, Y. Yan, Surface modification of chitosan membranes by alkane vapor plasma, J. Mater. Chem. 11 (2001) 1374–1377. doi:10.1039/b009688l.

[29]   S.S. Silva, S.M. Luna, M.E. Gomes, J. Benesch, I. Pashkuleva, J.F. Mano, R.L. Reis, Plasma surface modification of chitosan membranes: Characterization and preliminary cell response studies, Macromol. Biosci. 8 (2008) 568–576. doi:10.1002/mabi.200700264.

[30]   S.A. Sukhishvili, Responsive polymer films and capsules via layer-by-layer

assembly, Curr. Opin. Colloid Interface Sci. 10 (2005) 37–44. doi:10.1016/j.cocis.2005.05.001.

[31]   H. Sakaguchi, T. Serizawa, M. Akashi, Layer-by-Layer Assembly on Hydrogel Surfaces and Control of Human Whole Blood Coagulation, Chem. Lett. 32 (2003) 174–175. http://www.journal.csj.jp/doi/pdf/10.1246/cl.2003.174 (accessed August 28, 2017).

[32]   L. Grossin, D. Cortial, B. Saulnier, O. Félix, A. Chassepot, G. Decher, P. Netter, P. Schaaf, P. Gillet, D. Mainard, J.C. Voegel, N. Benkirane-Jessel, Step-by-step build-up of biologically active cell-containing stratified films aimed at tissue engineering, Adv. Mater. 21 (2009) 650–655. doi:10.1002/adma.200801541.

[33]   S. Mehrotra, D. Lynam, R. Maloney, K.M. Pawelec, M.H. Tuszynski, I. Lee, C. Chan, J. Sakamoto, Time controlled protein release from layer-by-layer assembled multilayer functionalized agarose hydrogels, Adv. Funct. Mater. 20 (2010) 247–258. doi:10.1002/adfm.200901172.

[34]   D. Choi, J. Heo, J.H. Park, Y. Jo, H. Jeong, M. Chang, J. Choi, J. Hong, Nano-film coatings onto collagen hydrogels with desired drug release, J. Ind. Eng. Chem. 36 (2016) 326–333. doi:10.1016/j.jiec.2016.02.023.

[35]   P. Gentile, C. Ghione, A.M. Ferreira, A. Crawford, P. V. Hatton, Alginate-based hydrogels functionalised at the nanoscale using layer-by-layer assembly for potential cartilage repair, Biomater. Sci. (2017). doi:10.1039/C7BM00525C.

[36]   H. Hu, H. Hu, J.H. Xin, A. Chan, L. He, Glutaraldehyde-chitosan and poly (vinyl alcohol) blends, and fluorescence of their nano-silica composite films, Carbohydr. Polym. 91 (2013) 305–313. doi:10.1016/j.carbpol.2012.08.038.

[37]   A.K. Bajpai, S.K. Shukla, S. Bhanu, S. Kankane, Responsive polymers in controlled drug delivery, Prog. Polym. Sci. 33 (2008) 1088–1118. doi:10.1016/j.progpolymsci.2008.07.005.

[38]   D.D. Solomon, R.J. Sherertz, Antibiotic releasing polymers, J. Control.

207

Release. 6 (1987) 343–352. doi:10.1016/0168-3659(87)90087-3.

[39]   M. Haktaniyan, S. Atilla, E. Cagli, I. Erel-Goktepe, pH- and Temperature-Induced Release of Doxorubicin from Multilayers of Poly(2-isopropyl-2-oxazoline) and Tannic Acid, Polym. Int. (2017). doi:10.1002/pi.5458.

[40]   R. Osawa, T.P. Walsh, Effects of Acidic and Alkaline Treatments on Tannic-Acid and Its Binding Property to Protein, J. Agric. Food Chem. 41 (1993) 704–707. doi:10.1021/jf00029a004.

[41]   D.L. Ross, C.M. Riley, Aqueous solubilities of some variously substituted quinolone antimicrobials, Int. J. Pharm. 63 (1990) 237–250. doi:10.1016/0378-5173(90)90130-V.

[42]   E. Kharlampieva, S. Sukhishvili, Hydrogen-Bonded Layer-by-Layer Polymer Films, Polym. Rev. 46 (2006) 377–395. doi:10.1080/15583720600945386.

[43]   F. Zentz, L. Bédouet, M.J. Almeida, C. Milet, E. Lopez, M. Giraud, Characterization and quantification of chitosan extracted from nacre of the abalone haliotis tuberculata and the oyster pinctada maxima, Mar. Biotechnol. 3 (2001) 36–44. doi:10.1007/s101260000042.

[44]   A.A. Tager, A.P. Safronov, S. V. Sharina, I.Y. Galaev, Thermodynamic study of poly(N-vinyl caprolactam) hydration at temperatures close to lower critical solution temperature, Colloid Polym. Sci. 271 (1993) 868–872. doi:10.1007/BF00652769.

[45]   A.H. Zisch, M.P. Lutolf, M. Ehrbar, G.P. Raeber, S.C. Rizzi, N. Davies, H. Schmökel, D. Bezuidenhout, V. Djonov, P. Zilla, J. a Hubbell, Cell-demanded release of VEGF from synthetic, biointeractive cell ingrowth matrices for vascularized tissue growth, FASEB J. 17 (2003) 2260–2262. doi:10.1096/fj.02-1041fje.

[46]   C.C. Lin, A.T. Metters, Hydrogels in controlled release formulations: Network design and mathematical modeling, Adv. Drug Deliv. Rev. 58 (2006) 1379–1408. doi:10.1016/j.addr.2006.09.004.

[47] N. Bhattarai, J. Gunn, M. Zhang, Chitosan-based hydrogels for controlled, localized drug delivery, Adv. Drug Deliv. Rev. 62 (2010) 83–99. doi:10.1016/j.addr.2009.07.019.

[48] M. Hosseinnejad, S.M. Jafari, Evaluation of different factors affecting antimicrobial properties of chitosan, Int. J. Biol. Macromol. 85 (2016) 467–475. doi:10.1016/j.ijbiomac.2016.01.022.

[49] K.T. Chung, Z. Lu, M.W. Chou, Mechanism of inhibition of tannic acid and related compounds on the growth of intestinal bacteria., Food Chem. Toxicol. 36 (1998) 1053–1060. doi:10.1016/S0278-6915(98)00086-6.

[50] M. LeBel, Ciprofloxacin: chemistry, mechanism of action, resistance, antimicrobial spectrum, pharmacokinetics, clinical trials, and adverse reactions., Pharmacotherapy. 8 (1988) 3–33. http://www.ncbi.nlm.nih.gov/pubmed/2836821.

[51] J.M. Sorrell, M.A. Baber, A.I. Caplan, Site-matched papillary and reticular human dermal fibroblasts differ in their release of specific growth factors/cytokines and in their interaction with keratinocytes, J. Cell. Physiol. 200 (2004) 134–145. doi:10.1002/jcp.10474.

[52] S. Balaji, A. King, T.M. Crombleholme, S.G. Keswani, The Role of Endothelial Progenitor Cells in Postnatal Vasculogenesis: Implications for Therapeutic Neovascularization and Wound Healing, Adv. Wound Care. 2 (2013) 283–295. doi:10.1089/wound.2012.0398.

[53] C. Chatelet, O. Damour, a Domard, Influence of the degree of acetylation on some biological properties of chitosan films., Biomaterials. 22 (2001) 261–268. doi:10.1016/S0142-9612(00)00183-6.

[54] V. Patrulea, N. Hirt-Burri, A. Jeannerat, L.A. Applegate, V. Ostafe, O. Jordan, G. Borchard, Peptide-decorated chitosan derivatives enhance fibroblast adhesion and proliferation in wound healing, Carbohydr. Polym. 142 (2016) 114–123. doi:10.1016/j.carbpol.2016.01.045.

[55] Jin Ho Lee, Jong Woo Park, Hai Bang Lee, Cell adhesion and growth on polymer surfaces with hydroxyl groups prepared by water vapour plasma treatment, Biomaterials. 12 (1991) 443–448. doi:10.1016/0142-9612(91)90140-6.

CHAPTER 5

CONCLUSIONS AND OUTLOOK

This PhD thesis study developed functional surface coatings using LbL technology which may find use in various biomedical applications.

In Chapter 2, dual functional ultra-thin surface coatings which exhibited both bacterial anti-adhesive and antibacterial properties were developed using LbL self-assembly technique. Zwitterionic block copolymer micelles with pH-responsive cores and PSS were used as building blocks for the multilayer assembly. Zwitterionic units on the micellar coronae assured the bacterial anti-adhesiveness, while pH-responsive polybasic micellar cores provided the release of an antibacterial agent, Triclosan under mild acidic conditions. These LbL films exhibited anti-adhesive property against *Escherichia coli* and *Staphylococcus aureus*. Triclosan release from the surface decreased the number of viable bacteria that were adherent on the surface compared to LbL films composed of empty zwitterionic micelles. Considering the slightly acidic environment in sites of bacterial infection, such multilayer coatings may be promising for surface modification of hospital equipment and medical devices, such as catheters and stents. Such LbL coatings can be further improved by using hyaluronic acid (HA) as the polyanion counterpart rather than PSS. Hyaluronic acid is a natural polysaccharide, thus highly biocompatible. It has a very large water holding capacity which could impart enhanced bacterial anti-adhesive property to the multilayer films. As a future work, these ultra-thin films can be used to be deposited on medical devices, such as catheters, to see their efficacy in reducing multiple drug resistant (MDR) bacteria-related infections at hospitals.

In Chapter 3, the use of a biodegradable polycation, poly(4-hydroxy-L-proline ester) (polyhydroxyproline) (PHPE) was described to prepare osteoconductive surfaces. Briefly, water soluble complexes of PHPE and TA were prepared and then used as building blocks to construct LbL films. PHPE-TA complexes were unique in terms of a building block as it did not require a polymer counterpart to drive the LbL assembly. It was found that multilayers of PHPE-TA complexes conducted the adherence and the proliferation of SaOS-2 cells (human osteosarcoma cells). They induced the alkaline phosphatase activity of the adherent cells, indicating enhanced mineralization of the surface. It was also found that PHPE could be used as an osteoinductive agent which was quite promising for bone regeneration. The osteoinductive effect was observed most probably because the enhanced penetration of PHPE inside the cell, through the membrane. PHPE hydrolyzes into *trans*-hydroxyproline residues or can transit into proline residues and get incorporated in collagen. PHPE holds promise as an agent to promote bone regeneration, through the induction of collagen synthesis. As a future work, PHPE-TA LbL films can be coated on bone implants or other orthopedic medical devices that are in contact with the bone to assess their efficacy in conducting bone formation around the device. Additionally, the treatment of mesenchymal stem cells with PHPE can be assessed to observe the differentiation of stem cells towards primary lineages.

In Chapter 4, we have described the surface modification of hydrogel membranes composed of chitosan and poly(ethylene glycol). As chitosan forms brittle structures, PEG was incorporated within the hydrogel matrix to increase the ductility of the hydrogel membrane, making it more suitable for practical applications such as wound dressings. A wound dressing should be biocompatible, non-cytotoxic and induce the regeneration of the wounded tissue at the shortest time possible. Chitosan is an antibacterial agent with high biocompatibility and hemocompatibility, but it does not provide adhesive surfaces for fibroblasts cells, which are the most abundant cells in the dermis. In this part of the thesis, the surface of chitosan/PEG hydrogel membranes was modified via LbL self-assembly of TA and PVCL. Ciprofloxacin, a broad spectrum antibiotic, with known antibacterial activity against MRSA, was loaded into the LbL films. These hydrogels were capable of releasing Ciprofloxacin via

temperature-trigger due to LCST-type phase behavior of PVCL and conformational changes occurred within the multilayer films at physiological temperature. Ciprofloxacin release from the surface enhanced the antibacterial activity of the hydrogel membranes. Hydrogels coated with LbL films of PVCL and TA also provided better adherence of CCD-18Co primary fibroblast cells on the surface and improved their viability. Such hydrogel modifications could be useful in overcoming bacteria-related infections during wound healing. As a future work, multilayers can be loaded with other bioactive molecules, such as peptides with RGD sequence or variety of other designed peptides that can signal the cells to adhere on surfaces. These modifications can improve the fibroblast proliferation on surfaces and reduce the tissue integration time for these hydrogels.

CURRICULUM VITAE

PERSONAL INFORMATION

Surname, Name: ONAT, Bora

Nationality: Turkish

Date and Place of Birth: 1986, İstanbul, Eminönü

Phone: +90 536 479 2959

e-mail: onatbora@gmail.com

EDUCATION

Middle East Technical University, Ankara, Turkey - Ph.D. candidate in the department of Biotechnology - from Sep. 2012
Advisor: Assoc. Prof. Irem Erel Goktepe

Co-advisor: Assoc. Prof. Sreeparna Banerjee

University of Bedfordshire, Luton, U.K. - M.Sc. in Biotechnology (Molecular Microbiology) - Feb. 2011 to Mar. 2012

Graduation grade: Upper second class honoursAdvisor: Dr. Arthur Hosie

Project: Escherichia coli was transfected with lambda bacteriophage to assess the genes of a pathogenic oral bacterium *Tannerella forsythia*.

Middle East Technical University, Ankara, Turkey - B.Sc. in Molecular Biology and Genetics - Sep 2004 to Jan 2011

Graduation project advisor: Assoc. Prof. Aysegul Gozen

EXPERIENCE

Intern, Scripps Institution of Oceanography, **University of California San Diego**, CA, USA — 2007

Advisor: Prof. Dr. Douglas H. Bartlett

SKILLS

I have experience in HPLC, ellipsometer, Dynamic Light Scattering, fluorescence and light microscope, UV and fluorescence spectrometry and well-reader, RT-PCR and qPCR techniques, cell culture methods, bacteriophage transfection of bacteria, and major microbial cultivation and cell culture techniques.

ACADEMIC AWARDS AND SCHOLARSHIPS

2011 - 2012 Second best graduation grade in class, University of Bedfordshire

2014 - 2017 Primary fields research projects Ph.D. scholarship of the Turkish Science and Technology Association (TUBITAK)

PUBLISHED SCIENTIFIC ARTICLES

- Bacterial anti-adhesive and pH-induced antibacterial agent releasing ultra-thin films of zwitterionic copolymer micelles, Bora ONAT, Vural BÜTÜN, Sreeparna BANERJEE, Irem EREL GOKTEPE, **Acta Biomaterialia**, Volume 40, August 2016, Pages 293-309, DOI: 10.1016/j.actbio.2016.04.033

MANUSCRIPTS IN PREPARATION

- Onat, B.; Ozcubukcu, S.; Banerjee, S.; **Erel-Goktepe, I**. "Polyhydroxyproline ester promotes osteogenic differentiation of SaOS-2 cells"

- Onat, B.; Banerjee, S.; **Erel-Goktepe, I**. "Osteoconductive layer-by-layer films of biodegradable polymers"

- Onat, B.; Banerjee, S.; **Erel-Goktepe, I.** "Temperature-Induced Antibiotic Release from Chitosan/PEG Hydrogel Membranes Functionalized Using Layer-by-Layer Technology"

- Onat, B.; Cagli, E.; **Erel-Goktepe, I**. "Layer-by-layer films of stimuli responsive block copolymer micelles" (review article)

CONFERENCE ABSTRACTS

- Onat, B.; Butun, V.; Banerjee, S.; **Erel-Goktepe, I**. "Anti-Biofouling Films Prepared by Layer-by-Layer Formation of Zwiterionic Micelles" *NanoTR 11*, 2015 ODTÜ, Ankara, Turkey. (Oral speech)

- Onat, B.; Butun, V.; Banerjee, S.; **Erel-Goktepe, I**. "Multifunctional Anti-Adhesive Films Prepared by Layer-by-Layer Formation of Zwitterionic Micelles" *27th European Conference on Biomaterials*, 2015, Poland. (Poster presentation and short speech)

- Onat, B.; **Erel-Goktepe, I**. "Implant surfaces modified by completely biodegradable and antibacterial multilayer films for osteoconduction" *Frontiers in Bioengineering and Biotechnology*, Volume 4, 2016, DOI: 10.3389/conf.fbioe.2016.01.02288, *10th World Biomaterials Congress,* 2016, Canada.

- Onat, B.; Ozcubukcu, S.; Banerjee, S.; **Erel-Goktepe, I**. "Osteoconductivity of layer--by--layer films of poly(4--hydroxy--L--proline) ester" *7th International Colloids Conference,* 2017, Spain. (Poster presentation)

REFERENCES

1. Assoc. Prof. Irem Erel Goktepe, Department of Chemistry, Middle East Technical University, Turkey

erel@metu.edu.tr, (90) 312 2103233

2. Assoc. Prof. Sreeparna Banerjee, Department of Biology, Middle East Technical

University, Turkey

banerjee@metu.edu.tr, (90) 312 2106468

3. Dr. Arthur Hosie, Division of Science, University of Bedfordshire, U.K.

arthur.hosie@beds.ac.uk, (44) 1234 400 400 (ext. 2146)